Institut für Ernährungswissenschaft

Lehrstuhl für Lebensmittelchemie

Characterization of selenium and copper in cell systems of the neurovascular unit

Dissertation

zur Erlangung des akademischen Grades

„doctor rerum naturalium" (Dr. rer. nat.)

in der Wissenschaftsdisziplin

„Lebensmittelchemie"

kumulativ eingereicht an der

Mathematisch-Naturwissenschaftlichen Fakultät

der Universität Potsdam

vorgelegt von

Stefanie Raschke

aus Strausberg

2023

TABLE OF CONTENTS

LIST OF FIGURES

LIST OF TABLES

INDEX OF ABBREVIATIONS

AD	Alzheimer´s disease
ALS	Amyotrophic lateral sclerosis
ALXN1840	bis-choline tetrathiomolybdate
ANOVA	Analysis of variance
APEX1	DNA-(apurinic or apyrimidinic site) lyase
ApoER2	Apolipoprotein E receptor 2
ATOX1	Antioxidant 1 copper chaperone
ATP	Adenosine triphosphate
ATP7A/B	ATPase copper transporting alpha/beta
Aβ	Amyloid beta
BBB	Blood-brain barrier
BCB	Blood-liquor barrier
BER	Base excision repair
CA	Comet assay
Carboxy-DCFH-DA	5(&6)-carboxy-2',7'-dichlorodihydrofluoresceindiacetate
CCF-STTG1	Human astrocytoma cells
CCK8	Cell Counting Kit-8
CCS	Copper chaperone for superoxide dismutase
CIAAW	Commission on Isotopic Abundances and Atomic Weights
CNS	Central nervous system
COX17	Cytochrome c oxidase copper chaperone 17
CP	Ceruloplasmin
CSF	Cerebrospinal fluid
Cu	Copper
CVDs	Cardiovascular diseases
Cys	Cysteine
D-A-Ch	Germany, Austria, Switzerland
DBH	Dopamine-β-hydroxylase
DHE	Dihydroethidium
DIO	Iodothyronine deiodinase
DIV	Day *in vitro*
DMSe	Dimethylselenide
DMT1	Divalent metal transporter 1

DNA	Deoxyribonucleic acid
DPA	D-penicillamine
DTNB	5,5'-dithiobis(2-nitrobenzoic acid)
EC$_{30}$	Effective concentration with 30% impact
EFSA	European Food Safety Authority
ER	Endoplasmatic reticulum
ET	Ergothioneine
ETS	Electron transport system
FCS	Fetal calf serum
Fpg	Formamidopyrimidine DNA glycosylase
GPX	Glutathione peroxidase
GSH	Reduced glutathione
GS-SeH	Glutathione selenol
GS-Se-SG	Diglutathione selenide
GSSG	Glutathione disulfide
HepG2	Human liver carcinoma cells
HO-1	Heme oxygenase 1
HPLC	High performance liquid chromatography
ICP	Inductively coupled plasma
IUPAC	International Union of Pure and Applied Chemistry
LC	Locus coeruleus
LUHMES	Lund human mesencephalic cells
m/z	Mass-to-charge ratio
MeSeCys	Methylselenocysteine
MeSeN	Se-methylselenoneine
Met	Methionine
MMP	Mitochondrial membrane potential
MNKD	Menkes disease
MRI	Magnetic resonance imaging
MS/MS	Tandem mass spectrometry
MT	Metallothionein
NADPH	Nicotinamide adenine dinucleotide phosphate
NCC	Nonceruloplasmin copper
ND	Neurodegenerative disease
NEIL	Nei like DNA glycosylase

NIH	U.S. National Institute of Health
NOAEL	No observed adverse effect level
NPC	Nutritional Prevention of Cancer
NQO1	NAD(P)H quinone dehydrogenase 1
NRF2	Nuclear factor (erythroid-derived 2)-like 2
OCTN-1	Organic cation/carnitine transporter 1
OGG1	8-oxoguanine DNA glycosylase
PAM	peptidyl-α-monooxygenase
PARP	Poly(ADP-ribose) polymerase 1
PBCEC	Primary porcine endothelial cells
PD	Parkinson´s disease
RO(N)S	Reactive oxygen (and nitrogen) species
SD	Standard deviation
Se	Selenium
SECIS	Selenocysteine insertion sequence
SeCT	Selenocystathionine
SeCys	Selenocysteine
SELENOP	Selenoprotein P
SeMet	Selenomethionine
SeN	Selenoneine
SEPHS	Selenophosphate synthetase
SN	Substantia nigra
SOD	Superoxide dismutase
T2D	Type 2 diabetes
t-BOOH	*Tert*-butylhydroperoxide
TEER	Transepithelial electrical resistance
TGN	*trans*-Golgi network
TMSe	Trimethylselenonium
TNB	2-nitro-5-thiobenzoic acid
TPC	Tripartite complex
TRX	Thioredoxin
TXNRD	Thioredoxin reductase
WD	Wilson´s disease
WHO	World Health Organization
ZO-1	Zonula occludens-1

ELUCIDATIONS

- References for chapter 1 (General Introduction) and chapter 7 (General Discussion) are listed together at the end of this thesis (Bibliography), references for the manuscripts (chapters 2 – 6) are listed at the end of each chapter in a separate reference section.

- Figures and tables are consecutively numbered in chapter 1 (General Introduction) and chapter 7 (General Discussion), while figures and tables of the manuscripts (chapters 2 – 6) are numbered separately according to their appearance within the respective manuscript.

- Owing to the complex terminology of IUPAC nomenclature, the chemical compounds studied in this thesis are referred to using their trivial names.

- Registered and legally protected trademarks are marked by the following symbols ™ or ®

- Genes or proteins of human origin are capitalized (e.g., SELENOP), and those of non-human origin are written with the initial letter capitalized only (e.g., Selenop).

DECLARATION

The present cumulative doctoral thesis comprises five scientific studies (chapters 2 – 6), which were prepared as independent manuscripts. They have been published (chapters 2, 3, and 5) or submitted (chapter 4 and 6) to international peer-reviewed journals. The articles include suggestions of co-authors as well as of referees and journal editors as outcome of the peer-review process.

As the leading author of two of five manuscripts (chapters 4 and 6), I developed the concepts of the studies with support of my supervisor Prof. Dr. Tanja Schwerdtle, performed most of the experiments, conducted the analysis and wrote the main text. I am first author together with Dr. Evgenii Drobyshev (shared first authorship) in the manuscript presented in chapter 2. For this article, I was equally involved in conducting the experiments as well as their evaluation, the interpretation of the results, and the writing and editing of the manuscript.

As co-author of two manuscripts (chapter 3 and 5), I performed parts of the experiments within the study. Experiments carried out by co-authors were performed as mentioned in chapter *1.5 Structure of the thesis* for each manuscript. When using published data and methods or when citing statements and results provided by others, it is indicated by appropriate references in the respective manuscripts. All co-authors provided feedback of the concept of the studies and for revision of the manuscripts.

_____
Stefanie Raschke
(Doctoral candidate)
26th February 2023

SUMMARY

The trace elements, selenium (Se) and copper (Cu) play an important role in maintaining normal brain function. Since they have essential functions as cofactors of enzymes or structural components of proteins, an optimal supply as well as a well-defined homeostatic regulation are crucial. Disturbances in trace element homeostasis affect the health status and contribute to the incidence and severity of various diseases. The brain in particular is vulnerable to oxidative stress due to its extensive oxygen consumption and high energy turnover, among other factors. As components of a number of antioxidant enzymes, both elements are involved in redox homeostasis. However, high concentrations are also associated with the occurrence of oxidative stress, which can induce cellular damage. Especially high Cu concentrations in some brain areas are associated with the development and progression of neurodegenerative diseases such as Alzheimer's disease (AD). In contrast, reduced Se levels were measured in brains of AD patients. The opposing behavior of Cu and Se renders the study of these two trace elements as well as the interactions between them being particularly relevant and addressed in this work.

In the first part, the transfer of the individual elements into the brain as well as their combination was investigated using a well-established *in vitro* model of the blood-brain barrier (BBB). The study demonstrated that the Se transfer is strongly dependent on the Se species used. In the *in vitro* model of the BBB, the newly discovered Se species, selenoneine, and two reference species were investigated regarding their transfer and metabolism. While previous studies have demonstrated side-directed transfer of selenonein across the intestinal barrier and partial metabolization, here it was transferred only in small amounts staying in the non-metabolized form across the *in vitro* BBB.

In the next section, as part of a collaboration, the impact of Cu on primary porcine brain capillary endothelial cells (PBCECs) forming the *in vitro* BBB as well as transfer behavior was studied. Furthermore, a combined approach was selected to evaluate the efficacy of a newly developed Cu chelator for the treatment of Wilson´s disease (WD) patients in this model. It was shown that the PBCECs are particularly sensitive to Cu, weakening the barrier integrity resulting in higher Cu transfer into the brain. Combined administration with ALXN1840 prevented the impairment of the barrier as well as Cu transfer to the brain. These results are promising for further development of ALXN1840 as a clinical treatment for WD.

In vivo models of neurodegenerative diseases have already shown the protective effect of Se supplementation. Therefore, the *in vitro* BBB model was applied to investigate whether insufficient Se supply to PBCECs results in higher Cu transfer to the brain. Here, PBCECs were supplemented with physiologically relevant concentrations of selenite already during cultivation and subsequently the transfer of Cu was measured *via* ICP-MS/MS. Supplementation with Se did not demonstrate any effect

on the transfer of Cu. However, the Se status of PBCECs improved, as evidenced by increased cellular Se content, improved the barrier integrity accompanied by higher levels of selenoprotein P (SELENOP). In addition, transfer rates were decreased upon incubation of supraphysiological Cu concentrations, presumably indicating saturation of the transporters involved.

After considering the transfer of Se and Cu, the focus has shifted to the brain, where the effect of Cu on brain cells, was characterized. Furthermore, the effect of Cu on the Se status of cells was of particular interest. Astrocytes are the first cells encountered by the transmitted Cu in the brain. Moreover, they effectively accumulate and store redox-active Cu to protect the highly specialized neurons. Exposure of cells to Cu exhibited substantial cytotoxicity both in astrocytes as well as neurons. This remained unchanged even after Se supplementation. In addition, it was shown that the cells accumulate Cu efficiently, which was also independent of additional Se administration. Investigations observing the mode of action demonstrated an increased formation of reactive species especially in the mitochondria. Cu seems to trigger structural and functional changes in these organelles and consequently causes a decline in membrane potential. In addition, changes in the glutathione balance were observed, whereby increased GSH is formed, presumably to bind excess free Cu. With increasing Cu concentrations, the GSH/GSSG ratio also decreased. Oxidative DNA damage formation and neurite network loss were also induced by Cu. Additional supplementation with Se exhibited only a protective effect on neurite degeneration, whereas the other mechanistic endpoints remained largely unaffected. However, Cu significantly affected Se status, which was evident from reduced glutathione peroxidase activity, decreased cellular Se as well as SELENOP levels, and decreased excretion of this selenoprotein. This could be partially protected by supplementation with selenite or SeMet, although a dependence on the Se species used was clearly evident.

The present work demonstrated an impact of Cu on cells of the neurovascular unit. Whereby Se supplementation did not provide a clear positive effect on Cu-induced toxicity. However, an interaction of the two trace elements has been demonstrated, especially regarding the cellular Se status. Deteriorations of the Se status may have a negative effect on cellular redox regulation and presumably on the development and progression of neurodegenerative diseases.

ZUSAMMENFASSUNG

Die Spurenelemente Selen (Se) und Kupfer (Cu) spielen eine wichtige Rolle bei der Aufrechterhaltung einer normalen Gehirnfunktion. Da sie wesentliche Funktionen als Cofaktoren von Enzymen oder Strukturbestandteile von Proteinen haben, sind eine optimale Versorgung sowie eine genau definierte homöostatische Regulierung von entscheidender Bedeutung. Störungen der Spurenelement-homöostase beeinträchtigen den Gesundheitszustand und tragen zum Auftreten und zur Schwere verschiedener Krankheiten bei. Insbesondere das Gehirn ist aufgrund seines hohen Sauerstoffverbrauchs und seines hohen Energieumsatzes anfällig für oxidativen Stress. Als Bestandteile einer Reihe von antioxidativen Enzymen sind beide Elemente an der Redox-Homöostase beteiligt. Hohe Konzentrationen werden jedoch auch mit dem Auftreten von oxidativem Stress in Verbindung gebracht, der zu Zellschäden führen kann. Besonders hohe Cu-Konzentrationen in einigen Hirnregionen werden mit der Entwicklung und der Progression neurodegenerativer Erkrankungen wie Alzheimer in Verbindung gebracht. Im Gegensatz dazu wurden in den Gehirnen von Alzheimer-Patienten geringere Se-Konzentrationen gemessen. Das gegensätzliche Verhalten von Cu und Se verdeutlicht die Relevanz der Untersuchung dieser beiden Spurenelemente sowie deren Wechselwirkungen und wird in dieser Arbeit thematisiert.

Im ersten Teil wird der Transfer der beiden Elemente einzeln, sowie in deren Kombination in das Gehirn anhand eines gut etablierten *in-vitro*-Modells der Blut-Hirn-Schranke (BHS) untersucht. Die Untersuchung des Se-Transfers konnte zeigen, dass dieser stark von der verwendeten Se-Spezies abhängig ist. In diesem Modell wurden die neu entdeckte Se-Spezies, Selenonein, sowie zwei Referenzverbindungen hinsichtlich Transfer und Metabolismus untersucht. Während frühere Studien einen gerichteten Transfer von Selenonein über die Darmbarriere und eine teilweise Metabolisierung nachgewiesen haben, wird dieses in der *in vitro*-BHS nur in geringen Mengen unverstoffwechselt transferiert.

Im folgenden Abschnitt wurden im Rahmen einer Kooperation die Auswirkungen von Cu auf primäre porcine Hirnkapillarendothelzellen (PBCECs), die die *in vitro*-BHS bilden, sowie das Transferverhalten untersucht. Darüber hinaus wurde ein kombinierter Ansatz gewählt, um die Wirksamkeit eines neu entwickelten Cu-Chelators (ALXN1840) für die Behandlung von Wilson Patienten zu testen. Es konnte gezeigt werden, dass PBCECs besonders empfindlich auf Cu reagieren, wodurch die Integrität der Barriere geschwächt und mehr Cu in das Gehirn transferiert wird. Die Kombination mit ALXN1840 konnte sowohl die Beeinträchtigung der Barriere als auch den Cu-Transfer ins Gehirn verhindern. Diese Ergebnisse sind vielversprechend für die weitere Entwicklung von ALXN1840 zur Behandlung der Wilson Erkranung.

In vivo-Modelle für neurodegenerative Erkrankungen konnten bereits eine protektive Wirkung einer Se-Supplementierung zeigen. Daher wurde das *in vitro* BHS-Modell verwendet, um zu untersuchen, ob

eine unzureichende Se-Versorgung der PBCECs zu einem höheren Cu-Transfer in das Gehirn führt. Dabei wurden PBCECs bereits während der Kultivierung mit physiologisch relevanten Konzentrationen von Selenit supplementiert und anschließend der Cu-Transfer mittels ICP-MS/MS gemessen. Die Se-Gabe zeigte keinen Einfluss auf den Cu-Transfer. Allerdings verbesserte sich der Se-Status der PBCECs, was durch einen erhöhten zellulären Se-Gehalt, eine verbesserte Barriereintegrität und höhere Selenoprotein P Gehalte nachgewiesen wurde. Darüber hinaus zeigte sich, dass die Transferraten bei der Inkubation mit supraphysiologischen Cu-Konzentrationen abnahmen, was vermutlich auf eine Sättigung der beteiligten Transporter hinweist.

Nach der Betrachtung des Transfers wurde das Gehirn in den Fokus gestellt, wo die Wirkung von Cu auf Gehirnzellen charakterisiert wurde. Darüber hinaus war die Wirkung von Cu auf den zellulären Se-Status von besonderem Interesse. Astrozyten sind die ersten Zellen, auf die das übertragene Cu im Gehirn trifft. Außerdem akkumulieren und speichern sie redox-aktives Cu, als Schutzmechanismus der hochspezialisierten Neuronen. Die Exposition gegenüber Cu konnte sowohl bei Astrozyten als auch bei Neuronen eine erhebliche Zytotoxizität zeigen. Dies blieb auch nach Se-Supplementierung unverändert. Darüber hinaus konnte gezeigt werden, dass die Zellen Cu effizient akkumulieren konnten, was auch unabhängig von einer zusätzlichen Se-Gabe war. Untersuchungen zur Wirkungsweise zeigten eine vermehrte Bildung reaktiver Spezies insbesondere in den Mitochondrien. Cu scheint in diesen Organellen strukturelle und funktionelle Veränderungen auszulösen und in der Folge eine Reduzierung des Membranpotentials zu bewirken. Darüber hinaus konnte eine Veränderung des Glutathionhaushalts beobachtet werden, wobei vermehrt GSH gebildet wird, vermutlich um freies Cu zu binden. Die Induktion oxidativer DNA-Schäden und der Verlust des Neuritennetzwerks wurden ebenfalls durch Cu untersucht. Eine zusätzliche Se-Gabe konnte jedoch nur eine protektive Wirkung auf die Neuritendegeneration zeigen, während die anderen mechanistischen Endpunkte weitgehend unbeeinflusst blieben. Allerdings beeinträchtigt Cu den Se-Status erheblich, was sich in einer verringerten Glutathionperoxidase-Aktivität, verringerten Se- und Selenoprotein P-Gehalten und einer verringerten Ausscheidung des Selenoproteins zeigte. Dies konnte teilweise durch Zugabe von Selenit oder SeMet protektiert werden, obwohl eine Abhängigkeit von den verwendeten Se-Spezies deutlich zu erkennen war.

In der vorliegenden Arbeit konnte ein Einfluss von Cu auf Zellen der neurovaskulären Einheit nachgewiesen werden. Dabei zeigte die Se-Gabe keine eindeutig positive Wirkung auf die Cu-induzierte Toxizität. Allerdings konnte eine Wechselwirkung der beiden Spurenelemente nachgewiesen werden, insbesondere hinsichtlich des zellulären Se-Status. Eine Verschlechterung des Se-Status könnte sich negativ auf die zelluläre Redox-Regulation und vermutlich auf die Entwicklung und das Fortschreiten neurodegenerativer Erkrankungen auswirken.

1. GENERAL INTRODUCTION

1.1 Selenium - Occurrence and physiological relevance

1.1.1 Physicochemical characteristics

Selenium (Se) is a member of the 16th group (VIa subgroup) of the periodic table, with atomic number 34 and characterized by a relative mass of 78.971 u [1,2]. Along with oxygen, sulfur, tellurium and polonium, Se forms the group of chalcogens. It occurs in the following valence states: 0 (elementary), +IV (selenite), +VI (selenate) and -II (selenide). Organic compounds usually contain selenides and are therefore of particular relevance in biological systems. Influenced by various factors such as pH, redox potential, free oxygen availability, and humidity it can easily switch between oxidation levels [2]. Among the six naturally occuring Se isotopes, [78]Se and [80]Se are the most abundant ones (Figure 1) [1,3,4]. Elemental Se is found in five allotropic modifications, three being crystalline and two amorphous (red or black in colour) [2]. Crystalline allotropes are formed by either Se_6 or Se_8 polymer rings, grey or red in colour, or Se_n helical chains (grey colour). The last representing the most thermodynamically stable form with metal-like properties [5,6]. Se and sulfur, located one below the other in the periodic table, have similar chemical properties and are both involved in biological processes [7]. Both can be found at equivalent positions of different proteins as constituents of amino acids. Besides their similarities, those two elements are not completely interchangeable in biological systems [8]. Se differs from sulfur in terms of a slightly larger atomic radius and lower electronegativity, resulting in weaker bonds with carbon and hydrogen [9]. At physiological pH, selenol groups are present in their deprotonated selenolate form (pKa = 5.2), leading to higher reactivity, while their sulfur analog remains in the thiol form (pKa = 8.3) [9].

Atomic mass	34
Atomic weight [u]	78.971
Density [g/cm³]	4.808
Melting temperature [°C]	220
Boiling temperature [°C]	685
Oxidation states	-II, 0, +IV, +VI
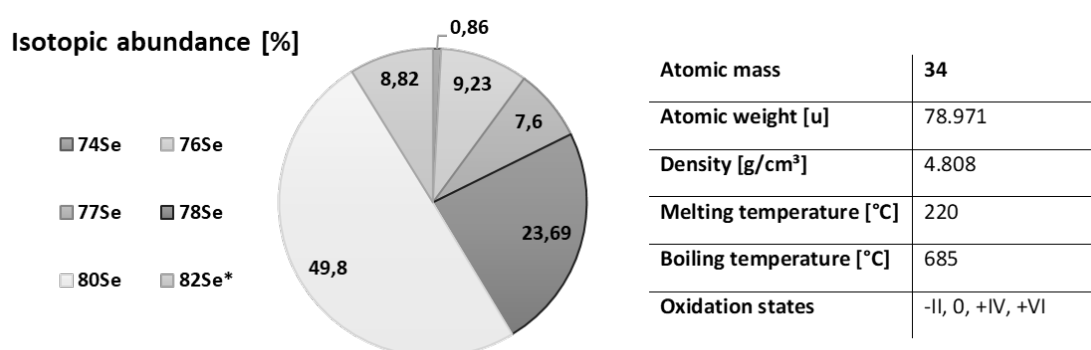
Figure 1. Percentage abundance of natural Se isotopes and chemical properties of Se. According to the Commission on Isotopic Abundances and Atomic Weights (CIAAW) from the International Union of Pure and Applied Chemistry (IUPAC). *radioactive

1.1.2 Environmental occurrence and food sources

Due to its diverse and complex chemical properties, Se is ubiquitously found in a variety of environmental compartments including air, water, soil, and plants. Se concentrations in water vary widely between surface water (0.06 to 0.12 µg/L) and groundwater (0.06 to 400 µg/L) and depend on pH, with higher contents in acidic (pH < 3.0) and alkaline (pH > 7.5) water [10]. Se concentrations in the atmosphere range between 0.1 and 10 ng/cm³. It is produced, among other things, by volcanic activity that releases Se-containing gases and dusts, but also by the industrial combustion of coal and fuels [10]. The average Se concentration in the Earth's crust ranges from 0.05 to 0.09 µg/g, but it is unevenly distributed and can reach very high levels in some areas. For example, volcanic rocks (120 µg/g) and shales (675 µg/g) can be particularly high in Se [5,10]. Most soils contain about 0.01 - 2.0 µg/g Se, although seleniferous soils can contain up to 1200 µg/g, depending mainly on the source rock material [10,11]. In addition to local weathering processes, other natural sources (e.g. volcanic eruptions) as well as anthropogenic inputs (combustion of fossil fuels, use of fertilizers, coal-generated fly-ash, non-ferrous metal production etc.) can contribute to soil and atmospheric Se concentrations [11]. Se-deficient areas are found in mountainous countries like Finland and Sweden, New Zealand, and some regions of China [12], whereas Venezuela, Canada, Western Australia, and parts of China, Russia, and the United States have particularly Se-rich soils [13,14].

Se content in plants depends on a number of factors such as soil properties, climate and geography. Moreover, the amount and chemical form of Se are of crucial importance for the plant availability of the element. Generally, the uptake and metabolism of Se follow the same pathways as for sulfur [15]. Based on the ability to accumulate Se, plants can be divided into non-accumulators and Se-accumulators [10]. Most plant species belong to the group of non-accumulators and tolerate only small amounts of Se (10 - 100 µg/g dry matter). Se-accumulating plants can contain Se levels up to 500 µg/g dry matter when grown on seleniferous soils [10,16]. Although Se is not essential for higher plants (angiosperms), there are so-called Se-hyperaccumulators, which include about 30 representatives of the families *Brassicaceae*, *Fabaceae* and *Asteraceae* and can contain up to 15,000 µg Se/g dry matter [17]. Nutritionally relevant plant products, which can be enriched in Se include onions, garlic and broccoli, which deposit Se mainly in the form of selenate, selenomethionine (SeMet), methyl-selenocysteine (MeSeCys) and γ-glutamyl-Se-methyl-selenocysteine [13,18]. Some plant products such as brazil nuts (*Bertholletia excels*), containing relatively high Se amounts (up to 320 µg Se/g) and metabolize the absorbed Se mainly to SeMet [18]. Most vegetables and fruits contain only low amounts of Se [10]. In animal products, Se concentration depends largely on feeding conditions and the use of supplements [7]. Se is mainly enriched in form of SeMet and SeCys, and especially offal and some fish (cod and tuna) contain high Se concentrations [19].

1.1.3 Human selenium intake and recommendations

Se is mainly absorbed through food, but the environment, occupation and smoking can also contribute to exposure [13]. Consumption of cereals and cereal products accounts for the largest share of Se intake, followed by meat, fish, eggs, and milk and dairy products [13,20]. The uptake *via* drinking water, mainly as selenate, is low; the maximum permissible amount of Se in drinking water in Germany is 10 µg/L [13,21]. Human bioavailability of Se is influenced by certain factors including content of protein and fat as well as heavy metals in the diet [2,22]. Generally, protein-rich foods contain higher Se amounts, while fat content correlates with lower Se [23]. In addition, the bioavailability of Se is negatively affected by the presence of heavy metals and sulfur, and positively affected by the presence of vitamins A, C and E [2].

Individual Se intakes vary widely around the world, ranging from 3 to 7000 µg per day, and both Se deficiency and intoxication, as described later in this section, can be observed. Particularly high daily intakes were observed in Venezuela, some parts of China and North America [13,24]. In contrast, Se intake in Europe is lower, ranging from 7 to 90 µg per day (average 40 µg/d) [19]. In the dietary supplement sector, a number of Se compounds (e.g. SeMet, Se-enriched yeasts, sodium selenate, -selenite) are approved in Europe and can increase the individual Se intake [25]. In order to achieve adequate Se contents in plant and animal products, Se-containing fertilizers or feed additives are applied. In Germany, the use of sodium selenate (as fertilizer and feed additives) and sodium selenite (as feed additives) is permitted [26–28].

According to the German, Austrian and Swiss Societies of Nutrition (D-A-Ch), average intake recommended for men is 70 µg and for women 60 µg Se per day, respectively. Accordingly, values for children and young people are set lower and nursing women have a higher requirement [29]. These recommendations were derived from a study in Se-deficient chinese participants supplemented with SeMet [30]. The U.S. National Institute of Health (NIH) recommends a daily intake of 55 µg Se per day on the basis of two intervention studies in China and New Zealand [31–33]. In contrast, intake recommendations from the World Health Organization (WHO) are based on two-thirds saturation of plasma glutathione peroxidase (GPX) activity, a representative of the selenoproteins that contain selenocysteine in their active center (see section *1.1.4 – Human selenium metabolism and selenoprotein synthesis*). From this, a daily Se intake of 26 µg for women and 34 µg for men was determined to be sufficient [34]. The differences in the recommendations result from different derivation methods used for the calculation. In addition, the choice of the ideal biomarker for Se supply is a matter of ongoing debate.

One of the most widely used biomarkers of Se status is the total concentration in serum or plasma and corresponds to the amount of Se that is absorbed and retained by the organism. However, the

nonspecific incorporation of SeMet, a Se compound commonly found in diet, may contribute to the total content without playing a functional role and consequently, not providing information about the capacity and saturation of functional selenoproteins. Therefore, additional assessment of parameters like selenoprotein P (SELENOP) level and GPX3 activity is used to gain more specific information about the functional Se fraction [35]. These parameters can easily be measured in plasma or serum samples and already respond to minor Se deficiency [36]. Plasma/serum SELENOP concentration is considered a more accurate biomarker of the Se status than total serum Se, as it is the physiological transport form of Se, ensuring systemic supply of the trace element [30,37]. GPX3, another functional biomarker, is synthesized in the kidney, which is dependent on external Se supply *via* SELENOP. A Selenop-knockout mouse model demonstrated decreased Gpx3 activity, which could be recovered by transgenic liver-specific expression of human SELENOP [38], demonstrating the link between both biomarkers. Urinary Se levels can be used to assess Se status at the population level as well [39]. Se concentration in hair or toenails is used as a non-invasive long-term biomarker [40]. To obtain a complete picture of the Se status, the combination of biomarkers is useful [35,40].

1.1.4 Human selenium metabolism and selenoprotein synthesis

The uptake of Se takes place mainly in the upper part of the duodenum and depends on the chemical structure of the Se species ingested. Absorption of the various Se species is achieved by different mechanisms, some of which have not yet been fully elucidated, as in case of selenite. The organic selenoamino acids, equivalent to the sulfur-containing analogues, are actively transported into the enterocytes *via* amino acid transporters. After uptake of selenate by the anion transporter (SLC26), it is reduced to selenite and then further metabolized. In general, absorption of selenoamino acids and selenate is highly efficient with absorption rates ranging from 70% to 90% [41]. In contrast, selenite uptake is less efficient with about 60% and depends on the availability of reduced glutathione (GSH) in the intestine [41]. The rate of absorption can be negatively affected by the presence of other elements like iron (Fe) (III), calcium, arsenic, lead and sulfur. As selenite is complexed by Fe(III) it can no longer be absorbed by enterocytes [12].

Human Se metabolism at cellular level is depicted in Figure 2. The main metabolite of Se homeostasis is selenide (Se^{2-}) and the Se species are converted to it albeit *via* different metabolic pathways before Se can specifically be incorporated into selenoproteins. Metabolism of selenate and selenite involves a series of reduction steps facilitated by thioredoxin reductase (TXNRD) system or GSH to selenide. Ingested SeMet can be incorporated non-specifically into proteins, so-called selenized proteins that have no additional function, or it can be enzymatically converted into SeCys. This is further metabolized into selenide *via* SeCys-β-lyase to be subsequently used for the synthesis of selenoproteins or for

transport in the blood. In this process, selenide is bound to various proteins such as very low density lipoprotein (VLDL), low density lipoprotein (LDL) as well as albumin or globulin and then transported to the liver, which represents the central organ of Se homeostasis [18]. Hepatic Se is then either provided to selenoprotein synthesis or undergo further transformation for excretion [42]. For further distribution of Se within the body, it is incorporated into SELENOP in the liver, which is considered as major Se transporter [43]. In plasma, the largest proportion of Se is composed of SELENOP (53%), followed by GPX3 (19%) and others (28%) [44]. Uptake of SELENOP into extrahepatic tissues is receptor-mediated by apolipoprotein E receptor 2 (ApoER2) (brain, testis) or megalin (kidney) [2,45]. Excess Se is excreted mainly in the form of selenosugars, dimethylselenide (DMSe) and trimethylselenide (TMSe) *via* urine and faeces [46].

Starting from the central metabolite selenide, selenoprotein synthesis happens selectively at the translational level through a highly complex process. Normally recognized as a stop codon, SeCys is encoded *via* UGA codon. Recognition of this as SeCys requires the so-called SeCys insertion element (SECIS), a hair structure in the 3'-untranslated region (3'-UTR) of eukaryotic selenoprotein mRNA that prevents premature chain termination [47]. In addition to the SECIS element, Sec-tRNA$^{[Ser]Sec}$ is needed, which is complementary to the UGA codon. Beginning with a serine-loaded tRNA, the synthesis of SeCys takes place directly at the tRNA. Initially the serine residue is phosphorylated by phosphoseryl tRNA kinase (PSTK) and then converted to Sec-tRNA$^{[Ser]Sec}$ by SeCys synthetase (SEPSECS) in the presence of selenophosphate. Selenide is enzymatically activated to selenophosphate by selenophosphate synthetase (SEPHS) under consumption of ATP. Subsequently, SeCys-loaded tRNA is recognized by a specific elongation factor (eEFsec) and directed to the ribosomes. There, a complex consisting of SECIS, SECIS binding protein 2 (SBP2), eL30, EFsec and tRNA is formed and referred to as SeCys insertion complex [48].

The observation that individual selenoproteins respond differently to Se deficiency is known as selenoprotein hierarchy. Some selenoproteins, such as GPX4, deiodinases (DIOs) and TXNRDs, are expressed with higher priority than other selenoproteins (e.g., GPX1), while SELENOP has medium priority. However, this hierarchy is not yet fully known for all selenoproteins. Furthermore, the individual organs are also governed by a hierarchy, which means that under Se deficiency, brain and testis can maintain their Se levels constant at the expense of other organs (e.g. liver, kidney or lung) [49,50].
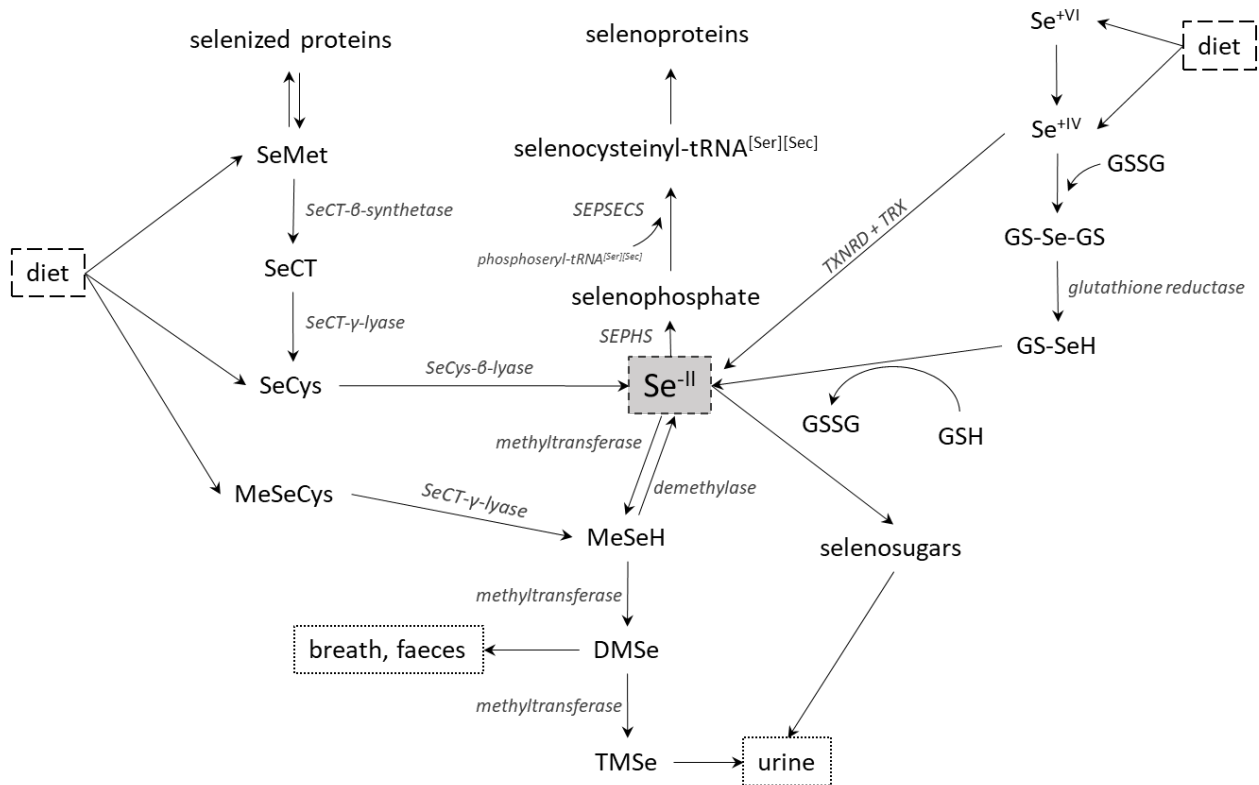
Figure 2. Schematic overview of the human Se metabolism. (Figure was adapted from [13]). In principle, dietary Se is metabolized to the central Se metabolite selenide (Se^{2-}) *via* different pathways depending on the Se species. Organic selenomethionine (SeMet) can be incorporated into proteins instead of methionine or undergo further metabolism by different enzymes. It is first converted to selenocystathionine (SeCT) *via* SeCT-β-synthethase and subsequently over selenocysteine (SeCys) to selenide *via* two different lyases. Methylselenocysteine (MeSeCys) is metabolized to methylselenole (MeSeH), which can be either demethylated to selenide or further methylated to form the excretion products dimethylselenide (DMSe) or trimethylselenide (TMSe). Inorganic selenate is reduced to selenite, which can be converted into selenide either *via* the glutathione/glutathione disulfide (GSH/GSSG) or *via* the thioredoxin reductase/thioredoxin (TXNRD/TRX) system. At high Se concentrations, selenide is excreted in the urine by formation of selenosugars. Selenoprotein synthesis starts with selenide, which is first activated to selenophosphate *via* selenophosphate synthetase (SEPHS) and subsequently loaded to a specific phosphoseryl-tRNA[Ser/Sec]. Incorporation of SeCys into selenoproteins takes place *via* a sophisticated system in which a number of other proteins are involved [13].

1.1.5 Physiological functions of selenoproteins

In 1817, the swedish chemist Jöns Jakob von Berzelius discovered Se and for a long time it was only known for its toxic properties. The essential nature of Se was first described by Schwarz and Foltz in 1957 on the basis of experiments in which prophylactic administration of Se prevented liver necrosis in rats [51]. In the 1970s, the discovery of Se in the GPX1 enzyme allowed for the first time the identification of a specific biochemical function of Se in mammalian cells [52,53]. Nowadays, Se is considered an essential trace element for all vertebrates including humans. In contrast to metals, Se does not interact with proteins solely as a cofactor, but it is incorporated into proteins as a constituent of the proteinogenic amino acid SeCys. The majority of the biological action of Se is based on these selenoproteins [47]. In humans, there are 25 coding genes known for Se-dependent enzymes, with GPXs, TXNRDs, and DIOs representing the most well-known selenoproteins [2]. Although the functional properties of several selenoproteins have already been well characterized, there are a number of representatives whose functions have not yet been fully elucidated. An overview of the individual selenoproteins with regard to function and localization is shown inTable 1. Based on their function, some selenoproteins can be classified into different families with five members belonging to the GPX, three to the TXNRD and three to the DIO family. The GPX and TXNRD families are major participants in the antioxidant defense system. While the GPXs are responsible for the detoxification of peroxides, the TXNRD family regulates the redox status of disulfides [54]. Members of the DIO family are important mediators of thyroid hormone metabolism *via* activation and inactivation of thyroid hormones [55]. SELENOP has a special role among the selenoproteins. Up to ten SeCys are incorporated in the amino acid sequence, rendering SELENOP responsible for the systemic distribution of Se in the body. Moreover, antioxidant and metal-binding properties have already been observed, making SELENOP a multifunctional selenoprotein [44]. The functions of other selenoproteins have not yet been fully elucidated. Thus, SELENOM, SELENON, and SELENOT appear to be involved in the regulation of Ca homeostasis [56–58]. While others, such as SELENOF, SELENOK, and SELENOS, appear to play a role in protein folding and degradation [59–61]. Moreover, structural similarities may be useful in predicting the functions of currently less understood selenoproteins. A number of selenoproteins contain a TRX-like motif (C-X-X-U), suggesting involvement in redox regulation.

*Table 1. Overview of the 25 human selenoproteins, their functions and localization. *selenoprotein with TRX-like redox motif (C-X-X-U). General reviews used for the overview:* [54,62]*. Abbreviations: AD - Alzheimer´s disease, CNS - central nervous system, Cys – cysteine, ER - endoplasmatic reticulum, Met - methionine, PM – plasma membrane, TRX – thioredoxin*

Selenoprotein	Function	Localization Organ (subcellular localization)	Source
Iodothyronine deiodinases (DIO)			
DIO1*	activation of thyroid hormones (T4), inactivation of thyroid hormones (T3 → rT3, T4 → T2)	liver, kidney, thyroid (PM)	[63]
DIO2*	activation of thyroid hormones (T4)	thyroid, CNS, pituitary, skeletal muscle (ER)	
DIO3*	inactivation of thyroid hormones (T3, T4)	pregnant uterus, placenta, fetal and neonatal tissues (PM)	
Glutathione peroxidases (GPX)	(Cys-containing homologs: GPX5, GPX7 & GPX8)		
GPX1	reduction of hydroperoxides	ubiquitous, kidney, liver, erythrocytes (cytosol)	[64]
GPX2		gastrointestinal tract, liver (cytosol)	
GPX3		plasma, kidney (extracellular)	
GPX4	reduction of phospholipid & cholesterol hydroperoxides, embryogenesis, sperm maturation	ubiquitous, testes, spermatozoa, brain (cytosol, mitochondria, nucleus)	
GPX6	reduction of hydroperoxides	olfactory epithelium, embryo (cytosol)	
Thioredoxin reductases (TRXND)			
TRXND1*	NADPH-dependent reduction of TRX	ubiquitous (cytosol, nucleus)	[65]
TRXND2*		ubiquitous (mitochondria)	
TRXND3*	reduction of TRX, sperm maturation	testis	
Other selenoproteins			
Methionine-R-sulfoxide reductase 1 (MSRB1, SELENOR)	reduction of Met sulfoxide to Met	ubiquitous (cytosol, nucleus)	[54,66]
Selenophosphate synthetase 2 (SEPHS2)	selenophosphate synthesis	ubiquitous (cytosol, nucleus)	[67]
Selenoprotein F (SEP15)*	control of protein folding, redox regulation	ubiquitous (ER)	[59,68]
Selenoprotein H*	redox-sensitive DNA-binding protein, antioxidative defense	ubiquitous (nucleoli)	[69,70]
Selenoprotein I	phosphatidylethanolamine synthesis, role in T-cell function	ubiquitous (PM)	[71]
Selenoprotein K	ER-associated protein degradation, immune function, regulation of myogenesis	ubiquitous (ER membrane)	[60,72–74]
Selenoprotein M*	Ca homeostasis regulation, neuroprotective role in AD	ubiquitous, most abundant in brain (ER)	[56,75]
Selenoprotein N	Ca homeostasis regulation, SEPN1-related myopathies	ubiquitous, embryonic development (ER membrane)	[57,76]
Selenoprotein O*	AMPylation, redox regulation	ubiquitous (mitochondria)	[77,78]
Selenoprotein P*	Se transport & homeostasis, antioxidative function	plasma (secreted)	[44,79]
Selenoprotein S	ER-associated protein degradation, regulation of inflammation and oxidative stress	ubiquitous (ER membrane, PM)	[61,80]
Selenoprotein T*	Ca homeostasis regulation, neuroendocrine function, neuroprotective role, involved in glucose homeostasis	ubiquitous (Golgi apparatus, ER, PM)	[58,81]
Selenoprotein V*	ER-stress mediated signaling, regulation of Se metabolism, male reproduction	testis (cytosol, nucleus)	[82–84]
Selenoprotein W*	regulation of bone metabolism, redox regulation	ubiquitous, muscle, brain (cytosol)	[85,86]

1.1.6 Imbalances of selenium homeostasis

An intake below 20 μg Se per day or Se serum level <25 μg/L is referred to as Se deficiency and is associated with alterations in expression of selenoproteins. Although there is usually no obvious Se deficiency in Western industrialized countries, there are a number of people who are at risk of developing Se deficiency, including patients on total parenteral nutrition or gastrointestinal malabsorption, vegetarians, and alcoholics [20]. Symptoms of Se deficiency include fatigue, poor performance, hair loss, whitening of fingernails, muscle weakness and infertility [20]. Additionally, a number of conditions are associated with Se deficiency: decreased immune function, increased viral virulence, cognitive decline or dementia [87]. Furthermore, endemic Se deficiency diseases are known, especially in Se-poor regions such as parts of China or Siberia. The Keshan disease, a cardiomyopathy that mainly affects children and women of childbearing age, is the best-known Se deficiency disease. However, infection with Coxsackie virus together with a coexistent Se deficiency seems to be a trigger for this disease [13]. Kashin-Beck is another endemic Se deficiency disease that occurs in Se-deficient areas of China, Korea, and Siberia. This disease is a dystrophic osteoarthropathy leading to deformation of bones and joint structure [13].

Though Se is one of the essential trace elements for humans, excessive intake can lead to toxic effects. Cases of Se intoxication can arise due to occupational exposure, suicidal intent, and overdosage of supplements [13,88,89]. Acute Se poisoning (serum levels of 400 to 30.000 μg/L) is associated with abdominal (vomiting, nausea, diarrhea, abdominal pain, and garlicky bad breath) and neurological symptoms (tremors, muscle spasms, agitation, confusion, delirium, and coma). In severe poisoning, cardiac and pulmonary symptoms such as hypotension and pulmonary edema may develop, causing possible death [89,90]. Endemic cases of chronic Se poisoning, known as selenosis can be observed in particularly seleniferous areas of China [91]. Symptoms of chronic Se intoxication (serum levels of 500 to 1400 μg/L), include abdominal symptoms (nausea, diarrhea, vomiting, garlicky breath odor), alopecia, nail changes, fatigue, skin lesions, peripheral paresthesias accompanied with hyperreflexia, and pain in the extremities [90]. Neurological symptoms such as a decline in cognitive function, weakness and paralysis may also be seen [90]. Due to the adverse effects, a tolerable upper intake level of 300 μg per day (adults) and for children depending of the age ranging from 60 μg (age: 1 – 3 yrs) to 250 μg (age: 15 – 17 yrs) has been established by the European Food Safety Authority (EFSA) [92]. In a similar range, the WHO and the U.S. Institute of Medicine of the National Academies established a maximum safe dose of 400 μg Se per day (age >14 yrs) and for children ranging from 45 μg (age up to 6 months) to 280 μg (age: 9 – 13 yrs) [31,34].

The substantial role of Se and selenoproteins in inflammatory processes and the immune response has been extensively studied (detailed reviews on this topic [93,94]). Deficiency of this trace element can

lead to decreased immune competence resulting in increased susceptibility to infection and possibly other diseases. Lower Se status could be observed in patients with chronic inflammation (including cystic fibrosis [95], rheumatoid arthritis [96] and inflammatory bowel disease [97]), critical illness (sepsis [98]), trauma patients with wound healing disorders [99] and virus infections (AIDS [100] and COVID-19 [101]). In this context, Se and selenoproteins have been shown to be involved in immune cell activation, proliferation, and differentiation [94]. Antioxidant selenoproteins (GPXs and TXNRDs) play a role in the homeostasis of redox-active components like hydrogen peroxide, which together with other mediators trigger proper immune response [93]. The role of specific selenoproteins in immune function is not yet conclusively understood. However, some appear to have regulatory roles like SELENOR [102], SELENOK [73] and SELENOS [103].

The fact that Se deficiency can negatively affect the cardiovascular system has already been shown in the endemic cardiomyopathy known as Keshan disease. Association between physiological Se status and reduced cardiovascular diseases (CVDs) incidence and mortality could be shown by meta-analysis of observational studies indicating a possible U-shaped relationship (Figure 3) [104–106]. Possible mechanisms at the cellular level include an increased antioxidant function, inhibition of apoptosis and influence on cell survival [107]. However, the use of Se supplements for the prevention of CVDs remains controversial. Meta-analysis of randomized controlled trials (RCTs) regarding the benefit of Se supply failed to identify an association between Se alone and reduced risk of CVDs and mortality [108].

Recent analyses of observational studies on Se and risk of type 2 diabetes (T2D) suggest a positive association [109,110], which was first reported in 2007 after re-evaluation of data from the Nutritional Prevention of Cancer (NPC) study [111]. However, there seems to be an interrelation between SELENOP secretion from the liver and insulin signaling. This balance is disturbed in T2D, and SELENOP is increasingly released into the blood [112,113]. This raises the question of whether elevated Se is a risk factor for T2D or the consequence of it and highlights the need for well-designed studies in this field.

A number of studies have demonstrated an association between Se status and decline in cognitive function in elderly patients. In this context, a low Se plasma or toenail content is related to a higher cognitive decline over time [114–116]. Similar observations could be made in AD patients [117,118]. In a later section of this work, the importance of Se in the context of the brain and neurodegenerative diseases (NDs) is discussed in more detail (see section *1.3.2 – Physiological relevance of selenium for brain function*).

Human reproductive function can also be influenced by Se status. Especially male fertility is associated with the selenoproteins GPX4 and SELENOP [119]. Thereby, GPX4 plays an important role in spermatogenesis as well as in sperm motility [120]. Male Selenop[(-/-)] mice show reduced fertility, lower

Se levels in the testes, and even supplementation with Se failed to raise Se levels to Selenop$^{(+/+)}$ levels indicating the high relevance of this selenoprotein [121]. The involvement of Se in female reproduction is less well understood, although a possible role in follicular development is assumed [122].

Aiming to investigate the potential benefits of Se supplementation on the development of cancer, the NPC study was initiated. Initial results were promising, showing reductions in cancer incidence, cancer mortality, and incidence of lung, colon, and prostate cancer [123]. However, these results were weakened by re-evaluation, resulting in only patients with low Se status at study entry (<106 ng/mL) who showed a reduced incidence of total and prostate cancer [124]. Additionally, a second re-evaluation even revealed an increase in skin cancer risk in patients with high Se status (>123 ng/mL) [125]. Another large study, the Selenium and Vitamin E Cancer Prevention Trial (SELECT), failed to show any benefits of supplementation on the development of prostate cancer and other cancer types [126]. In contrast to the NPC study, these patients already had a relatively optimal Se status (122 to 152 ng/mL) at baseline, which might be a reason for the absence of effect. The Swedish Mammography Cohort Study indicated a potential benefit of Se administration in patients with low Se intake (<20.5 µg/day), as breast cancer mortality was highest in this group [127]. In summary, the results of the studies are heterogeneous and highly dependent on the baseline Se status of the patients. These observations have given rise to the concept of the U-shape risk-response curve of Se-dependent health effects (Figure 3). Consistent with this widely accepted concept, people with low Se status may benefit from Se supplementation and reduce their risk for developing certain diseases, in contrast to people with adequate or high Se status who may be adversely affected by supplemental Se intake.
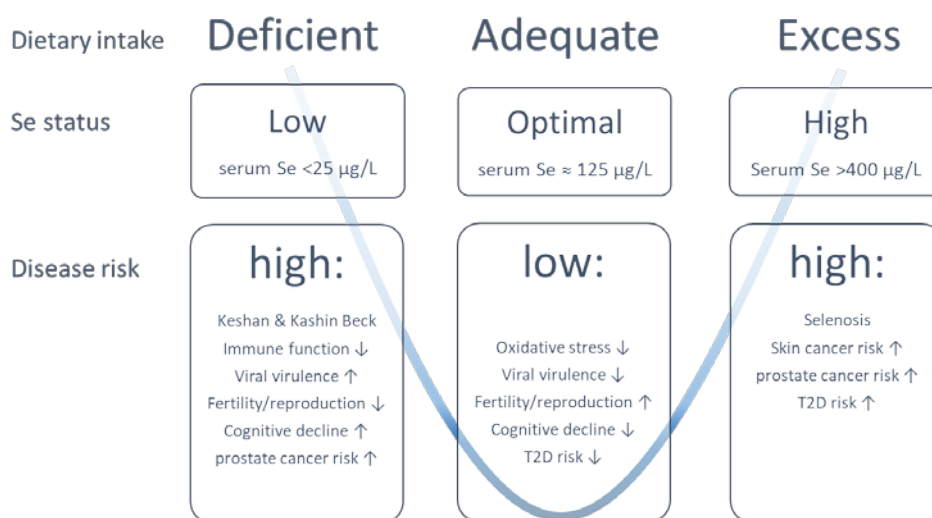
Figure 3. U-shaped relationship between Se status/intake and disease risk. (Modified from [87]).

1.2 Copper - Occurrence and physiological relevance

1.2.1 Chemical characteristics

Copper (Cu) is a transition metal with atomic number 29 and a relative mass of 63.55 Da [1]. Together with silver and gold, it belongs to the 11th group of the periodic table. ^{63}Cu and ^{65}Cu are the two stable naturally occurring Cu isotopes with abundances of 69.2% and 30.8%, respectively (Figure 4) [3]. In addition to the two stable isotopes, there are 27 radioactive isotopes (half-life ranging from 0.16 to 62 h), with some like ^{64}Cu and ^{67}Cu being applied for medical imaging and therapeutical purposes [128,129]. Pure Cu has a reddish-brown metal color and, with a density of 8.9 g/cm³, belongs to the heavy metals. As a semi-precious metal, it is characterized by very good thermal and electrical conductivity and, in terms of physical-technical properties, Cu is a very solid but at the same time ductile material [130]. It occurs in following oxidation states: 0, +I, +II and +III (rarely +IV), whereby only +I and +II are of relevance for biological systems. There, Cu (primarily as +II) is mainly bound to amino acids like histidine or to proteins with imidazole residues such as albumin. Under hydrophilic and oxidizing conditions, Cu(II) salts are the most stable compounds and appear blue or green in colour [131]. Characteristics of Cu are summarized in Figure 4.

Isotopic abundance [%]

■ 63Cu   ■ 65Cu

30,8

69,2

Atomic mass	29
Atomic weight [u]	63.546
Density [g/cm³]	8.94
Melting temperature [°C]	1083
Boiling temperature [°C]	2595
Oxidation states	0, +I, +II, +III
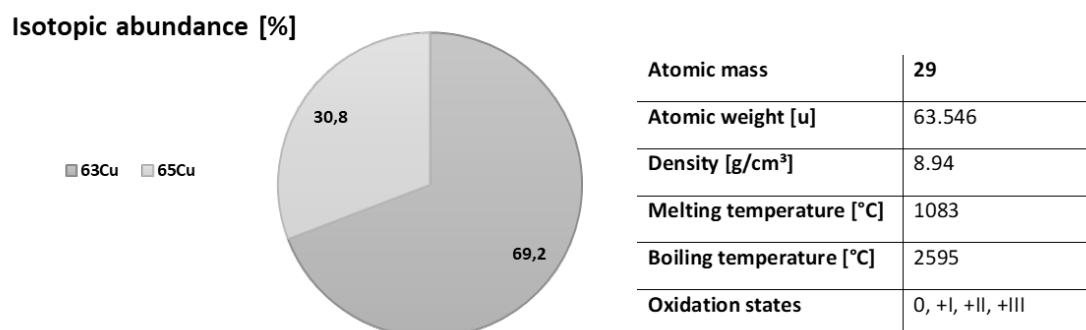
Figure 4. Percentage abundance of natural Cu isotopes and chemical properties of Cu. According to the Commission on Isotopic Abundances and Atomic Weights (CIAAW) from the International Union of Pure and Applied Chemistry (IUPAC).

1.2.2 Natural occurrence and industrial uses

As the 25th most abundant element in the earth's crust, concentrations of Cu range from 25 to 75 mg/kg. High concentrations can be found in igneous rocks (up to 120 mg/kg) and coal (up to 280 mg/kg), while in sedimentary rocks, Cu concentrations are lower (limestone (2 to 10 mg/kg), sandstone (2 to 30 mg/kg), shales (40 to 60 mg/kg)) [132]. Contents in soils vary widely from country to country, with values ranging from 14 to 110 mg/kg [132]. The concentrations of Cu depend on a number of factors, such as the parent material, the physico-chemical properties and exogenous inputs

from industry and agriculture. Anthropogenic sources of Cu release to the environment include industrial and mining operations, incineration processes, domestic sewage, and the use of fertilizers and fungicides [130]. Also contributing to Cu levels in the environment are natural sources such as windblown dust, volcanic activity, and forest fires [130]. In seawater, Cu levels range from 1 to 5 µg/L, while rain and river water contain less Cu with 0.02 to 0.3 µg/L and 0.3 to 3.6 µg/L, respectively [132]. However, in dependence of natural soil erosion and anthropogenic sources concentrations can be higher in rivers and lakes [132]. Atmospheric Cu concentrations range from 5 to 200 ng/cm³, with higher concentrations possible in urban or other polluted areas, such as near non-ferrous metal producing industries [130].

Cu is the 3rd most used metal in the world and is mainly used in its elemental form. A large part of it is utilized in the electrical engineering industry for the production of wires, conductors and generators, but also for the production of water pipes [131]. In addition to the use of the pure metal, Cu compounds are used in agriculture as fungicides and fertilizers [26], in antifouling paints and in animal lifestock as a feed additive [27,130].

1.2.3 Human intake and recommendations

Food and drinking water are the main sources of Cu intake for humans, although the natural Cu content is subject to wide variations [133,134]. Several factors play a role, including the season, soil quality, geographical location, water sources and the use of fertilizers [135,136]. Offal, seafood, cocoa products, some nuts and seeds contain high levels of Cu and are therefore good sources of Cu [130,134]. In addition to food, drinking water can also contribute to the Cu supply. The Cu content in drinking water is subject to strong fluctuations depending on the natural mineral content, the pH value as well as the use of Cu pipes [130]. In Germany, a limit value of 2 mg/L Cu in drinking water has been set [21]. Depending on the Cu content of the diet, the absorption rate can vary between 12% and 65% [137–139]. Absorption is determined by several factors, including protein content, dietary fiber, and presence of divalent cations. In this context, protein-containing foods and the amino acid histidine appear to have a resorption-promoting effect. In contrast, the presence of dietary fiber and high concentrations of zinc (Zn) and iron (Fe) reduce absorption [131].

Generally, the worldwide Cu supply is considered to be adequate for healthy adults [133,140]. Average values for intake vary from 0.9 to 2.1 mg per day in Europe and USA [133,134]. The main contribution to Cu intake comes from cereals and cereal products, but also meat and meat products account for it. Other groups such as starchy roots/tubers (potatoes) and their products, coffee, tea, fish and seafood are also among the important sources of Cu in Europe [133].

According to the German, Austrian and Swiss Societies for Nutrition (D-A-CH), the estimated values for adequate intake range from 1.0 to 1.5 mg Cu per day for adults with correspondingly lower values for children [141]. Calculation was based on the compensation of Cu losses *via* feces and urine. Other organizations have established reference values between 0.9 and 3.5 mg per day for adults. Various markers have been used for the calculation, such as plasma/serum Cu levels, ceruloplasmin (CP) and erythrocyte superoxide dismutase (SOD) activity [133]. These are the most frequently used biomarkers for assessing the Cu status. However, application of those indicators is partly limited, as they can be influenced by various factors such as hormones and inflammatory processes [142]. A new diagnostic biomarker for individual Cu status is the labile Cu fraction, which is not tightly bound to ceruloplasmin and is referred to as exchangeable Cu. It is proposed to be a specific marker for Cu overload in WD [143]. However, further research is needed to establish a robust and sensitive biomarker for Cu status.

1.2.4 Human copper metabolism

Dietary Cu, mostly in the cupric form (Cu^{2+}), is absorbed mainly in the stomach or proximal intestine after being previously reduced to cuprous Cu (Cu^+) by various reductases such as duodenal cytochrome B (DCYTB) or STEAP2 [144–146]. Cellular uptake occurs *via* high affinity copper uptake protein 1 (CTR1), but also CTR2 or divalent metal transporter 1 (DMT1) might contribute to cellular Cu absorption [144,147]. High Cu concentrations in the intestinal lumen induce internalization of CTR1 to endosomes in order to reduce uptake of the element [148]. Within the cell, cuprous ions are directly sequestered by GSH [149] and subsequently bound to metallothioneins (MT) [150,151] or transported to the target organelle *via* specific chaperones to prevent the accumulation of free Cu ions in the cytoplasm [152]. The chaperones include, for instance, the Cu chaperone for superoxide dismutase (CCS) [153], the cytochrome c oxidase copper chaperone 17 (COX17) [154], and the antioxidant 1 copper chaperone (ATOX1) [155]. In the cytosol, CCS is responsible for the activation of SOD1, while COX17 transports Cu to the mitochondria, where it is incorporated into complex IV (cytochrome c oxidase) of the respiratory chain. ATOX1 is responsible for Cu transport to ATP7A or ATP7B, which are located either in the *trans*-Golgi network (TGN) or in the plasma membrane [156]. Export of Cu into the portal system is primarily mediated by ATP7A [157]. In the blood system, Cu is bound to albumin, transcuprein (α2-macroglobulin) or post-hepatic to ceruloplasmin (CP) [146,158]. The main storage organ for Cu is the liver and the regulation of Cu homeostasis is accomplished mainly by absorption and excretion [159,160]. In the liver, biliary excretion and loading of CP with Cu is mediated by ATP7B in dependence of the Cu concentration [161,162]. At physiological Cu concentrations, Cu^+ ions are transported to the TGN, loaded onto CP, and subsequently released into the blood for systemic distribution [163]. In contrast, high Cu concentrations induce translocation of ATP7B to the apical membrane, resulting in

excretion of excess Cu *via* the bile duct [164]. This process is presumably mediated by Cu metabolism domain containing 1 (COMMD1) because mutation in this gene caused a Wilson´s disease (WD)-typical Cu accumulation within the liver in dogs [165].
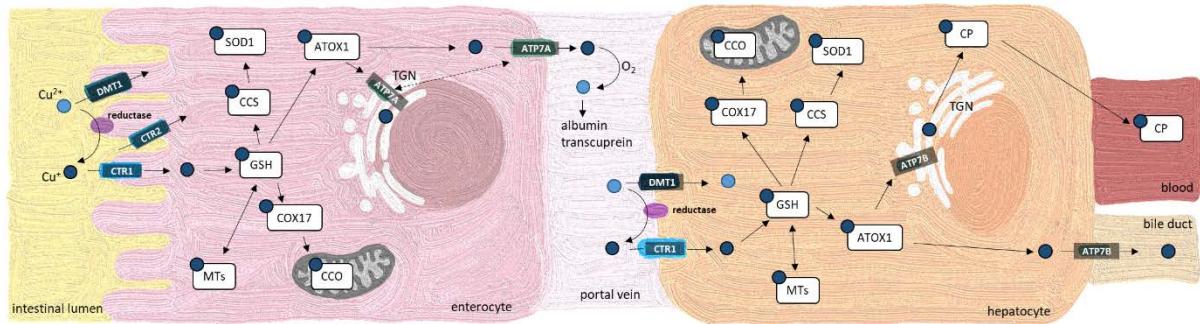
Figure 5. Overview of Cu metabolism in human enterocytes and hepatocytes. In the intestinal lumen, cupric ions (Cu^{2+}) are reduced to Cu^+ prior to uptake into the enterocyte *via* copper uptake protein 1 (CTR1). High Cu concentrations in the intestinal lumen induce an internalization of CTR1 into endosomes to reduce Cu uptake. Other transporters such as CTR2 and the divalent metal transporter 1 (DMT1) can also contribute to cellular Cu uptake. In the cell, cuprous ions are sequestered by GSH and subsequently either stored by binding to metallothioneins (MT) or transferred to specific Cu chaperones for transport to the target organelles. CCS is the Cu chaperone for superoxide dismutase 1 (SOD1), while cytochrome c oxidase chaperone (COX17) transports Cu to the mitochondria and antioxidant 1 copper chaperone (ATOX1) shuttles Cu to the *trans*-Golgi network (TGN) or directly to the exporting ATPase copper transporting alpha (ATP7A in enterocytes or ATP7B in hepatocytes). In dependence of the Cu status of the cells, the transporters can translocate between the TGN and the plasma membrane. In the blood, Cu is loaded to different proteins such as albumin and transcuprein or posthepatic to ceruloplasmin (CP). Figure was modified according to Doguer et al. [148].

1.2.5 Physiological functions and disturbances of copper homeostasis

Cu is an essential trace element whose essentiality was first demonstrated in anemic rats, in which only combined administration of Fe and Cu resulted in an increase in hemoglobin concentration [166,167]. Through its redox activity, Cu acts as a cofactor of various enzymes in reactions that involve single electron transfer between a substrate and molecular oxygen [142]. These enzymes are referred to as cuproenzymes and play an important role in cellular respiration, antioxidant protection, and Fe metabolism, among other functions (summarized in Table 2) [142].

Table 2. Functions of cuproenzymes. For a detailed overview, it is referred to a recent review from Collins et al. [142]

Cuproenzyme (Abbreviation)	Functions
Amine oxidase	deamination of mono- and diamines
Lysyl oxidase (LOX)	crosslinking of collagen fibers
Ceruloplasmin (CP)	ferroxidase, Fe release from storage
Hephaestin (HEPH)	ferroxidase, intestinal Fe transport
Cytochrome c oxidase	ATP production, electron transfer system
Tyrosinase (TYR)	pigmentation, melanin synthesis
Peptidylglycine α-amidating monooxygenase (PAM)	activation of peptide hormones
Superoxide dismutases (SOD)	reduction of superoxide
Dopamine β-hydroxylase (DBH)	activation of catecholamines

Based on a 12-week double-blind study, a no observed adverse effect level (NOAEL) of 10 mg per day and, considering an uncertainty factor, a tolerable upper intake level of 5 mg Cu per day for adults were established [132,164]. While under normal physiological conditions, Cu overload is prevented by increased excretion as part of Cu homeostasis, imbalances in Cu homeostasis can occur in certain genetic diseases, such as Menkes (MNKD) or Wilson´s diseases (WD), which are characterized by mutations in the *ATP7A* and *ATP7B* genes, respectively [161,168].

In X-linked recessive-inherited MNKD, the mutation in the *ATP7A* gene causes a dysfunction of Cu export [168]. This results in an accumulation of Cu in the intestine and, as a consequence, in a systemic Cu deficiency. Patients with MNKD die early in life if untreated and show clinical symptoms such as hypopigmentation of skin and hair, growth retardation, and connective tissue abnormalities [168]. In addition, neurological symptoms occur because the transport of Cu across the blood-brain barrier (BBB) is also affected, resulting in neurodegeneration and demyelination [169]. So far, a cure for the disease does not exist, but progression can be delayed or symptoms alleviated by subcutaneous or parenteral administration of Cu histidine. However, an early diagnosis and the presence of partially functional ATP7A are crucial for the success of the therapy [168].

WD is caused by an autosomal recessive mutation in the *ATP7B* gene [161,170,171] that results in impaired biliary Cu export as well as trafficking to the TGN for incorporation into CP [172]. This causes a massive accumulation of Cu, especially in the liver and brain, resulting in liver damage and neurological defects [173]. Characteristic changes occur in the eyes, the so-called Kayser-Fleischer corneal ring appears as a golden brown to greenish rim [172]. Treatment of the disease is based on complexation, which decreases absorption or bioavailability, or decreased absorption of Cu through Zn supplementation [174–176].

1.3 Relevance of selenium and copper for brain functions

1.3.1 Fundamentals of the blood brain barrier

The tasks of the central nervous system (CNS), consisting of the brain and spinal cord, involve the conversion of stimuli received from the sensory organs, control of motor activity, control of metabolism and maintenance of homeostasis, among others. To ensure the regulation of homeostasis, the brain has developed two sophisticated barrier systems - the blood-brain (BBB) and blood-liquor barrier (BCB). In the following only the BBB will be considered in detail (an overview of the BCB is reviewed elsewhere [177]). To maintain the physiological environment of the brain, the barrier systems are indispensable, and act as a combination of physical (prevention of paracellular transport by tight junctions), metabolic (intracellular and extracellular enzymes for the maintenance of metabolism and an inactivation of neurotoxic substances), and transport barriers (regulated transcellular transport by specific proteins) [178,179]. Dysfunction of the protective barrier systems are associated with various NDs including stroke, Alzheimer's disease (AD), Parkinson's disease (PD), amyotrophic lateral sclerosis (ALS) and brain tumors [180–182]. Highly specialized capillary endothelial cells encircling blood capillaries form the BBB and act as an interface between brain tissue and blood circulation. A number of characteristics account for the unique properties of the brain capillary endothelial cells, including the absence of fenestration, the presence of tight and adherent junctions, low rates of endocytosis and transcytosis [183–185]. Furthermore, in contrast to other endothelial cells, the large number of mitochondria emphasizes the high requirement for ATP-dependent transporters [186]. The cells of the BBB grow in a monolayer and account for 95% of the area between the blood and brain tissue [187]. Endothelial cells together with neurons, non-neuronal cells (astrocytes, microglia and pericytes) and components of the extracellular matrix form a functional whole, the neurovascular unit (Figure 6) [188].

Astrocytes occupy a central position in the brain, mediating the interactions between neurons and the cerebral vasculature [189]. Generally, regulation of CNS homeostasis is one of the most important functions of astroglia. This includes, among other things, the supply of nutrients and energy substrates to neurons, maintenance of molecular homeostasis through ion transport, modulation of synaptic activity through removal and degradation of neurotransmitters, and provision of neurotransmitter precursors [189]. Moreover, end feet of the astrocytes cover up to 99% of the area of the parenchymal microvasculature [190] and contributing to regulation and remodeling of BBB properties as well as neurovascular coupling [191,192]. Embedded between astrocytes and endothelial cells are pericytes, which play an important role in modulation of BBB integrity and permeability, clearance of toxic substances and regulation of cerebral blood flow. Moreover, they are thought to have immune cell properties and stem cell activity [193–196]. Underneath the endothelial cells lies the basal lamina

which is predominantly composed of extracellular matrix proteins such as collagen type IV, laminin and fibronectin [197]. Functions include structural support, cell anchorage, and signal transduction [198]. Neurons are specialized in reception and transmission of nerve impulses and represent the functional unit of the CNS.
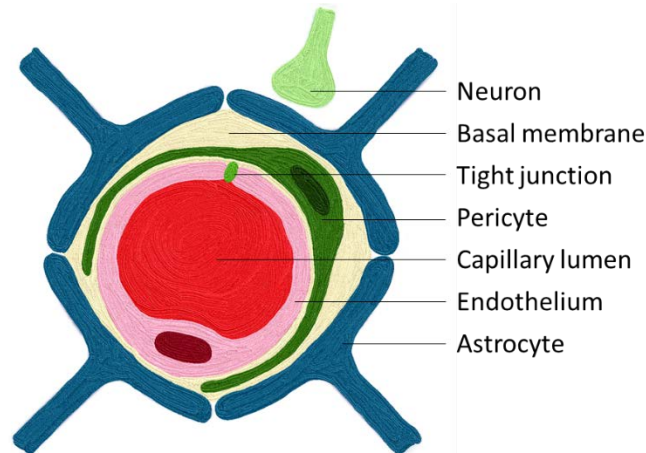
Figure 6. The neurovascular unit. Schematic drawing of the neurovascular unit consisting of endothelial cells, pericytes, neurons and astrocytes. Figure was modified according to Abbott et al. [185]

The BBB represents a tight barrier between the blood system and brain parenchyma. Cell-cell contacts are sealed by tight and adherent junctions, resulting in high transendothelial resistance and low paracellular and transcellular permeability [199]. This is necessary to prevent uncontrolled passage of blood-born substances into the CNS. Moreover, the BBB offers protection against neurotoxic substances (e.g. xenobiotics or endogenous metabolites) by so-called ATP-binding cassette (ABC) transporters [200]. To ensure the supply of required nutrients to the CNS, the BBB has a series of transporters that can shuttle hexoses, amino acids, nucleosides, and ions [199]. Furthermore, receptor-mediated transport and adsorptive-mediated transcytosis also contribute to substrate transfer across the BBB [201].

Even though the BBB provides protection against neurotoxins and harmful substances from outside, endogenous factors can also damage the brain. In particular, oxidative stress is a major threat to the brain. To maintain physiological functions, the brain requires about 20% of the body's total oxygen consumption to cover the high energy demand of neuronal activity [202]. In addition to ATP, by-products such as superoxide anions and hydroxyl radicals are also produced during oxidative respiration [203]. Under physiological conditions, reactive oxygen and nitrogen species (RONS) play an important role in fine-tuning of brain functions *via* redox-sensitive signaling, while uncontrolled production has detrimental consequences. Increased occurrence of RONS in combination with exceeding the antioxidant capacity of the cell causes oxidative stress, which is closely associated with

neurodegeneration [202,204]. Moreover, the brain is particularly vulnerable to oxidative stress due to several factors. As mentioned above, the brain has a high energy turnover, which is ensured by a neuronal accumulation of mitochondria that provide the necessary higher metabolic turnover in the respiratory chain [205]. Moreover, the brain is enriched in polyunsaturated fatty acids [206], which are particularly susceptible to lipid peroxidation, representing another source of oxidative stress [207]. This is further enhanced by a moderate antioxidant capacity. The neuronal concentration of cytosolic GSH is only 50% compared to other organs, which also reduces the activity of GSH-dependent enzymes like GPXs [203,208]. Especially in the context of trace elements, the abundance of redox-active elements such as Fe, Mn, and Cu is increased in the brain. As part of the Fenton or Fenton-like reaction, high concentrations of these transition metals can lead to an increased production of hydroxyl radicals [209]. In addition to the factors described above, there are a variety of other factors that illustrate the brain's susceptibility to oxidative stress, such as the synthesis of neurotransmitters and their autooxidation [202]. These factors can have negative effects on the cells of the brain, especially with regard to post-mitotic non-self-replenishing neurons. Loss of these neurons can inevitably lead to functional decline associated with NDs like AD [210].

1.3.2 Physiological relevance of selenium for brain function

The trace element Se is essential for proper brain function. The brain is one of the organs that are preferentially supplied with it under Se deficiency conditions [43,211]. In Se-deficient fed mice, Se levels in brain and testis were only mildly diminished in contrast to other organs [211,212]. Yet, the levels of Se in the human brain (around 110 ng Se/g wet weight) are relatively low compared to other organs (e.g. liver or kidney with 291 or 771 ng Se/g wet weight, respectively), corresponding to about 2% of the body's total Se content [213,214]. Brain areas of the telencephalon (e.g. the putamen, caudate nucleus) and the cerebellum (cerebellar vermix) are particularly Se-rich under physiological conditions [215].

The physiological functions of Se are mostly exerted *via* the incorporation of the proteinogenic amino acid SeCys into selenoproteins (for details on selenoprotein synthesis see section *1.1.4 – Human selenium metabolism and selenoprotein synthesis*). In humans, impaired expression of selenoproteins is known to cause various syndromes, some of which are associated with neurological abnormalities, pointing to an essential function of these proteins in the brain [216]. In addition, a large proportion of selenoproteins possess antioxidant properties. The change in expression of these proteins during aging has implications for their antioxidative function and the development of NDs [217]. Increased oxidative stress is considered one hallmark of various NDs such as AD [218,219], PD [220,221], ALS [222,223] and multiple sclerosis [224,225].
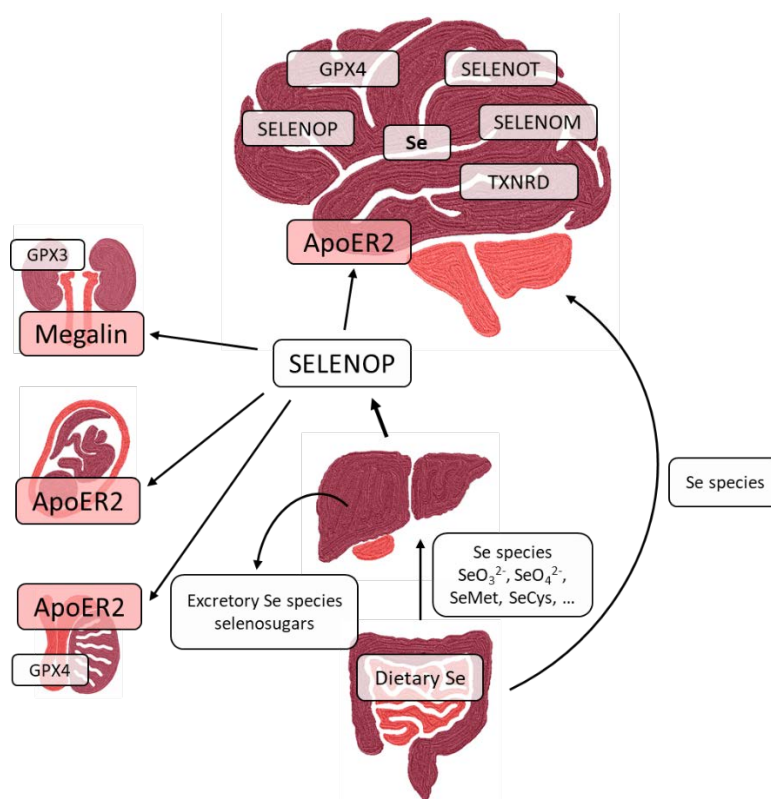
Figure 7. Schematic overview of body Se transport. Dietary Se in the form of various Se species (e.g., SeO_3^{2-}, SeO_4^{2-}, SeMet, SeCys, MeSeCys) is transported to the liver, where selenoprotein biosynthesis occurs. SELENOP formed there is released into the blood for systemic distribution of Se. Excess Se is excreted by the liver in the form of excretory Se species, mainly selenosugars. Systemic SELENOP can be taken up by various receptors (megalin or ApoER2) into the respective organ, where it is then used for further selenoprotein synthesis. In particular, the brain is dependent on an external SELENOP supply, although low-molecular-weight Se species [226] and selenosugars [46] can also be transported *via* the BBB. Figure was modified from [227]. Abbreviations: ApoER2 - Apolipoprotein E receptor 2, GPX – glutathione peroxidase, TXNRD – thioredoxin reductase.

SELENOP plays a unique role, as it is the main supplier of Se to the brain (for systemic Se distribution see Figure 7). In mice with genetic *SelenoP* knockout or its receptor *ApoER2*, reduced brain Se levels were associated with neurological symptoms such as ataxia, seizures and poor motor coordination [121,228,229]. By adding Se to the diet (8 weeks, torula yeast-based diet, 2 mg Se/kg as sodium selenite), brain Se concentrations could be raised to Selenop$^{+/+}$ level [121]. Mice with a liver-specific knockout of the selenoprotein demonstrated decreased plasma Se levels comparable to Selenop$^{-/-}$ mice, but exhibited no neurological symptoms. This indicates that local expression of Selenop is responsible for maintaining Se levels in the brain under Se-deficient conditions [38]. SELENOP expression could be detected in human brain [230] and non-neuronal cells like astrocytes are known to secrete it for further Se distribution in the brain [231,232]. In addition to SELENOP, other Se species are able to cross the BBB and thus contribute to local Se supply [226]. SELENOP not only functions as a Se transporter, but also has an affinity for binding transition metals such as Cu, Zn, and Fe, which is attributed to the presence of two histidine-rich domains [233,234]. On the one hand, the high

reactivity of transition metals is essential for the organism, as they are mainly involved as cofactors of enzymes catalyzing redox reactions. On the other hand, altered homeostasis of these can result in uncontrolled production of reactive species *via* Fenton or Fenton-like reaction and as a consequence in oxidative stress and cellular damage. Thus, transition metals are associated with the development and progression of NDs such as AD and WD [235,236]. *In vitro* studies have shown that SELENOP possibly competes with amyloid-beta and tau-protein with divalent ions. In addition, the formation of tertiary complexes of SELENOP, cations and amyloid-beta or tau-protein reduces their toxicity [234,237]. Furthermore, an increase in *SELENOP* mRNA expression was observed in post-mortem brain tissue from AD patients [238], which was further co-localized with amyloid-beta and neurofibrillary tangles [239]. Additionally, levels were also higher in the choroid plexus and in the cerebrospinal fluid (CSF) of AD patients compared to healthy controls [240]. *SELENOP* expression is increased during aging, which may indicate an increased need for Se [241]. In conclusion, there seems to be an association between the pathological changes and SELENOP; however, further studies are needed to establish a direct relationship because the evidence from post-mortem and *in vitro* studies is limited.

Another important selenoprotein family for brain function are the GPXs with GPX4 being the most widely expressed isoform in the brain. This enzyme is anchored in the membrane, which catalyzes the reduction of complex hydroperoxide lipids [242]. Homozygous knockouts of this selenoprotein were embryonically lethal in mice, highlighting its importance in cell development and maintenance [243]. The relevance for male fertility has already been described in section *1.1.6 – Imbalances of selenium homeostasis*. GPX4 is implicated to protect neurons from the non-apoptotic pathway driven by Fe-mediated production of RONS, called ferroptosis [244]. In mice, neuron-specific knockout of *Gpx4* caused neurodegeneration of hippocampal, cerebral and motor neurons leading to cognitive impairment with deficits in learning and memory function as well as paralysis *via* ferroptotic pathways [245,246].

The TXNRD family is involved in redox regulation, but also a role in neuroprotection has been described [247]. Trxnd1 and Trxnd2 are essential for development, and knockout resulted in retardation of development and growth leading to early embryonic lethality in mice [248,249]. While neural-specific knockout of *Trxnd2* exerts no abnormal brain phenotype, knockout of *Trxnd1* displays symptoms of cerebellar dysfunctions with growth retardation and movement disorders [249,250]. Moreover, neuronal ablation of *Trxnd1* did not cause any abnormalities indicating a role in radial glia development [250]. In a murine model of *Trxnd1* overexpression, the selenoprotein provided neuroprotective effects and decreased damage to neurons after induced brain injury by ischemic conditions [251] or excitotoxin [252].

Knockout of *Selenot* in mice is embryonal lethal, while mice with brain-specific ablation displays severe motor impairments when treated with PD-inducing agents like 1-methyl-4-phenyl-1,2,3,6-tetrahydropyridine (MPTP) [253]. Moreover, treatment with MPTP induced Selenot in the degenerating substantia nigra compacta in wildtype mice, which was consistent with high *SELENOT* expression in caudate putamen tissue of PD patients [253]. Additionally, overexpression of *SELENOT* in a human dopaminergic cell line (SH-SY5Y) protected the cells from oxidative stress after exposure to 1-methyl-4-phenylpyridinium [253]. These data indicate a neuroprotective role of SELENOT of dopaminergic neurons.

In addition to the selenoproteins mentioned, other selenoproteins appear to play a role in brain function; for more information, the reader is referred to recent reviews [254,255].

1.3.3 Importance of copper for brain function

Cu is essential for proper brain function, and both deficiency and excess lead to neurological dysfunction [146,256]. Brain-specific Cu-dependent enzymes such as peptidyl-α-monooxygenase (PAM) and dopamine-β-hydroxylase (DBH) are involved in the synthesis of neuropeptides and neurotransmitters. The Cu content in human serum (993 ± 340 µg/L) is significantly higher than in CSF (21.7 ± 8.5 µg/L), thus the brain barriers restrict the entry of Cu into the brain parenchyma [257]. Main entry route for Cu into the brain parenchyma is through the BBB, while the choroid epithelial cells of the BCB are able to take up Cu from the CSF and regulate homeostasis [258] (Figure 8). CTR1 has been shown to be present on brain capillary endothelial cells and cells of the choroid plexus that form the BBB and BCB, respectively, and is the major transporter for Cu uptake, similar to other cell types [258]. The Cu transporter ATP7A is responsible for Cu export from cells and mutation of the gene, as seen in MNKD patients, or knockout of the transporter in mouse models of MNKD resulted in severe Cu deficiency in the brain [259]. In epithelial cells of the choroid plexus, ATP7B plays an important role in the regulation of Cu homeostasis. In response to elevated Cu, ATP7B translocates from intracellular compartments to the basolateral or blood-facing membrane to increase Cu efflux into the blood. In WD patients, ATP7B function is disturbed and as a consequence, Cu accumulates within the brain [256,260].

Cu concentrations in the human brains range around 3.1 to 5.1 µg/g wet weight, and generally, gray matter contains more Cu than white matter [261,262]. Moreover, glial cells seem to contain higher Cu concentrations than neuronal cells, especially in the subventricular zone where mainly astrocytes are located [256]. These cells are able to store Cu and regulate the distribution within the brain parenchyma [263]. Other Cu-rich brain areas include the locus coeruleus (LC) and substantia nigra (SN),

both of which contain catecholamus neurons. The dentate nucleus, basal ganglia, hippocampus, and cerebellum may also be rich in Cu [256,264].

NDs like AD and PD are associated with a disturbed Cu homeostasis resulting in a misdistribution of the trace element [265]. In brains of PD patients, Cu levels were decreased in the SN while it accumulates in Lewis bodies by forming a complex with α-synuclin [266]. Similar misdistributions have been observed in brains of AD patients, where Cu accumulates in the senile plaques in association with amyloid-β and neurofibrillary tangles while other brain areas were depleted of Cu [267].
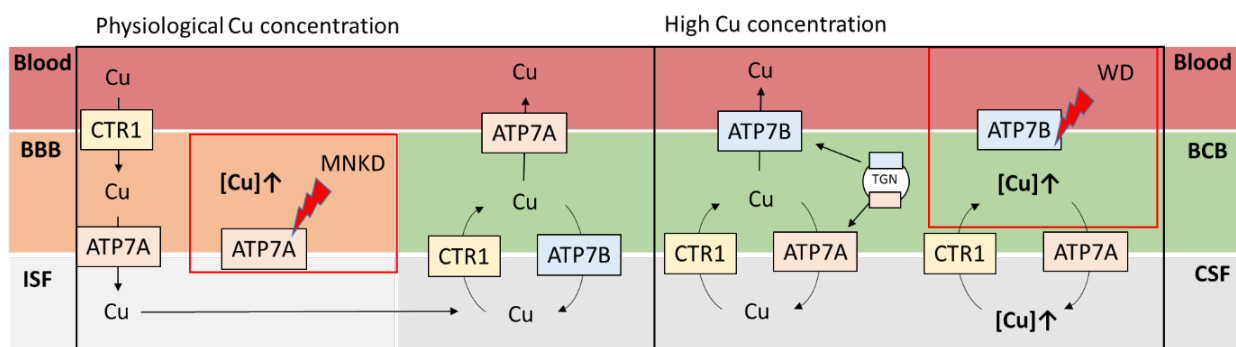
Figure 8. Entry routes for Cu into the brain. Cu transport across the endothelial cells of the blood-brain barrier occurs *via* CTR1 (high affinity copper uptake protein 1) into the cell and *via* ATP7A (ATPase copper transporting alpha) out of the cell into the interstitial fluid (ISF) of the brain. A mutation in the ATP7A gene, as occurs in Menkes disease (MNKD), leads to a dysfunction of the transporter, resulting in Cu accumulation in the endothelial cells of the BBB. Regulation of Cu homeostasis occurs mainly through the blood-cerebrospinal fluid barrier (BCB). Copper enters the cerebrospinal fluid (CSF) *via* diffusion and is taken up by the endothelial cells of the BCB *via* the CTR1. At physiological Cu concentrations, it can be transported either back into the CSF by ATP7B or into the blood *via* ATP7A. High Cu concentrations cause translocation of the transporters responsible for export from the *trans*-Golgi network (TGN). Thus, ATP7B is translocated to the apical and ATP7A to the basolateral membrane of BCB endothelial cells. In Wilson´s disease (WD), dysfunctional ATP7B and leads to accumulation of Cu in the brain. Figure was modified according to [262,268].
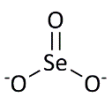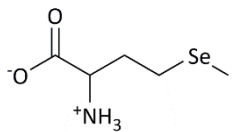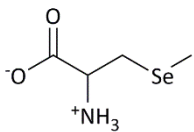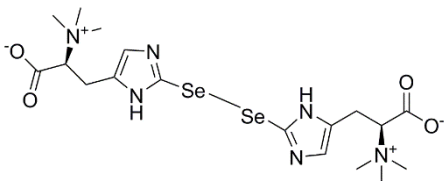
1.4 Objective of the thesis

Essential trace elements such as Se and Cu are vital components of enzymes and lead to impaired health when deficient. Furthermore, both trace elements are involved in the regulation of the redox homeostasis of the organism. This arises, on the one hand, because they are components of antioxidant enzyme systems and, on the other hand, because at high intracellular concentrations they can themselves contribute to the induction of oxidative stress and consequently to cell damage.

The brain represents a particularly sensitive organ to alterations in trace element homeostasis. Neurological disorders can occur in both deficiency and excess. In addition to the BCB, the BBB provides, among other things, a stable homeostasis of the internal environment of the brain. The transfer of trace elements mostly takes place *via* the BBB. Therefore, the present thesis aimed to investigate the transfer of Se and Cu across the BBB, alone and in combination (Chapter 2 to 4). Furthermore, this work addresses the effects of Cu overload in different cells of the brain, as an accumulation of Cu can be observed in different NDs such as WD and AD [256,267]. Proposed mode of action of Cu induced toxicity is thought to be *via* induction of oxidative stress. For this reason, effect of an overload of Cu was focusing especially on oxidative stress related endpoints (Chapter 5). With respect to oxidative stress, selenoproteins with antioxidative properties may play an important role in the defense of Cu induced cellular stress. Therefore, chapter 6 aimed to characterize the influence of prior Se supplementation on Cu overload in human astrocytes and neurons. Different endpoints related to cytotoxicity, Cu bioavailability, oxidative stress markers, genomic stability and cellular Se status were measured.

Se mediated effects are known to be dependent on the chemical form and Table 3 provides an overview of the Se species used in this thesis, which are either common natural dietary Se sources, and/or frequently used in food supplements.

Table 3. Se species which are of relevance for the present thesis. *Selenoneine is depicted in its oxidized, dimeric form, which is reported to be stable at cold to room temperatures* [269]. *Selenoneine (dimeric form) was isolated and purified by Kuehnelt and colleagues* [270].

| Selenite | Selenomethionine (SeMet) | Methylselenocysteine (MeSeCys) | Selenoneine* (SeN) |

Following research questions and objectives are the subject of this thesis:

- Transfer of SeN and reference Se species across an *in vitro* BBB model (chapter 2)
- Effects of Cu on an *in vitro* BBB model and protective effects of chelating agents (chapter 3)
- Influence of Se supplementation on Cu transfer across the *in vitro* BBB (chapter 4)
- Characterization of the effects of Cu on astrocytes with focus on oxidative stress (chapter 5)
- Effects of Cu on human neuronal cell lines and modulation by Se supplementation (chapter 6)

On the one hand, this thesis provides insights into the transfer of the trace elements Se and Cu across the BBB *in vitro* model. On the other hand, Cu overload, which is associated with various NDs, is characterized in human astrocytes. These cells are known to serve as buffer by efficiently storing Cu and subsequently protecting other cells of the brain such as neurons. Furthermore, combinational approaches aimed to shed light into rarely investigated trace element interactions. *In vivo*, changes in trace element homeostasis do not occur in isolation, but in combinations highlighting the relevance of further investigations of trace element interactions.

1.5   Structure of the thesis

To achieve the first objectives of this thesis, the well-established porcine *in vitro* model of the BBB was used to study the transfer of the trace elements Se and Cu as wells as the combination of both elements. Besides the transfer of the two trace elements into the brain, the impact of Cu overload and also in combination with additional Se supplementation was be investigated using human astrocytic and differentiated neuronal cell lines.

Selenoneine (SeN) (2-selenyl-Nα,Nα,Nα-trimethyl-L-histidine), a recently discovered Se species with similar properties to its isolog ergothioneine, is present in high amounts in edible fish [271]. A previous work demonstrated transfer across the intestinal barrier using Caco-2 cells and partial metabolization of SeN by these cells [272]. Therefore, in **Chapter 2**[1] (*Capabilities of Selenoneine to Cross the In Vitro Blood-Brain Barrier Model*), the transfer, cytotoxicity as well as metabolization of SeN was investigated applying the well-established *in vitro* model of the BBB. Primary porcine brain capillary endothelial cells (PBCECs) were isolated from freshly slaughtered pigs (for the isolation protocol see Appendix A: *The In vitro blood-brain barrier*). PBCECs are representative cells of the BBB and are tightly connected to each other *via* tight junction, preventing paracellular transfer of substances. SeN was synthezised from genetically modified fission yeast Schizosaccharomyces pombe, isolated, purified and kindly provided by Ao.-Prof. Dr. Doris Kuehnelt in the working group of Univ.-Prof. Dr. Kevin A. Francesconi from the University of Graz [270]. At first, cytotoxicity of SeN and the reference Se species selenite and MeSeCys was investigated using the neutral red and CCK8 assay. Subsequently, non-cytotoxic concentrations (1 and 10 µM) of the Se species were used for transfer experiments. Additionally, barrier integrity was monitored *via* impedance-based spectroscopy using the CellZscope® during the experiment (Appendix B: *Monitoring by impedance spectroscopy*). Se concentrations of the medium and cell lysate samples were quantified *via* ICP-MS/MS. Design and implementation of transfer experiments, measurement of Se contents and cytotoxicity were performed by Dr. Evgenii Drobyshev and myself in equal proportions. Ao.-Prof. Dr. Doris Kuehnelt from the univisity of Graz performed the speciation analysis of the cell lysates and medium samples. This study provides information about the transfer across the BBB and metabolisation by the barrier-forming cells of the newly identified Se specie SeN.

Chapter **3**[2] (*Bis-choline tetrathiomolybdate prevents copper-induced blood–brain barrier damage*) focuses on Cu transfer across the in vitro BBB and Cu-induced toxicity to BBB-forming cells. Furthermore, the efficacy of a newly developed chelating agent for the treatment of WD was investigated. Due to a mutation in the *ATP7B* gene [161,170,171], Cu accumulation occurs in the liver and later also in the brain, causing neurological symptoms [273–276]. Common therapeutic approach is the complexation of Cu by using chelating agents. However, neurological symptoms may worsen with the administration of chelators such as DPA [277–281]. A tetrathiomolybdate, ALXN1840, is currently under development to minimize these side effects [282–284].

In this collaboration with the Technical University of Munich, the effect of combined administration of ALXN1840 upon Cu exposure on the BBB was investigated. This work includes the entire manuscript, but only the experiments I performed using the *in vitro* model of BBB are discussed. In the first step, cytotoxic effects of Cu in combination with DPA or ALX1840 were conducted using the CCK8 and neutral red assay. Subsequently, Cu concentrations of 250 µM were choosen for transfer experiments. Barrier integrity was continuously monitored throughout the experiment using the CellZscope®. Subsequently, the Cu contents in medium samples taken during the experiment were quantified by ICP-MS/MS. The filters containing the PBCECs were used for immunohistochemical visualization of the tight junctions. Some filters were also sent to the TU Munich to the research group of Prof. Dr. Zischka for electron microscopy. Dr. Sabine Borchard and I designed the experimental setup. I conducted most of the transfer experiments, the Cu measurement, cytotoxicity assays in the PBCECs and immunohistochemistry of the tight junctions. Accordingly, this study provides information on the Cu transfer into the brain, and the impact of Cu on the cells of the BBB as well as the protective effects of the novel chelator ALXN1840.

Human studies could identify an association between Se and the protection against cognitive decline [285]. Moreover, Se levels in brains were shown to be lower in AD patients compared to healthy controls [286]. Thus, these data suggest a possible protective role of an adequate Se supply with respect to the development of NDs. In contrast, Cu accumulation in specific brain areas is associated with the development and progression of NDs such as AD [267]. Against the background of an opposite behavior of the two trace elements, the investigation of a possible interaction is of high relevance. Therefore, chapter **4**[3] (*Se supplementation to an in vitro blood-brain barrier does not affect Cu transfer into the brain*) provides a combined approach between the two trace elements Se and Cu in the *in vitro* model of the BBB.

Cultivation protocol of the PBCECs were adapted to ensure adequate Se supplementation of the cells. This incubation protocol provided sufficient time for the incorporation of Se into selenoproteins and allow for adjustments of the antioxidant defense system and metabolism. Development of the protocol was done together with Prof. Dr. Schwerdtle. For transfer experiments, a physiologically relevant (15 µM) and a supraphysiological (50 µM) Cu concentration were chosen. During the experiment, the barrier integrity was monitored by impedance spectroscopy using the CellZscope®. Subsequently, both Se and Cu concentrations were quantified in medium samples and cell lysates by ICP-MS/MS. Additionally, the basolateral (brain side) medium samples were used to quantify content of SELENOP by affinity chromatographic separation followed by ICP-MS/MS. The conception, execution of the experiments and writing the manuscirpt was done by myself under the supervision of Prof. Dr. Schwerdtle.

In the last two chapters brain cell lines were applied to study the impact of excess Cu of the cells within the brain. Especially dyshomeostasis of Cu is associated with serveral NDs such as AD and WD, causing Cu accumulation in certain brain areas [265]. High concentrations of redox-active Cu can increase the formation of RONS *via* Fenton-like reactions and consequently causing oxidative stress. Therefore, chapter **5**[4] (*Characterizing effects of excess copper levels in a human astrocytic cell line with focus on oxidative stress markers*) includes studies in human astrocytes aiming to shed light into the toxic mechanism of Cu with special focus on oxidative stress.

Dr. Barbara Witt conducted mechanistic studies and established a microscopic approach to specifically visualize ROS production in mitochondria. Additionally, Dr. Michael Stiboller performed analysis and quantification of target elements (Ca, Fe, Mg, Mn, Cu and Zn). I performed cytotoxicity tests and measurement of mitochondrial membrane potential together with Dr. Barbara Witt. Furthermore, I carried out essential preparatory work in the cell culture laboratory. In summary, this study provides data on the toxic mode of action with regard to oxidative stress of Cu in human astrocytes. Additionally, a first attempt was made to characterize the interaction between multiple elements.

Chapter **6**[5] (*Selenium homeostasis in human brain cells: Effects of copper (II) and Se species*) follows on from the studies in the previous chapter. Here, the focus lies on the interaction between the two trace elements Se and Cu. Furthermore, the protective potential of Se supplementation on various markers in human astrocytes and neurons was investigated. The cultivation conditions were adjusted for optimal Se supply to the cells. Subsequently, the cells were enriched with two different Se species (selenite and SeMet) already during cultivation to enable the incorporation of Se into selenoproteins, followed by treatment with increasing $CuSO_4$ concentrations for 48 h. At first, a viability study was conducted to screen different cytotoxicity endpoints for Cu toxicity. Subsequently, cellular concentrations of Cu and Se were quantified using ICP-MS/MS. To further characterize the Se status of the cells, GPX activity using a photospectroscopic assay was measured. Additionally, an analytical method to quantify SELENOP was established by Dr. Johannes Kopp, and I performed the measurement of medium samples and cell lysates. To investigate the protective potential of Se against Cu-induced toxicity, alkaline and Fpg-modified comet assay was performed in both cell lines. Furthermore, a gene screening was conducted in astrocytes to assess the effects of Cu alone and in combination with Se on genes involved in DNA repair, antioxidative defense and Se status. Selection of the appropriate genes as well as design of the primers was performed by me under supervision of Dr. Fransiska Ebert. Additionally, generation of RONS and the GSH/GSSG ratio were determined using carboxy-DCFH-DA and DTNB-based colorimetric assay, respectively. In neurons, the effects of Cu with prior Se supplementation on the neurite network were assessed by staining of tubulin followed by microscopic evaluation. The study design was planned under the direction of Prof. Dr. Tanja Schwerdtle. I performed the experiments, did the analysis, and wrote the manuscript. The presented study sheds light on the interaction between Cu and Se, especially in the context of an impact of Cu on Se homeostasis.

Chapter **7** concludes by discussing the overall outcomes of the studies conducted (chapters 2 - 5) and places the results in the context of the relevant literature. The appendix contains additional content related to the applied systems.

---

2.   CAPABILITIES OF SELENONEINE TO CROSS THE IN VITRO BLOOD-BRAIN BARRIER MODEL

2.1   Graphical abstract
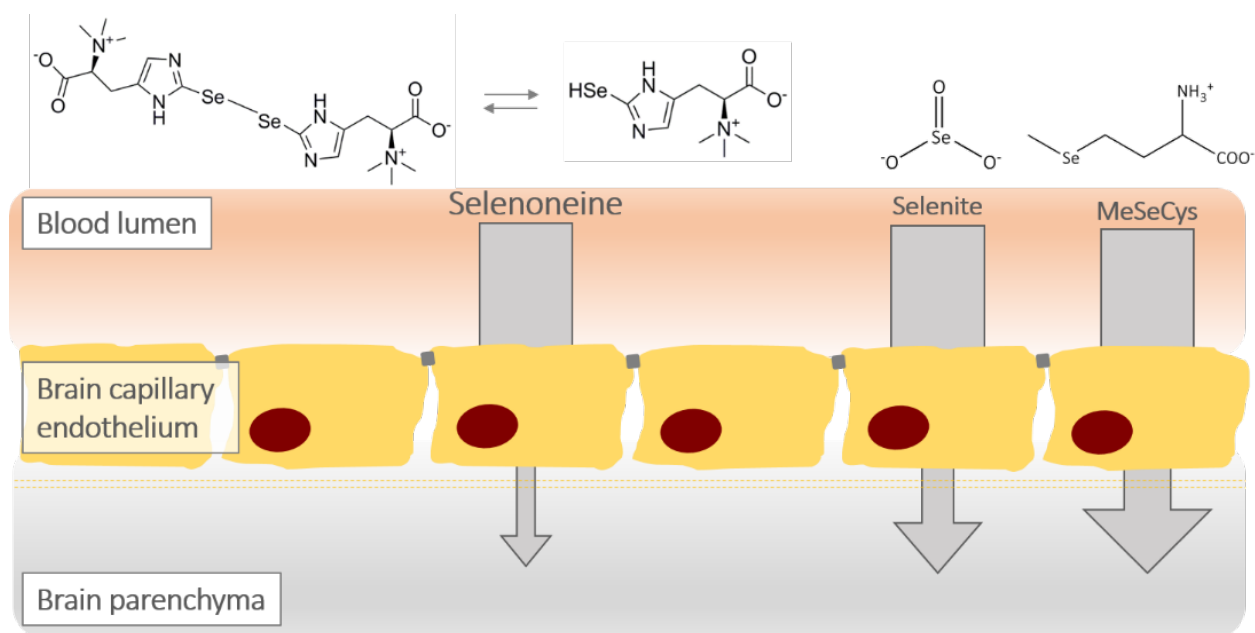
2.2   Abstract

The naturally occurring selenoneine (SeN), the selenium analogue of the sulfur-containing antioxidant ergothioneine, can be found in high abundance in several marine fish species. However, data on biological properties of SeN and its relevance for human health is still scarce. This study aims to investigate the transfer and presystemic metabolism of SeN in a well-established *in vitro* model of the blood-brain barrier (BBB). Therefore, the SeN and the reference Se species selenite and Se-methylselenocysteine (MeSeCys) were applied to primary porcine endothelial cells (PBCECs). Se content of culture media and cell lysates were measured *via* ICP-MS-MS. Speciation analysis was conducted by HPLC-ICP-MS. Barrier integrity was shown to be unaffected during transfer experiments. SeN demonstrated the lowest transfer rates and permeability coefficient (6.7 x 10-7 cm s-1) in comparison to selenite and MeSeCys. No side-directed accumulation was observed after both-sided application of SeN. However, concentration dependent transfer of SeN indicate possible presence of transporters on the both sides of the barrier. Speciation analysis demonstrated no methylation of SeN by the PBCECs. Several derivatives of SeN detected in the media of the BBB model were also found in cell free media containing SeN and hence not considered to be true metabolites of the PBCEC cells. Concluding, SeN is likely to have a slow transfer rate to the brain and not being metabolized by the brain endothelial cells. Since this study demonstrates, that SeN may reach the brain tissue, further studies are needed to investigate possible health-promoting effects of SeN in humans.

2.3   Introduction

Selenium (Se) is an essential trace element, which attracted high attention in the field of nutritional science due to the fundamental importance for human health [1–3]. Se is necessary for the normal functioning of almost all living organisms. In humans, Se manifests its functions by incorporation as the amino acid selenocysteine into selenoproteins. These selenoproteins represent a broad variety of enzymes in mammals and are necessary for proper function of antioxidant, immune and thyroid hormone system [4,5]. The importance of Se is particularly evident in the brain, since Se deficiency can cause irreversible damage to neuronal tissue [6]. Moreover, it was shown in mice that brain Se homeostasis underlies a strictly regulated hierarchy, which protects the brain from Se depletion at the expense of other tissues in time of Se deficiency [7,8].

Exposure to Se occurs mainly *via* diet in form of different Se species in plant and animal-derived food. In addition to that, Se is commonly used in dietary supplements [1]. Beside its physiological importance, Se can also induce toxic effects depending on the chemical structure as well as intake level [9,10]. The highly Se species-dependent impact on human health is characterized by differing bioavailability, metabolism and toxicity [6,11]. More precisely, some Se species are discussed to have potential neuroprotective effects [12]. In this light, a comprehensive investigation of Se species, which

can be found in human diet, is needed to gain insight of the possible health-promoting effects. The naturally occurring Se species selenoneine (2-selenyl-Nα,Nα,Nα-trimethyl-L-histidine, SeN), was identified in blood and other tissues of the bluefin tuna (Thunnus thynnus) [13]. Since its discovery in 2010, SeN has attracted considerable attention not only due to its high abundance in edible fish [13–15] but also as an isologue of the antioxidant ergothioneine (ET) [16]. Therefore, similar properties have been proposed for SeN, but to date there are limited data concerning the properties of SeN. In comparison to ET, SeN demonstrated higher radical-scavenging activity against 1,1-diphenyl-2-picrylhydrazyl [13]. Furthermore, data suggest a potential role in methyl mercury detoxification in zebrafish embryos [17] and dolphin liver [18]. In addition, SeN demonstrated a protective effect against iron-mediated auto-oxidation in erythrocytes under hypoxic conditions [19] and against tumor progression in two types of colorectal cancer models in mice [20]. The limitation of these pilot studies is the use of SeN-enriched fish extracts due to the limited availability of pure species in sufficient quantity. However, a recent study with synthetic SeN reported higher stability of SeN under hydrogen peroxide treatment [21]. Moreover, the intermediate seleninic acid was shown to be rapidly converted back to SeN by glutathione under physiological conditions, thus promoting the quenching of peroxide radicals [21]. In contrast to other naturally occurring Se species like selenite or Se-methylselenocysteine (MeSeCys), there are no data on the usability of SeN as a Se source for the selenoproteome.

Recently, the specific transport of SeN across the intestinal barrier has been assessed using the Caco-2 intestinal barrier model system [22]. Moreover, SeN was highly bioavailable to the cells and the metabolite Se-methylselenoneine (MeSeN) was detected. These findings are consistent with previously reported data on the detection of SeN in human blood [23] and its metabolite MeSeN in blood and urine [24,25]. However, to date there are no data on the transport of SeN to the nervous system. In hindsight to potential neuroprotective effects of SeN, it is of importance to investigate the transport to the brain. The SeN isologue ET has been detected in the brain raising the question of possible transfer of SeN across the blood-brain barrier (BBB) [26].

Considering the nutritional relevance of SeN and the still unknown effects on human health, further characterization of SeN is essential. Therefore, a well-established *in vitro* BBB model system was applied by utilizing primary porcine brain endothelial cells (PBCECs). In the current study, it has been investigated how SeN affected the BBB in comparison to selenite and MeSeCys with special focus on the integrity of the BBB and transfer across the model system. Furthermore, this work provides data on cellular bioavailability as well as pre-systemic metabolism of SeN in PBCECs.

2.4   Materials and Methods

2.4.1   Chemicals and Reagents

Fetal calf serum (FCS), Earle's media 199, Ham's F12 media, L-glutamine, and gentamycin were purchased from Biochrom GmbH (Berlin, Germany). Neutral red powder was supplied by Carl Roth GmbH + Co. KG (Karlsruhe, Germany) and (2-(2-methoxy-4-nitrophenyl)-3-(4-nitrophenyl)-5-(2,4-disulfophenyl)-2H-tetrazolium sodium salt (WST-8) by Dojindo EU GmbH (Munich, Germany). Sodium selenite pentahydrate ($Na_2SeO_3 \cdot 5H_2O$, ≥ 99%, Lot # BCBJ3980V) was obtained from Sigma Aldrich Chemie GmbH (Munich, Germany). Se (Methyl)seleno-L-cysteine (MeSeCys, > 98%, Lot # GR159180-9) was obtained from Abcam (Cambridge, UK). Selenoneine (SeN) with a Se purity of ≥ 98% was isolated from genetically modified fission yeast Schizosaccharomyces pombe at the University of Graz [27]. Isotopically enriched ^{77}Se (97.20 ± 0.20%) was purchased from Eurisotop SAS (Saarbrücken, Germany). All other chemicals not stated were purchased from Sigma Aldrich Chemie GmbH (Munich, Germany) or Roth GmbH + Co. KG (Karlsruhe, Germany).

For Se speciation analysis analytical grade chemicals were used throughout. Ammonium formate (≥ 95%), formic acid (≥ 98%, p.a.), tris-(2-carboxyethyl)phosphine hydrochloride (TCEP, > 98%, for biochemistry) and ammonia solution (≥ 25%, p.a.) were obtained from Carl Roth GmbH + Co. KG. Malonic acid (99%) and methanol (HPLC gradient grade) were purchased from Sigma-Aldrich and VWR International (Fontenay-sous-Bois, France), respectively. Sodium selenite was purchased from Merck, sodium selenate and D,L-selenomethionine (> 99%) were obtained from Fluka (Buchs, St. Gallen, Switzerland), and MeSeCys was purchased from Sigma-Aldrich.

2.4.2   Cell Culture

The *in vitro* model of the BBB has already been described in detail and successfully applied in characterization of the transfer of arsenic-containing hydrocarbons [28], organic and inorganic mercury species [29], mangenese [30] as well as different other compounds [31,32]. Brains of freshly slaughtered pigs were kindly provided by a local slaughterhouse (Görzke, Brandenburg, Germany).

Primary porcine brain capillary endothelial cells were isolated and cultivated according to published protocol [33]. For experiments, cryopreserved cells were thawed quickly at 37 °C and seeded (250,000 cells cm^{-2}) on rat tail collagen-coated Transwell® microporous polycarbonate membrane inserts (1.12 cm2, 0.4 µm pore size; Corning, Wiesbaden, Germany) or on rat tail collagen-coated 96-well plates (TPP, Trasadingen, Switzerland) as previously described [28]. Earle's Media 199 supplemented with 10% FCS, 50 U mL-1 penicillin, 50 µg mL-1 streptomycin, 100 µg mL-1 gentamycin and 0.7 mM L-glutamine was used for cultivation at cell culture conditions (37 °C, 5% CO2, 100% humidity). After 48 hours of proliferation medium were changed to serum-free Ham's F12 media supplemented with 50

U mL-1 penicillin, 50 µg mL-1 streptomycin, 100 µg mL-1 gentamycin, 4.1 mM L-glutamine and 550 nM hydrocortisone to start cell differentiation [34]. After additional 48 hours, cells were ready for following experiments.

2.4.3 Dosage Information and Administration

Stock solutions of the Se species (10 – 100 mM) were prepared and diluted in purified water. Aliquots of SeN were stored at -80 °C, while solutions of sodium selenite and MeSeCys were prepared freshly before each experiment. For cytotoxicity testing, cells were incubated with concentrations ranging from 10 – 100 µM of each Se species for 48 hours, respectively. For transfer studies, 1 µM or 10 µM of Se species were applied in the apical (blood-side) compartment for 72 hours. Basal Se concentration was 3.38 µg Se L-1 in the serum-containing medium and 0.127 µg Se L-1 in the serum-free medium, which were used during transfer studies.

2.4.4 Cytotoxicity Testing

To assess the cytotoxic effects of the Se species neutral red uptake and dehydrogenase activity (cell counting kit-8, CCK8) assays were conducted as viability markers. Following treatment of confluent PBCECs with the Se species, WST-8 solution was added to the cell culture media. Cellular dehydrogenases mediate the reduction of tetrazolium salt to an orange formazan dye and the change in absorbance correlates with the dehydrogenase activity [35]. Absorbance was measured with an Infinite 200 Pro microplate reader (Tecan Group Ltd., Männedorf, Switzerland) at 470 nm.

Following CCK8 assay, cell culture media was gently removed and replaced by media treated with neutral red (200 µg neutral red mL-1). The dye accumulates in intact lysosomes through binding to anionic residues of the lysosomal membrane [36]. After 3 hours of staining the cells were washed and fixed with 0.5% formaldehyde (v/v) in phosphate buffered saline (PBS). After extraction of the dye by acidified ethanolic solution in PBS, the absorbance was measured with an Infinite 200 Pro microplate reader at a wavelength of 540 nm.

2.4.5 Evaluation of Barrier Integrity

The PBCECs grow as a monolayer on the Transwell® inserts resulting in two compartments, the apical (blood-facing) and basolateral (brain parenchyma) compartment. Se species were applied to the apical compartment in 1 or 10 µM concentrations for 72 hours. Transendothelial electrical resistance (TEER) and capacitance of PBCEC monolayer were continuously monitored during the transfer experiments using the CellZscope® (nanoAnalytics, Münster, Germany). The TEER values are proportional to the barrier integrity and capacitance correlates to the plasma membrane surface, providing additional

information about cell viability. Measurements were conducted every 90 minutes. For the PBCECs barrier, starting TEER values were in the range from 674 to 741 $\Omega \cdot cm^2$ and capacitance in range from $5.07 \times 10\text{-}7$ to $5.70 \times 10\text{-}7$ $\mu F/cm^2$. Obtained TEER and capacitance values were normalized to the starting values of each experiment.

2.4.6   Total Selenium Quantification

Total Se content in media and cell lysates was quantified using triple quadrupole Agilent 8800 inductively-coupled plasma mass spectrometer (ICP-MS/MS) with standard nickel cones, concentric glass nebulizer and Peltier cooled (2 °C) Scott spray chamber. For the Se quantification an established isotope dilution method (IDA-ICP-MS) [37] was applied. Media samples were taken after 0, 6, 24, 48 and 72 hours of incubation from apical and basolateral compartments. Media samples were diluted with nitric acid and 77Se isotope to obtain solutions with a final concentration of 3 µg 77Se L-1 and 2% (v/v) nitric acid. The Transwell® membranes with the PBCECs were cut out and washed with PBS. Cells were lysed using RIPA buffer (10 mM TRIS, 150 mM NaCl, 1 mM EDTA, 1% v/v Triton X-100, 1% v/v sodium deoxycholate, 0.1% v/v SDS) for 15 minutes at 4 °C. Cell lysates were centrifuged (10,000 x g, 20 min, 4 °C), diluted with nitric acid and 77Se spike as mentioned above. Before measurements, 3% (v/v) of isopropanol was mixed to all samples for signal enhancement. Operation parameters were optimized for Se detection. Following masses were monitored: $^{80}Se^+ \rightarrow {}^{80}Se^{16}O^+$ and $^{77}Se^+ \rightarrow {}^{77}Se^{16}O^+$. Protein content of the cell lysates was quantified *via* Bradford assay (Bio-Rad, Munich, Germany) following manufacturer's instructions.

2.4.7   Speciation Analysis

For Se speciation analysis, media and cell lysates from transfer experiments (incubation with 10 µM of the respective selenium species) were shipped to Graz on dry ice, and stored at -80 °C until analysis. Before analysis samples were thawed and centrifuged (21,000 x g, 10 min, 4 °C). The centrifuged samples were either diluted with MilliQ (18.2 MΩ*cm) water or directly subjected to HPLC-ICP-MS analysis.

Quantitative determination of Se species was performed with an Agilent 1100 HPLC system (Agilent, Waldbronn, Germany) including a degasser (G1379A), a binary pump (G1312A), a thermostated autosampler (G1329A, G1330A) and a thermostated column compartment (G1316A). Media and cell lysate samples treated with SeN were analyzed by reversed-phase-HPLC with and without 0.1 mM TCEP (condition I, Table S1, Supporting Information), whereas samples treated with MeSeCys were analyzed without TCEP in the mobile phase (condition I, Table S2, Supporting Information). Samples exposed to selenite were analyzed by anion-exchange chromatography (condition II, Table S1, Supporting Information). The HPLC system was connected *via* PEEK capillary tubing (i.d. 0.125 mm) to

an Agilent 7900 ICP-MS equipped with a Micro Mist nebulizer and a Scott-type spray chamber. The ICP-MS was operated in H2-reaction mode (H2 flow rate: 3.5 mL min-1) and selenium signal enhancement was achieved by using 1% CO2 in Ar as optional gas at a flow rate of 12% of the carrier gas flow. The signals at m/z 77, 78, 80, and 82 were monitored and m/z 78 was used for quantification against aqueous standard solutions of selenite (for samples treated with selenite), as well as MeSeCys and selenomethionine (for samples treated with MeSeCys and SeN).

Unknown Se species in the media incubated with SeN were identified by HPLC-ESI-Orbitrap-MS under chromatographic condition I without TCEP in the mobile phase (Table S1, Supporting Information) using a Dionex Ultimate 3000 HPLC system (ThermoFisher Scientific, Waltham, USA) consisting of a Rapid Separation (RS) pump, an RS autosampler and an RS column compartment coupled to a Q-Exactive Orbitrap Mass Spectrometer (ThermoFisher Scientific) equipped with a heated electrospray ionization (HESI-II) source. The following source settings were used to operate the electrospray ionization source in positive mode: gas temperature 350 °C, gas flow rates 65 (sheath) and 20 (aux) instrument units, spray voltage 3500 V and capillary temperature 300 °C. The resolution was 70,000 (full width at half maximum, FWHM) for full scan ranges of m/z 150 to 370 and m/z 350 to 1,000. For the automatic gain control (AGC) target and the maximum injection time (IT) 3 x 106 and 100 ms were used, respectively. Further structural information on precursor ions was gained by data dependent MS/MS (ddMS/MS), which was performed with stepped collision energies of 10, 20, and 30 instrument units. MS/MS settings were the following: resolution 17,500 FWHM, maximum IT 50 ms, AGC target 1 x 105 and isolation window 8 Thomson (mass/charge).

2.4.8 Statistics

Presented results were obtained with at least three independent PBCEC stocks. The transfer studies were conducted in duplicates. For cytotoxicity tests four replicates were taken for each concentration point. GraphPad Prism 8.0.1 (GraphPad Software Inc.) was used for statistical analysis. Results are presented as mean + SD. Data were analyzed using one-way ANOVA followed by Dunnett's multiple comparison post hoc tests. Significance levels are: $*P < 0.05$, $** P < 0.01$, and $*** P < 0.001$.

2.5 Results and Discussion

The naturally occurring Se species selenoneine, which is an isologue of the antioxidant ergothioneine, was first identified in blood and tissue of bluefin tuna [13]. Due to its high abundance in fish [13–15], SeN is of nutritional relevance, but comprehensive investigations of the physiological role in the human metabolism are still lacking. Taking into consideration, that SeN might be transferred to the brain, there could be a possible protective or antioxidant effect of SeN on the nervous system. In addition to that, to date it is still unclear if SeN can be utilized as a Se source for the selenoproteome.

In the current study cytotoxicity, transfer and bioavailability of SeN were assessed in comparison to the reference Se species selenite and MeSeCys using the PBCECs BBB model. Additionally, speciation studies were conducted using HPLC-ICP-MS and HPLC-ESI-Orbitrap-MS to investigate a possible metabolization of the Se species by PBCECs.

2.5.1 Impact of Se Species on the Viability of PBCECs

In order to identify the non-cytotoxic concentration range for subsequent transfer studies, dehydrogenase activity and neutral red uptake were assessed after incubation with the respective Se species for 48 hours. SeN and MeSeCys exerted no cytotoxic effects on PBCECs in concentrations up to 100 µM (Fig. 1 A). This goes in line with other studies investigating the cytotoxicity of SeN in a human Caco-2 [22] and a murine melanoma cell line [38]. However, SeN affected the lysosomal integrity already at a concentration of 10 µM (Fig. 1 B), but not reaching effective concentration reducing the cell viability by 30% (EC30). To date, there are limited data on cytotoxicity of SeN and no data are available in primary cells. There are no studies on cytotoxic effects of selenite and MeSeCys in brain endothelial cells. Most studies regarding toxicity of Se species are conducted in human cancer cell lines. In these studies selenite was toxic already at low micromolar concentrations while MeSeCys caused toxic effects only at higher concentrations [37,39–43]. Furthermore, results from rodent studies reported higher toxicity of selenite compared to organic Se species [44,45]. In agreement with *in vitro* and *in vivo* data, selenite caused substantial cytotoxic effects on PBCECs in both tested viability endpoints whereby the lysosomal integrity (EC_{30} value: 15 µM) was more sensitive as compared to the dehydrogenase activity (EC_{30} value: 30 µM). MeSeCys only had an impact on lysosomal integrity but could not reduce viability below 70% (Fig. 1 B). Regarding EC_{30} values of selenite, PBCECs were less sensitive compared to cancer cell lines [37]. Possible reasons for the different sensitivity could be explained with the differentiation status of cells and the usage of primary cells.
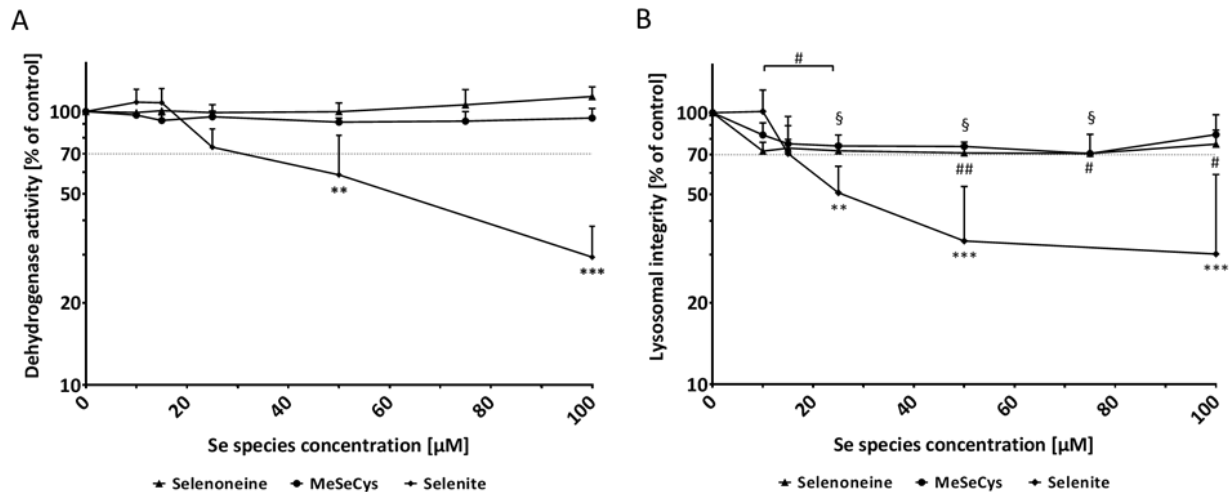
Figure 1. Cell viability determined by dehydrogenase activity (A) and neutral red uptake (B) after 48 hours incubation with three Se species in differentiated primary porcine endothelial cells (PBCECs). Shown are mean values of at least two individual experiments with at least four replicates each + SD. ($^{*/#/§}P$ < 0.05, $^{**/##}P$ < 0.01 and $^{***}P$ < 0.001 vs. untreated control cells, SeN – ▲ (#), MeSeCys – ● (§), Selenite – ◆ (*)).

2.5.2   Effect of Se Species on the Integrity of In Vitro BBB Model

To verify the integrity of the PBCEC barrier during incubation with SeN and the reference Se species selenite and MeSeCys, online monitoring of TEER and capacitance was performed. An intact barrier is essential for transfer studies and a disruption of the barrier by cytotoxic effects has to be avoided. Therefore, sub-cytotoxic concentrations of each Se species were used for transfer studies. Neither TEER nor capacitance decreased during incubation with 1 µM (Fig. 2) and 10 µM (data not shown) Se species, thus indicating the absence of barrier disruption. Capacitance remained unaffected during transfer experiments. TEER demonstrated noticeable increase after incubation with MeSeCys, which could be explained by an altered expression of tight junctions (TJs) [46]. Altogether, no barrier disruption was observed during 72-hour incubation with 1 µM selenite, MeSeCys or SeN. The same Se species also did not affect TEER and capacitance of the Caco-2 intestinal barrier model at concentrations up to 10 µM [22].
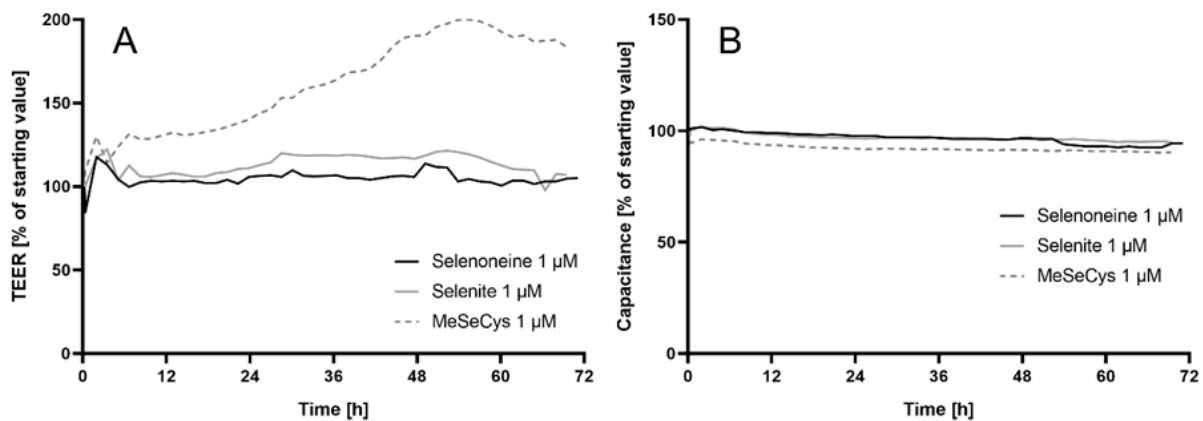
Figure 2. PBCEC barrier integrity (A) and capacitance (B) after application of 1 µM of Se species in the apical compartment for 72 hours. Barrier integrity was assessed by online monitoring of the TEER and capacitance values. Shown are mean values, expressed as % of starting value, calculated from at least three independent experiments with two replicates each. Standard deviation did not exceed 18% for TEER and 3% for capacitance (not shown).

2.5.3   Se Transfer Across the In Vitro BBB Model and Se Uptake

To investigate the bioavailability of the Se species to the nervous system, time-dependent Se transfer was studied after application of Se species to the apical side of the PBCEC barrier, thus imitating Se entry from the blood vessel lumen. For the selenite incubation, Se transfer was statistically not significant ($P > 0.05$) due to the high standard deviation (Fig. 3). Nevertheless, transfer of 33 ± 13% Se content to the basolateral compartment indicates that a considerable part of selenite passed across the barrier (permeability coefficient ($8.7 \pm 3.7) \times 10^{-7}$ cm s^{-1}). In contrast to selenite, MeSeCys demonstrated the fastest and the most efficient transport among the applied Se species and mostly reached equilibrium after 72 hours. Permeability coefficient of MeSeCys (($10.4 \pm 0.2) \times 10^{-7}$ cm s^{-1}) was almost identical to the coefficient of sucrose (1.0×10^{-6} cm s^{-1}) reported for the same PBCEC model [47]. Most probably, this is attributed to the Se-unspecific active transport of amino acids. MeSeCys can potentially be carried by the alanine, serine, cysteine, and threonine transporter 1 (ASCT1) and 2 (ASCT2), which are responsible for the delivery of cysteine to the brain [48]. The kinetics of SeN transfer was the slowest among applied Se species. SeN application resulted in a statistically significant increase of the Se concentration in the basolateral compartment after 48 hours. Nevertheless, SeN permeability coefficient is the lowest with ($6.7 \pm 2.3) \times 10^{-7}$ cm s^{-1} and only 22 ± 7% of Se was transferred after incubation with 1 µM SeN, which is very close to those for incubation with 0.1 µM SeN – 24 ± 6% (Fig. S1, Supporting Information), but significantly higher than that for 10 µM SeN – 9 ± 2% (Fig. S2, Supporting Information). After the application of SeN on the both sides of the PBCEC barrier, no side-directed transfer was observed (data not shown). However, the concentration-dependent differences of the transport of SeN indicated that transporters on both sides possibly facilitate SeN transport in dependence on SeN gradient rather than a transport by passive

diffusion. In contrast to the results in the BBB model, the studies using the Caco-2 intestinal barrier model demonstrated side-directed transport of SeN from the intestinal lumen to the blood side [22]. This may be due to the expression of organic cation/carnitine transporter 1 (OCTN1) in Caco-2 cells, which was shown to be responsible for SeN transport in HEK293 cells [17]. Nevertheless, it is known that ET can pass across BBB and accumulate in the brain of rats [49], while OCTN1 is not expressed in rats BBB [50]. Therefore, we cannot exclude other possible transfer mechanism for SeN in the model used.

Se concentration in PBCEC cell lysates was measured at the end of the transfer experiment to determine the Se uptake into the cells. The obtained Se contents in PBCECs demonstrated a slight increase in intracellular Se content, but did not differ significantly from the control cells (data not shown), thus indicating no accumulation of the studied Se species within the cells.
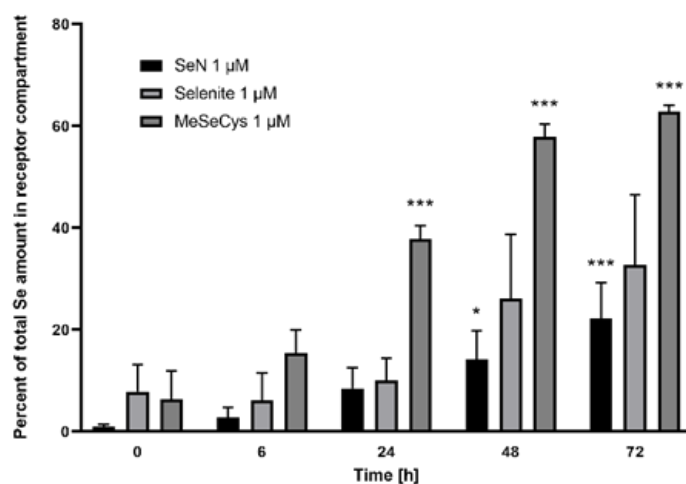
Figure 3. Percentage of Se transferred from the apical to the basolateral compartment after the application of 1 µM Se species in the apical compartment for 72 hours. Shown are mean values + SD calculated from at least three independent experiments with two replicates each. Presented mean values were calculated based on the average values from each experiment. Statistically significant difference was calculated in relation to the starting value (0 hours) for corresponding Se compound using one-way ANOVA followed by Dunnett's test, $* P < 0.05$, $*** P < 0.001$.

2.5.4   Speciation Studies

To date, the mammalian metabolism of SeN is mostly unknown. Therefore, a HPLC-based speciation study of SeN was carried out in PBCECs. For the speciation studies 10 µM of SeN or of the reference Se species MeSeCys or selenite were applied to the apical compartment of the *in vitro* BBB model for 72 hours and obtained media from both compartments as well as cell lysates were analysed by HPLC-ICP-MS. Incubation with SeN resulted in the formation of at least eight unknown Se-peaks (U1 – U8) in addition to SeN in both compartments with U1 being major and in the same concentration range as the originally applied species in all media investigated (Fig. 4). This unknown peak was also detectable

in high concentrations in media containing SeN without presence of cells (data not shown). In general, no significant differences in the concentrations of the selenium species were observed, when TCEP was added to the mobile phase.

Table 1. Se species concentrations (results from two independent experiments) in the media of apical and basolateral compartments and cell lysates after 72-hour incubation with 10 µM of SeN, selenite or MeSeCys.

		SeN	Selenite	MeSeCys
Apical	Total Se [µg Se L^{-1}]	1312; 1296	132; 117	151; 153
	Incubated species [µg Se L^{-1}]	394; 559	19; 21	185; 176
	% of total Se	**30; 43**	**14; 18**	**123; 115**
	Sum of species [µg Se L^{-1}]	1342; 1364	19; 21	188; 187
	Column recovery [%]	102; 105	14; 18	125; 122
Basolateral	Total Se [µg Se L^{-1}]	61;78	104; 94	127; 132
	Incubated species [µg Se L^{-1}]	24; 21	35; 30	151; 162
	% of total Se	**39; 27**	**34; 32**	**119; 123**
	Sum of species [µg Se L^{-1}]	66; 67	35; 30	154; 164
	Column recovery [%]	108; 86	34; 32	121; 124
Cell lysate	Total Se [µg Se L^{-1}]	3.1; 1.7	5.0; 4.5	1.4; 0.7
	Incubated species [µg Se L^{-1}]	1.8; 0.5	1.6; 1.6	0.5; 0.3
	% of total Se	**57; 29**	**32; 36**	**36; 43**
	Sum of species [µg Se L^{-1}]	1.8; 0.5	1.6; 1.6	0.5; 0.3
	Column recovery [%]	57; 29	32; 36	36; 43

To elucidate the nature of the unknowns HPLC-ESI-Orbitrap-MS was performed and all unknowns could be assigned accurate candidate masses with Δm < 2 ppm, corresponding elemental compositions, and we propose structures based on the recorded fragmentation patterns in comparison to that of SeN (Figs. S3 – S7 and Table S2, Supporting Information). We propose the major unknown U1 is an adduct of SeN with pyruvate, which is always present in the DMEM/Ham's F12 culture media as sodium pyruvate, and likely reacts spontaneously to SeN-pyruvate ([C12H18O5N3Se]+; m/z = 364.0407; Δm = -0.8 ppm). Although only U1 could be clearly detected by HPLC-ICP-MS when pure SeN containing media without PBCEC cells were analysed, all unknowns except for U2 were detectable by HPLC-ESI-Orbitrap-MS, albeit with considerably weaker signals than in the media from the transfer experiments with the cells. We proposed structures for U2 to U8 based on similarities to fragmentation spectra measured for SeN (Fig. S7, Supporting Information) and U1 (Fig. S3, Supporting Information), and

suggest that several isomers eluting at different retention times are present in the samples (Fig. S8, Supporting Information). As U2's structure is likely similar to that of the other unknowns, it is also not considered a "true metabolite" of the PBCEC cells.

Although the concentration of SeN itself did not exceed 43% of the total Se (Table 1), the sum of species (SeN plus U1 to U8) closely matched the total selenium concentration. If U1 to U8 are already formed without the PBCECs this indicates negligible metabolism of SeN by the PBCEC cells at the blood-brain barrier themselves. In contrast to the results in the intestinal barrier model [22] no methylation of SeN to Se-methylselenoneine could be observed by high resolution MS in the BBB model. In the lysate samples SeN was only detected at trace levels and the detection of the other peaks in lysates seems to be unachievable in the current setup.

MeSeCys was the major Se species in media and cell lysate samples (Table 1). Additionally, four minor unknown Se species in low concentrations were detected in media (Fig. S9, Supporting Information). As their concentrations were low, identification by HPLC-ESI-Orbitrap-MS was not attempted. Column recovery showed quantitative elution of the Se species in the media.

In samples treated with selenite, selenite was the only form of Se detected with the anion-exchange separation (Fig. S10, Supporting Information). However, in contrast to SeN and MeSeCys treated media, the column recovery was low in the case of selenite-treated media (only 14 – 36% of the total selenium, Table 1). Spiking of one of the media with an aqueous selenite standard solution showed retention time matching between the species in the media and the pure standard (Fig. S10, Supporting Information) and yielded quantitative recovery of the added selenite (111%). Hence, the low column recovery is most likely due to the presence of other selenium metabolites strongly retained on the column under the used chromatographic conditions. As these suspected species make up for a major part of the total selenium in the media further investigations into their identification are needed.
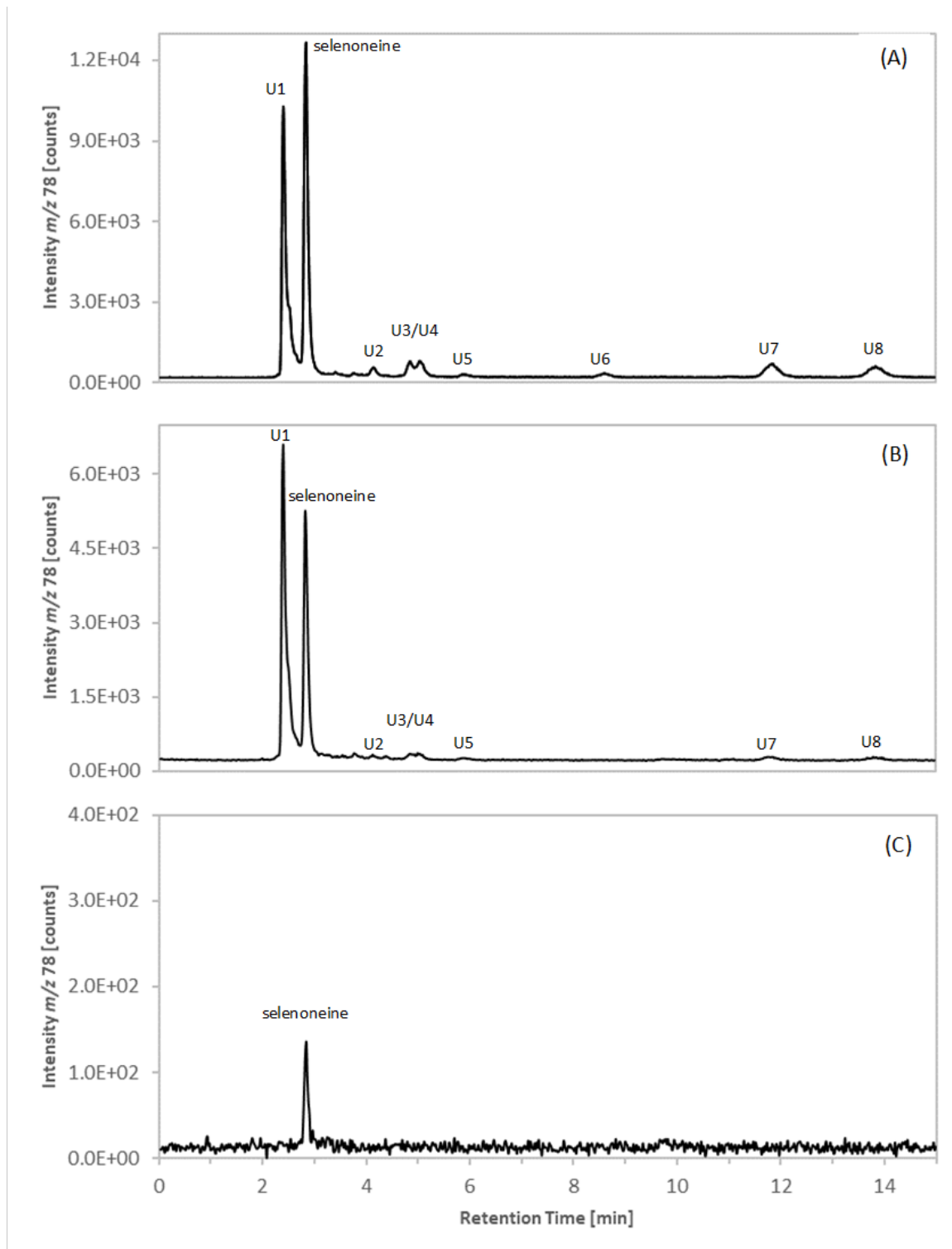
Figure 4. HPLC-ICP-MS chromatogram of the media from apical (A) and basolateral (B) compartments as well as cell lysate (C) after 72-hour incubation with 10 µM SeN from the apical side of the PBCEC barrier. Chromatographic conditions: column: Waters Atlantis dC18, 4.6 x 150 mm; mobile phase: 20 mM ammonium formate 3% (v/v) methanol 0.1 mM TCEP pH 3.0; flow rate: 1 mL min^{-1}; column temperature: 30 °C; injection volume: 10 µL. Apical medium (A) was diluted 1 + 9 with water before analysis.

2.6 Conclusion

The current study demonstrated capability of SeN, a naturally-occurring Se species, to pass the blood-brain barrier by applying a well-established BBB model based on primary porcine capillary endothelial cells. Se transport and biotransformation were studied after application of SeN, selenite and MeSeCys. Obtained data indicate the absence of toxic manifestations in BBB model during long-term incubation with supra-physiological concentrations of all Se species. Transfer studies indicate slow but substantial transport of SeN from the blood-facing to the brain-facing side of the BBB. Additionally, speciation study revealed negligible metabolism of SeN by PBCECs. Our results are indispensable for advances towards the assessment of possible health-promoting effects of SeN. Nevertheless, taking into consideration the complexity of the brain, consisting not only of one cell type, and more complex transport mechanism of inorganic Se species, the limitations of the model system are indisputable. Therefore, further studies regarding the human health-related properties of SeN are required.

2.7 Supporting Information

Supporting Information is available online or from the authors.

2.8 Acknowledgement

2.9 Conflict of Interest

The authors declare no conflict of interest.

2.10 References

[1]   M. Kieliszek, S. Błazejak, Current knowledge on the importance of selenium in food for living organisms: A review, Molecules, 2016, 21, 609.

[2]   S.J. Fairweather-Tait, Y. Bao, M.R. Broadley, R. Collings, D. Ford, J.E. Hesketh, R. Hurst, Selenium in Human Health and Disease, Antioxid. Redox Signal., 2011, 14, 1337–1383.

[3]   M. Vinceti, T. Filippini, L.A. Wise, Environmental Selenium and Human Health: an Update, Curr. Environ. Health Reports, 2018, 5, 464–485.

[4]   V.M. Labunskyy, D.L. Hatfield, V.N. Gladyshev, Selenoproteins: Molecular Pathways and Physiological Roles, Physiol. Rev., 2014, 94, 739–777.

[5]   G. V. Kryukov, Characterization of Mammalian Selenoproteomes, Science, 2003, 300, 1439–1443.

[6]   N.D. Solovyev, Importance of selenium and selenoprotein for brain function: From antioxidant protection to neuronal signalling, J. Inorg. Biochem., 2015, 153, 1–12.

[7]   A. Nakayama, K.E. Hill, L.M. Austin, A.K. Motley, R.F. Burk, All Regions of Mouse Brain Are Dependent on Selenoprotein P for Maintenance of Selenium, J. Nutr., 2007, 137, 690–693.

[8]   N. Akahoshi, Y. Anan, Y. Hashimoto, N. Tokoro, R. Mizuno, S. Hayashi, S. Yamamoto, K. Shimada, S. Kamata, I. Ishii, Dietary selenium deficiency or selenomethionine excess drastically alters organ selenium contents without altering the expression of most selenoproteins in mice, J. Nutr. Biochem., 2019, 69, 120–129.

[9]   European Commission, Scientific Committee on Food Opinion of the Scientific Committee on Food on the Tolerable Upper Intake Level of Vitamin E, Heal. Consum. Prot. Dir., 2000, 1–24.

[10]   M. Vinceti, J. Mandrioli, P. Borella, B. Michalke, A. Tsatsakis, Y. Finkelstein, Selenium neurotoxicity in humans: Bridging laboratory and epidemiologic studies, Toxicol. Lett., 2014, 230, 295–303.

[11]   Z. Hu, A. Shiokawa, N. Suzuki, H. Xiong, Y. Ogra, Evaluation of chemical species and bioaccessibility of selenium in dietary supplements, Eur. Food Res. Technol., 2019, 245, 225–232.

[12]   N.D. Solovyev, E. Drobyshev, G. Bjørklund, Y. Dubrovskii, R. Lysiuk, M.P. Rayman, Selenium, selenoprotein P, and Alzheimer's disease: is there a link?, Free Radic. Biol. Med., 2018, 127, 124–133.

[13]   Y. Yamashita, M. Yamashita, Identification of a novel selenium-containing compound, selenoneine, as the predominant chemical form of organic selenium in the blood of bluefin tuna, J. Biol. Chem., 2010, 285, 18134–18138.

[14]   A. Achouba, P. Dumas, N. Ouellet, M. Little, M. Lemire, P. Ayotte, Selenoneine is a major selenium species in beluga skin and red blood cells of Inuit from Nunavik, Chemosphere, 2019, 229, 549–558.

[15]   Y. Yamashita, M. Yamashita, H. Iida, Selenium Content in Seafood in Japan, Nutrients, 2013, 5, 388–395.

[16]   I.K. Cheah, B. Halliwell, Ergothioneine; antioxidant potential, physiological function and role in disease, Biochim. Biophys. Acta - Mol. Basis Dis., 2012, 1822, 784–793.

[17]   M. Yamashita, Y. Yamashita, T. Suzuki, Y. Kani, N. Mizusawa, S. Imamura, K. Takemoto, T. Hara, M.A. Hossain, T. Yabu, K. Touhata, Selenoneine, a Novel Selenium-Containing Compound, Mediates Detoxification Mechanisms against Methylmercury Accumulation and Toxicity in Zebrafish Embryo, Mar. Biotechnol., 2013, 15, 559–570.

[18]   Z. Pedrero Zayas, L. Ouerdane, S. Mounicou, R. Lobinski, M. Monperrus, D. Amouroux, Hemoglobin as a major binding protein for methylmercury in white-sided dolphin liver, Anal. Bioanal. Chem., 2014, 406, 1121–1129.

[19]   Y. Yamashita, Discovery of the strong antioxidant selenoneine in tuna and selenium redox metabolism, World J. Biol. Chem., 2010, 1, 144.

[20]   J. Masuda, C. Umemura, M. Yokozawa, K. Yamauchi, T. Seko, M. Yamashita, Y. Yamashita, Dietary supplementation of selenoneine-containing tuna dark muscle extract effectively reduces pathology of experimental colorectal cancers in mice, Nutrients, 2018, 10,.

[21]   D. Lim, D. Gründemann, F.P. Seebeck, Total Synthesis and Functional Characterization of Selenoneine, Angew. Chemie Int. Ed., 2019, 58, 15026–15030.

[22]   I. Rohn, N. Kroepfl, J. Bornhorst, D. Kuehnelt, T. Schwerdtle, Side-Directed Transfer and Presystemic Metabolism of Selenoneine in a Human Intestinal Barrier Model, Mol. Nutr. Food Res., 2019, 63, 1–11.

[23]   M. Yamashita, Y. Yamashita, T. Ando, J. Wakamiya, S. Akiba, Identification and determination of selenoneine, 2-Selenyl-N α, N α, N α -Trimethyl-l-histidine, as the major organic selenium in blood cells in a fish-eating population on remote Japanese Islands, Biol. Trace Elem. Res., 2013, 156, 36–44.

[24]   M. Klein, L. Ouerdane, M. Bueno, F. Pannier, Identification in human urine and blood of a novel selenium metabolite, Se-methylselenoneine, a potential biomarker of metabolization in mammals of the naturally occurring selenoneine, by HPLC coupled to electrospray hybrid linear ion trap-orbital ion tra, Metallomics, 2011, 3, 513.

[25]   N. Kroepfl, K.A. Francesconi, T. Schwerdtle, D. Kuehnelt, Selenoneine and ergothioneine in human blood cells determined simultaneously by HPLC/ICP-QQQ-MS, J. Anal. At. Spectrom., 2019, 34, 127–134.

[26] N. Nakamichi, K. Nakayama, T. Ishimoto, Y. Masuo, T. Wakayama, H. Sekiguchi, K. Sutoh, K. Usumi, S. Iseki, Y. Kato, Food-derived hydrophilic antioxidant ergothioneine is distributed to the brain and exerts antidepressant effect in mice, Brain Behav., 2016, 6, e00477.

[27] N.G. Turrini, N. Kroepfl, K.B. Jensen, T.C. Reiter, K.A. Francesconi, T. Schwerdtle, W. Kroutil, D. Kuehnelt, Biosynthesis and isolation of selenoneine from genetically modified fission yeast, Metallomics, 2018, 10, 1532–1538.

[28] S.M. Müller, F. Ebert, G. Raber, S. Meyer, J. Bornhorst, S. Hüwel, H.-J. Galla, K.A. Francesconi, T. Schwerdtle, Effects of arsenolipids on in vitro blood-brain barrier model, Arch. Toxicol., 2018, 92, 823–832.

[29] H. Lohren, J. Bornhorst, R. Fitkau, G. Pohl, H.-J. Galla, T. Schwerdtle, Effects on and transfer across the blood-brain barrier in vitro—Comparison of organic and inorganic mercury species, BMC Pharmacol. Toxicol., 2016, 17, 63.

[30] J. Bornhorst, C.A. Wehe, S. Hüwel, U. Karst, H.-J. Galla, T. Schwerdtle, Impact of Manganese on and Transfer across Blood-Brain and Blood-Cerebrospinal Fluid Barrier in Vitro, J. Biol. Chem., 2012, 287, 17140–17151.

[31] F. Matthes, P. Wölte, A. Böckenhoff, S. Hüwel, M. Schulz, P. Hyden, J. Fogh, V. Gieselmann, H.-J. Galla, U. Matzner, Transport of Arylsulfatase A across the Blood-Brain Barrier in Vitro, J. Biol. Chem., 2011, 286, 17487–17494.

[32] D. Mulac, S. Hüwel, H. Galla, H. Humpf, Permeability of ergot alkaloids across the blood-brain barrier in vitro and influence on the barrier integrity, Mol. Nutr. Food Res., 2012, 56, 475–485.

[33] H. Franke, H.-J. Galla, C.T. Beuckmann, Primary cultures of brain microvessel endothelial cells: a valid and flexible model to study drug transport through the blood–brain barrier in vitro, Brain Res. Protoc., 2000, 5, 248–256.

[34] D. Hoheisel, T. Nitz, H. Franke, J. Wegener, A. Hakvoort, T. Tilling, H.-J. Galla, Hydrocortisone Reinforces the Blood–Brain Barrier Properties in a Serum Free Cell Culture System, Biochem. Biophys. Res. Commun., 1998, 244, 312–316.

[35] J. Bornhorst, F. Ebert, A. Hartwig, B. Michalke, T. Schwerdtle, Manganese inhibits poly(ADP-ribosyl)ation in human cells: a possible mechanism behind manganese-induced toxicity?, J. Environ. Monit., 2010, 12, 2062.

[36] G. Repetto, A. del Peso, J.L. Zurita, Neutral red uptake assay for the estimation of cell viability/cytotoxicity, Nat. Protoc., 2008, 3, 1125–1131.

[37] T.A. Marschall, J. Bornhorst, D. Kuehnelt, T. Schwerdtle, Differing cytotoxicity and bioavailability of selenite, methylselenocysteine, selenomethionine, selenosugar 1 and trimethylselenonium ion and their underlying metabolic transformations in human cells, Mol. Nutr. Food Res., 2016, 60, 2622–2632.

[38] T. Seko, S. Imamura, K. Ishihara, Y. Yamashita, M. Yamashita, Selenoneine suppresses melanin synthesis by inhibiting tyrosinase in murine B16 melanoma cells and 3D-cultured human melanocytes, Fish. Sci., 2020, 86, 171–179.

[39] K. Takahashi, N. Suzuki, Y. Ogra, Bioavailability comparison of nine bioselenocompounds in vitro and in vivo, Int. J. Mol. Sci., 2017, 18, 1–11.

[40] L.L. Flores Villavicencio, G. Cruz-Jiménez, G. Barbosa-Sabanero, C. Kornhauser-Araujo, M.E. Mendoza-Garrido, G. De La Rosa, M. Sabanero-López, Human lung cancer cell line A-549 ATCC is differentially affected by supranutritional organic and inorganic selenium, Bioinorg. Chem. Appl., 2014, 2014,.

[41] C.S. Hoefig, K. Renko, J. Köhrle, M. Birringer, L. Schomburg, Comparison of different selenocompounds with respect to nutritional value vs. toxicity using liver cells in culture, J. Nutr. Biochem., 2011, 22, 945–955.

[42] K. Lunøe, C. Gabel-Jensen, S. Stürup, L. Andresen, S. Skov, B. Gammelgaard, Investigation of the selenium metabolism in cancer cell lines, Metallomics, 2011, 3, 162–168.

[43]   A.P. Kipp, J. Frombach, S. Deubel, R. Brigelius-Flohé, Selenoprotein W as biomarker for the efficacy of selenium compounds to act as source for selenoprotein biosynthesis, 1st ed., Elsevier Inc., .

[44]   E.M. Ammar, D. Couri, Acute toxicity of sodium selenite and selenomethionine in mice after ICV or IV administration., Neurotoxicology, 1981, 2, 383–6.

[45]   X. Wang, Y. Yang, H. Zhang, J. Liu, Safety assessment and comparison of sodium selenite and bioselenium obtained from yeast in mice, Biomed Res. Int., 2017, 2017,.

[46]   T.A. Martin, T. Das, R.E. Mansel, W.G. Jiang, Synergistic regulation of endothelial tight junctions by antioxidant (Se) and polyunsaturated lipid (GLA) via Claudin-5 modulation, J. Cell. Biochem., 2006, 98, 1308–1319.

[47]   H. Franke, H.-J. Galla, C.T. Beuckmann, An improved low-permeability in vitro-model of the blood–brain barrier: transport studies on retinoids, sucrose, haloperidol, caffeine and mannitol, Brain Res., 1999, 818, 65–71.

[48]   Q.R. Smith, H. Mandula, J.M.R. Parepally, Amino Acid Transport Across The Blood-Brain Barrier, in: Handb. Biol. Act. Pept., Elsevier, : pp. 1415–1422.

[49]   T. Mayumi, H. Kawanc, Y. Sakamoto, E. Suehisa, Y. Kawai, T. Hama, Studies on Ergothioneine. V.1) Determination by High Performance Liquid Chromatography and Application to Metabolic Research, Chem. Pharm. Bull., 1978, 26, 3772–3778.

[50]   L. Pochini, M. Galluccio, M. Scalise, L. Console, C. Indiveri, OCTN: A Small Transporter Subfamily with Great Relevance to Human Pathophysiology, Drug Discovery, and Diagnostics, SLAS Discov., 2019, 24, 89–110.

2.11 Supporting Information
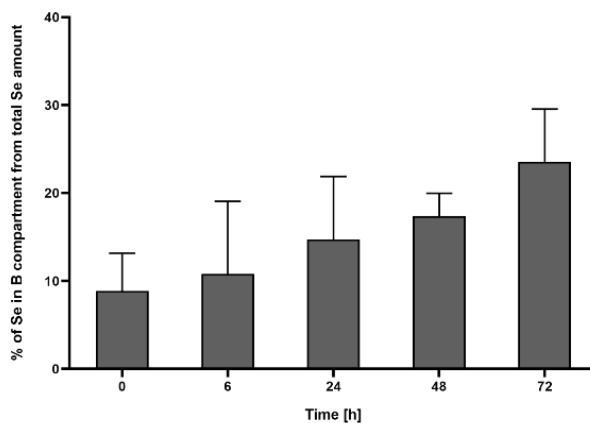
Figure S1. Se transfer after application of 0.1 µM SeN in the apical compartment for 72 hours. Shown are mean values + SD calculated from three independent experiments with two replicates each.
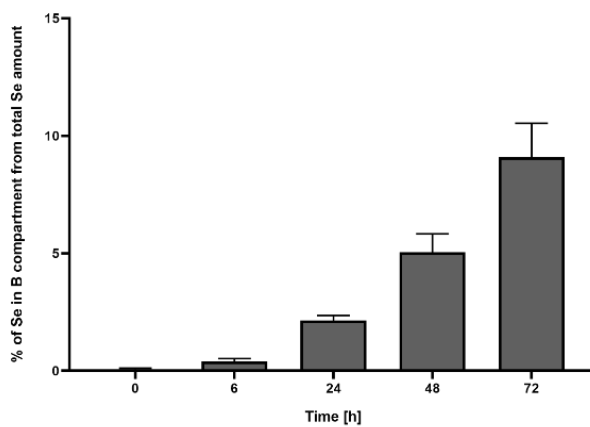
Figure S2. Se transfer after application of 10 µM SeN in the apical compartment for 72 hours. Shown are mean values + SD calculated from a single experiment with three replicates each.
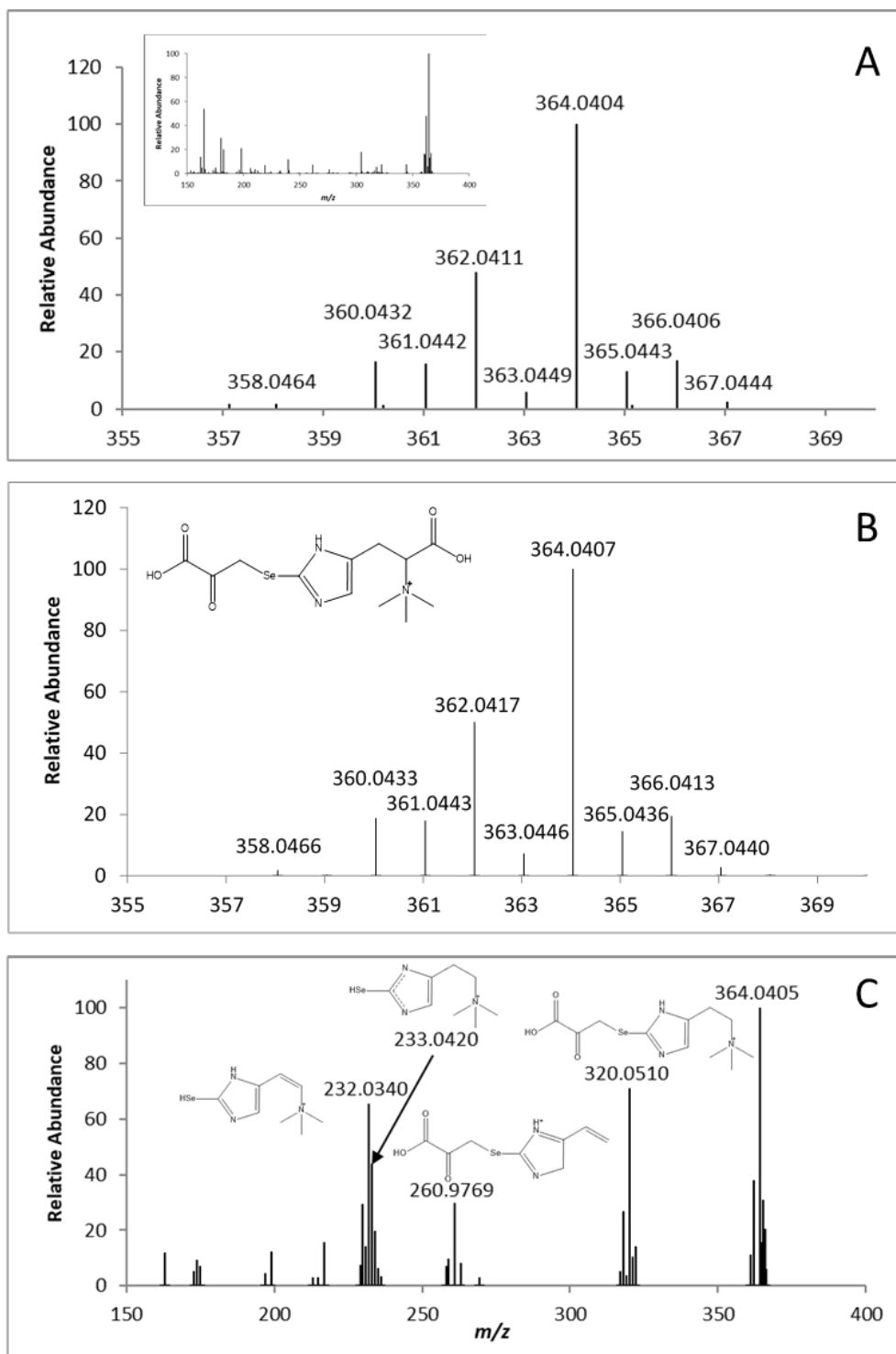
Figure S3: HPLC-ESI-Orbitrap-MS mass spectrum of U1 (A), simulated mass spectrum of the candidate structure (B), and fragmentation of the molecular ions at *m/z* 364.0 ± 4.0 with 10, 20, 30 NCE (C); Chromatographic conditions: Condition I without TCEP (Table S1). The R-$C_3H_3O_3$ moiety was proposed to be pyruvic acid based on the presence of sodium pyruvate in the culture medium; we show one possible isomer for this sidechain.
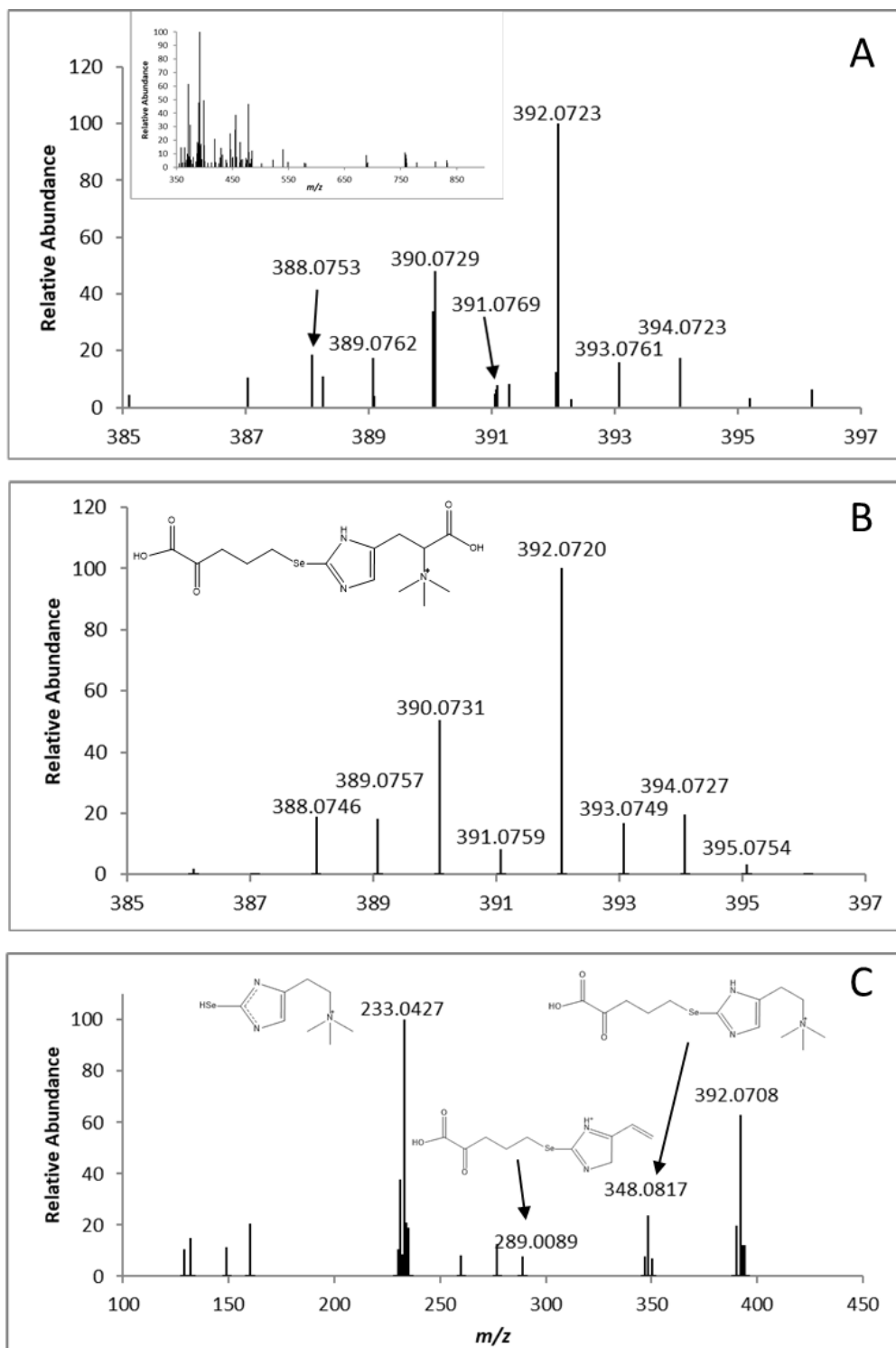
Figure S4: HPLC-ESI-Orbitrap-MS mass spectrum of U2 (A), simulated mass spectrum of the candidate structure (B), and fragmentation of the molecular ions at m/z 392.1 ± 4.0 with 10, 20, 30 NCE (C); Chromatographic conditions: Condition I without TCEP (Table S1). We show only one possible isomer of the R-C5H7O3 moiety based on the structural similarity to pyruvate, which is contained in the culture medium.
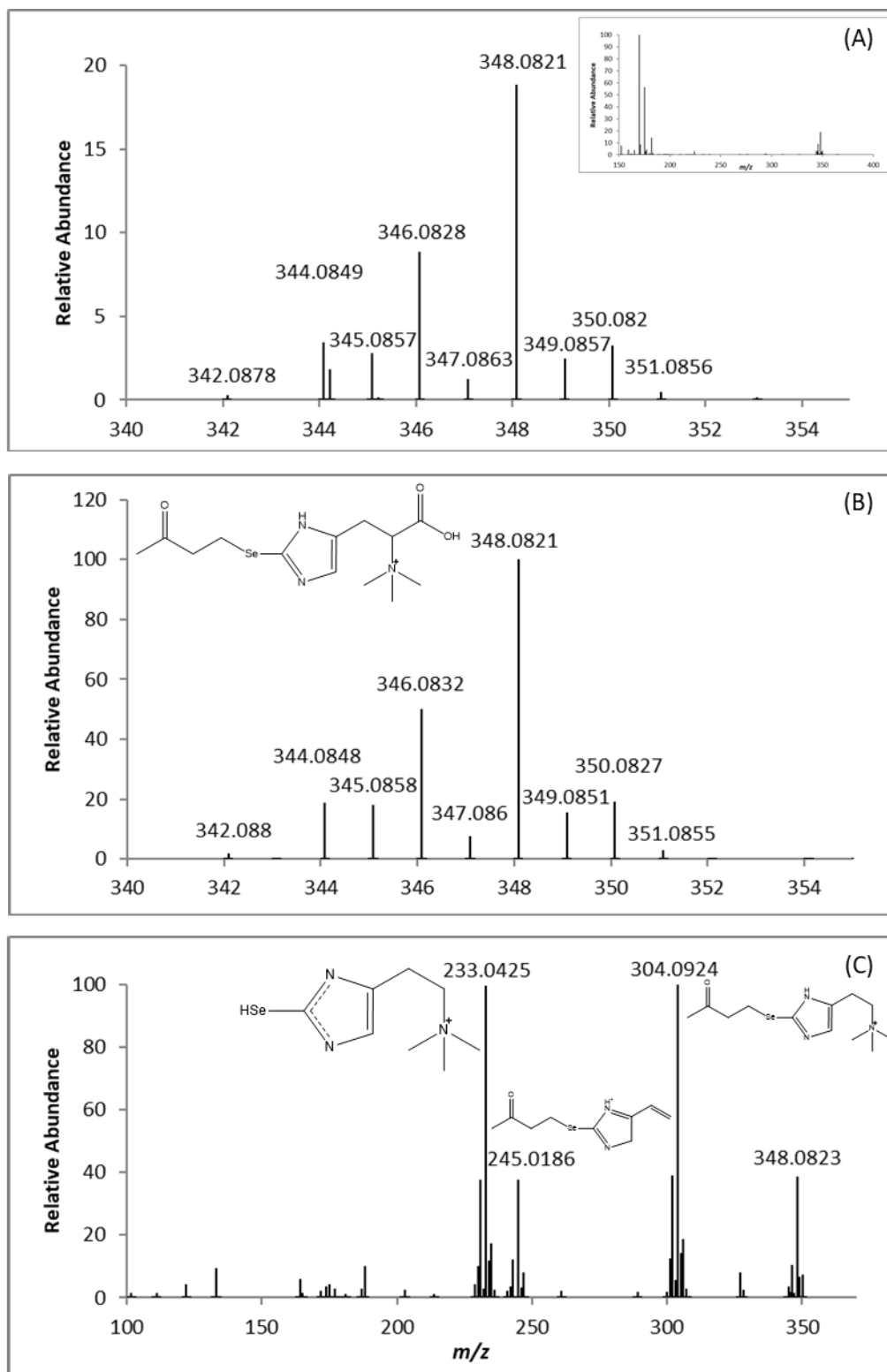
Figure S5: HPLC-ESI-Orbitrap-MS mass spectrum of U3/U4 (A), simulated mass spectrum of the candidate structure (B), and fragmentation of the molecular ion at m/z 348.1 ± 4.0 with 10, 20, 30 NCE (C); Chromatographic conditions: Condition I without TCEP (Table S1). We show only one possible isomer of the R-C4H7O moiety; several isomers of this moiety are likely present (peaks U3-U5 in Fig. S8 E).
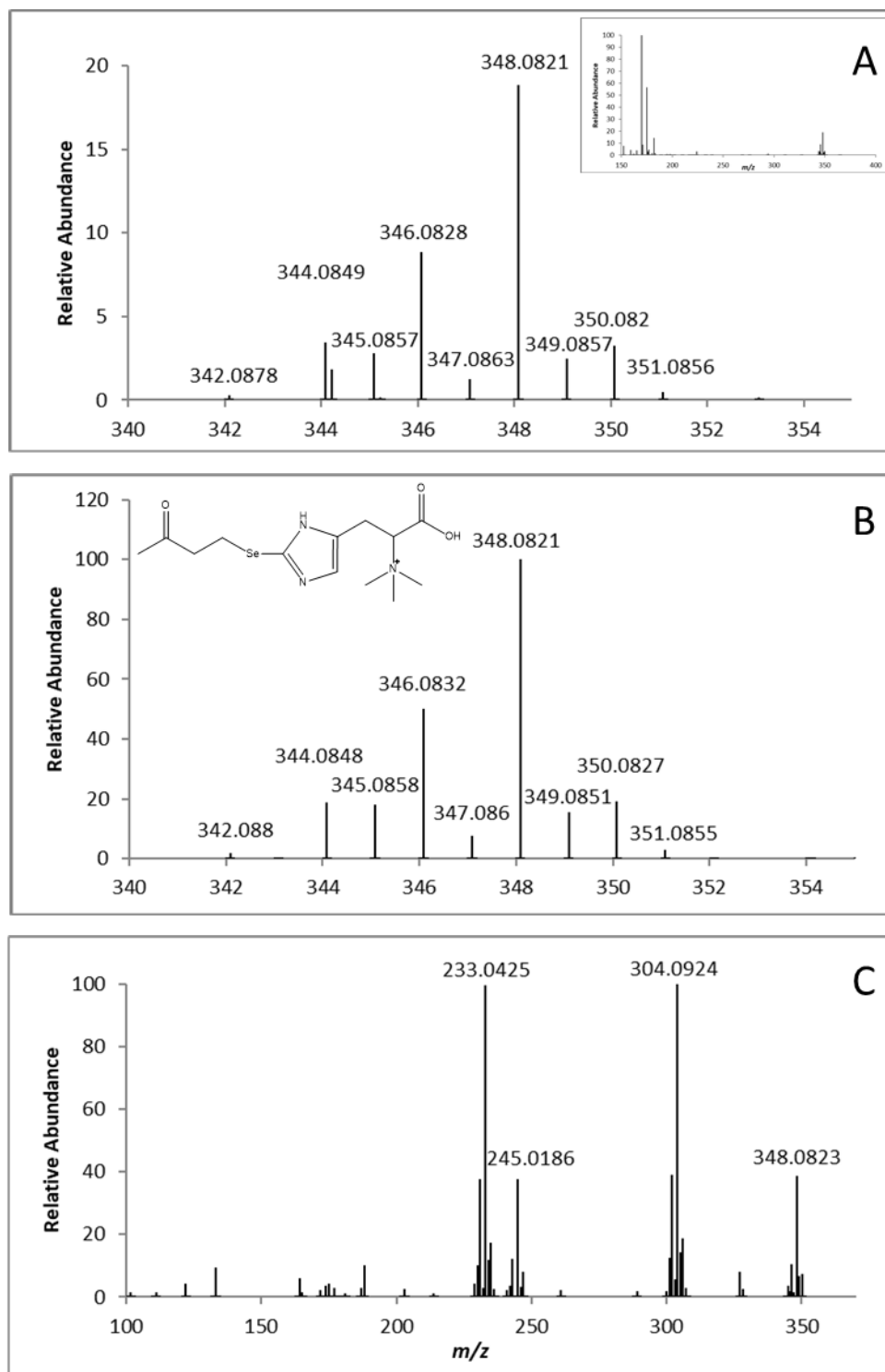
Figure S6: HPLC-ESI-Orbitrap-MS mass spectrum of U7 (A), simulated mass spectrum of the candidate structure (B), and fragmentation of the molecular ion at m/z 406.1 ± 4.0 with 10, 20, 30 NCE (C); Chromatographic conditions: Condition I without TCEP (Table S1). We show only one possible isomer of the R-C6H9O3 moiety; several isomers of this moiety are likely present (peaks U6-U8 in Fig. S8 F).
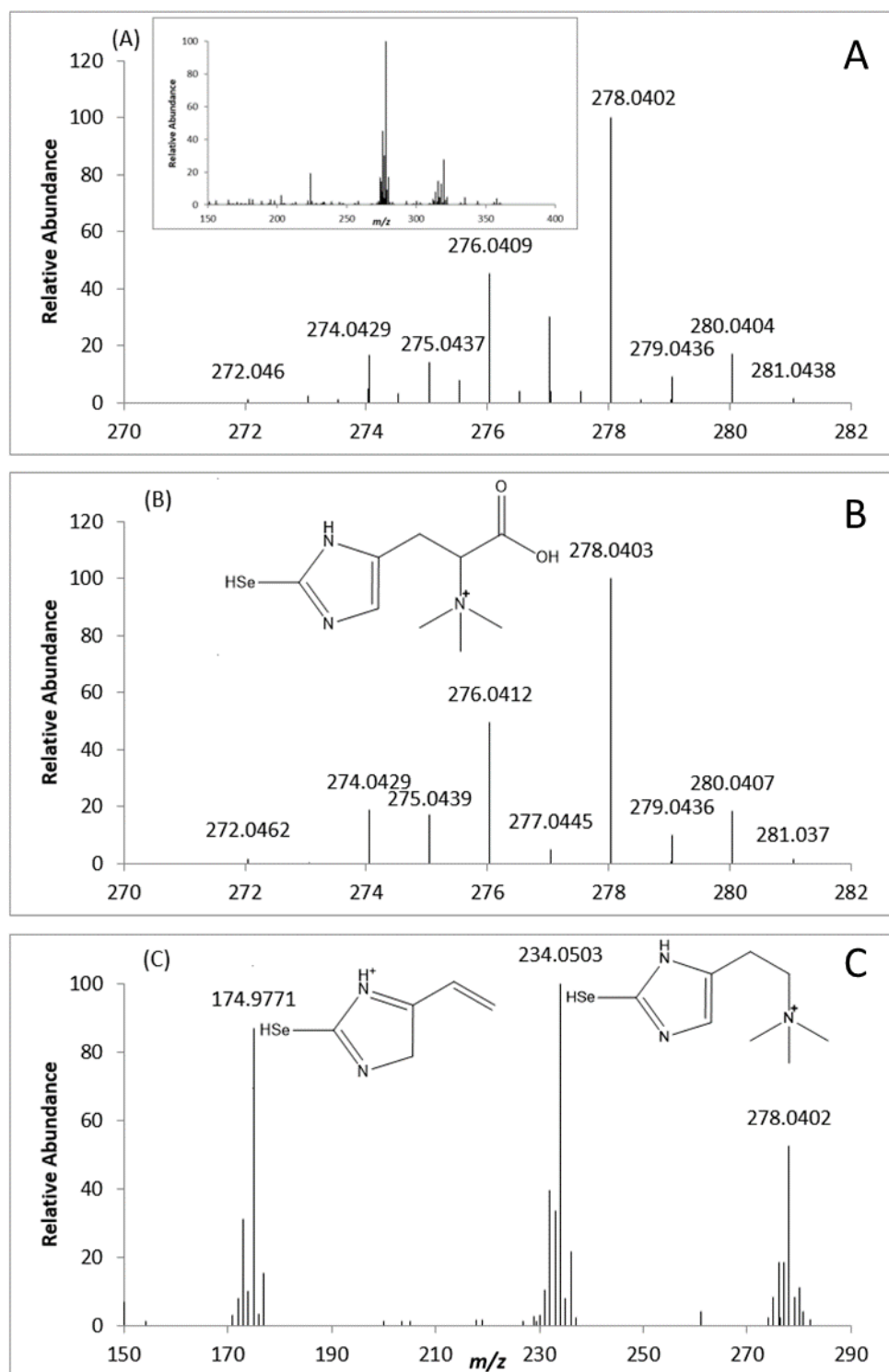
Figure S7: HPLC-ESI-Orbitrap-MS mass spectrum of SeN (A), simulated mass spectrum of the structure (B), and fragmentation of the molecular ion at m/z 278.0 ± 4.0 with 10, 20, 30 NCE (C); Chromatographic conditions: Condition I without TCEP (Table S1).
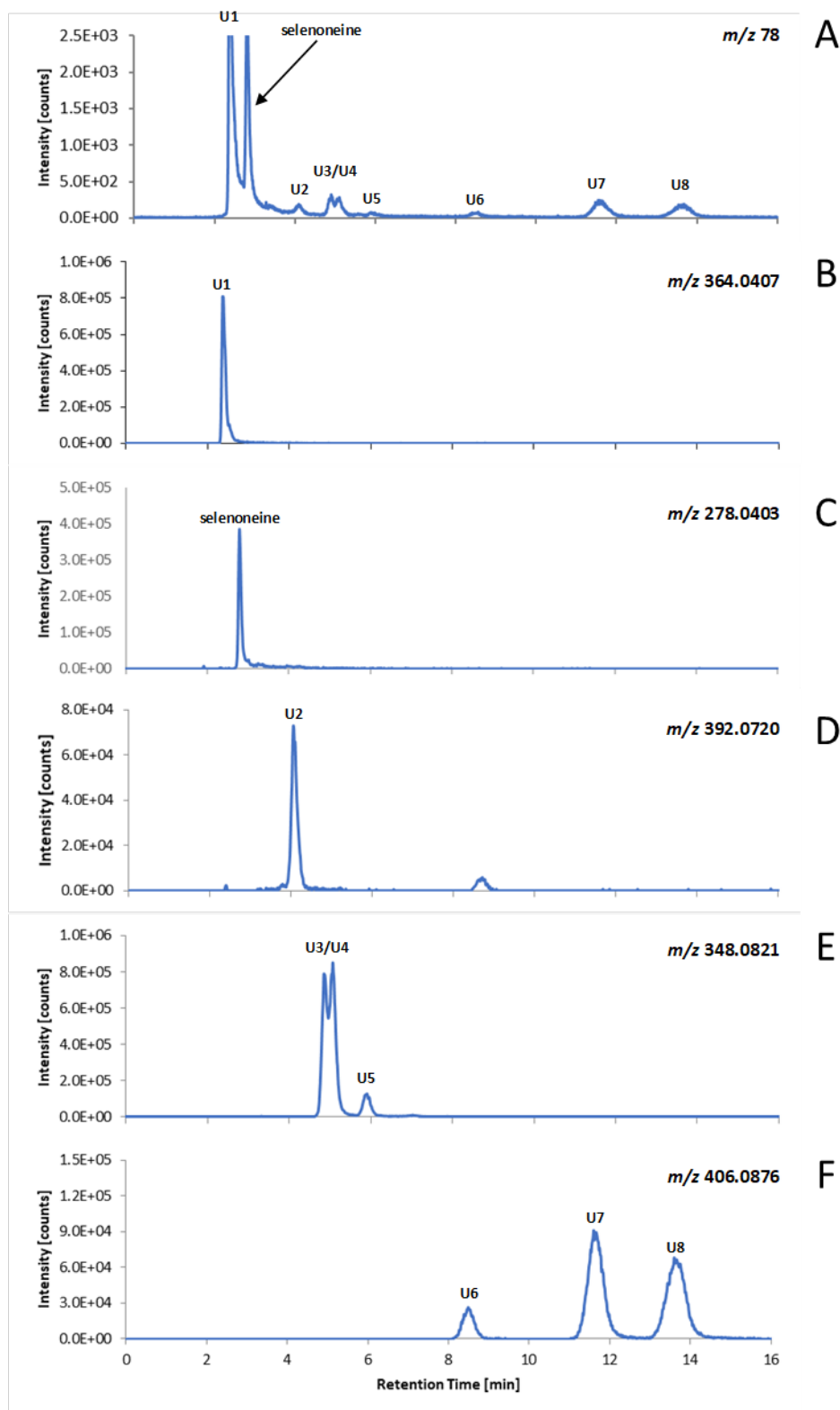
Figure S8: HPLC-ICP-MS chromatogram (m/z 78) (A) and HPLC-ESI-Orbitrap-MS chromatograms (m/z of selenoneine and candidate base peak masses for U1 to U8 extracted from positive full scan with Δm ± 3 ppm) (B)-(F); Chromatographic conditions: Condition I without TCEP (Table S1)
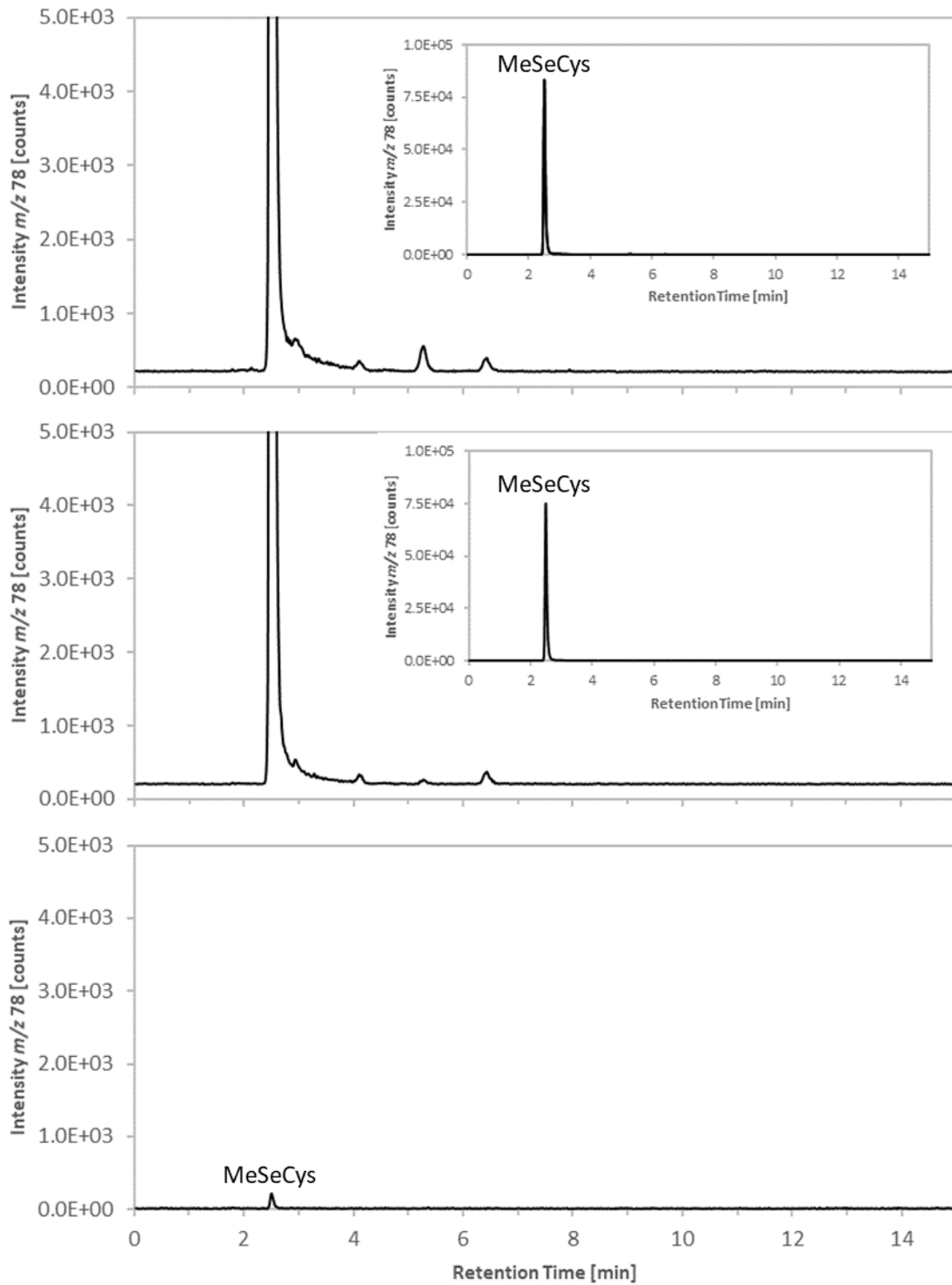
Figure S9. HPLC-ICP-MS chromatogram of the medium from apical (A) and basolateral (B) compartments as well as cell lysate (C) after 72-hour incubation with 10 µM MeSeCys from the apical side of the PBCEC barrier. Chromatographic conditions: column: Waters Atlantis dC18, 4.6 x 150 mm; mobile phase: 20 mM ammonium formate 3% (v/v) methanol pH 3.0; flow rate: 1 mL min-1; column temperature: 30 °C; injection volume: 10 µL.
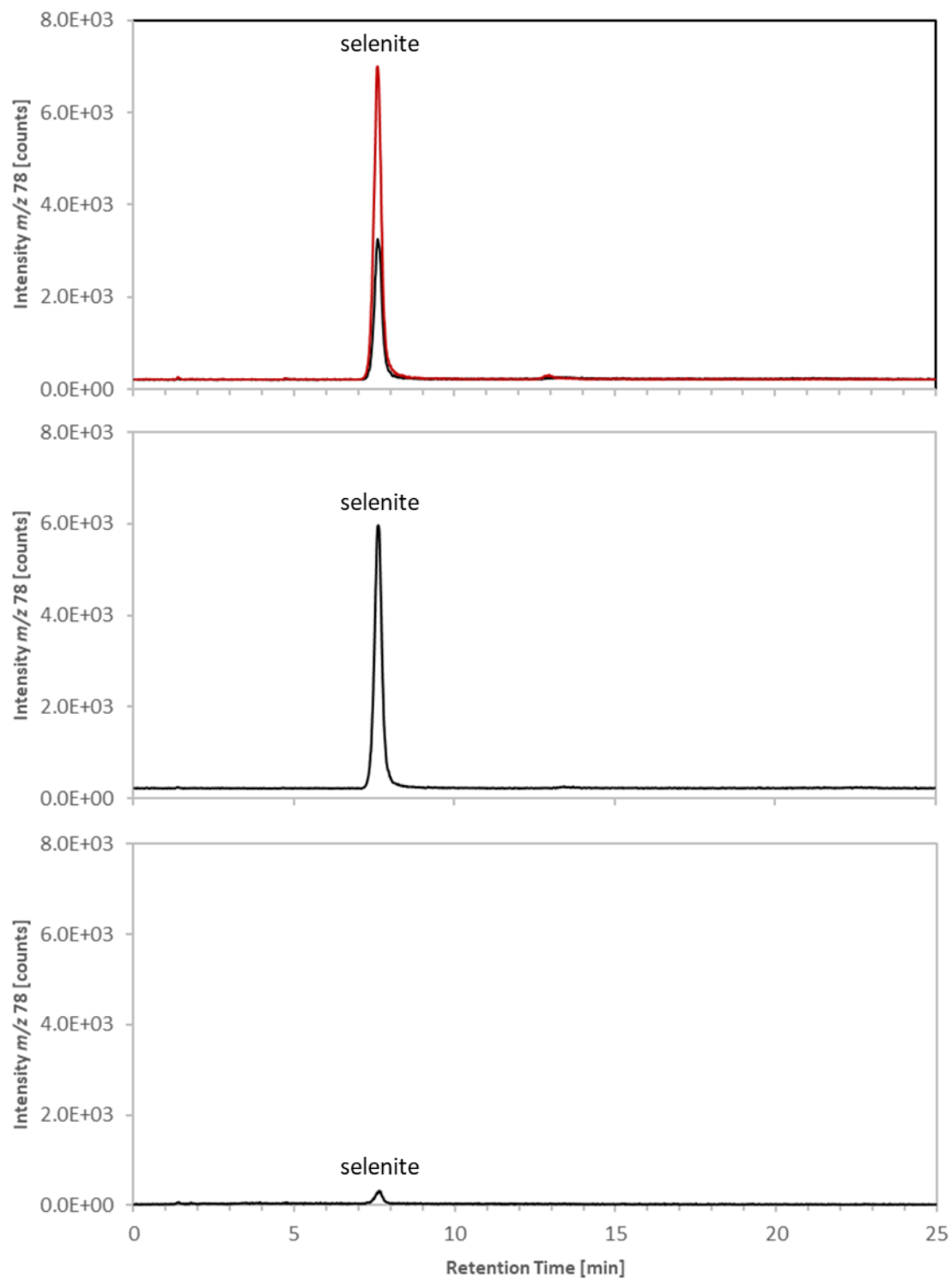
Figure S10. Anion-exchange-HPLC/ICP-MS chromatogram of medium from the apical compartment (black line) and medium from the apical compartment spiked with an aqueous selenite standard solution (final spike concentration 20 μg Se/L) (A), medium from the basolateral compartment (B) as well as cell lysate (C) after 72-hour incubation with 10 μM selenite from the apical side of the PBCEC barrier. Chromatographic conditions: column: Dionex IonPacTM AS14, 3 x 150 mm; mobile phase: 5 mM malonate pH 9.5; flow rate: 0.5 ml/min; column temperature: 30°C; injection volume: 10 μL

Table S1. Chromatographic conditions for the quantitative determination of Se species in PBCEC cell lysates and culture media. For all conditions, the column temperature was 30 °C and the injection volume was 10 μL.

	Condition	Column	Mobile Phase	Flow Rate [mL min^{-1}]
I	reversed-phase	Atlantis® dC18 (5 μM; 4.6 x 150 mm; Waters Corporation, Milford, USA)	20 mM ammonium formate, 3% MeOH pH 3.0*	1.0
II	anion-exchange	Dionex IonPac^{TM} AS14 (5 μM; 3 × 150 mm; ThermoFisher Scientific, Waltham, USA)	5 mM malonate pH 9.5**	0.5

* adjusted with formic acid; ** adjusted with 25% aqueous ammonia

Table S2. High resolution mass spectral data for Selenoneine (SeN) and previously unknown Se species (U1 - U8) observed in cell cultures and media.

Compound	Elemental composition	Elemental composition of the side chain	Calculated mass [M]$^+$	Measured mass [M]$^+$	Mass difference [ppm]
Selenoneine (SeN)	$C_9H_{16}O_2N_3Se$	H-(SeN)	278.0403	278.0402	-0.1
U1 (SeN-pyruvate*)	$C_{12}H_{18}O_5N_3Se$	$C_3H_3O_3$-(SeN)	364.0407	364.0404	-0.8
U2 (SeN-oxopentanoate*)	$C_{14}H_{22}O_5N_3Se$	$C_5H_7O_3$-(SeN)	392.0720	392.0723	+0.7
U3/U4/U5 (SeN-butanone*)	$C_{13}H_{22}O_3N_3Se$	C_4H_7O-(SeN)	348.0821	348.0821	+0.1
U6/U7/U8 (SeN-oxohexanoate*)	$C_{15}H_{24}O_5N_3Se$	$C_6H_9O_3$-(SeN)	406.0876	406.0883	+1.6

* We propose compound names for only one of the possible isomers of U1 - U8.

3. BIS-CHOLINE TETRATHIOMOLYBDATE PREVENTS COPPER-INDUCED BLOOD-BRAIN BARRIER DAMAGE

3.1 Abstract

In Wilson disease, excessive copper accumulates in patients' livers and may, upon serum leakage, severely affect the brain according to current viewpoints. Present remedies aim at avoiding copper toxicity by chelation, for example, by D-penicillamine (DPA) or bis-choline tetrathiomolybdate (ALXN1840), the latter with a very high copper affinity. Hence, ALXN1840 may potentially avoid neurological deterioration that frequently occurs upon DPA treatment. As the etiology of such worsening is unclear, we reasoned that copper loosely bound to albumin, that is, mimicking a potential liver copper leakage into blood, may damage cells that constitute the blood-brain barrier, which was found to be the case in an *in vitro* model using primary porcine brain capillary endothelial cells. Such blood–brain barrier damage was avoided by ALXN1840, plausibly due to firm protein embedding of the chelator bound copper, but not by DPA. Mitochondrial protection was observed, a prerequisite for blood–brain barrier integrity. Thus, high-affinity copper chelators may minimize such deterioration in the treatment of neurologic Wilson disease.

3.2   Introduction

In 1912, Samuel Alexander Kinnier Wilson reported a fatal neurological disease characterized by a progressive degeneration of the lenticular nucleus that additionally was associated with liver cirrhosis [1]. Today, we know that Wilson disease (WD) is due to an impairment of the mostly liver-residing copper-transporting ATPase ATP7B [2, 3, 4]. ATP7B defects cause massive liver copper accumulation and current viewpoints state that this copper may leak into the circulation [5]. In WD, patients' blood copper is not tightly incorporated into the copper-bearing plasma protein ceruloplasmin, but potentially available for its accumulation in peripheral organs, especially the brain [6]. Indeed, a correlation between a progressively elevated serum concentration of nonceruloplasmin copper (NCC) and the neurological severity has been described [7]. Moreover, in the WD animal model toxic milk mouse, there is some experimental evidence for this route. These mice appear with enormous liver copper accumulations, whereas modest elevations are seen in the spleen, kidney, and brain [8]. Upon intragastric D-penicillamine (DPA) administration, within days, a significant increase in copper in the serum and also in the brain was demonstrated in these mice [9], and thus one may conclude that it is the DPA taken up by the portal vein that liberates liver copper to cause serum and brain copper elevations.

In WD patients, upon years or even decades of accumulation, brain copper concentrations may reach up to 450 µg/g dry weight (versus 7 - 60 µg/g dry weight in controls) [10, 11, 12], considered to be the prime toxic condition that causes brain lesions and neurologic symptoms (e.g., dysarthria and parkinsonism) [13]. Nevertheless, many aspects of the pathophysiology of neurologic WD are still rather circumstantial, lack clinical evidence, or are unknown. Among them is the issue how elevated NCC enters and accumulates in the brain.

In WD patients, blood copper is mainly bound to albumin and amino acids [14, 15, 16]. Being the most abundant plasma protein (35 - 50 g/L; 500 - 750 µM), albumin has a huge copper binding capacity and may bind up to five copper ions at pH 7.4 (17). A first copper ion is tightly bound to the N terminus (K_d = 0.9 x 10^{-12} M [18] – 6.7 x 10^{-17} M [19]), a second one to a multi-metal binding site with intermediate affinity (K_d = 1.91 x 10^{-7} M [17]), and the remaining three copper ions are relatively loosely attached to presently uncharacterized sites (K_d = 6.25 x 10^{-6} M [17]). In this respect, the amino acid histidine may play a minor role because of its comparatively lower plasma concentration (≈100 µM [15]) and intermediate copper affinity ($K_d \approx 10^{-9}$ M [20]). Thus, in plasma, several binding partners for copper exist with either high capacity and/or high affinity. In WD patients, total blood copper concentrations of 0.5 - 16.6 µM have been observed [21, 22], among them a relatively low concentration of 1 - 5 µM copper that may be exchangeable as determined by EDTA (K_d = 1.26 × 10^{-16} M [18]) chelation experiments [23]. This raises the issue of how excess brain copper accumulation may occur. One mechanism may be a constant competition for and uptake of copper into the brain *via* the high-affinity

transporter CTR1 (Kd ≈ 10^{-14} M), possibly linked to an impaired copper re-export into the blood due to ATP7B defects [24]. CTR1 and ATP7B are present at the blood-facing membrane of endothelial cells that form the blood–brain barrier (BBB) along with astrocytes and pericytes [25]. Such competition at relatively low NCC blood copper, together with a one-way copper route into the brain due to ATP7B absence, may explain the observed long clinical silence, sometime lasting decades, of neurologic complications in WD patients. Another, not mutually exclusive possibility is that periods of copper induced liver damage may cause intense "blood copper pulses," thereby causing brain copper accumulation and damage. In fact, clinically relevant fluctuations in neurologic symptoms, sometimes multiple times per day, with varying degrees of severity have been reported. These symptoms may be exacerbated by stress, concurrent illnesses, or medications [26]. Such brain damage of NCC may start at the BBB that then may facilitate further unregulated copper entry into the brain. In agreement with this hypothesis, Stuerenburg described disturbances of the BBB in neurologic WD patients, as indicated by an increased ratio of albumin presence in cerebrospinal fluid versus serum [27]. Moreover, copper chelation treatments that bind excess liver copper, may secondarily cause such copper pulses. Here, as has been demonstrated in toxic milk mice, the chelator DPA directed copper to the blood, causing elevations in brain [9]. Indeed, treatment of neurologic WD patients with DPA can lead to dramatic symptom worsening as reported in 19 - 52% of the patients [28, 29, 30, 31, 32, 33, 34], especially shortly upon treatment onset. Such neurological worsening is not typically reported in tetrathiomolybdate (TTM)-treated patients [35, 36, 37]. As DPA has a lower copper affinity (Kd = 2.4 × 10^{-16} M [38]) than TTM (Kd = 2.3 × 10^{-20} M [38]), because of its tight binding, competition for copper in the blood may be diminished by the latter, possibly leading to lower BBB and/or brain damage.

To shed light into these hypotheses, we have studied the dose dependent copper-induced damage to the constituting cells of the BBB using increasing copper amounts bound to albumin, that is, from tightly to more loosely albumin-bound copper, thereby mimicking hypothetical blood copper pulses. Importantly, we find that such damage can be avoided upon presence of the high-affinity chelator bis-choline TTM (ALXN1840), but not by DPA.

3.3 Results

3.3.1 Copper chelators elevate blood copper differentially

Currently, chelation is the main therapeutic approach in WD to avoid copper toxicity upon its accumulation occurring primarily in the liver. However, if chelators mobilize excess hepatic copper, this may cause increased blood copper. Although such mobilization is a prerequisite for renal clearance of chelated copper, it could nevertheless lead to potentially undesirable systemic copper effects, for example, "neurological worsening" as suggested by DPA treatment studies in toxic milk mice [9]. Indeed, upon intravenous ^{64}Cu-injection, within minutes the metal can be largely traced by positron emission tomography (PET) in brain supporting vessels in wild-type rats (Fig 1A). In contrast, by intraperitoneal 64Cu-injection, that is, mimicking nutritional uptake, copper is not detected in brain by PET, even hours later (Figs 1A and S1).

We therefore investigated if or to what extent copper appears in serum in untreated Atp7b$^{+/-}$ control and Atp7b$^{-/-}$ rats (alternatively termed WD rats), but also in Atp7b$^{-/-}$ rats treated with either DPA or ALXN1840 (Fig 1B). As in WD patients, WD rats lack copper incorporation into ceruloplasmin [39], and therefore untreated Atp7b$^{-/-}$ animals have a very low serum copper level. Treatment of WD rats with ALXN1840 resulted in a significant increase in serum copper levels (likely due to ALXN1840–Cu–albumin tripartite complex formation, see below). This did not occur with DPA treatment (Fig 1B). As this latter absence may be due to fast renal copper clearance, we next investigated the excretion of copper *via* urine (Fig 1C), but also feces (Fig 1D). Whereas untreated Atp7b$^{+/-}$ and Atp7b$^{-/-}$ rats had low copper levels in either urine or feces collected over 24 h, DPA treatment of WD rats led to a significantly increased copper excretion into urine, in agreement with typical diagnostic findings in WD patients. In contrast, no profoundly elevated net copper excretion was noted upon ALXN1840 treatment under the chosen conditions (i.e., an observation period of 96 h [40]). Thus, these chelators elevate blood copper levels to different extent. Whereas in the case of DPA a rapid renal clearance (blood peak between 1 and 3 h after application [41]) may have avoided the detection of elevated serum copper levels here, it was significantly elevated upon ALXN1840 treatment in WD rats.
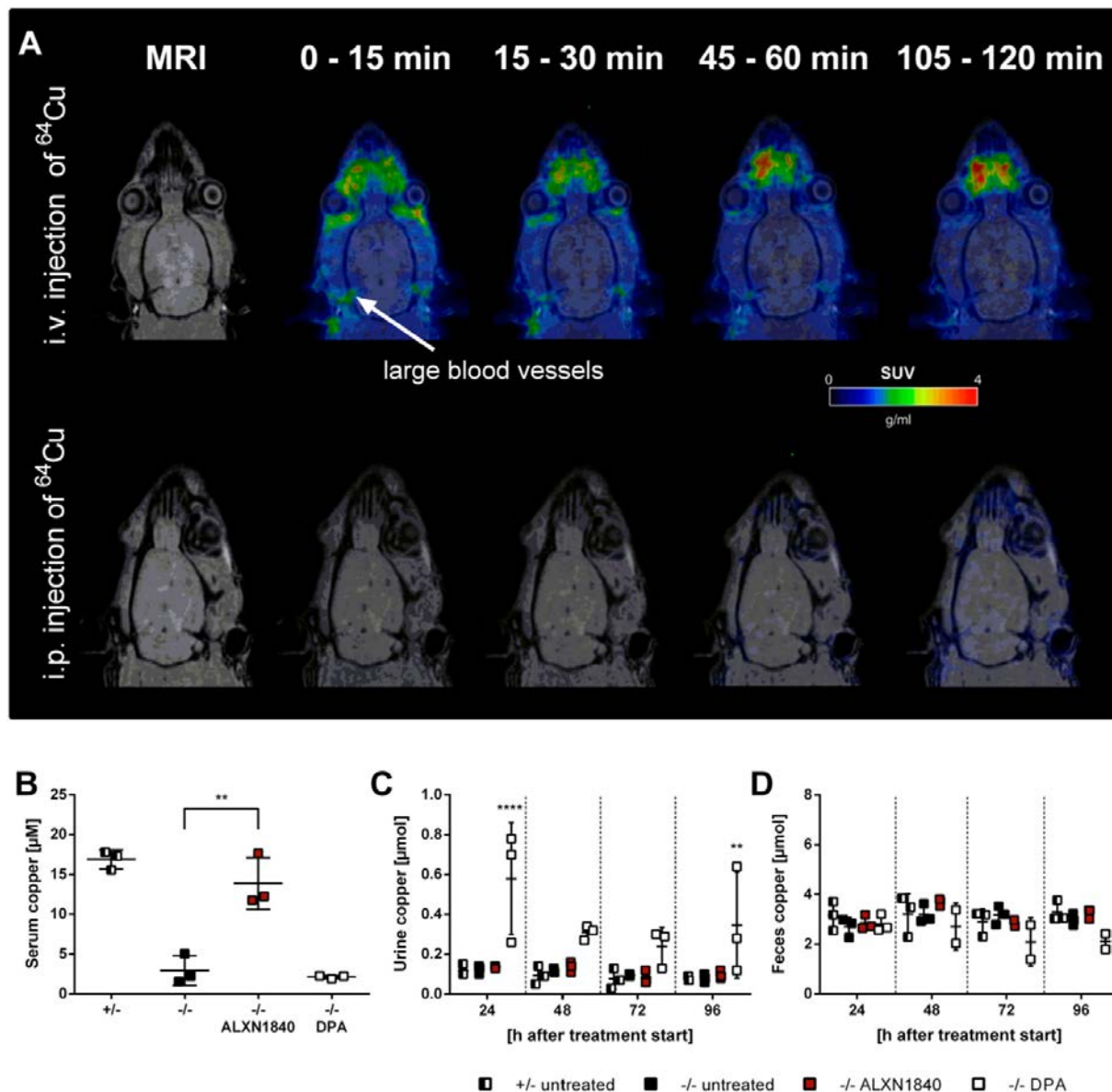
Figure 1. ALXN1840 and DPA increase blood copper levels. (A) Positron emission tomography scan of wild-type rats with ^{64}Cu injected either i.v. or i.p. I.v. injection results in a fast and high ^{64}Cu signal in brain proximate vessels in contrast to i.p.–injected rats. (B) Significantly increased serum copper levels are detected in Atp7b$^{-/-}$ rats treated with ALXN1840 (for 4 d) upon euthanasia, in contrast to DPA treatment (N = 3). (C) During DPA treatment of Atp7b$^{-/-}$ rats, a significantly increased urinary copper excretion is detected (N = 3). (D) No increased fecal copper excretion is observed during ALXN1840 and DPA treatments (N = 3). One-way ANOVA with Dunnett's multiple comparisons test was used for statistical analysis. *P < 0.05, **P < 0.01, ***P < 0.001, ****P < 0.0001.

3.3.2 ALXN1840 forms a stable complex with copper and albumin

In WD, blood copper may be loosely bound to albumin [14]. In fact, upon mixing 750 µM copper with 250 µM albumin (i.e., a molar ratio 3:1), a subsequent gel filtration removed about half to two thirds of the copper from albumin (Fig 2A top panel). Clearly, such easily removable loosely bound copper may present a potential threat when present in WD patients' blood. Moreover, when incubated with DPA (at a molar ratio Cu–albumin-DPA of 3:1:3), a portion of the copper pool stayed with albumin,

likely due to DPA's lower copper affinity in comparison to the high-affinity albumin binding site (Kd (DPA) = 2.4×10^{-16} M [38] versus Kd (N terminus of albumin) = 6.7×10^{-17} M [19]), whereas the residual copper co-migrated with DPA (Fig 2A lower panel). Therefore, it appears that the capacity of DPA to de-copper albumin is limited to the loosely bound copper at the applied molar ratios.

Intriguingly, when co-incubated with ALXN1840 (Kd = 2.3×10^{-20} M [38]), which has an affinity for copper that is magnitudes greater than that of DPA or albumin, albumin was not fully de-coppered but rather one prominent gel filtration peak appeared (Fig 2A middle panel), comprising the protein and large parts of copper as well as ALXN1840 (detected as molybdenum). This feature has been described for ALXN1840 in man [35] or for TTM in LEC rats (TTM is the active molecule in ALXN1840) [42, 43, 44, 45] and is due to the formation of a Cu–albumin–ALXN1840/TTM complex, previously termed the "tripartite complex" (TPC).

How is copper bound to the TPC? The single TPC gel filtrationbpeak clearly indicated its tight binding to the protein. Consequently, we used X-ray crystallography of the TPC (Fig 2B) and, upon data refinement, we could track ALXN1840 with two bound copper ions in the so-called Sudlow Site 1, a profound cleft in albumin formed by His241, Tyr149, Arg256, Lys237, and Ala290 (Fig 2B). Thus, in the presence of albumin, copper and ALXN1840 get deeply embedded into the protein. This finding may explain the lack of urinal copper excretion in ALXN1840-treated WD rats (Fig 1C), as renal albumin clearance is very limited [46]. In addition, electron paramagnetic resonance (EPR) studies demonstrated a change in copper redox status in the TPC versus Cu–albumin (Fig 2C). Whereas the latter revealed the typical cupric Cu(II) signal [47], in the presence of ALXN1840, the signal intensity of the EPR-active cupric copper dropped by around 50%, suggesting the reduction of one cupric copper ion to EPR-silent cuprous Cu(I) (Fig 2C second trace). Indeed, upon addition of sodium dithionite that fully reduces Cu(II) to Cu(I), no EPR signal was detected in both, Cu–albumin and TPC (Fig 2C lower traces).

In summary, using the above molar ratios, only the tightly bound copper stays with albumin, whereas more loosely bound copper is either set free upon gel filtration, bound to DPA, or relocated to the Sudlow site of albumin by ALXN1840 forming the TPC. Thus, if excess liver copper appears in blood in untreated WD, it represents a potential toxic threat to secondarily affected tissues like the brain, but this situation may change depending on the particularly used chelator.
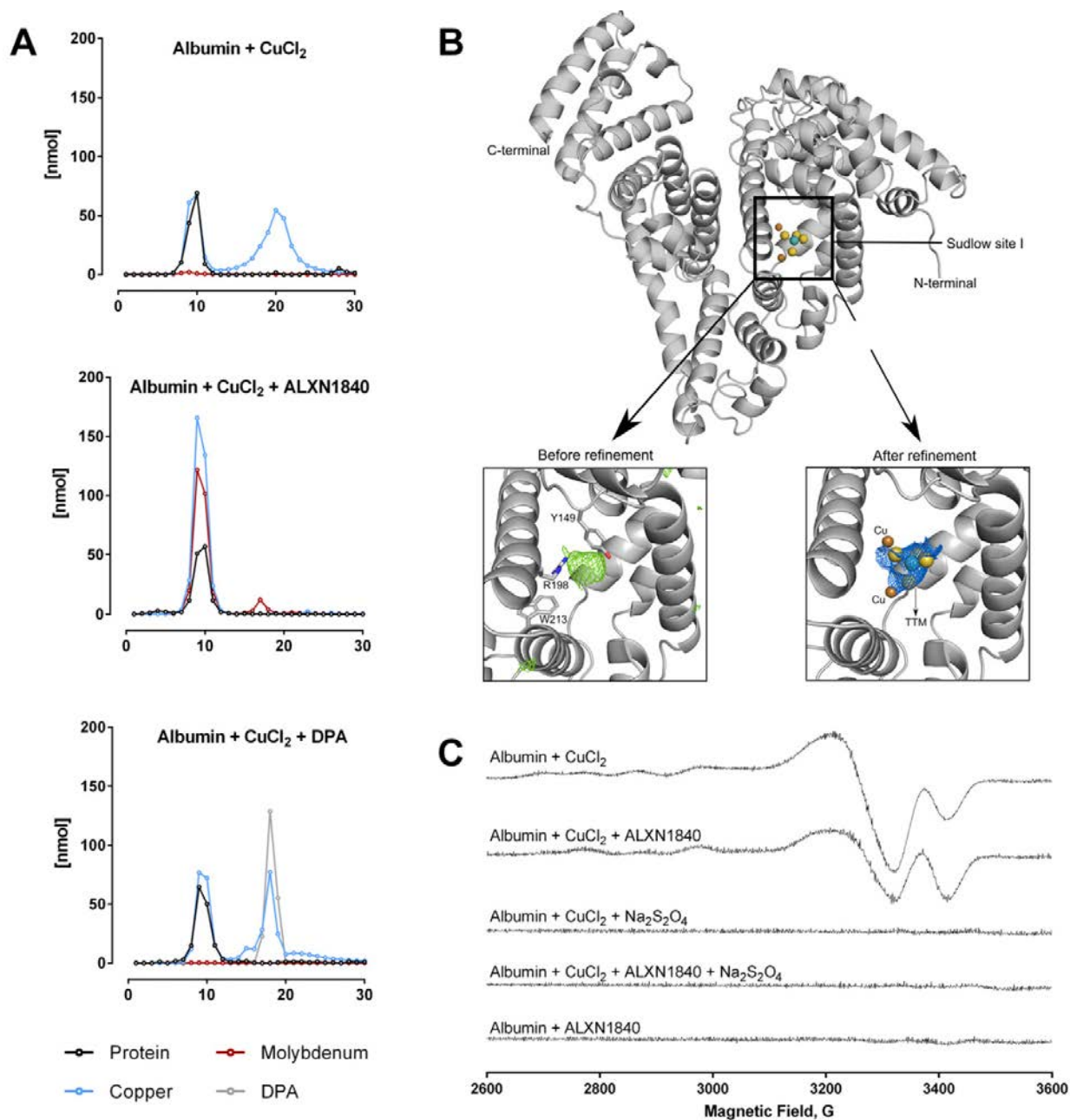
Figure 2. ALXN1840 forms a stable complex with albumin and copper. (A) Size-exclusion chromatography demonstrates that a Cu–albumin mixture of a molar ratio of 3:1 causes the formation of a Cu–albumin complex as well as a second peak representing unbound copper. In the additional presence of ALXN1840, a single peak is encountered, suggesting the formation of an albumin–Cu–ALXN1840 complex, in contrast to the addition of DPA (N = 2). (B) Structural analysis of albumin (upper panel) and its Sudlow site I (SsI). The lower panels present close-ups of SsI with calculated difference map (F_{obs}–F_{calc}, colored green) before (left) and after (right) refinement. ALXN1840 and copper atoms are covered by calculated $2F_{obs}$–F_{calc} map (colored blue), indicating the presence of these molecules inside SsI. (C) Electron paramagnetic resonance measurements reveal a partial reduction of Cu^{2+} in the albumin/Cu/ALXN1840 tripartite complex. Complete Cu^{2+} reduction is achieved by excess sodium dithionite ($Na_2S_2O_4$).

3.3.3 High-affinity chelation prevents Cu–albumin–induced cell toxicity

To demonstrate loosely albumin-bound copper toxicity, we tested hepatic HepG2 cells (human hepatocellular carcinoma) (Figs 3A and S2A) and surrogate brain cell types, such as EA.hy926 (human endothelium) (Figs 3B and S2B), U87MG (human astrocytoma) (Figs 3C and S2C) and SHSY5Y (human neuroblastoma) (Figs 3D and S2D) cells for their vulnerability against Cu–albumin. Albumin was at a concentration of 250 μM and increasing molar ratios of Cu versus albumin (1:1–10:1) were used to mimic its progressive copper load. Whereas at a molar ratio of 1:1, copper is rather tightly bound to albumin, at higher ratios (especially when ≥3:1) an increasing amount of loosely bound copper is available (exemplarily shown in Fig 2A top panel for a ratio of 3:1).
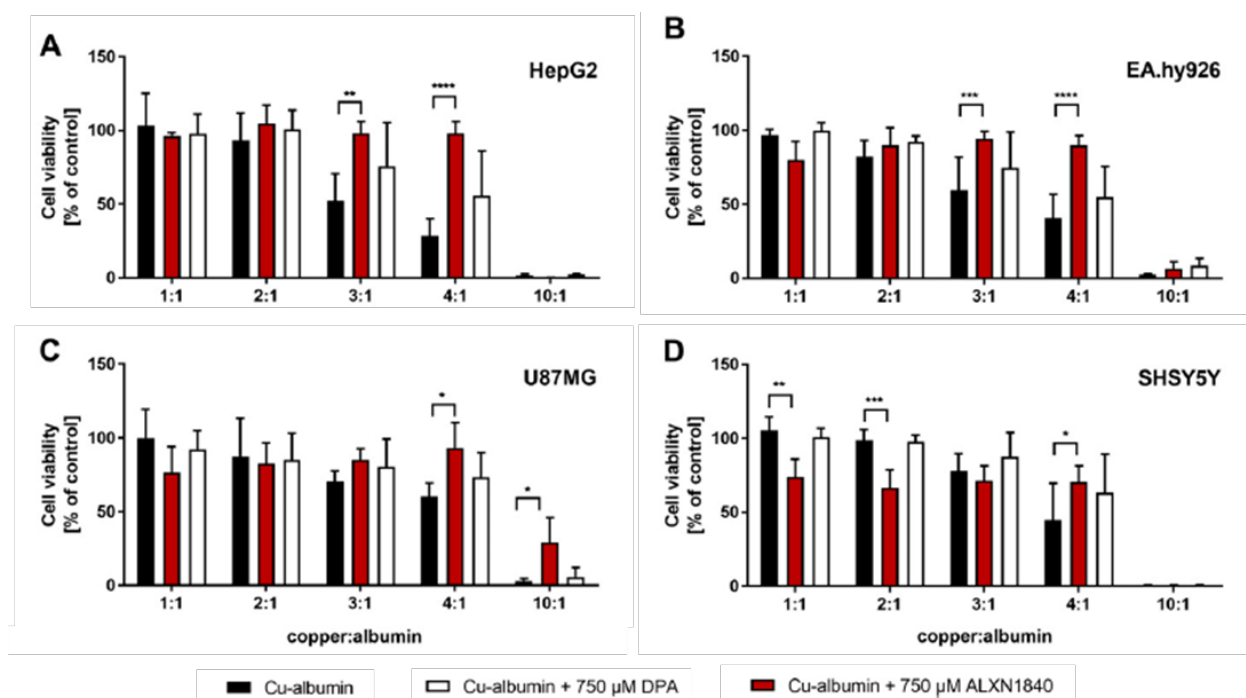
Figure 3. Cu–albumin ratio dependent toxicity. (A, B, C, D) Increasing molar Cu–albumin ratios cause a ratio dependent decrease in CellTiter-Glo-assessed cell viability in (A) HepG2, (B) EA.hy926, (C) U87MG, and (D) SHSY5Y cells. Such cytotoxicity is largely avoided by ALXN1840 but to a very minor part by DPA (both 750 μM, N = 3–5, n = 6–10). Two-way ANOVA with Dunnett's multiple comparisons test was used for statistical analysis. *P < 0.05, **P < 0.01, ***P < 0.001, ****P < 0.0001.

After 24 h of incubation, all tested cell lines demonstrated cellular toxicity against a dose-dependent increase in loosely albumin-bound Cu, as assessed by the CellTiter-Glo assay (Fig 3A–D, black bars). Importantly, the high-affinity chelator ALXN1840 at a concentration of 750 μM fully avoided toxicity up to a Cu–albumin ratio of 4:1 (Fig 3, red bars). In contrast, DPA was much less effective. Only in HepG2 cells, and only at a high 750 μM dose, a modest rescuing effect was observed upon DPA addition (Figs 3A and S2A, white bars) that was, however, completely absent, in, for example, endothelial EA.hy926 cells. Despite this admittedly artificial (with respect to total copper amount and observed time frame of 24 h for toxicity) testing scenario, these results nevertheless suggest that endothelial

cells may be particularly vulnerable to Cu–albumin and that DPA cannot block this Cu toxicity. Importantly, the lack of DPA rescue was not due to toxicity of DPA itself, as in a copper-free setting even DPA concentrations up to 2 mM were found to be nontoxic (Fig S3A). However, as a note of caution, at such settings, i.e. without external Cu–albumin addition, rather the high-affinity chelator ALXN1840 becomes toxic at elevated concentrations (Fig S3A), possibly because of an interference with copper containing vital enzymes such as the cytochrome c oxidase (Fig S3B).

3.3.4   ALXN1840 may prevent copper toxicity because of its high copper affinity

As can be seen in Fig 4, a profound dose of Cu–albumin (here at a ratio of 3:1) increased the cellular copper content more than 100-fold in all tested cell types (Fig 4, left panels), paralleled by massive cell death, with SHSY5Y cells being the least and EA.hy926 and HepG2 cells being the most affected (Fig 4 right panels). This copper toxicity could not be avoided even by high doses of DPA, that is, equimolar to copper (Figs 3 and 4, right panels). Moreover, a significant de-coppering was not noted in any of the cell lines upon DPA co-treatment despite a tendency for lower copper content in EA.hy926 and SHSY5Y cells (Fig 4, left panels). In remarkable contrast, co-treatment with the high-affinity chelator ALXN1840 significantly decreased the copper content in EA.hy926 and U87MG cells, and cellular viability was significantly maintained (Fig 4, right panels). These data indicate that the cell viability protection exerted by the high-affinity chelator, however, is at best only in part due to its capacity to lower the cellular copper content. In HepG2 cells, for example, highly similar cellular copper contents were found in cells either co-treated by ALXN1840, DPA, or treated by Cu–albumin alone (Fig 4, upper left panel). Despite this equal copper burden, ALXN1840 rescued HepG2 cells, whereas DPA did not (Fig 4, upper right panel). It therefore appears much more plausible that it is the enormous copper affinity of ALXN1840 (Kd ≈ 10 - 20) that avoided copper toxicity by its tight binding whether out- or inside cells. Indeed, even the highest known copper affinities of potential cellular binding partners are orders of magnitude lower (Kd ≈ 10–16 (48)). In contrast, as its dissociation constant is exactly in this latter range, this may also explain why DPA was unable to ensure or only tendentiously increased cellular viability.
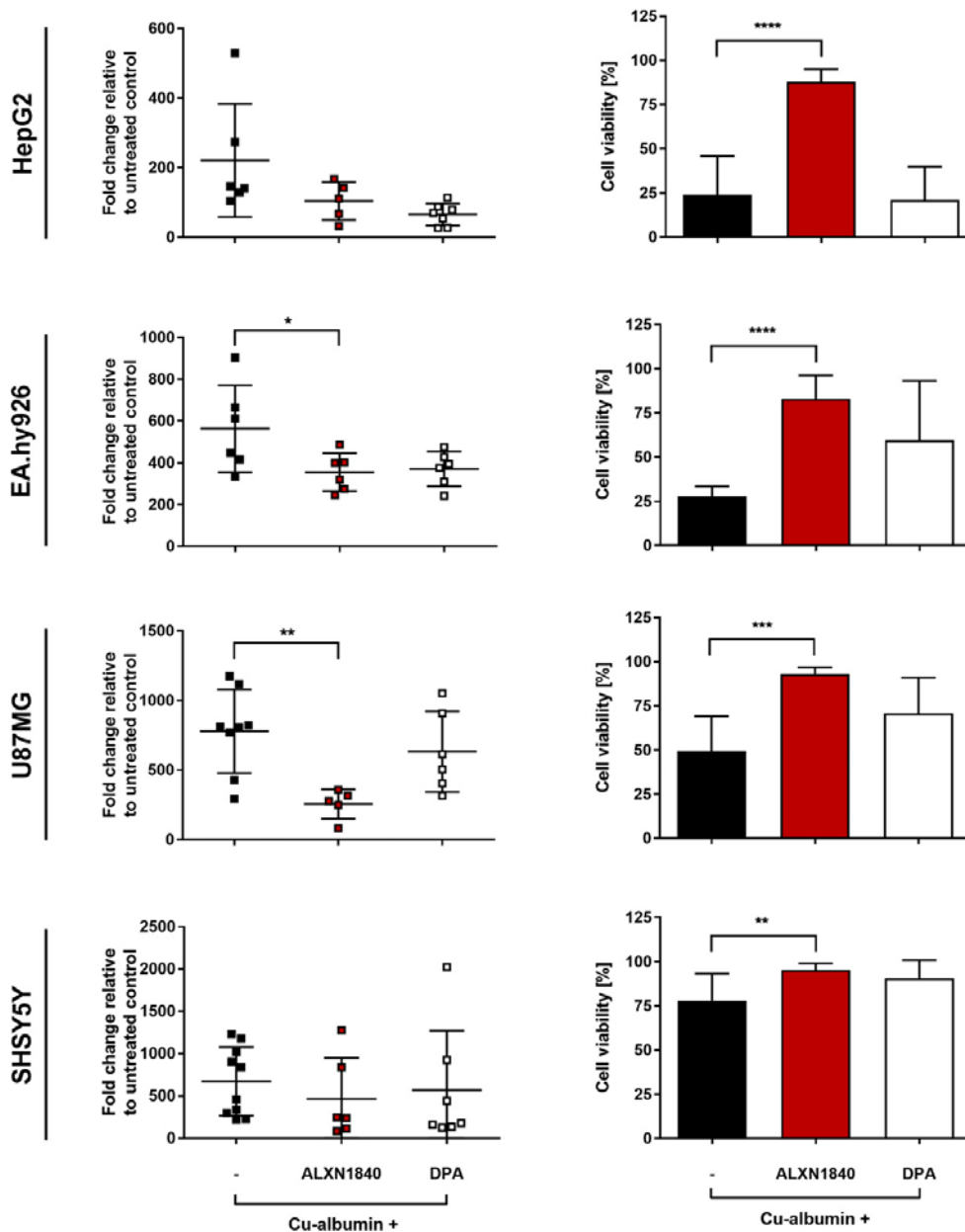
Figure 4. Massive cellular copper accumulations are partially resolved by ALXN1840. (Left panels) Cu–albumin incubation at a molar ratio of 3:1 (i.e., 750 µM Cu2+ and 250 µM albumin) leads to massive copper accumulation in all investigated cell lines. In the co-presence of ALXN1840, U87MG, and EA.hy926 cells, but not HepG2 and SHSY5Y cells, present with significantly lower copper content, not observed in the copresence of DPA (N = 4–12). One-way ANOVA with Dunnett's multiple comparisons test was used for statistical analysis. (Right panels) Such Cu–albumin incubations lead to massive cell viability loss of HepG2, EA.hy926, U87MG, and SHSY5Y as assessed by trypan blue staining. Co-presence of ALXN1840, but not of DPA, significantly protects all tested cell lines (N = 4–12). One-way ANOVA with Sidak's multiple comparisons test was used for statistical analysis. *P < 0.05, **P < 0.01, ***P < 0.001, ****P < 0.0001.

3.3.5   ALXN1840 ameliorates Cu–albumin–induced mitochondrial damage

In WD, reports have amply demonstrated that copper severely affects hepatocyte mitochondria [49, 50, 51]. Only very recently have comparative studies shown a high copper sensitivity of brain mitochondria [52]. Here, we have specifically looked to evaluate whether Cu–albumin could also impose structural and/or functional damage on mitochondria in cells that constitute the BBB, that is, endothelial cells and astrocytes. This was foremost because a clinical report had suggested copper-induced BBB damage to occur in neurologic WD patients [27]. To exclude mitochondrial impairment as secondary effect of copper-induced cell demise, we adjusted the Cu–albumin concentration (ratio 3:1) such that cell viability was comparable with untreated controls (Fig S4A). Besides, neither cellular protein content nor cell size were affected by such settings that, however, caused an enormous increase in cellular copper content with respect to untreated controls (Fig S4A).

Electron micrographs of Cu–albumin versus untreated cells demonstrated prominent mitochondrial structural alterations in EA.hy926 cells, and present, but more modest, alterations in U87MG cells (Fig 5A). A loss or structural disorientation of the mitochondrial cristae and membranous inclusions were observed (arrows in Fig 5A). Importantly, ALXN1840 co-treatment partially avoided these structural abnormalities, demonstrating mitochondria with electron-dense matrices and structured cristae similar to untreated control cells. In contrast, DPA was of no/minor effect as mitochondria presented with short and unstructured cristae and membranous inclusions (Fig 5A).

These structural deficits were paralleled by functional mitochondrial impairments (Fig 5B), which were especially apparent in high-resolution respiratory measurements of treated cells under fully uncoupled conditions (i.e., forcing mitochondria to maximal respiration, electron transport system [ETS], Fig S4B). When calculating the respiratory control ratios (the paradigm markers for mitochondrial integrity and functionality) by dividing either the "routine" (R, i.e., in presence of ADP) or the fully uncoupled state (ETS, i.e., upon titration with carbonyl cyanide m-chlorophenyl hydrazine (CCCP)) oxygen consumption rate by the so-called leak state (L, i.e., respiration w/o ADP), especially the E/L ratio demonstrated clear mitochondrial bioenergetic deficits, that again could, either significantly in the case of EA.hy926 cells or tendentiously in the case of U87MG cells, be avoided by the presence of ALXN1840, but not by DPA (Fig 5B).
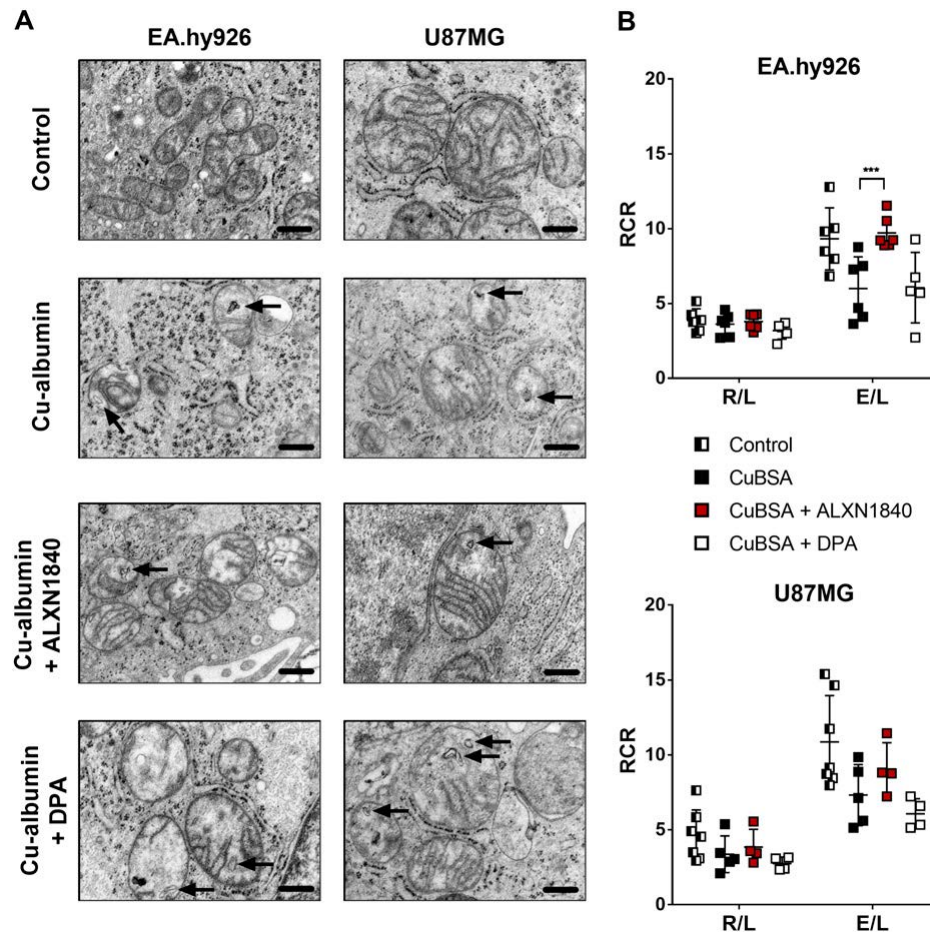
Figure 5. Cu–albumin–induced structural and functional mitochondrial alterations. (A) Cu–albumin incubation causes membranous inclusions and unorganized/shortened cristae in mitochondria of EA.hy926 and U87MG cells. In the co-presence of ALXN1840, but not of DPA, these alterations are partially resolved (Scale bars 500 nm). (B) Respiratory control ratios (RCR), defined as routine to leak respiration (R/L) or electron transport system to leak respiration (E/L). Co-presence of ALXN1840, but not of DPA, significantly/markedly augments the Cu–albumin induced E/L ratio drop in EA.hy926 and U87MG cells, respectively (N = 4–7). Two-way ANOVA with Dunnett's multiple comparisons test was used for statistical analysis. *P < 0.05, **P < 0.01, ***P < 0.001, ****P < 0.0001.

3.3.6   Disruption of the tight endothelial cell layer of the BBB by Cu–albumin is prevented by ALXN1840, but not by DPA

Human EA.hy926 endothelial (and U87MG astrocytoma) cells were highly vulnerable to increasing Cu–albumin challenges (Fig 3B) and demonstrated prominent mitochondrial structural and functional deficits (Fig 5). We thus reasoned that especially the endothelial cell layer that requires mitochondrial integrity and functionality for remaining tightly sealed within the BBB [53, 54], may constitute a pivotal target of Cu–albumin toxicity.

Consequently, we used a well-characterized *in vitro* model of the endothelial BBB using primary porcine brain capillary endothelial cells (PBCECs) cultivated on Transwell inserts [55, 56]. As in the BBB, these primary cells form a mono-cellular tight epithelial barrier, as can be biophysically assessed by

the continuous measurement of their transepithelial electrical resistance (TEER) and their monolayer capacitance as measure for cellular integrity [57].

First, we validated that increasing Cu–albumin concentrations (all at a molar ratio of 3:1) progressively decreased the TEER (Fig S5A). Of note, only the highest used Cu–albumin concentration (300 µM copper/100 µM albumin) caused a massive capacitance increase, that is, cell death, after 36 h of incubation (Fig S5A) that was additionally validated *via* the neutral red assay (Fig S5B). Thus, the leakiness of the endothelial cell layer of the BBB induced by lower Cu–albumin concentrations is not due to the mere induction of cell death but is a clear sign of endothelial cell stress.
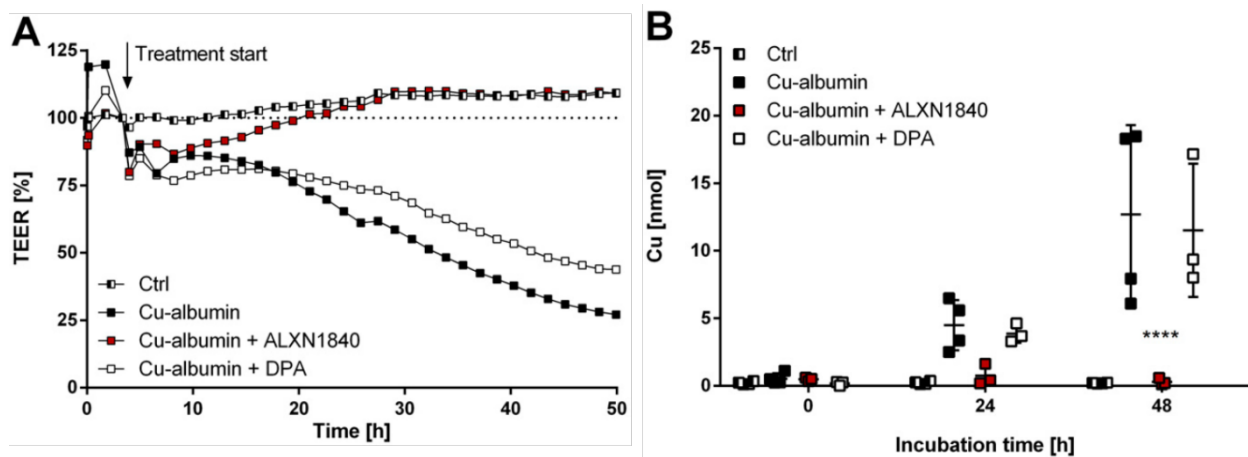
Figure 6. Cu–albumin permeabilizes blood–brain barrier constituting endothelial cell monolayers. (A) Cu–albumin (250 µM copper, 83.3 µM albumin), either alone or in the co presence of DPA, leads to a time-dependent reduction in the transepithelial electrical resistance (TEER) of primary porcine brain capillary endothelial cell monolayers that is avoided by the co-presence of 250 µM ALXN1840 (N = 2, n = 4). (B) Such decreased resistance is paralleled by progressive copper appearance in the basolateral compartment (resembling the brain parenchyma) (N = 2, n = 4). Two-way ANOVA with Dunnett's multiple comparisons test was used for statistical analysis. *P < 0.05, **P < 0.01, ***P < 0.001, ****P < 0.0001.

We subsequently determined the capability of the copper chelators ALXN1840 and DPA to prevent such Cu–albumin–induced endothelial BBB damage (Fig 6). Thereto, a Cu–albumin concentration (250 µM Cu/83.3 µM albumin, molar ratio of 3:1) was chosen that readily caused the BBB to become leaky (i.e., decrease the TEER, Fig 6A), but did not induce cell death within the observed time frame as evidenced by time-stable capacitance of the PBCEC monolayers (Fig S5C). Importantly, DPA co-treatment was not able to prevent the copper-induced TEER loss (Fig 6A). In contrast, PBCEC monolayers treated with Cu–albumin in the presence of ALXN1840 demonstrated stable TEER values for 48 h, indistinguishable from untreated monolayers (Fig 6A). This was further validated by determining the copper influx into the basolateral compartment of the Transwell system that is not directly accessible in tight PBCEC monolayers (control in Fig 6B). In fact, copper influx progressively occurred upon Cu–albumin treatment that could not be avoided by DPA but was fully avoided by

ALXN1840 co-treatments (Fig 6B). Thus, elevated Cu–albumin causes leakiness of the endothelial BBB layer already in the absence of endothelial cell death that is associated

with copper influx into the otherwise shielded compartment, and this can be avoided by the presence of ALXN1840, but not by DPA.

Finally, Cu–albumin–induced PBCEC monolayer damage can be visualized by either immunocytochemistry or electron microscopy (Fig 7). First, Claudin-5, an integral membrane protein of tight junction strands [58], demonstrated a continuous and uninterrupted distribution at the cell margins in untreated control cells. In contrast, Cu–albumin–treated PBCECs displayed gap formations between cells as well as serrated and diffuse Claudin-5 presence. Of note, this structural damage happens already at incubation conditions that do not elicit cell toxicity/death, that is, that do not kill the cells as their intact nuclei can be seen in the immunofluorescence (Fig 7) and also biophysically confirmed by a lack of capacitance increase (Fig S5A). In the presence of ALXN1840, Claudin-5 expression was continuous and uninterrupted, whereas the presence of DPA could not prevent copper-induced gap formation (Fig 7, left panels). Second, Zonula occludens-1 (ZO-1), an intracellular tight junction-associated protein [59], appeared continuously present and uninterrupted at the cell borders in untreated control PBCEC monolayers (Fig 7, middle panels). Upon Cu–albumin treatment, a pronouncedly more diffuse staining of ZO-1 occurred that could be fully protected by ALXN1840 co-treatment, but not by DPA (Fig 7, middle panels). Such a protein loss at the tight junctions was also apparent from, third, electron micrographs. In control PBCEC monolayers, because of deposition of the contrasting agent at protein-richmoieties, these structures appear electron dense. Upon Cu–albumin treatment, however, these structures were much more electron permissive, not protected for by DPA, but by ALXN1840 (Fig 7, right panels).
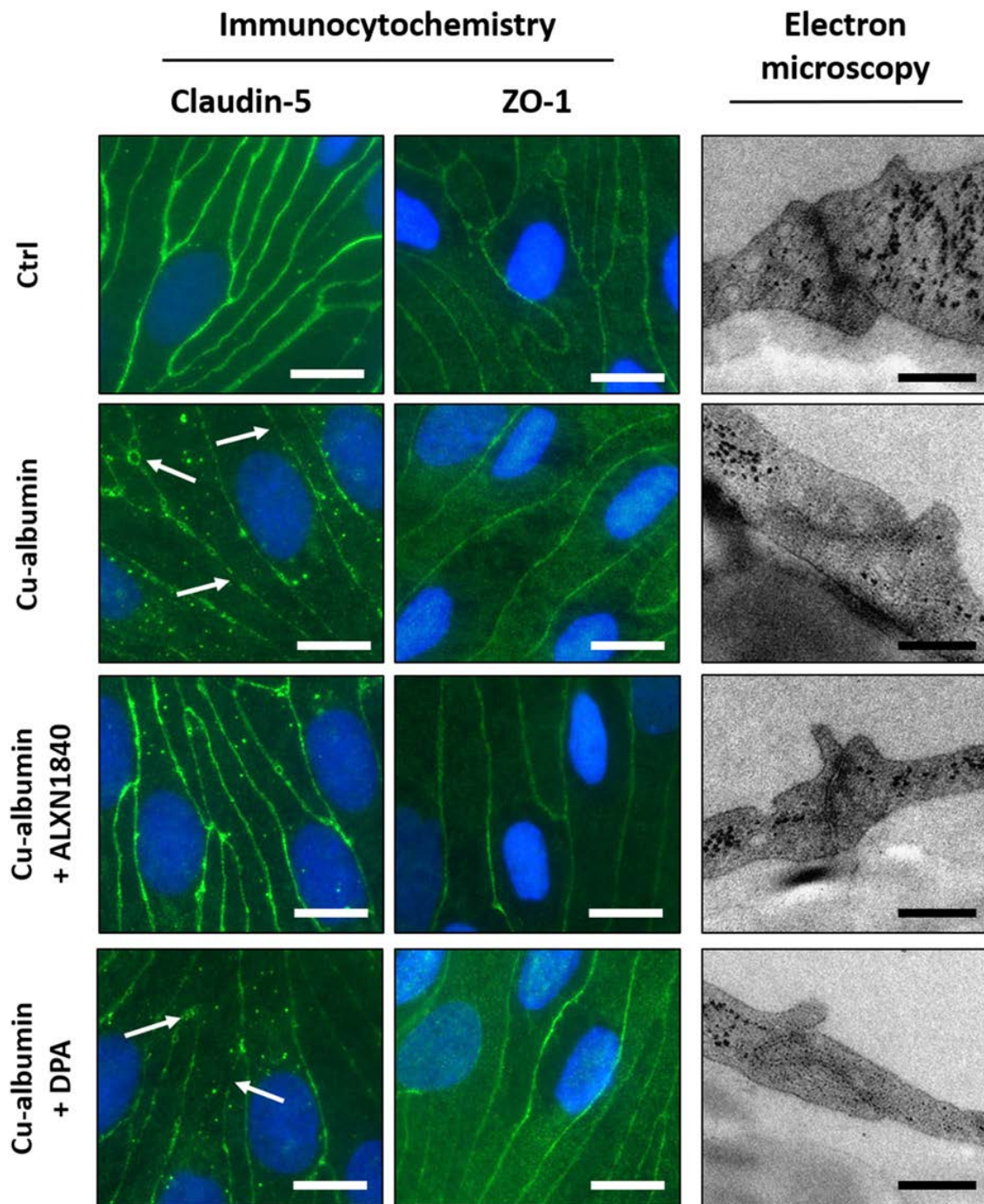
Figure 7. Cu–albumin disrupts tight junctions in blood brain barrier constituting endothelial cell monolayers. (Left panels) Immunocytochemistry staining against the tight junction protein Claudin-5 shows a continuous staining of the cell margins in control PBCECs, being disrupted upon Cu–albumin treatment (250 µM copper and 83.3 µM albumin). Co-presence of ALXN1840 (250 µM), but not of DPA, alleviates these morphologic alterations. (Middle panels) The tight junction–associated protein Zonula occludens-1 (ZO-1) reveals a plasma membrane associated or more diffuse cytosolic localization in either untreated control or Cu–albumin–treated PBCECs, respectively. Co-presence of ALXN1840, but not of DPA, avoids such diffuse localization. Scale bars equal 10 µm. Electron micrographs of Cu–albumin–treated versus control PBCECs reveal less electron-dense tight junction structures. Tight junctions appear electron dense upon co-presence of ALXN1840 but not of DPA. Scale bars equal 250 nm.

3.4 Discussion

In this study, we have demonstrated that intravenously present copper can easily access the brain supporting vessels (Fig 1) and that upon increase, copper is progressively loosely bound to serum albumin (Fig 2). Such Cu–albumin is cell-toxic (Figs 3 and 4) and endothelial cells that constitute the tight barrier to protect the brain are especially vulnerable. At Cu–albumin concentrations that do not exert immediate cell death, mitochondria are a vulnerable target (Fig 5) and affected cells of the endothelial barrier demonstrate leaky tight junctions, resulting in a progressive copper cross-transition (Figs 6 and 7). Importantly, all these features were largely avoided by co-treatment with the high-affinity copper chelator ALXN1840, but not with DPA (Figs 2, 3, 4, 5, 6, and 7).

How do these findings relate to *in vivo* situations in WD patients, where 18–68% have been reported to suffer from neurological symptoms, for example, tremor, dysarthria, and dystonia [13], and their disease severity has been suggested to correlate with increased available serum copper?

First, massively elevated copper brain levels have been observed in WD patients. This may be realized as counterintuitive because serum albumin has an enormous capacity to tightly bind the metal at a binding site with very high affinity. Moreover, blood copper concentrations in neurologic WD patients are considerably lower than albumin's binding capacity. A possible explanation for how copper could nevertheless slowly accumulate in the brain may be a constant competition for Cu between serum albumin and the copper uptake transporter CTR1 at the BBB, which would result (after years/decades) in brain damage. The other not mutually exclusive possibility is repeated focal hepatocyte death in the liver to cause repetitive intense copper pulses in the blood that may overwhelm the serum albumin binding capacity, thus allowing copper uptake into brain. Indeed, in Atp7b$^{-/-}$ rat livers, copper is not evenly distributed but rather present in "copper hotspots" with 3.5 times higher copper concentration than the surrounding liver tissue [60]. Demise of such hotspots could possibly result in transient copper pulses. In a collaborative effort, we have very recently determined an extractable serum Cu of 4.0 ± 2.3 µM in healthy control rats, 2.1 ± 0.6 µM Cu in healthy Atp7b$^{-/-}$ rats, and 27 ± 16 µM Cu in diseased Atp7b$^{-/-}$ rats, using a Cu-specific column that separates bound Cu from extractable Cu [61]. In agreement with these data, we did not see elevated urinary copper excretion in untreated but still healthy Atp7b$^{-/-}$ rats similar to controls (Fig 1C), but in contrast to findings in WD patients. Thus, it is only upon hepatocyte death in the Atp7b$^{-/-}$ rats (i.e., when they become diseased) that there are up to 10-fold higher amounts of "free" copper in serum that may be taken up by the brain. However, when hepatitis starts animals die shortly after and before developing neuronal symptoms, thereby precluding the study of neurological deficits in these animals. Furthermore, as ATP7B is present in the blood-facing membrane of the cerebral endothelium [24], mutations in ATP7B could lead to a reduced/blocked re-transport of excessive copper into the blood, thereby causing a one-way entry of the metal into the brain parenchyma. Here, only ATP7A-mediated copper transport *via* the

cerebrospinal fluid back into the systemic circulation would allow lowering brain copper [24]. Taken together, these results would explain the observed correlation in WD patients of neurological severity and increasing NCC correlating with such insults [7]. Perhaps, the strongest indication for such a "copper pulse" scenario is the worsening of neurological symptoms observed in up to 50% of neurologic WD patients seen shortly after starting the treatment with the copper chelator DPA [28, 29, 30, 31, 32, 33, 34]. This unwanted drug effect was attributed to the (abrupt) mobilization of copper from the liver into the bloodstream, thereby leading to an increased copper accumulation in the brain [9]. Indeed, in the WD animal model toxic milk mouse, there is some experimental evidence for this viewpoint. Upon intragastric D-penicillamine (DPA) administration, within days, a significant increase in copper in serum and also in brain was demonstrated in these mice [9], and thus one may conclude that it is the DPA taken up by the portal vein that liberates liver copper to cause serum and brain copper elevations. Consequently in WD patients, current clinical guidelines follow a "start low and go slow" strategy, that is, a careful upward titration of DPA over weeks and months to avoid a rapid transitory increase in toxic, non-ceruloplasmin–bound copper in the blood [62, 63].

As Atp7b$^{-/-}$ rats shortly die upon hepatitis onset, we thus switched to cellular studies here to investigate potential toxicity to such copper pulses, that is, loosely albumin-bound copper. As the by far major copper binder in Atp7b$^{-/-}$ rat serum is albumin, we thus used an albumin concentration close to the physiological range. Furthermore, using the reported affinity values for the diverse albumin copper-binding sites, we came up with the setting of different molar copper/albumin ratios to mimic situations with tightly versus more loosely bound copper. Clearly, these conditions are artificially high with respect to the added copper (in absolute amounts) here. It should, however, be mentioned that we investigated 24-h incubations (in contrast to years/decades of clinical silence in neurological WD). In fact, when a low ratio (1:1) was used, no cell toxicity in any of the tested cell types was encountered. This demonstrates the enormous binding capacity of albumin thereby avoiding acute cell toxicity. However, when the Cu to albumin ratio rose, cell viability went down, with endothelial cells being especially vulnerable. Importantly, an increased mitochondrial impairment and disruption of the cellular connectivity of endothelial cell layers resembling the first barrier of the BBB, appeared as early signs of such Cu–albumin toxicity, that is, without the initiation of cell death. Moreover, such an initial damage already allowed for progressive trans/para-epithelial copper passage. We therefore suggest endothelial BBB damage upon elevated loosely plasma protein-bound copper as one potential initial damage mechanism in neurologic WD that would subsequently allow for facilitated copper entry into the brain. It will be highly interesting to see in clinical settings whether this conceptual conclusion from our study can be validated.

Second, neurological worsening has been reported to occur frequently with DPA treatment but much less frequently upon TTM treatment. This could be due to a differentially altered presence of loosely

plasma protein-bound copper upon diverse chelator treatment. The high-affinity copper chelator ALXN1840 caused the removal of loosely bound copper from albumin and its embedding into a deep cleft of the protein itself (termed tripartite complex TPC). Although it is unclear (due to the obtained low-resolution crystallography data) whether copper has also been removed from the high-affinity copper-binding site by ALXN1840, loosely bound copper was removed. Indeed, such TPC formation upon ALXN1840/TTM administration (either orally or injected) has been demonstrated *in vivo* in Atp7b$^{-/-}$ rats and WD patients as well [35, 42, 64, 65]. Consequently, hardly any signs of Cu–albumin toxicity were encountered in our study upon TPC formation. This may either be due to a lower cellular TPC uptake versus loosely bound copper resulting in lower cellular copper levels, or a firm continuous association of copper and ALXN1840 (even within cells in the studied time frames of 1–2 d). In contrast, DPA routed copper to the urine, demonstrating its passage into the blood and renal clearance. Such DPA-initiated copper urinal excretion was, however, quantitatively limited as only 10% of the net copper intake of Atp7b$^{-/-}$ rats can be found in the urine upon DPA treatment (i.e., 0.4 µmol/24 h of a total net uptake of ~3.95 µmol/24 h, unpublished observation). Nevertheless, renal copper clearance by DPA occurred fast [41], as 3 d after treatment stop, we did not observe elevated blood copper. As DPA is administered several times daily to WD patients, rapidly elevated blood copper peaks may arise. Such DPA-initiated copper peaks would be subjected to redistribution, positively to the urine but negatively to the brain. In fact, upon co-incubating different cell types with Cu–albumin and DPA, that is, avoiding an excretion route, these potentially negative effects became amply visible in our study. As with Cu–albumin alone, hardly any beneficial effect was encountered upon DPA presence. Thus, only when DPA-bound blood copper is excreted fast such negative effects may be avoided. Of note, another potential binding partner for DPA-mobilized liver copper may be the high-affinity binding site of albumin itself, potentially resulting in recirculating copper liver reuptake, thereby plausibly explaining why WD patient livers, even years after DPA treatment are still heavily burdened with copper [66].

And finally, neurological damage occurs frequently in WD patients. Given the early studies by Vogel et al [67, 68], who demonstrated direct copper toxicity in cat brains, but also other species, together with the strongly elevated copper levels in neurologic WD patients [10, 11, 12], the current consensus holds that copper is the prime responsible neurotoxin in these patients. Indeed, we found that all tested cell lines including surrogate neuronal and astrocytic cells, are highly vulnerable to copper that dissociates from albumin. As we and others have earlier reported that neurons have comparatively very low-protective metallothioneins [52, 69, 70], these cells appear relatively unprotected against copper insults. In this respect, copper-induced damage to the protective barrier cells, as demonstrated in our study, presents an enormous threat as it would cause a comparatively uncontrolled copper entry into the brain. In agreement, Stuerenburg suggested an involvement of the BBB in four neurologic WD

patients showing neurological deterioration under DPA treatment paralleled by an increased BBB damage [27]. As we did not observe a rescue of the endothelial BBB by DPA co-treatment, but DPA may cause massive copper mobilization into blood, this could have two detrimental consequences. First, especially neurologic WD patients with pre-damaged BBB would be highly vulnerable to such chelator-induced copper pulses, and second, elevated presence of such DPA-bound copper in blood could even worsen pre-existing BBB damage. This suggests that neurologic patients may be tested for BBB damage (e.g., by determination of S100B levels in blood or of the albumin ratio cerebrospinal fluid/serum) before DPA treatments are initiated. Importantly, we find that such damage or leakiness occurs already at non-toxic doses and identified endothelial cell mitochondria as one vulnerable target. In fact, Doll et al. described mitochondria as "key players in BBB permeability" [53]. In agreement with our study, manipulation of mitochondrial respiration was paralleled with a rapid increase in BBB permeability and disruption of the tight junctions.

In summary, we propose the BBB as a highly sensitive structure to abrupt blood copper overload. In addition, we linked the occurrence of neurological worsening upon DPA co-treatment to its inability to rescue such damage. In contrast, high-affinity chelators seem to be much more protective in this respect. Indeed, ALXN1840 was found to effectively bind loosely attached albumin copper (in this case forming the tripartite complex), and largely avoided BBB copper toxicity. It will be interesting to extend the concept of this study in the future to further WD treatments, either already existing, that is, to zinc and trientine, or in development. Although we have admittedly used an *in vitro* system to demonstrate acute toxicity on the BBB constituting cells, this study nevertheless suggests such damage to be checked for in neurological WD patients. Given that earlier findings of such impairments in a few neurological WD cases hold true in more patients, our study suggests that BBB damage pre-screening should be envisioned before treatments with low/ intermediate copper affinity chelators are initiated.

3.5 Materials and Methods

3.5.1 MicroPET/magnetic resonance imaging (MRI)

Wild-type rats underwent anatomical MRI 1T and dynamic PET (Mediso Medical Imaging Systems). Anesthesia with isoflurane was initiated with the rat placed in an acrylic glass chamber and maintained with respiration in a mask during the scan. A bolus of ^{64}Cu (≈10 MBq/animal) was injected *via* a tail vein catheter or intraperitoneal. PET scanning was performed the first 120 min after injection, followed by a 25-min T1-weighted MRI scan. Body temperature and respiration frequency were monitored during anesthesia. PET images were reconstructed with a three-dimensional ordered subset expectation algorithm (Tera-Tomo 3D; Mediso Medical Imaging Systems) with four iterations and six subsets and a voxel size of 0.6 × 0.6 × 0.6mm3. Data were corrected for dead-time, decay, and randoms using delayed coincidence window without corrections for attenuation and scatter. The 120-min

dynamic PET scans were reconstructed as 8 frames of 15 min and presented as standardized uptake value. The animal study was approved by Dyreforsøgstilsynet under the Danish Ministry for Veterinary and Food Administration. The study was carried out in strict accordance with the recommendations in the Guide for the Care and Use of Laboratory Animals, EEC Council Directive 2010/63/EU.

3.5.2 Animal studies

Animals were maintained under the Guidelines for the Care and Use of Laboratory Animals of the Helmholtz Center Munich. Animal experiments were approved by the government authorities of the Regierung von Oberbayern. Control Atp7b$^{+/-}$ and WD Atp7b$^{-/-}$ rats were fed ad libitum with normal chow (1314; 13.89 mg Cu/kg; Altromin Spezialfutter GmbH) and tap water. All rats were healthy at treatment start and presented no signs of acute liver damage (serum aspartate aminotransferase <200 U/l and serum bilirubin <0.5 mg/dl). Atp7b$^{-/-}$ rats (age: 79–96 d) were treated intraperitoneally for 4 consecutive days with 2.5 mg/kg body weight (bw) ALXN1840 once daily or 100 mg/kg bw DPA once daily. Untreated Atp7b$^{+/-}$ and Atp7b$^{-/-}$ rats served as controls. Urine and feces were collected at 24 h intervals for which rats were housed individually in metabolic cages for 4 d. After a 2 d resting period off treatment in normal cages and group housing, rats were euthanized for serum collection. Copper levels in urine, serum, and feces were analyzed by inductively coupled plasma optical emission spectrometry (ICP-OES, ARCOS, SPECTRO Analytical Instruments) as previously described [49].

3.5.3 Gel filtration chromatography

10 mg of fatty acid–free bovine serum albumin (subsequently referred to as albumin, Carl Roth) was resuspended in 10 mM Tris–HCl buffer (pH 7.4) and mixed with 45 µl of 10 mM copper chloride. Where indicated, 45 µl of 10 mM ALXN1840 or DPA was added to the Cu–albumin complex before loading the samples onto a Superdex 75 10/300 GL column (GE Healthcare). 1 ml fractions were analyzed for protein content by the Bradford assay [71], molybdenum and copper levels by ICP-OES [49], and DPA content using 1,2-naphthoquinone-4-sulfonate (NQS) as previously described [72] with minor modifications. Briefly, 50 µl of each fraction was mixed with 10 µl 0.2% NQS, 10 µl of 0.2 M sodium phosphate buffer (pH 12.0), and 30 µl ddH2O in a clear 96-well plate. The samples were incubated for 20 min and absorbance was measured at 452 nm. Absolute levels of DPA were calculated using equally treated DPA standard solutions (25–250 µM).

3.5.4 X-ray crystallography of the tripartite complex copper–albumin–ALXN1840 (TPC)

100 mg albumin was suspended in buffer containing 50 mM potassium phosphate and 150 mM sodium chloride (pH 7.5). Copper chloride and ALXN1840 were added in double molar excess and the mixture was incubated for 30 min at 37°C. The Cu–albumin–ALXN1840 mixture was loaded onto an S200 gel filtration column equilibrated with PBS (pH 7.4). Fractions corresponding to the Cu–albumin–

ALXN1840 (TPC) in the monomeric state were pooled and protein was concentrated to 100 mg/ml. Screening for crystallization conditions was performed using commercially available buffer sets in a sitting-drop vapor-diffusion setup by mixing 0.2 µl of protein complex solution and 0.2 µl of buffer solution. Crystals were obtained at room temperature from a solution containing 0.1 M succinic acid, sodium dihydrogen phosphate, glycine buffer (pH 7.0), and 0.25% PEG 1500. Crystals were cryo-protected in 30% glycerol in the mother liquor and flash-cooled in liquid nitrogen. The diffraction data were collected at the ID23-2 beamline at the European Synchrotron Radiation Facility. The data were indexed and integrated using X-ray detector software [73, 74], scaled and merged using Scala [75]. The initial phases were obtained by molecular replacement calculated using Phaser [76] and albumin structure as a search model (protein database 4F5S and reference 77). The initial model was manually rebuilt because of the resulting electron density maps using Coot [78]. Because of the low resolution of data, refined structure did not reach Rfree values below 0.40. Nevertheless, we were able to analyze a final model in terms of presence of ALXN1840 because of the high scattering factor of the molybdenum complex resulting in a strong detectable signal.

3.5.5 EPR

For EPR measurements, complexes of Cu–albumin (2 mM/1 mM), Cu–albumin–ALXN1840 (TPC, 2 mM/1 mM/1 mM), and albumin– ALXN1840 (1 mM/1 mM) were prepared in 10 mM Tris/HCl (pH 7.4) buffer and reduced with an excess of sodium dithionite (Merck) shortly before measurements where indicated. EPR spectra were recorded at 77 K using an ECS106 spectrometer (Brucker BioSpin) operating in X-band at about 9.5 GHz.

3.5.6 Cell culture

SHSY5Y (human neuroblastoma), U87MG (human astrocytoma), EA.hy926 (human endothelium), and HepG2 (human hepatocellular carcinoma) cells were from ATCC and were cultured in DMEM supplemented with 10% FCS (Biochrom) and 1% antibiotic-antimycotic (Life Technologies). All cells were maintained at 37°C in a humidified atmosphere with 5% CO2.

3.5.7 Cell toxicity assays

2×10^4 cells were seeded into each well of a 96-well plate and incubated overnight. On the next day, cells were treated for 24 h with increasing copper concentrations (0–2,500 µM) and 250 µM albumin (resulting in Cu–albumin molar ratios of 1:1, 2:1, 3:1, 4:1, and 10:1) in the absence or presence of 750 µM ALXN1840 or DPA in DMEM (2% FCS). Cell toxicity was either determined by CellTiter-Glo assay (Promega) or Trypan blue exclusion test [79].

3.5.8   Cellular copper content

2×10^6 cells were incubated for 24 h with 750 µM copper and 250 µM albumin (i.e., at a Cu–albumin molar ratio of 3:1) in the absence or presence of 750 µM ALXN1840 or DPA, respectively, in DMEM (2% FCS). Afterwards, cells were trypsinized and counted. Cell viability was determined by Trypan blue exclusion test. Copper and molybdenum content of cells was analyzed by ICP-OES (Ciros Vision, SPECTRO Analytical Instruments) as previously described [49].

3.5.9   Electron microscopy

Electron microscopy of cells was performed as previously described (50) on a 1200EX electron microscope (JEOL) at 60 kv. Pictures were taken with a KeenView II digital camera (Olympus) and processed by the iTEM software package (analySIS FIVE, Olympus).

3.5.10   Mitochondrial function

U87MG and EA.hy926 cells were pretreated for 24 h with DMEM (2% FCS) alone or with DMEM (2% FCS) containing 750 µM copper chloride and 250 µM albumin in the absence or presence of 750 µM ALXN1840 or DPA. Oxygen consumption was assessed by high resolution respirometry using the Oxygraph-2k and DatLab 7.0 (Oroboros Instruments GmbH) as described previously [80]. Per chamber, $1.5–2 \times 10^6$ living cells were supplied in 2 ml of MiR05 buffer (0.5 mM EGTA, 3 mM $MgCl_2$, 60 mM lactobionic acid, 20 mM taurine, 10 mM KH_2PO_4, 20 mM Hepes, 110 mM sucrose, 1 g/l albumin, pH 7.1) and routine respiration was measured. Addition of 2.5 µM oligomycin (inhibitor of the FOF1-ATPase) enabled the measurement of leak respiration and stepwise addition of CCCP (1 µl steps from 1 mM stock solution) allowed the determination of the maximum oxygen flux and thereby the capacity of the ETS. The oxygen flux was baseline-corrected for non-mitochondrial oxygen consuming processes (ROX) by the addition of 2.5 µM of the complex III–inhibitor antimycin A. For complex IV activity measurements, cells were pretreated for 24 h with DMEM (2% FCS) alone or with DMEM (2% FCS) containing 750 µM copper chloride and 250 µM albumin in the absence or presence of 750 µM ALXN1840 or DPA. Complex IV activity was measured as previously described [81]. Briefly, about 2.5×10^6 cells were detached, washed two times with PBS by centrifugation and the cell pellet was resuspended in 200 µl of 20 mM hypotonic potassium buffer. After three freeze-thaw cycles, complex IV activity was measured by adding 10 µl of the sample to 90 µl of 50 mM potassium phosphate buffer (pH 7.0) containing 50 µM reduced cytochrome c with or without 0.3 mM KCN. Absorbance was measured at 550 nm for 10 min in a plate reader (Synergy 2, BioTek Instruments, Inc.) and complex IV activities were calculated from the linear slopes of the initial rates corrected for unspecific activity (in the presence of KCN) and normalized to the protein content determined by the Bradford assay [71].

3.5.11 Endothelial BBB model

For transepithelial resistance (TEER) experiments [82], cryopreserved primary porcine brain capillary endothelial cells (PBCECs) were thawed and seeded either on rat tail collagen coated 96-well plates for cytotoxicity testing using the neutral red assay [83] or Transwell inserts (area: 1.12 cm^2, pore size: 0.4 µm; Corning) for barrier integrity studies. Cells were cultured for 48 h in Earle's Medium 199 supplemented with 10% FCS, 50 U penicillin/ml, 50 µg/ml streptomycin, 100 µg/ml gentamycin, and 0.7 mM l-glutamine and maintained at 37°C in a humidified atmosphere with 5% CO2. Subsequently, the medium was changed to DMEM/Ham's F 12 (1:1) containing 50 U penicillin/ml, 50 µg/ml streptomycin, 100 µg/ ml gentamycin, and 4.1 mM L-glutamine and 550 nM hydrocortisone for additional 48 h upon which the medium was changed to the treatment solution containing 250 µM copper (and 83.3 µM albumin, Cu–albumin molar ratio 3:1) in the absence or presence of 250 µM DPA or ALXN1840, respectively. TEER and capacitance values were continuously monitored over 48 h using a CellZscope device (nanoAnalytics). Only PBCEC monolayers with initial TEER values >600 Ω × cm^2 and capacitance values between 0.45 and 0.6 µF/cm^2 were used for permeability studies [84]. The barrier integrity was calculated by normalizing the TEER values to the respective start values. At treatment start, after ~24 and 48 h exposure to the test substances, 20 µl of the apical medium as well as 40 µl of the basolateral medium were collected for subsequent copper determination. Total copper was determined by ICP-MS/MS as previously described [85].

For the immunocytochemical staining of tight junction proteins, confluent PBCECs cultivated on Transwell membrane inserts were processed as previously described [55]. Briefly, PBCECs were fixed with formaldehyde and permeabilized using Triton X-100. After blocking of unspecific binding sites by albumin, the cells were incubated with the either anti–Claudin-5 or anti-ZO-1 antibody (Zytomed Systems GmbH). After a second blocking step, the cells were treated with an Alexa Fluor 488-conjugated secondary antibody (Invitrogen, Molecular Probes Inc.). Hoechst 33258 (Merck) was used to stain cell nuclei. Subsequently, membranes were cut out of the inserts and mounted in Aqua Poly/Mount (Polysciences Inc.). After a solidification period of 24 h, the samples were evaluated using a DM6 B fluorescence microscope by Leica Microsystems CMS GmbH in combination with the Leica Application Suite X. Electron microscopy of PBCECs grown on Transwell inserts was performed as previously described [86] with minor modifications. Briefly, after fixation with 2.5% glutaraldehyde, cell monolayers were post-fixed with 1% osmium tetroxide for 30 min and dehydrated by ethanol. Cell monolayers were gradually embedded in epoxy resin in ethanol (1:2, 1:1, 2:1 for 20 min each) and finally embedded in 100% epoxy resin for 48 h at 60°C without preembedding before cutting and image acquisition.

3.5.12   Miscellaneous/statistics

Chemicals were obtained from Sigma-Aldrich if not stated otherwise. DPA was a kind gift from Heyl Pharma. ALXN1840 was a kind gift from Alexion AstraZeneca Rare Disease. Cellular protein levels were determined by the BCA assay [87]. Cell size was determined using a LUNA-II Automated Cell Counter (Logos biosystems). Throughout this manuscript "N" designates the number of biological replicates and "n" the number of technical replicates. Data are mean values with SD. Statistical significance was analyzed with the respective tests indicated in the figure legends using GraphPad Prism 7 (GraphPad Software Inc.).

3.6   Supplementary Information

Supplementary Information is available at https://doi.org/10.26508/lsa.202101164.

3.7   Acknowledgements

3.8   Author Contributions

S Borchard: conceptualization, data curation, investigation, and methodology.
S Raschke: investigation and methodology.
KM Zak: investigation.
C Eberhagen: investigation.
C Einer: investigation.
E Weber: investigation.
SM Müller: investigation.
B Michalke: investigation and methodology.
J Lichtmannegger: data curation, investigation, and methodology.
A Wieser: investigation and methodology.
T Rieder: investigation and methodology.
GM Popowicz: data curation, formal analysis, validation, investigation, and methodology.
J Adamski: validation.
M Klingenspor: validation.
AH Coles: validation.
R Viana: formal analysis, funding acquisition, and validation.
MH Vendelbo: investigation.
TD Sandahl: resources and investigation.
T Schwerdtle: investigation and methodology.
T Plitz: conceptualization.
H Zischka: conceptualization, data curation, supervision, funding acquisition, and writing—original draft.

3.9 Conflict of Interest Statement

AH Coles and R Viana are employees and shareholders of Alexion Astra-Zeneca Rare Disease. T Plitz was an employee of Wilson Therapeutics.

3.10 References

[1] Wilson SAK (1912) Progressive lenticular degeneration: A familial nervous disease associated with cirrhosis of the liver. Brain 34: 295–507. doi:10.1093/brain/34.4.295

[2] Bull PC, Thomas GR, Rommens JM, Forbes JR, Cox DW (1993) The Wilson disease gene is a putative copper transporting P-type ATPase similar to the Menkes gene. Nat Genet 5: 327–337. doi:10.1038/ng1293-327

[3] Petrukhin K, Fischer SG, Pirastu M, Tanzi RE, Chernov I, Devoto M, Brzustowicz LM, Cayanis E, Vitale E, Russo JJ (1993) Mapping, cloning and genetic characterization of the region containing the Wilson disease gene. Nat Genet 5: 338–343. doi:10.1038/ng1293-338

[4] Tanzi RE, Petrukhin K, Chernov I, Pellequer JL, Wasco W, Ross B, Romano DM, Parano E, Pavone L, Brzustowicz LM (1993) The Wilson disease gene is a copper transporting ATPase with homology to the Menkes disease gene. Nat Genet 5: 344–350. doi:10.1038/ng1293-344

[5] Bearn AG, Kunkel HG (1954) Abnormalities of copper metabolism in Wilson[R8S2Q1M7]s disease and their relationship to the aminoaciduria. J Clin Invest 33: 400–409. doi:10.1172/JCI102912

[6] Scheinberg IH, Sternlieb I (1984) Major problems in internal medicine Wilson[R8S2Q1M7]s Disease. Philadelphia: Saunders: 171. leaves of plates.

[7] Poujois A, Trocello JM, Djebrani-Oussedik N, Poupon J, Collet C, Girardot- Tinant N, Sobesky R, Habès D, Debray D, Vanlemmens C, et al (2017) Exchangeable copper: A reflection of the neurological severity in Wilson [R8S2Q1M7]s disease. Eur J Neurol 24: 154–160. doi:10.1111/ene.13171

[8] Allen KJ, Buck NE, Cheah DM, Gazeas S, Bhathal P, Mercer JF (2006) Chronological changes in tissue copper, zinc and iron in the toxic milk mouse and effects of copper loading. Biometals 19: 555–564. doi:10.1007/ s10534-005-5918-5

[9] Chen DB, Feng L, Lin XP, Zhang W, Li FR, Liang XL, Li XH (2012) Penicillamine increases free copper and enhances oxidative stress in the brain of toxic milk mice. PLoS One 7: e37709. doi:10.1371/journal.pone.0037709

[10] Cumings JN (1948) The copper and iron content of brain and liver in the normal and in hepato-lenticular degeneration. Brain 71: 410–415. doi:10.1093/brain/71.4.410

[11] Faa G, Lisci M, Caria MP, Ambu R, Sciot R, Nurchi VM, Silvagni R, Diaz A, Crisponi G (2001) Brain copper, iron, magnesium, zinc, calcium, sulfur and phosphorus storage in Wilson[R8S2Q1M7]s disease. J Trace Elem Med Biol 15: 155–160. doi:10.1016/S0946-672X(01)80060-2

[12] Litwin T, Gromadzka G, Szpak GM, Jabłonka-Salach K, Bulska E, Członkowska A (2013) Brain metal accumulation in Wilson[R8S2Q1M7]s disease. J Neurol Sci 329: 55–58. doi:10.1016/j.jns.2013.03.021

[13] Lorincz MT (2010) Neurologic Wilson[R8S2Q1M7]s disease. Ann N Y Acad Sci 1184: 173–187. doi:10.1111/j.1749-6632.2009.05109.x

[14] Gubler CJ, Lahey ME, Cartwright GE, Wintrobe MM (1953) Studies on copper metabolism. IX. The transportation of copper in blood. J Clin Invest 32: 405–414. doi:10.1172/JCI102752

[15] Neumann PZ, Sass-Kortsak A (1967) The state of copper in human serum: Evidence for an amino acid-bound fraction. J Clin Invest 46: 646–658. doi:10.1172/JCI105566

[16] Liu N, Lo LS, Askary SH, Jones L, Kidane TZ, Trang T, Nguyen M, Goforth J, Chu YH, Vivas E, et al (2007) Transcuprein is a macroglobulin regulated by copper and iron availability. J Nutr Biochem 18: 597–608. doi:10.1016/j.jnutbio.2006.11.005

[17] Zgirski A, Frieden E (1990) Binding of Cu(II) to non-prosthetic sites in ceruloplasmin and bovine serum albumin. J Inorg Biochem 39: 137–148. doi:10.1016/0162-0134(90)80022-p

[18] Kirsipuu T, Zadoroˇznaja A, Smirnova J, Friedemann M, Plitz T, Tõugu V, Palumaa P (2020) Copper(II)-binding equilibria in human blood. Sci Rep 10: 5686. doi:10.1038/s41598-020-62560-4

[19] Eom JE, Lee E, Jeon KH, Sim J, Suh M, Jhon GJ, Kwon Y (2014) Development of an albumin copper binding (ACuB) assay to detect ischemia modified albumin. Anal Sci 30: 985–990. doi:10.2116/analsci.30.985

[20] Jones CE, Abdelraheim SR, Brown DR, Viles JH (2004) Preferential Cu2+ coordination by His96 and His111 induces beta-sheet formation in the unstructured amyloidogenic region of the prion protein. J Biol Chem 279: 32018–32027. doi:10.1074/jbc.M403467200

[21] Walshe JM (2012) Serum [L8D2Q2M0]free[R8D2Q2M1] copper in Wilson disease. QJM 105: 419–423. doi:10.1093/qjmed/hcr229

[22] Guillaud O, Brunet AS, Mallet I, Dumortier J, Pelosse M, Heissat S, Rivet C, Lachaux A, Bost M (2018) Relative exchangeable copper: A valuable tool for the diagnosis of Wilson disease. Liver Int 38: 350–357. doi:10.1111/liv.13520

[23] El Balkhi S, Trocello JM, Poupon J, Chappuis P,Massicot F, Girardot-Tinant N, Woimant F (2011) Relative exchangeable copper: A new highly sensitive and highly specific biomarker for Wilson[R8S2Q1M7]s disease diagnosis. Clin Chim Acta 412: 2254–2260. doi:10.1016/j.cca.2011.08.019

[24] Telianidis J, Hung YH, Materia S, Fontaine SL (2013) Role of the P-Type ATPases, ATP7A and ATP7B in brain copper homeostasis. Front Aging Neurosci 5: 44. doi:10.3389/fnagi.2013.00044

[25] Persidsky Y, Ramirez SH, Haorah J, Kanmogne GD (2006) Blood-brain barrier: Structural components and function under physiologic and pathologic conditions. J Neuroimmune Pharmacol 1: 223–236. doi:10.1007/s11481-006-9025-3

[26] Vierling JM, Sussman NL (2019) Wilson disease in adults. In Clinical and Translational Perspectives on Wilson Disease. Kerkar N, Roberts EA (eds.). pp 165–177. London: Academic Press.

[27] Stuerenburg HJ (2000) CSF copper concentrations, blood-brain barrier function, and coeruloplasmin synthesis during the treatment of Wilson [R8S2Q1M7]s disease. J Neural Transm (Vienna) 107: 321–329. doi:10.1007/s007020050026

[28] Czlonkowska A, Litwin T, Karlin´ski M, Dziezyc K, Chabik G, Czerska M (2014) D-penicillamine versus zinc sulfate as first-line therapy for Wilson [R8S2Q1M7]s disease. Eur J Neurol 21: 599–606. doi:10.1111/ene.12348

[29] Kalita J, Kumar V, Chandra S, Kumar B, Misra UK (2014) Worsening of Wilson disease following penicillamine therapy. Eur Neurol 71: 126–131. doi:10.1159/000355276

[30] Kalita J, Kumar V, Ranjan A, Misra UK (2015) Role of oxidative stress in the worsening of neurologic Wilson disease following chelating therapy. Neuromolecular Med 17: 364–372. doi:10.1007/s12017-015-8364-8

[31] Merle U, Schaefer M, Ferenci P, Stremmel W (2007) Clinical presentation, diagnosis and long-term outcome of Wilson[R8S2Q1M7]s disease: A cohort study. Gut 56: 115–120. doi:10.1136/gut.2005.087262

[32] Walshe JM, Yealland M (1993) Chelation treatment of neurological Wilson's disease. Q J Med 86: 197–204.

[33] Litwin T, Dziez˙ yc K, Karlin´ski M, Chabik G, Czepiel W, Członkowska A (2015) Early neurological worsening in patients with Wilson[R8S2Q1M7]s disease. J Neurol Sci 355: 162–167. doi:10.1016/j.jns.2015.06.010

[34] Brewer GJ, Terry CA, Aisen AM, Hill GM (1987) Worsening of neurologic syndrome in patients with Wilson[R8S2Q1M7]s disease with initial penicillamine therapy. Arch Neurol 44: 490–493. doi:10.1001/archneur.1987.00520170020016

[35] Weiss KH, Askari FK, Czlonkowska A, Ferenci P, Bronstein JM, Bega D, Ala A, Nicholl D, Flint S, Olsson L, et al (2017) Bis-choline tetrathiomolybdate in patients with Wilson[R8S2Q1M7]s disease: An open-label, multicentre, phase 2 study. Lancet Gastroenterol Hepatol 2: 869–876. doi:10.1016/S2468-1253(17)30293-5

[36]   Brewer GJ, Askari F, Lorincz MT, Carlson M, Schilsky M, Kluin KJ, Hedera P, Moretti P, Fink JK, Tankanow R, et al (2006) Treatment of Wilson disease with ammonium tetrathiomolybdate: IV. Comparison of tetrathiomolybdate and trientine in a double-blind study of treatment of the neurologic presentation of Wilson disease. Arch Neurol 63: 521–527. doi:10.1001/archneur.63.4.521

[37]   Brewer GJ, Hedera P, Kluin KJ, Carlson M, Askari F, Dick RB, Sitterly J, Fink JK (2003) Treatment of Wilson disease with ammonium tetrathiomolybdate: III. Initial therapy in a total of 55 neurologically affected patients and follow-up with zinc therapy. Arch Neurol 60: 379–385. doi:10.1001/archneur.60.3.379

[38]   Smirnova J, Kabin E, J¨arving I, Bragina O, Tõugu V, Plitz T, Palumaa P (2018) Copper(I)-binding properties of de-coppering drugs for the treatment of Wilson disease. α-Lipoic acid as a potential anti-copper agent. Sci Rep 8: 1463. doi:10.1038/s41598-018-19873-2

[39]   Kojimahara N, Nakabayashi H, Shikata T, Esumi M (1995) Defective copper binding to apo-ceruloplasmin in a rat model and patients with Wilson[R8S2Q1M7]s disease. Liver 15: 135–142. doi:10.1111/j.1600-0676.1995.tb00660.x

[40]   Plitz T, Boyling L (2019) Metabolic disposition of WTX101 (bis-choline tetrathiomolybdate) in a rat model of Wilson disease. Xenobiotica 49: 332–338. doi:10.1080/00498254.2018.1443352

[41]   Butler M, Carruthers G, Harth M, Freeman D, Percy J, Rabenstein D (1982) Pharmacokinetics of reduced D-penicillamine in patients with rheumatoid arthritis. Arthritis Rheum 25: 111–116. doi:10.1002/art.1780250120

[42]   Ogra Y, Suzuki KT (1995) Removal and efflux of copper from Cumetallothionein as Cu/tetrathiomolybdate complex in LEC rats. Res Commun Mol Pathol Pharmacol 88: 196–204.

[43]   Mills CF, El-Gallad TT, Bremner I, Weham G (1981) Copper and molybdenum absorption by rats given ammonium tetrathiomolybdate. J Inorg Biochem 14: 163–175. doi:10.1016/s0162-0134(00)80037-9

[44]   Gooneratne SR, Howell JM, Gawthorne JM (1981) An investigation of the effects of intravenous administration of thiomolybdate on copper metabolism in chronic Cu-poisoned sheep. Br J Nutr 46: 469–480. doi:10.1079/bjn19810055

[45]   Mills CF, El-Gallad TT, Bremner I (1981) Effects of molybdate, sulfide, and tetrathiomolybdate on copper metabolism in rats. J Inorg Biochem 14: 189–207. doi:10.1016/s0162-0134(00)80000-8

[46]   Peterson PA, Evrin PE, Bergga° rd I (1969) Differentiation of glomerular, tubular, and normal proteinuria: Determinations of urinary excretion of beta-2-macroglobulin, albumin, and total protein. J Clin Invest 48: 1189–1198. doi:10.1172/JCI106083

[47]   Martins DA, Gouvea LR, Muniz GSV, Louro SRW, Batista DdGJ, Soeiro MdNC, Teixeira LR (2016) Norfloxacin and N-donor mixed-ligand copper(II) complexes: Synthesis, albumin interaction, and antitrypanosoma cruzi activity. Bioinorg Chem Appl 2016: 5027404. doi:10.1155/2016/5027404

[48]   Banci L, Bertini I, Ciofi-Baffoni S, Kozyreva T, Zovo K, Palumaa P (2010) Affinity gradients drive copper to cellular destinations. Nature 465: 645–648. doi:10.1038/nature09018

[49]   Zischka H, Lichtmannegger J, Schmitt S, J¨agemann N, Schulz S, Wartini D, Jennen L, Rust C, Larochette N, Galluzzi L, et al (2011) Liver mitochondrial membrane crosslinking and destruction in a rat model of Wilson disease. J Clin Invest 121: 1508–1518. doi:10.1172/JCI45401

[50]   Einer C, Leitzinger C, Lichtmannegger J, Eberhagen C, Rieder T, Borchard S, Wimmer R, Denk G, Popper B, Neff F, et al (2018) A high-calorie diet aggravates mitochondrial dysfunction and triggers severe liver damage in Wilson disease rats. Cell Mol Gastroenterol Hepatol 7: 571–596. doi:10.1016/j.jcmgh.2018.12.005

[51]   Lichtmannegger J, Leitzinger C, Wimmer R, Schmitt S, Schulz S, Kabiri Y, Eberhagen C, Rieder T, Janik D, Neff F, et al (2016) Methanobactin reverses acute liver failure in a rat model of Wilson disease. J Clin Invest 126: 2721–2735. doi:10.1172/JCI85226

[52] Borchard S, Bork F, Rieder T, Eberhagen C, Popper B, Lichtmannegger J, Schmitt S, Adamski J, Klingenspor M, Weiss KH, et al (2018) The exceptional sensitivity of brain mitochondria to copper. Toxicol In Vitro 51: 11–22. doi:10.1016/j.tiv.2018.04.012

[53] Doll DN, Hu H, Sun J, Lewis SE, Simpkins JW, Ren X (2015) Mitochondrial crisis in cerebrovascular endothelial cells opens the blood-brain barrier. Stroke 46: 1681–1689. doi:10.1161/STROKEAHA.115.009099

[54] Bukeirat M, Sarkar SN, Hu H, Quintana DD, Simpkins JW, Ren X (2016) MiR-34a regulates blood-brain barrier permeability and mitochondrial function by targeting cytochrome c. J Cereb Blood Flow Metab 36: 387–392. doi:10.1177/0271678X15606147

[55] Müller SM, Ebert F, Raber G, Meyer S, Bornhorst J, Hüwel S, Galla HJ, Francesconi KA, Schwerdtle T (2018) Effects of arsenolipids on in vitro blood-brain barriermodel. Arch Toxicol 92: 823–832. doi:10.1007/s00204-017-2085-8

[56] Hoheisel D, Nitz T, Franke H, Wegener J, Hakvoort A, Tilling T, Galla HJ (1998) Hydrocortisone reinforces the blood-brain barrier properties in a serum free cell culture system. Biochem Biophys Res Commun 244: 312–316. doi:10.1006/bbrc.1997.8051

[57] Golowasch J, Nadim F (2013) Capacitance, membrane. In Encyclopedia of Computational Neuroscience. Jaeger D, Jung R (eds.). pp 1–5. New York, NY: Springer New York.

[58] Greene C, Hanley N, Campbell M (2019) Claudin-5: Gatekeeper of neurological function. Fluids Barriers CNS 16: 3. doi:10.1186/s12987-019-0123-z

[59] Fanning AS, Jameson BJ, Jesaitis LA, Anderson JM (1998) The tight junction protein ZO-1 establishes a link between the transmembrane protein occludin and the actin cytoskeleton. J Biol Chem 273: 29745–29753. doi:10.1074/jbc.273.45.29745

[60] Müller JC, Lichtmannegger J, Zischka H, Sperling M, Karst U (2018) High spatial resolution LA-ICP-MS demonstrates massive liver copper depletion in Wilson disease rats upon Methanobactin treatment. J Trace Elem Med Biol 49: 119–127. doi:10.1016/j.jtemb.2018.05.009

[61] Quarles CD Jr., Macke M, Michalke B, Zischka H, Karst U, Sullivan P, Field MP (2020) LC-ICP-MS method for the determination of [L8D2Q2M0] extractable copper[R8D2Q2M1] in serum. Metallomics 12: 1348–1355. doi:10.1039/d0mt00132e

[62] European Association for Study of Liver (2012) EASL clinical practice guidelines: Wilson[R8S2Q1M7]s disease. J Hepatol 56: 671–685. doi:10.1016/j.jhep.2011.11.007

[63] Litwin T, Członkowska A, Socha P (2019) Oral chelator treatment of Wilson disease. In Clinical and Translational Perspectives on Wilson disease. Kerkar N, Roberts EA (eds.). pp 357–364. London: Academic Press.

[64] Sugawara N, Li D, Sugawara C (1994) Removal of copper from the liver of long-evans cinnamon (LEC) rats by tetrathiomolybdate (TTM) injection: The main excretion route is via blood, not bile. Res Commun Mol Pathol Pharmacol 85: 217–226.

[65] Ogra Y, Miyayama T, Anan Y (2010) Effect of glutathione depletion on removal of copper from LEC rat livers by tetrathiomolybdate. J Inorg Biochem 104: 858–862. doi:10.1016/j.jinorgbio.2010.04.001

[66] Scheinberg IH, Sternlieb I, Schilsky M, Stockert RJ (1987) Penicillamine may detoxify copper in Wilson[R8S2Q1M7]s disease. Lancet 2: 95. doi:10.1016/s0140-6736(87)92753-x

[67] Vogel FS, Evans JW (1961) Morphologic alterations produced by copper in neural tissues with consideration of the role of the metal in the pathogenesis of Wilson[R8S2Q1M7]s disease. J Exp Med 113: 997–1004. doi:10.1084/jem.113.6.997

[68] Vogel FS, Kemper L (1963) Biochemical reactions of copper within neural mitochondria, with consideration of the role of the metal in the pathogenesis of Wilson's disease. Lab Invest 12: 171–179.

[69] Aschner M (1996) The functional significance of brain metallothioneins. FASEB J 10: 1129–1136. doi:10.1096/fasebj.10.10.8751715

[70] Thirumoorthy N, Sunder AS, Kumar KM, Kumar MS, Ganesh G, Chatterjee M (2011) A review of metallothionein isoforms and their role in pathophysiology. World J Surg Oncol 9: 54. doi:10.1186/1477-7819-9-54

[71] Bradford MM (1976) A rapid and sensitive method for the quantitation of microgram quantities of protein utilizing the principle of protein-dye binding. Anal Biochem 72: 248–254. doi:10.1006/abio.1976.9999

[72] Elbashir A (2013) A new spectrophotometric method for determination of penicillamine in pharmaceutical formulation using 1, 2-naphthoquine-4-sulfonate (QS). PharmacoVigilance Rev 1: 1–5. doi:10.4172/jp.1000105

[73] Krug M, Weiss MS, Heinemann U, Mueller U (2012) Xdsapp: A graphical user interface for the convenient processing of diffraction data usingXDS. J Appl Cryst 45: 568–572. doi:10.1107/s0021889812011715

[74] Kabsch W (2010) Xds. Acta Crystallogr D Biol Crystallogr 66: 125–132. doi:10.1107/s0907444909047337

[75] Evans P (2006) Scaling and assessment of data quality. Acta Crystallogr D Biol Crystallogr 62: 72–82. doi:10.1107/S0907444905036693

[76] McCoy AJ (2017) Acknowledging errors: Advanced molecular replacement with phaser. Methods Mol Biol 1607: 421–453. doi:10.1007/ 978-1-4939-7000-1_18

[77] Bujacz A (2012) Structures of bovine, equine and leporine serum albumin. Acta Crystallogr D Biol Crystallogr 68: 1278–1289. doi:10.1107/S0907444912027047

[78] Emsley P, Lohkamp B, Scott WG, Cowtan K (2010) Features and development of Coot. Acta Crystallogr D Biol Crystallogr 66: 486–501. doi:10.1107/S0907444910007493

[79] Strober W (2015) Trypan blue exclusion test of cell viability. Curr Protoc Immunol 111: A3.B.1-A3.B.3. doi:10.1002/0471142735.ima03bs111

[80] Pesta D, Gnaiger E (2012) High-resolution respirometry: OXPHOS protocols for human cells and permeabilized fibers from small biopsies of human muscle. Methods Mol Biol 810: 25–58. doi:10.1007/978-1-61779-382-0_3

[81] Spinazzi M, Casarin A, Pertegato V, Salviati L, Angelini C (2012) Assessment of mitochondrial respiratory chain enzymatic activities on tissues and cultured cells. Nat Protoc 7: 1235–1246. doi:10.1038/nprot.2012.058

[82] Srinivasan B, Kolli AR, Esch MB, Abaci HE, Shuler ML, Hickman JJ (2015) TEER measurement techniques for in vitro barrier model systems. J Lab Autom 20: 107–126. doi:10.1177/2211068214561025

[83] Repetto G, del Peso A, Zurita JL (2008) Neutral red uptake assay for the estimation of cell viability/cytotoxicity. Nat Protoc 3: 1125–1131. doi:10.1038/nprot.2008.75

[84] Bornhorst J, Wehe CA, Hüwel S, Karst U, Galla HJ, Schwerdtle T (2012) Impact of manganese on and transfer across blood-brain and bloodcerebrospinal fluid barrier in vitro. J Biol Chem 287: 17140–17151. doi:10.1074/jbc.M112.344093

[85] Kopp JF, Müller SM, Pohl G, Lossow K, Kipp AP, Schwerdtle T (2019) A quick and simple method for the determination of six trace elements in mammalian serum samples using ICP-MS/MS. J Trace Elem Med Biol 54: 221–225. doi:10.1016/j.jtemb.2019.04.015

[86] Ye D, Dawson KA, Lynch I (2015) A TEM protocol for quality assurance of in vitro cellular barrier models and its application to the assessment of nanoparticle transport mechanisms across barriers. Analyst 140: 83–97. doi:10.1039/c4an01276c

[87] Smith PK, Krohn RI, Hermanson GT, Mallia AK, Gartner FH, Provenzano MD, Fujimoto EK, Goeke NM, Olson BJ, Klenk DC (1985) Measurement of protein using bicinchoninic acid. Anal Biochem 150: 76–85. doi:10.1016/ 0003-2697(85)90442-7

4.   SE SUPPLEMENTATION TO AN IN VITRO BLOOD-BRAIN BARRIER DOES NOT AFFECT CU TRANSFER INTO THE BRAIN

4.1   Graphical abstract
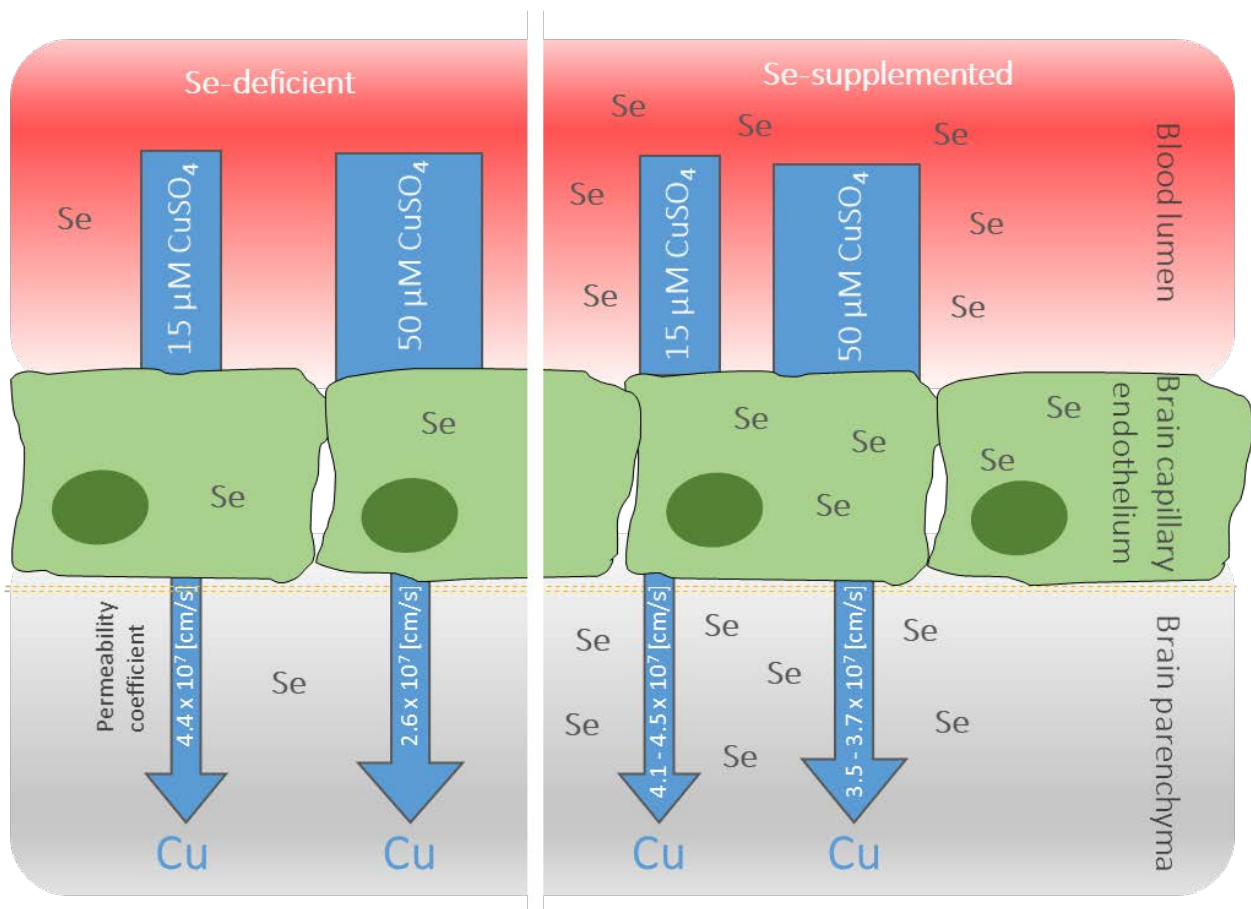
4.2   Abstract

Dyshomeostasis of copper (Cu) accompanied by Cu accumulation in certain brain areas has been associated with neurodegenerative diseases. One proposed toxic mode of action following Cu overload is oxidative stress associated with neuronal damage, whereas Selenium (Se) is assumed to play here a protective role. This study investigates the relationship between adequate Se supplementation and the respective consequences for Cu transfer into the brain applying an in vitro model of the blood-brain barrier (BBB). Primary porcine brain capillary endothelial cells (PBCECs) seeded on Transwell® inserts were supplemented with selenite starting at cultivation in both compartments. After apical application of 15 or 50 µM CuSO4, transfer of Cu to the basolateral compartment, the brain facing side, was assessed by ICP-MS/MS. Neither selenite supplementation nor Cu incubation negatively affected barrier properties. Transfer of Cu was not affected by selenite supplementation. Under Se-deficient conditions, Cu permeability coefficients decreased with increasing Cu concentrations. The results of this study do not indicate that under suboptimal Se supplementation more Cu transfers across the BBB to the brain.

4.3   Introduction

Maintaining the homeostasis of the essential trace elements selenium (Se) and copper (Cu) is of high relevance for normal brain function. Both deficiency and excess of these two trace elements can lead to neurological impairments [1–4]. Particularly, Cu dyshomeostasis seems to be associated with several neurodegenerative diseases such as Alzheimer´s (AD), Parkinson´s (PD) and Wilson´s disease (WD) being accompanied with Cu accumulation in some brain regions [5–7]. Several *in vivo* and *in vitro* studies have indicated a link between increased Cu levels in the brain and increased oxidative stress subsequently damaging macromolecules being associated with neuronal damage [8]. *In vitro studies* in primary neurons have previously demonstrated the protective potential of Se supplementation in the induction of oxidative stress [9,10]. Adequate expression of selenoproteins is important to counteract oxidative stress. Most selenoproteins have been described to be involved in redox regulation such as glutathione peroxidases or thioredoxin reductases, and reduced expression is exacerbating oxidative stress in the brain [4]. A number of studies have pointed out that chemical-induced brain damage appears to be dependent on Se supplementation of the animals [8]. Animals on a Se-deficient diet showed increased levels of brain damage and supplementation with Se could reduce levels of oxidative DNA damage [8]. Based on these studies it has been hypothesized that an adequate Se supplementation may have a protective role against Cu-induced damage. In recent studies changing homeostasis of the two trace elements during aging could be identified. The identified increasing serum Cu concentrations may contribute to the elevated Cu levels in the brain. In contrast, decreased Se serum concentrations were found in the elderly, which might contribute to decreased antioxidant

defense in the brain [11]. The observed changes in Se and Cu homeostasis during aging, namely decreased Se and increased Cu serum concentrations and Cu accumulation in the brain, opens among others the question whether a suboptimal Se supplementation of the endothelial cells of the blood-brain barrier (BBB) allows a higher transfer of Cu into the brain. This short communication assesses whether a Se supplementation to a well-established *in vitro* blood-brain barrier may affect the transfer of Cu into the brain.

4.4 Methods

Primary porcine brain capillary endothelial cells (PBCECs) were seeded on rat tail collagen-coated Transwell® membrane cell culture inserts and cultivated as described elsewhere [12]. To overcome suboptimal Se supplementation, PBCECs were supplemented with 100 or 200 nM selenite starting at cultivation (DIV 0) in both compartments. On DIV 4, PBCEC monolayers with TEER values of at least $600\ \Omega \cdot cm^2$ as well as a capacitance of 0.45-0.6 µF/cm² were used for transfer experiments [13]. For transfer studies, 15 or 50 µM $CuSO_4$ were incubated for 48 h to the apical compartment (Figure S1). Throughout the incubation period, barrier integrity was continuously monitored, using the transendothelial electrical resistance (TEER) as a measure of barrier tightness on the one hand and capacitance as an indicator of cell viability on the other. Total Cu and Se concentrations in medium samples were quantified by ICP-MS/MS as described before [14,15]. Selenoprotein P (SELENOP) determination was based on affinity chromatographic separation followed by ICP-MS/MS according to previously published protocol [16].

4.5 Results and discussion

4.5.1   Barrier integrity was not affected by Se supplementation or by co-incubation with Cu

Neither TEER values as a measure for barrier tightness (Figure 1A) nor capacities (Figure 1B) were affected by Se supplementation or by the co-incubation with Cu. Previously, cytotoxicity of selenite was observed at a 75-fold higher concentration in these cells, without showing negative effects on barrier integrity [17]. Likewise for Cu it has been demonstrated before that Cu concentrations up to 250 µM do not cause toxic effects to this BBB model [18]. Although such high concentrations seem to be less relevant, high serum Cu concentrations could be measured in diseased Atp7b$^{-/-}$ rats as a model for WD. Demise of liver cells in these animals presumably leads to a massive Cu release into the blood, where levels of 27 ± 16 µM Cu could be measured [19], highlighting the relevance of the investigated Cu concentrations in our study. In WD patients, a similar scenario was observed after treatment with the Cu chelator D-penicillamine [20,21].
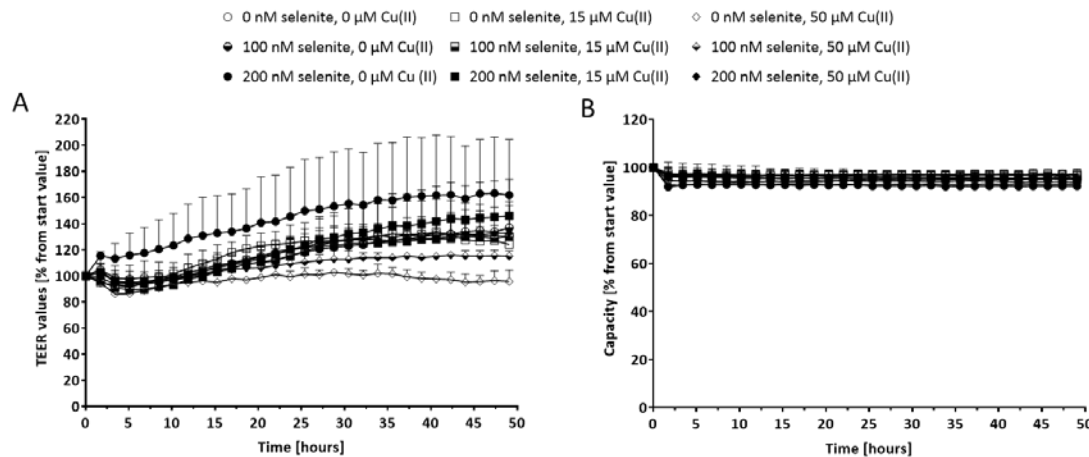
Figure 1. Neither selenite supplementation nor combined Cu(II) treatment showed negative effects on barrier integrity. PBCECs were supplemented with 100 or 200 nM selenite to ensure adequate Se supplementation (DIV 0). To determine the integrity of the barrier, TEER and capacitance were measured for 48 hours after apical application of 15 or 50 µM CuSO4 on DIV 4. Shown are mean of TEER (A) and capacitance values (B) from one representative experiment, expressed as % from starting value (two replicates per condition).

4.5.2   Selenite supply improves the Se status of PBCECs

Selenite supplementation to both compartments from the beginning of cultivation on resulted in concentration-dependent higher Se concentrations in both compartments (Figure 2), which did not change over 48 h indicating for no active side-directed Se transport as shown before [17]. No alterations in Se concentrations in the apical and basolateral compartments could be observed after co-treatment with Cu. Additionally, cellular Se concentrations were increased upon selenite supplementation (0 nM Selenite: 1.1 ± 0.1 ng Se/mg protein; 100 nM Selenite: 3.5 ± 0.1 ng Se/mg protein; 200 nM Selenite: 4.9 ± 1.2 ng Se/mg protein), but were not influenced by Cu (data not shown), indicating no interference of Cu with the Se homeostasis in this cell model. To further investigate Se homeostasis, SELENOP levels were measured in medium samples but were below the quantifiable range. Even after Se supplementation, the levels were higher than under deficient conditions, but still not quantifiable. Most of the Se was in the fraction containing Se-associated proteins or non-heparin-binding selenoproteins. This fraction was also significantly increased after Se administration (Figure S2). Overall, the improved TEER values in cells supplied with 200 nM selenite (Figure 1) and the increased cellular Se and SELENOP levels, indicate an improved Se status of the selenite supplied cells. This is consistent with previously published data showing that Se has protective effects on cell viability and barrier integrity in a co-culture system of murine brain microvascular endothelial (bEnd.3) and astrocyte (MA-h) cell lines [22]. Cells were cultured with 100 nM selenite 24 h prior to oxygen-glucose-deprivation challenge under hyperglycemic conditions. Expression of tight junctions (ZO-1, claudin-5

and occludin) were higher, and permeability of the barrier measured by fluorescein leakage was improved in the Se-supplemented system compared to cells without additional Se [22].
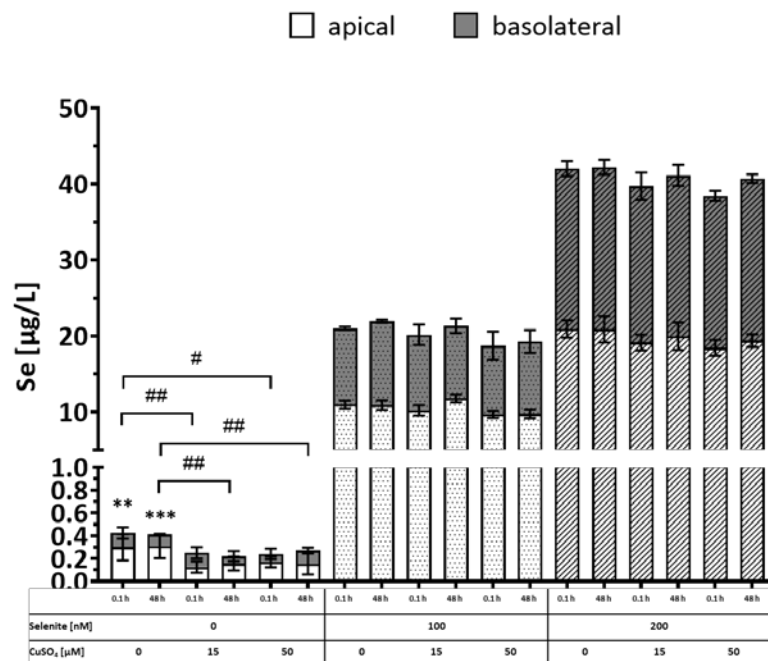
Figure 2. Se distribution between apical and basolateral compartments is altered under Se deficient conditions. Medium Se concentrations in apical and basolateral compartment after start of incubation (0.01 h) and after 48 h were measured using ICP-MS/MS. Shown are mean values of at three independent experiments, each with two replicates. Statistical analysis based on two-way ANOVA with Tukey´s post-test *$p<0.05$, **$p<0.01$, ***$p<0.005$ apical *vs.* basolateral compartment. #$p<0.05$, ##$p<0.01$, ###$p<0.005$ control *vs.* Cu(II) treatment.

Under Se-suboptimal (non-supplied) conditions, the distribution of Se between the two compartments is different, with significantly higher Se concentrations in the apical as compared to the basolateral compartment (apical: 0.3 ± 0.1 µg Se/L; basolateral: 0.1 ± 0.04 µg Se/L). This remained unchanged after the end of the 48-hour period (apical: 0.3 ± 0.1 µg Se/L; basolateral: 0.1 ± 0.01 µg Se/L). Combined application of Cu to the not-selenite supplied system resulted in a decrease in apical Se concentrations but no Se increase in the basolateral compartments (Figure 2). Cellular Se concentration were not significantly changed upon Cu exposure (0 µM Cu: 1.1 ± 0.1 ng Se/mg protein; 15 µM Cu: 1.2 ± 0.4 ng Se/mg protein; 50 µM Cu: 1.2 ± 0.4 ng Se/mg protein). However whether these minor cellular concentration changes can be reliable measured in the low number of cells applied on the barrier system is questionable. This is also shown by the relatively large standard deviations in the cellular concentrations.

4.5.3   Cu transfer via the BBB is not influenced by Se

To investigate whether selenite supplementation might influence Cu transfer into the brain facing compartment, Cu concentrations were measured by ICP-MS/MS in the both compartments at the beginning of the transfer experiment and after 48 h (Figure 3). At DIV 4, Cu concentrations in the basolateral compartments were similar in all Transwells and were not affected by prior selenite supplementation. After 48-hour incubation, Cu concentrations significantly increased in the basolateral compartment in a concentration-dependent manner, but were not affected by prior selenite supplementation (Figure 3). Incubation with physiological Cu concentration of 15 µM resulted in Cu permeability coefficients ranging from 4.1 to $4.5 \cdot 10^7$ cm/s (Table 1). Under Se deficiency, exposure to 50 µM Cu showed significantly lower Cu permeability coefficients compared to 15 µM Cu, while under Se adequate conditions the coefficients were only slightly lower. Transport of Cu into the brain is mostly facilitated *via* the copper uptake transporter 1 (CTR1) [23]. Lower permeability coefficients indicate saturation of the respective transporter resulting in lower transfer rates as shown for 50 µM Cu (single exposure). Surprisingly, permeability coefficients under selenite supplied conditions were not significantly different between 15 and 50 µM Cu, but there was a trend for a decrease with higher Cu concentrations.

Table 1. Cu permeability is negatively associated with higher Cu(II) incubation. Permeability coefficient was determined according to [24]. Shown are mean values of three independent experiments, each with two replicates per condition. Statistical analysis based on unpaired t-test §p<0.05 15 *vs.* 50 µM Cu(II).

Selenite [nM]	CuSO$_4$ [µM]	Permeability coefficient P x 10^7 [cm/s]
0	15	4.4 ± 1.3
	50	2.6 ± 0.5 §
100	15	4.5 ± 1.3
	50	3.7 ± 1.0
200	15	4.1 ± 1.7
	50	3.5 ± 1.3
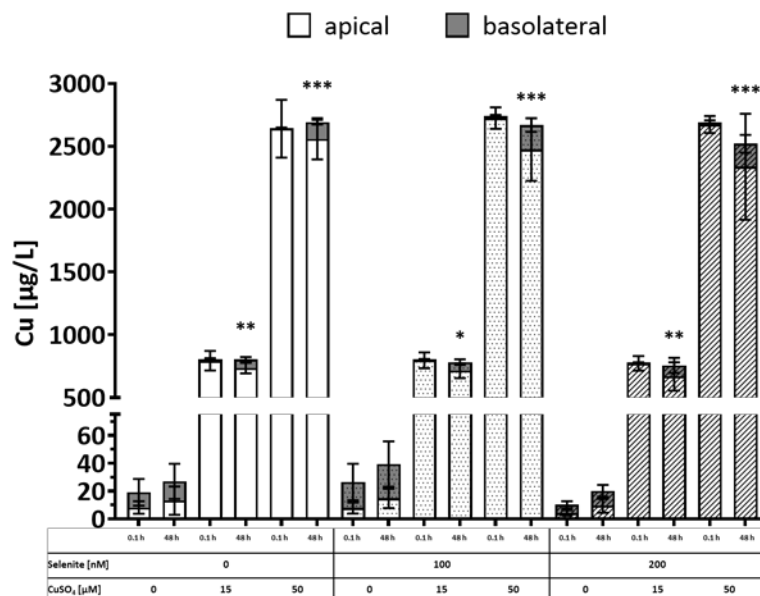
Figure 3. Selenite supplementation did not affected Cu transfer across the BBB. Medium Cu concentrations in apical and basolateral compartment after start of transfer experiment (0.01 h) and after 48 h were measured using ICP-MS/MS. Shown are mean values of three independent experiments, each with two replicates. Statistical analysis based on two-way ANOVA with Tukey´s post-test *$p<0.05$, **$p<0.01$, ***$p<0.005$ 0.1 *vs.* 48 h basolateral compartment.

4.6 Conclusion

The results of this study do not indicate that under suboptimal Se supplementation more Cu transfers across the BBB to the brain. Selenite supplementation improved the Se status of the cells, improved barrier integrity of the *in vitro* BBB but did not affect the Cu permeability coefficients.

4.7 Declaration of interest

The authors declare no conflicts of interest.

4.8 Acknowledgments

4.9 References

[1]   N. Kumar, P. Low, Myeloneuropathy and anemia due to copper malabsorption, J. Neurol. 251 (2004). https://doi.org/10.1007/s00415-004-0428-x.

[2]   U. Schweizer, N. Fradejas-Villar, Why 21? The significance of selenoproteins for human health revealed by inborn errors of metabolism, FASEB J. 30 (2016) 3669–3681. https://doi.org/10.1096/fj.201600424.

[3]   J. Chen, Y. Jiang, H. Shi, Y. Peng, X. Fan, C. Li, The molecular mechanisms of copper metabolism and its roles in human diseases, Pflügers Arch. - Eur. J. Physiol. 472 (2020) 1415–1429. https://doi.org/10.1007/s00424-020-02412-2.

[4]   N.D. Solovyev, Importance of selenium and selenoprotein for brain function: From antioxidant protection to neuronal signalling, J. Inorg. Biochem. 153 (2015) 1–12. https://doi.org/10.1016/j.jinorgbio.2015.09.003.

[5]   S. Genoud, B.R. Roberts, A.P. Gunn, G.M. Halliday, S.J.G. Lewis, H.J. Ball, D.J. Hare, K.L. Double, Subcellular compartmentalisation of copper, iron, manganese, and zinc in the Parkinson's disease brain, Metallomics. 9 (2017) 1447–1455. https://doi.org/10.1039/C7MT00244K.

[6]   M. Schrag, C. Mueller, U. Oyoyo, M.A. Smith, W.M. Kirsch, Iron, zinc and copper in the Alzheimer's disease brain: A quantitative meta-analysis. Some insight on the influence of citation bias on scientific opinion, Prog. Neurobiol. 94 (2011) 296–306. https://doi.org/10.1016/j.pneurobio.2011.05.001.

[7]   R. Squitti, R. Ghidoni, I. Simonelli, I.D. Ivanova, N.A. Colabufo, M. Zuin, L. Benussi, G. Binetti, E. Cassetta, M. Rongioletti, M. Siotto, Copper dyshomeostasis in Wilson disease and Alzheimer's disease as shown by serum and urine copper indicators., J. Trace Elem. Med. Biol. 45 (2018) 181–188. https://doi.org/10.1016/j.jtemb.2017.11.005.

[8]   V.K. Wandt, N. Winkelbeiner, J. Bornhorst, B. Witt, S. Raschke, L. Simon, F. Ebert, A.P. Kipp, T. Schwerdtle, A matter of concern – Trace element dyshomeostasis and genomic stability in neurons, Redox Biol. 41 (2021) 101877. https://doi.org/10.1016/j.redox.2021.101877.

[9]   D. Colle, D.B. Santos, V. de Souza, M.W. Lopes, R.B. Leal, P. de Souza Brocardo, M. Farina, Sodium selenite protects from 3-nitropropionic acid-induced oxidative stress in cultured primary cortical neurons, Mol. Biol. Rep. 46 (2019) 751–762. https://doi.org/10.1007/s11033-018-4531-y.

[10]   A. Salimi, N. Alyan, N. Akbari, Z. Jamali, J. Pourahmad, Selenium and L-carnitine protects from valproic acid-Induced oxidative stress and mitochondrial damages in rat cortical neurons, Drug Chem. Toxicol. 45 (2022) 1150–1157. https://doi.org/10.1080/01480545.2020.1810259.

[11] J . Baudry, J.F. Kopp, H. Boeing, A.P. Kipp, T. Schwerdtle, M.B. Schulze, Changes of trace element status during aging: results of the EPIC-Potsdam cohort study, Eur. J. Nutr. 59 (2020) 3045–3058. https://doi.org/10.1007/s00394-019-02143-w.

[12]   S.M. Müller, F. Ebert, G. Raber, S. Meyer, J. Bornhorst, S. Hüwel, H.-J. Galla, K.A. Francesconi, T. Schwerdtle, Effects of arsenolipids on in vitro blood-brain barrier model, Arch. Toxicol. 92 (2018) 823–832. https://doi.org/10.1007/s00204-017-2085-8.

[13]   J. Bornhorst, C.A. Wehe, S. Hüwel, U. Karst, H.-J. Galla, T. Schwerdtle, Impact of Manganese on and Transfer across Blood-Brain and Blood-Cerebrospinal Fluid Barrier in Vitro, J. Biol. Chem. 287 (2012) 17140–17151. https://doi.org/10.1074/jbc.M112.344093.

[14]   T.A. Marschall, J. Bornhorst, D. Kuehnelt, T. Schwerdtle, Differing cytotoxicity and bioavailability of selenite, methylselenocysteine, selenomethionine, selenosugar 1 and trimethylselenonium ion and their underlying metabolic transformations in human cells, Mol. Nutr. Food Res. 60 (2016) 2622–2632. https://doi.org/10.1002/mnfr.201600422.

[15]   B. Witt, M. Stiboller, S. Raschke, S. Friese, F. Ebert, T. Schwerdtle, Characterizing effects of excess copper levels in a human astrocytic cell line with focus on oxidative stress markers, J. Trace Elem. Med. Biol. 65 (2021) 126711. https://doi.org/10.1016/j.jtemb.2021.126711.

[16]   P. Heitland, H.D. Köster, Biomonitoring of selenoprotein P in human serum by fast affinity chromatography coupled to ICP-MS, Int. J. Hyg. Environ. Health. 221 (2018) 564–568. https://doi.org/10.1016/j.ijheh.2018.02.006.

[17]   E. Drobyshev, S. Raschke, R.A. Glabonjat, J. Bornhorst, F. Ebert, D. Kuehnelt, T. Schwerdtle, Capabilities of selenoneine to cross the in vitro blood–brain barrier model, Metallomics. 13 (2021). https://doi.org/10.1093/mtomcs/mfaa007.

[18]   S. Borchard, S. Raschke, K.M. Zak, C. Eberhagen, C. Einer, E. Weber, S.M. Müller, B. Michalke, J. Lichtmannegger, A. Wieser, T. Rieder, G.M. Popowicz, J. Adamski, M. Klingenspor, A.H. Coles, R. Viana, M.H. Vendelbo, T.D. Sandahl, T. Schwerdtle, T. Plitz, H. Zischka, Bis-choline tetrathiomolybdate prevents

copper-induced blood–brain barrier damage, Life Sci. Alliance. 5 (2022) e202101164. https://doi.org/10.26508/lsa.202101164.

[19] C.D. Quarles, M. Macke, B. Michalke, H. Zischka, U. Karst, P. Sullivan, M.P. Field, LC-ICP-MS method for the determination of "extractable copper" in serum, Metallomics. 12 (2020) 1348–1355. https://doi.org/10.1039/d0mt00132e.

[20] J. Kalita, V. Kumar, A. Ranjan, U.K. Misra, Role of Oxidative Stress in the Worsening of Neurologic Wilson Disease Following Chelating Therapy, NeuroMolecular Med. 17 (2015) 364–372. https://doi.org/10.1007/s12017-015-8364-8.

[21] T. Litwin, G. Gromadzka, G.M. Szpak, K. Jabłonka-Salach, E. Bulska, A. Członkowska, Brain metal accumulation in Wilson's disease, J. Neurol. Sci. 329 (2013) 55–58. https://doi.org/10.1016/j.jns.2013.03.021.

[22] B. Yang, Y. Li, Y. Ma, X. Zhang, L. Yang, X. Shen, J. Zhang, L. Jing, Selenium attenuates ischemia/reperfusion injury-induced damage to the blood-brain barrier in hyperglycemia through PI3K/AKT/mTOR pathway-mediated autophagy inhibition, Int. J. Mol. Med. 48 (2021) 178. https://doi.org/10.3892/ijmm.2021.5011.

[23] B.-S. Choi, W. Zheng, Copper transport to the brain by the blood-brain barrier and blood-CSF barrier, Brain Res. 1248 (2009) 14–21. https://doi.org/10.1016/j.brainres.2008.10.056.

[24] H. Franke, H.-J. Galla, C.T. Beuckmann, An improved low-permeability in vitro-model of the blood–brain barrier: transport studies on retinoids, sucrose, haloperidol, caffeine and mannitol, Brain Res. 818 (1999) 65–71. https://doi.org/10.1016/S0006-8993(98)01282-7.

4.10 Supporting information
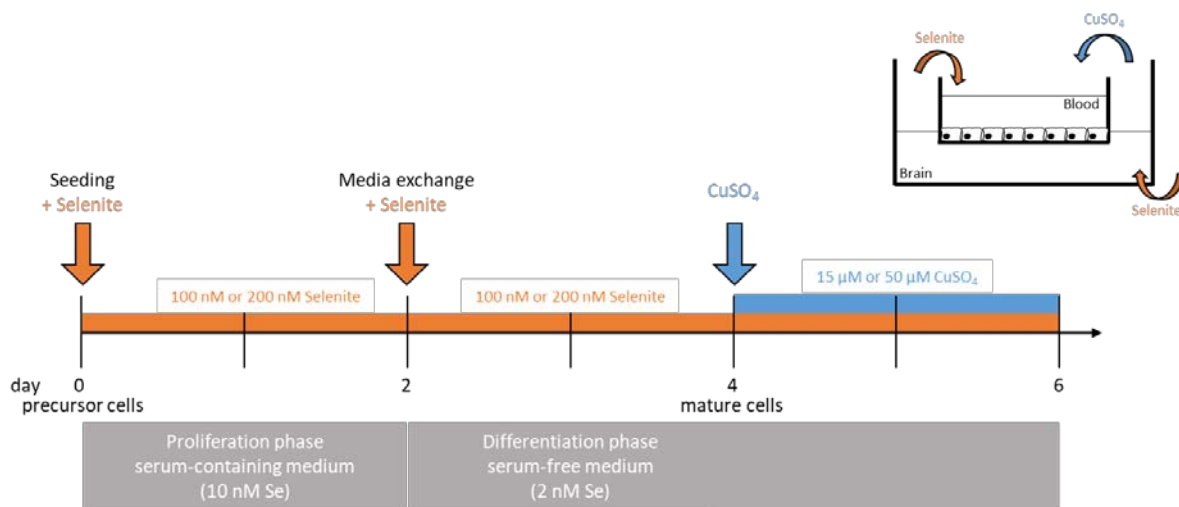
Figure S1. Incubation protocol of Cu transfer study with additional Se supplementation. PBCECs were supplemented with selenite (100 or 200 nM) or without addition of Se directly after seeding (DIV 0) in both compartments. After 48 h of proliferation, medium was changed to serum-free medium and added with selenite (100 or 200 nM) or without addition of Se to start differentiation phase. For transfer experiment (DIV 4), 15 or 50 μM $CuSO_4$ were incubated to the apical compartment for additional 48 h.
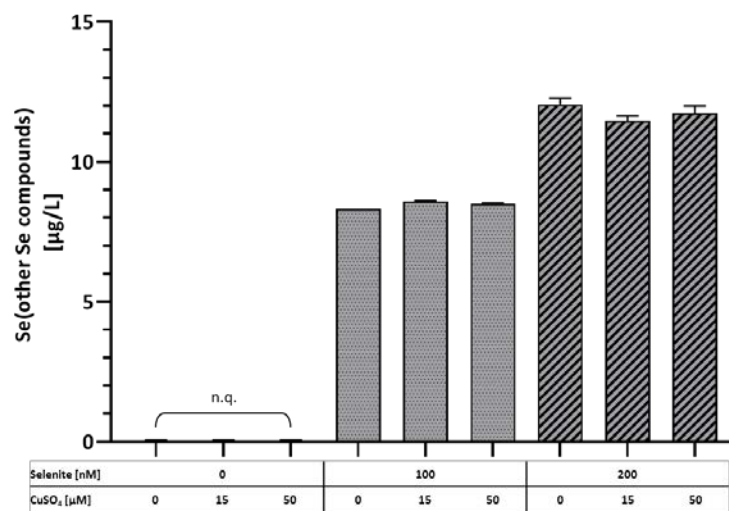
Figure S2. Se concentration in the fraction of Se-associated proteins and non-heparin-binding selenoproteins. PBCECs were supplemented with 100 or 200 nM selenite to ensure adequate Se supplementation during cultivation (DIV 0). For transfer experiment (DIV 4), 15 or 50 μM $CuSO_4$ were incubated to the apical compartment for additional 48 h. At the end of transfer, Se concentration of separated fraction of other Se compounds (Se-associated and non-heparin binding selenoproteins) were quantified by affinity chromatography coupled with ICP-MS/MS in basolateral medium samples. Abbreviations: n.q. – not quantifiable

5. CHARACTERIZING EFFECTS OF EXCESS COPPER LEVELS IN A HUMAN ASTROCYTIC CELL LINE WITH FOCUS ON OXIDATIVE STRESS MARKERS

5.1 Graphical abstract
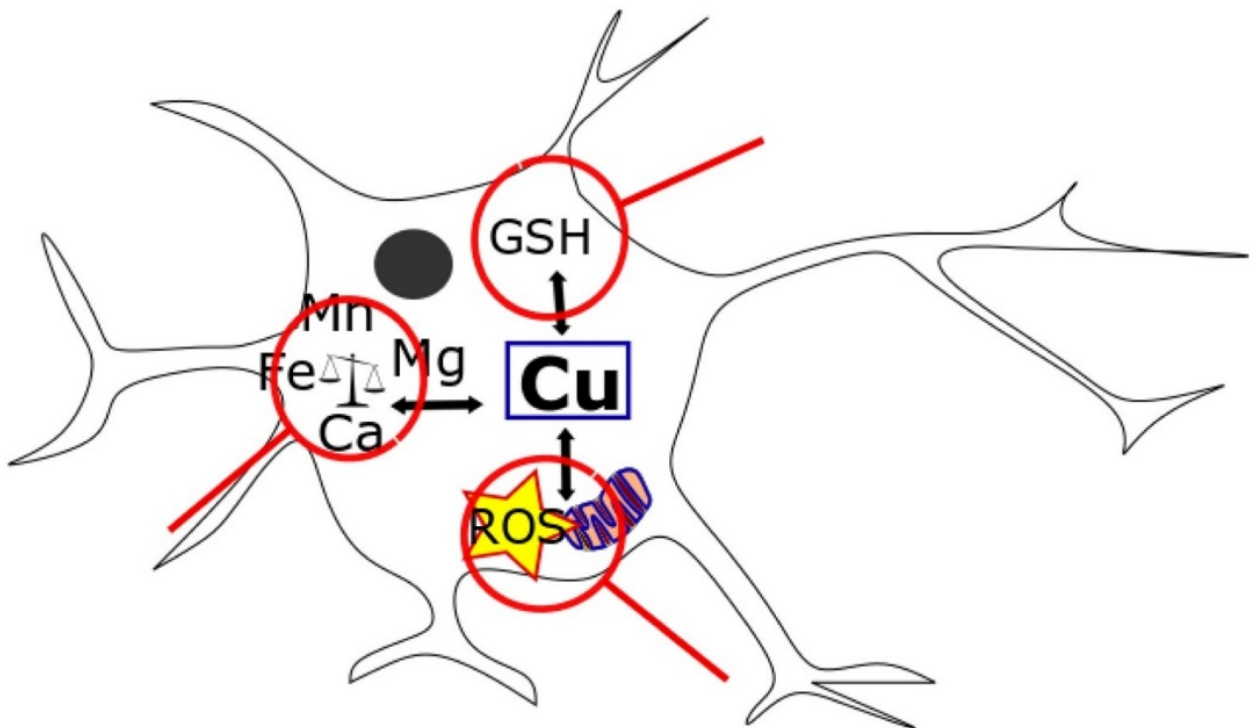
5.2 Abstract

Background: Being an essential trace element, copper is involved in diverse physiological processes. However, excess levels might lead to adverse effects. Disrupted copper homeostasis, particularly in the brain, has been associated with human diseases including the neurodegenerative disorders Wilson and Alzheimer's disease. In this context, astrocytes play an important role in the regulation of the copper homeostasis in the brain and likely in the prevention against neuronal toxicity, consequently pointing them out as a potential target for the neurotoxicity of copper. Major toxic mechanisms are discussed to be directed against mitochondria probably *via* oxidative stress. However, the toxic potential and mode of action of copper in astrocytes is poorly understood, so far. Methods: In this study, excess copper levels affecting human astrocytic cell model and their involvement in the neurotoxic mode of action of copper, as well as, effects on the homeostasis of other trace elements (Mn, Fe, Ca and Mg) were investigated. Results: Copper induced substantial cytotoxic effects in the human astrocytic cell line following 48 h incubation (EC30: 250 µM) and affected mitochondrial function, as observed *via* reduction of mitochondrial membrane potential and increased ROS production, likely originating from mitochondria. Moreover, cellular GSH metabolism was altered as well. Interestingly, not only cellular copper levels were affected, but also the homeostasis of other elements (Ca, Fe and Mn) were disrupted. Conclusion: One potential toxic mode of action of copper seems to be effects on the mitochondria along with induction of oxidative stress in the human astrocytic cell model. Moreover, excess copper levels seem to interact with the homeostasis of other essential elements such as Ca, Fe and Mn. Disrupted element homeostasis might also contribute to the induction of oxidative stress, likely involved in the onset and progression of neurodegenerative disorders. These insights in the toxic mechanisms will help to develop ideas and approaches for therapeutic strategies against copper-mediated diseases.

5.3 Introduction

As an essential trace element, Copper (Cu) is involved in diverse physiological processes. Particularly in the brain, it plays an important role to maintain the brain functions. Human exposure predominantly derives from diet (e.g. nuts, offal), industrial use and agricultural application (e.g. pesticides) [1,2]. In general, the Cu homeostasis is strictly regulated and well balanced, since both, overload and deficiency may lead to adverse effects. Homeostatic dysregulation is discussed to be associated with certain neurological disorders including Alzheimer's and Wilson disease [3–5]. In this context, glial cells, such as astrocytes, are supposed to play a key role in the regulation of the Cu homeostasis in the brain. Astrocytes efficiently take up Cu *via* the Cu transporters Ctr1 and DMT1. ATP7A has been discussed as most likely predominant Cu exporter in the astrocytes. Cellular distribution and trafficking is mediated by various Cu-binding proteins, which is described elsewhere [3,6–8]. However, it should be pointed

out here, that glial cells are discussed to tolerate distinct Cu accumulation, since they provide enhanced ability to store Cu by upregulating Cu transport and binding proteins such as glutathione (GSH) and metallothionein (MT). This emphasizes their pivotal role in maintaining the brain Cu homeostasis. Moreover, by providing enhanced storage capacity, astrocytes are discussed to protect other brain cells including neurons from Cu overload and consequently toxicity [9–11]. *In vitro* studies with cultured astrocytes showed that excess Cu levels reduce the cell viability. Toxic mode of action is supposed to be the induction of oxidative stress *via* ROS production and mitochondrial dysfunction [12,13]. However, the exact mode of action is not completely understood and still focus of investigation. The aim of this study was to elucidate the cellular mechanisms of Cu toxicity at excess, non-physiologic levels, likely occurring at disrupted copper homeostasis (e.g. due to Cu-related neurological diseases). The human astrocytic cell line CCF-STTG1 was applied as *in vitro* brain cell model. Particular focus is set on mitochondria as central target organelles and oxidative stress markers. Moreover, since there are hints, that Cu homeostasis is linked to other essential elements like Mg, Ca, Fe, Mn, interactions on cellular levels with these elements were investigated [14–17]. These experiments help to shed light on the role of astrocytes under excess Cu and how these brain cells are involved in the Cu homeostasis and in the protection against Cu-mediated neurotoxicity [18].

5.4 Materials and methods

5.4.1 Materials

CCF-STTG1 were obtained from the American Type Culture Collection (Bethesda, MD, USA). RPMI 1640 medium and glutamine were purchased from Biochrom (Berlin, Germany), Fetal calf serum (FCS) was from Merck KGaA (Darmstadt, Germany), penicillin-streptomycin solutions and trypsin were supplied by Sigma-Aldrich (Steinheim, Germany). Copper(II)sulphate (anhydrous, >99% purity) was purchased from Carl Roth (Karlsruhe, Germany). Resazurin dye, standards for GSH and GSSG, DTNB, DHE, antimycin A, sodium azide and tert-butylhydroperoxide were provided by Sigma- Aldrich (Steinheim, Germany), nitric acid (65%, suprapur) and Hoechst 33258 from Merck (Darmstadt, Germany), Carboxy-DCFH-DA and MitoTracker® Orange CMT-MRos from Life Technologies GmbH (Darmstadt, Germany) and MitoSOX™ Red from ThermoFisher Scientific (Dreieich, Germany). Alcian Blue was supplied by Fluka Biochemika (Munich, Germany) and DAPI from Vector Laboratories (Burlingame, USA). Single element standards for ICP-MS/MS measurements were purchased from Carl Roth (Karlsruhe, Germany) and Spetec (Erding, Germany). All other chemicals were obtained from Merck (Darmstadt, Germany), Carl Roth (Karlsruhe, Germany) or Sigma-Aldrich (Steinheim, Germany).

5.4.2   Cultivation and incubation of cells

Human astrocytic cell line (CCF-STTG1) was cultured as monolayer in RPMI 1640 supplemented with 10% FCS, 100 U/mL penicillin, 100 mg/mL streptomycin and 1.4 mM glutamine under standard conditions for human cell culture (37 °C, 5% CO_2 and 100% humidity). Cells were subcultured once a week and change of fresh media was performed every 2–3 days. 48 h after seeding in the respective experimental cell culture plates, the cells were treated with copper(II)sulphate ($CuSO_4$) solution and the respective experiments were performed another 48 h later following incubation. Stock solution of $CuSO_4$ (100 mM) was diluted in sterile distilled water and kept at 4 °C for up to two weeks. Further dilutions were prepared shortly before each experiment. Cu concentration of stock solutions was regularly checked by ICP-MS/MS (data not shown).

5.4.3   Cytotoxicity

Cytotoxic effects of Cu were studied in the human astrocytic cell model following 48 h incubation by investigating effects on cell number (indirectly *via* Hoechst) and cell viability (Resazurin). General cytotoxicity assays were performed in 96 well plates (30,000 cells/cm^2). *Cell number (Hoechst)* Cell number was indirectly determined using the bisbenzimidazole Hoechst 33258. This fluorescent dye binds to cellular DNA [19]. Consequently, applying this assay, the cell nuclei are detected and thus, cell number can be assessed. The method was performed as described before [20]. In brief, following a washing step with phosphate-buffered saline (PBS) and fixation with 3.7% formaldehyde/PBS for 10 min, the cells were permeabilized with 2.2% Triton™ X-100/PBS for 10 min and treated with 6 µM Hoechst/PBS for 30 min at 37 °C. The fluorescence was measured with a Tecan plate reader (Ex: 355 nm, Em: 460 nm; Tecan infinite 200 Pro, Tecan Austria GmbH, Gr¨odig, Austria). *Cell viability (Resazurin reduction assay)* Cell viability was monitored applying the Resazurin reduction assay. This endpoint is based on the reduction of Resazurin (Alamar Blue) to the fluorescent Resorufin by cellular dehydrogenases. In that way, the cellular metabolic activity can be assessed [21]. The assay was carried out as described before [22]. Briefly, Resazurin (5 µg/mL in culture media) was applied for 3 h at 37 °C. Thereafter, the fluorescence of Resorufin was detected with a Tecan plate reader (Ex: 540 nm, Em: 590 nm).

5.4.4   Mechanistic studies (with focus on mitochondria, oxidative stress)

To characterize the toxic mode of action, several more specific endpoints were studied with focus on mitochondria, as potential major target organelles, and oxidative stress. These experiments were performed either in 96 well plates (MitoTracker® Orange, Carboxy-DCFH-DA), 6 well plates (GSH/GSSG) or 12 well plates with cover slips (DHE, MitoSOX™) at a defined cell density (30,000 cells/cm^2).

Mitochondrial membrane potential (MitoTracker® Orange)

Effects on mitochondria were assessed *via* the mitochondrial membrane potential by applying MitoTracker® Orange CMT-MRos. This lipophilic cationic dye accumulates in the mitochondria depending on the mitochondrial membrane potential [23,24]. The assay was performed as described before [25]. Briefly, following treatment with the test compound, cells were incubated with 300 nM MitoTracker® Orange for 30 min at 37 °C. Thereafter, cells were fixed with 3.7% formaldehyde/PBS for 10 min at 37 °C. The fluorescence was measured with a Tecan plate reader (Ex: 544 nm, Em: 590 nm). To assess the mitochondrial activity, taking into account general cytotoxic effects, the mitochondrial membrane potential was related to the cell number, that was determined in parallel *via* Hoechst as described before. Sodium azide (NaN$_3$) was used as positive control (30 min incubation).

Cellular glutathione (GSH) and glutathione disulfide (GSSG) levels

Total glutathione levels (both reduced GSH and oxidized GSSG) were used as indicator for cellular redox status and measured by applying an enzymatic recycling assay [26]. This method is based on the conversion of DTNB to the yellow chromophore TNB and in parallel oxidation of GSH to GSSG, which is restored by glutathione reductase under the presence of NADPH. The amount of TNB is proportional to the total GSH and GSSG level. For the determination of GSSG only, the samples were treated with 2-vinylpyridine, leading to complexation of GSH. The method was performed as previously described [27,28]. Briefly, cell pellets (control and Cu-incubated) were prepared and cell number as TTCs, Roche Innovatis AG). Total GSH/GSSG and GSH was quantified in the supernatants of the lysed cell pellets using external calibration. Therefore, a kinetic measurement (5 readings) was performed at 412 nm with a Tecan plate reader.

Carboxy-DCFH-DA

Effects on the reactive oxygen and nitrogen species (RONS) were investigated applying a carboxy-DCFH-DA-based method. This endpoint relies on intracellular transformation of the carboxy-DCFH-DA to the fluorescent carboxy-DCFH due to RONS [29,30]. This assay was performed as described before [31]. In brief, cells were loaded with 15 µM carboxy-DCFH-DA for 20 min at 37 °C. Following two washing steps with media, cells were incubated with the test compound and RONS generation was periodically monitored *via* carboxy-DCFH formation up to 48 h with a Tecan plate reader (Ex: 485 nm, 535 nm). *Tert*butylhydroperoxide (TBH) was used as positive control.

Dihydroethidium (DHE) and MitoSOX™Red

Dihydroethidium (DHE) dye was applied to detect specific reactive oxygen and nitrogen species (RONS). This assay is based on the conversion of DHE to a fluorescent product due to superoxide anions [32]. This assay was performed as described before [30,33]. In brief, cells were seeded on cover slips,

that had been coated before with Alcian Blue to enhance cell adhesion and incubated with the test compound. Thereafter, 10 µM of DHE dye/medium was incubated for 30 min at 37 °C. Subsequently the cells were washed twice with PBS and microscopic images were taken with a Leica DM 6 (Wetzlar, Germany)(Ex: 540-580 nm, Em: 592-668 nm). Antimycin A was used as positive control (60 min incubation). To specifically detect mitochondrial superoxides, a method was developed, applying MitoSOX™ Red as superoxide indicator for live-cell imaging. In brief, cells were seeded on cover slips, that had been coated before with Alcian Blue and incubated with the test compound. Following incubation with the test compound, 5 µM MitoSOX™/media solution was applied for 10 min at 37 °C in the dark. Thereafter, the cells were washed thrice with PBS, the cover slips were mounted on DAPI on slides and subsequently, microscopic images were taken with a Leica DM 6 (Ex: 510 nm, Em: 580 nm (MitoSOX™); Ex: 350 nm, Em: 470 nm (DAPI)). Antimycin A was used as positive control (60 min incubation).

5.4.5   Cellular Bioavailability and interaction with other trace elements

To assess cellular bioavailability of $CuSO_4$, total Cu levels were determined in the human astrocytic cell line as described before [22]; and additionally, selected elements (Mg, Ca, Fe and Mn) were monitored in parallel. For assessing the cellular bioavailability, cells were seeded in 24 well plates (30,000 cells/cm^2) and incubated with $CuSO_4$ in a concentration range from 50 to 500 µM for 48 h. Before lysis of cells with RIPA buffer, the cells were washed twice with PBS. Protein levels of the cell lysates were measured *via* Bradford assay. For the determination of total element concentrations in cell lysates, 50 µL of cell lysate were placed in a 15 mL polypropylene tube, then 250 µL of an internal standard (ISTD) solution containing 100 µg Ge/L in 1% (v/v) and 500 µL of nitric acid, were added and the mixture was left to digest for 24 h at room temperature. Afterwards, the sample was diluted to a final volume of 2.5 mL with water. Total cellular levels of Cu and aforementioned elements, respectively, were measured by ICP-MS/MS (Agilent 8800 ICP-QQQ-MS, Agilent Technologies, Waldbronn, Germany). The ICP-MS/MS was operated in MS/MS mode using helium as collision cell gas at a flow rate of 4.3 mL/min. Additionally, 1% CO2 in Ar was introduced as optional gas (flow rate, 0.12 L/min) to maintain a constant carbon load of the plasma to compensate for any residual carbon in the digested samples. The monitored mass transitions (integration time of 0.5 s/point) for Mg, Ca, Mn, Fe, Cu and Ge (ISTD) were m/z 24 → m/z 24, m/z 44 → m/z 44, m/z 55 → m/z 55, m/z 56 → m/z 56, m/z 63 → m/z 63 and m/z 72 → m/z 72, respectively. Quantification was performed by external calibration based on the ISTD Ge. Mixed calibration standards were prepared in 20% (v/v) HNO_3 containing 10 µg Ge/L as ISTD for matrix matching. Calibration ranges were 0.1-500 µg/L and 10-500 µg/L for Mg, Mn, Fe, and Cu and Ca, respectively. Limit of detection (LOD) calculated from the mean value of chemical blanks plus 3 times the standard deviation (n = 4) divided by the calibration slope, ranged from 0.5-280 µg/L in the cell

lysates. All measured element concentrations in cell lysates were > LOD. Cell lysates were analyzed in triplicates and RSD were <15 %. The certified reference material NIST Trace Elements in Natural Water 1640A, purchased from LGC Standards GmbH (Wesel, Germany) was used for quality control and was treated in the same manner as cell lysates. This material has certified values of 85.75 ± 0.51 µg/L, 36.8 ± 1.8 µg/L, 40.39 ± 0.36 µg/L for Cu, Fe and Mn, respectively; values of 1059 ± 4 µg/L for Mg and 5615 ± 21 µg/L Ca are provided as reference values. We obtained 84.9 ± 1.4 µ/L, 37.2 ± 0.9 µg/L, 39.2 ± 1.1 µg/L for Cu, Fe and Mn, respectively; 1040 ± 31 µg/L for Mg and 6040 ± 430 µg/L for Ca throughout the study (n = 4). Cellular element concentrations were related to the respective protein levels. Furthermore, to assess the cellular molar concentrations, another approach was applied as described before [22]. In this study, the total cellular amount of the selected elements was related to the total cell volume (311,860,300 fL) derived from measurements by an automatic cell counter (Casy TTCs, Roche Innovatis AG).

5.4.6   Statistics

All experiments were independently carried out at least three times. Mean and standard deviations (SD) were calculated from raw data. Statistical analysis was done using ANOVA one-way test followed by Dunnett's test. Significance levels are $p < 0.05$, $p < 0.01$, $p < 0.001$.

5.5 Results and discussion

5.5.1   Cytotoxicity

Cell number and cell viability

To first assess the toxic potential of $CuSO_4$ in the human astrocytic cell model, endpoints with focus on general cytotoxicity were applied. Regarding both endpoints, $CuSO_4$ showed substantial toxic effects in the micromolar concentration range. Effects on cell viability, measured *via* cellular metabolic activity, turned out to be more sensitive as compared to effects on cell number, indicating that mitochondria might be potential target organelles of Cu toxicity. EC_{30} values (effective concentration with 30% impact) were found to be 250 µM (Resazurin) and 600 µM (Hoechst), respectively (see Fig. 1). So far, studies are limited with regard to cytotoxic effects of Cu in human glial cells. Studies with primary rat astrocytes revealed high cellular toxicity of Cu. 100 µM $CuCl_2$ reduced the cell viability to 60% following 24 h incubation, while 10 µM $CuCl_2$ did not affect the viability up to 48 h [34]. In another study with human astrocytes, significant toxic effects of $CuCl_2$ could be observed starting from 250 µM after 24 h incubation, where the cell viability was reduced to 60% [35]. It might be that there are species-specific differences in toxicity of Cu probably due to different metabolism or uptake mechanisms. Human astrocytes seem to be far less sensitive compared to primary rat astrocytes. To

better assess the cytotoxic potential of Cu, the toxic mode of action and cellular accessibility needs to be characterized and compared.
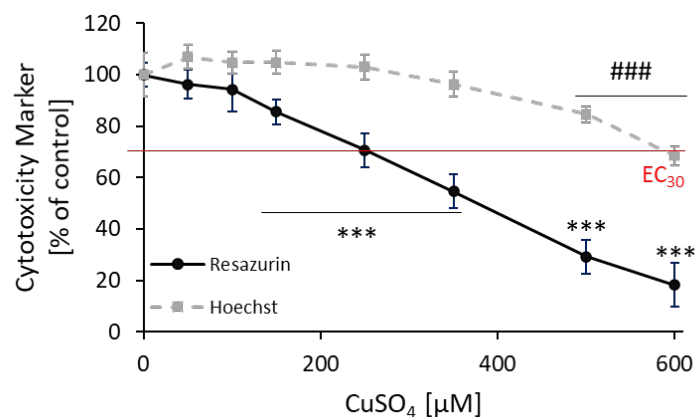
Fig. 1. General cytotoxicity – cell viability (Resazurin ——) and cell number (Hoechst - - -) were assessed in the human astrocytic cell line (CCF-STTG1) following 48 h incubation with CuSO$_4$. Shown are mean values of at least three independent experiments ± SD related to untreated control. EC$_{30}$: effective concentration with 30% impact. ###/*** p<0.001 (compared to untreated control) based on ANOVA-one way test followed by Dunnett's test.

5.5.2   Mechanistic studies

Mitochondria (Mitochondrial membrane potential)

To elucidate the toxic mode of action, selected endpoints with focus on oxidative stress and on mitochondria, as potential target organelles, have been conducted. Effects on mitochondria were investigated *via* mitochondrial membrane potential, which is supposed to be an early and quite sensitive marker [36,37]. CuSO$_4$ significantly reduced the mitochondrial membrane potential in the human astrocytic cell line. This decrease could be already observed following incubation with 100 µM Cu. Effects were significant, however, only at beginning cytotoxic concentrations. EC30 was around 300 µM, being slightly less sensitive compared to cell viability (see Fig. 2). The positive control NaN$_3$ effectively reduced the mitochondrial membrane potential to 54.7% *via* disruption of the mitochondrial electron transport. NaN$_3$ inhibits complex IV (cytochrome c oxidase) of the respiratory chain, leading to depolarization of mitochondria [38, 39]. Loss of mitochondrial membrane potential with increasing Cu levels has been reported in isolated rat brain mitochondria, before. Thereby, mitochondria of brain were found to be particularly sensitive towards Cu toxicity compared to liver or kidney [36]. Moreover, Cu depolarized the mitochondria and reduced the membrane potential in rat astrocytes [40]. This decrease of mitochondrial membrane potential is discussed to be mediated *via* induction of mitochondrial permeability but it could be also caused by disruption of the metalloenzymes of the respiratory chain [40]. Particularly complexes I, III and IV might be affected and could lead to massive ROS release [36]. Since effects on the mitochondrial membrane potential can be

associated with mitochondrial dysfunction and consequently impaired energy production, future studies should focus on energy state-related endpoints such as ATP levels [41]. *In vitro* and *in vivo* studies with rats have already indicated adverse effects on the energy levels as measured by reduction of ATP levels [42–44]. If the reduced mitochondrial membrane potential in human astrocytes is also associated with impaired energy production and lowered ATP levels, needs to be investigated in further studies. Moreover, disruption of mitochondrial membrane potential is linked to impaired mitochondrial function and might lead to uncontrolled, excessive ROS release [45,46]. Therefore, ROS-related endpoints were investigated in the next step.
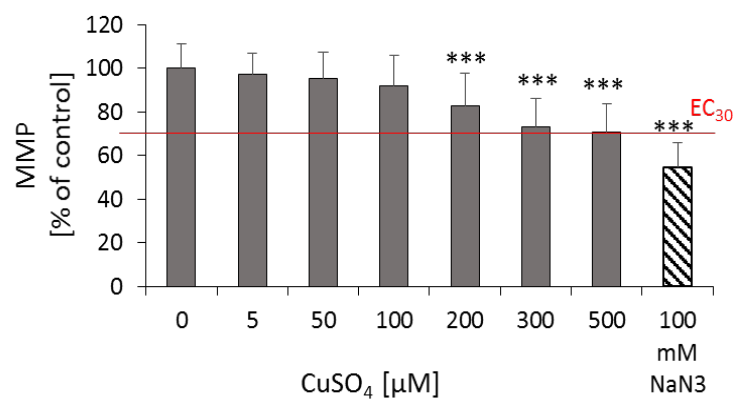
Fig. 2. Mitochondria – mitochondrial membrane potential (MMP) was assessed in the human astrocytic cell line (CCF-STTG1) following 48 h incubation with CuSO4 and the positive control NaN3, respectively (100 mM, 30 min). Mitotracker® Orange was related to cell number, to exclude cytotoxic effects. Shown are mean values of at least three independent experiments +SD. *** $p < 0.001$ (compared to untreated control) based on ANOVA-one way test followed by Dunnett's test.

Oxidative stress and ROS (GSH/GSSG, DHE, MitoSOX™ Red, Carboxy- DCFH-DA)

As oxidative stress marker, effects on cellular levels of glutathione (GSH) and glutathione disulfide (GSSG) were investigated. Levels of GSH / GSSG in untreated control cells were about 90% / 10% and decreased only slightly up to 250 µM CuSO4 to 84% / 26% (see Fig. 3 A). Massive effects were only observed at higher, cytotoxic concentrations of 500 µM (56% / 44%). Interestingly, total GSH levels increased with increasing concentrations of CuSO4 (see Fig. 3 B). This effect could be already observed at subcytotoxic effects. In control cells, the total GSH level accounted for 5.7 mM, while following 250 µM Cu incubation, the GSH level was found to be 6.9 mM. Thereby, levels of GSH decreased, whereas levels of GSSG increased following treatment with CuSO4. Excess Cu was reported to alter GSH metabolism, exerting effects on the overall cellular GSH levels. In primary rat astrocytes, total GSH levels were shown to increase concentration-dependently. Following incubation with 30 µM CuCl2, total GSH levels increased by 60% [47]. Likely underlying mechanisms are discussed to be enhanced uptake of GSH precursor amino acids or the upregulated enzyme for GSH synthesis [47]. The increase in total GSH levels probably helps to counteract toxic effects. This might be mediated by providing enhanced binding capacity of Cu rather than *via* its thiol activity (redox regulation) [48]. The GSH/GSSG

ratio, reflecting the cellular redox state, is discussed to be affected at excess Cu levels. GSH oxidation was induced by Cu in rat hepatocytes [49]. Moreover, reduced GSH/GSSG levels have been found in livers of Wilson disease patients compared to asymptomatic patients [50]. It seems, that imbalances in GSH/GSSG ratio are detected only in late stage diseased patients. This corresponds to the outcome of this study, where oxidation to GSSG and thus shifted levels of GSH/GSSG could be only observed at high, cytotoxic Cu concentrations. The tripeptide GSH exerts pivotal functions with regard to Cu metabolism in astrocytes. On the one hand GSH possesses antioxidative properties. Free radicals can be scavenged *via* its thiol group. Thus, a balanced GSH/GSSG homeostasis provides an essential defense system against oxidative stress. Moreover, GSH is involved in the cellular Cu transport [47]. Consequently, GSH is discussed as key player in the Cu homeostasis in human astrocytes. Since glial cells are supposed to supply other brain cells with GSH, these characteristics are discussed to carry out protective roles as well for neurons in the brain and might prevent the neurons from Cu toxicity [47]. Brain cells (besides glia also neurons) have been shown before, to be able to adapt to excess Cu conditions. Besides high levels of GSH, astrocytes also produce metallothionein, a Cu-binding protein, that is reported to enhance neuronal survival [8,18,51]. Following 24 h incubation with 100 μM $CuCl_2$, brain cells increased levels of this Cu-binding protein [35]. Supporting the assumption, that one defense strategy is to increase the cellular Cu-binding capacity. Interestingly, species-specific differences seem to occur here as well. Studies revealed that human astrocytes are able to maintain GSH levels better compared to primary rat astrocytes and thus seem to be less susceptible towards Cu toxicity [52]. When comparing the literature data of toxicity studies in primary rat cells with the here applied human astrocytes, this assumption can be confirmed.

A

B

$CuSO_4$	Total GSH [mM]	GSH [mM]	GSSG [mM]
0 μM	5.7 ± 0.4	4.9 ± 0.5	0.8 ± 0.2
50 μM	4.9 ± 0.3*	4.4 ± 0.2	0.4 ± 0.1
100 μM	5.9 ± 0.6	5.2 ± 0.6	0.8 ± 0.3
250 μM	6.9 ± 0.7**	5.7 ± 0.5	1.1 ± 0.2
500 μM	6.7 ± 0.6**	3.8 ± 0.9**	2.9 ± 0.6***
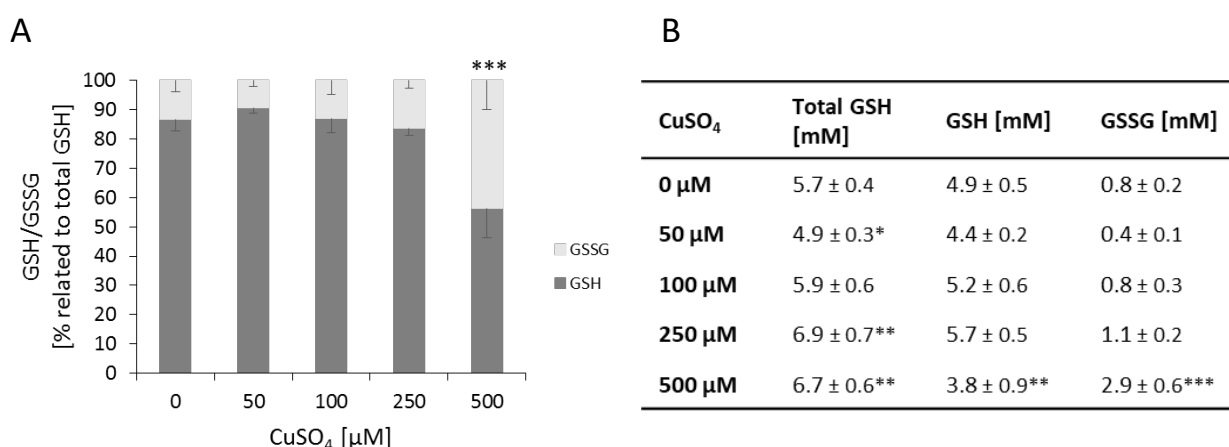
Fig. 3. Oxidative stress – levels of glutathione (GSH) und glutathione disulfide (GSSG) were investigated in the human astrocytic cell line (CCF-STTG1) following 48 h incubation with $CuSO_4$. Shown are mean values of at least three independent experiments ± SD. Effects on the ratio of GSH/GSSG [% related to total GSH] following treatment with $CuSO_4$ are depicted in (A). Cellular levels [mM] of total GSH, GSH and GSSG, respectively, are presented in (B). * $p < 0.05$, ** $p < 0.01$, *** $p < 0.001$ (compared to untreated control) based on ANOVA-one way test followed by Dunnett's test.

Oxidative stress is caused by imbalances between generation of ROS and antioxidative defense systems. Since there were hints, that Cu shows effects on oxidative stress markers, further studies focused on reactive oxygen species (ROS) to characterize the oxidative damage in the cells. First, ROS production was periodically monitored over time (for 48 h) *via* carboxy-DCFH-DA assay. Induction of ROS, assessed *via* increase in fluorescence, seems to occur concentration-dependently (see Fig. 4). At the lowest incubation concentration of 5 μM Cu, increase in fluorescence was already observed following one hour of incubation. At the highest incubation concentration of 600 μM, ROS was time-dependently induced up to 7 h, with maximum induction of 160% compared to control and finally decreased again. The positive control TBH massively increased ROS production, with maximum peak after 90 min (350 % compared to control). TBH can directly generate ROS such as peroxides *via* decomposition, leading to increased oxidative stress [53]. ROS induction in human astrocytes has been observed before *via* DCF-based assay. Following incubation with 10 μM Cu for 17 h, the ROS levels significantly increased 12-fold compared to control [54]. DCF-based assays specifically detect ROS including peroxyl, alkoxyl and NO2*, while not being sensitive for H_2O_2 and superoxides (O2*-), pointing out the importance, to include other ROS-related endpoints in order to check for a broad spectrum of reactive species [29]. To specifically characterize the cellular mechanisms, other types of ROS should be included in the studies as well.
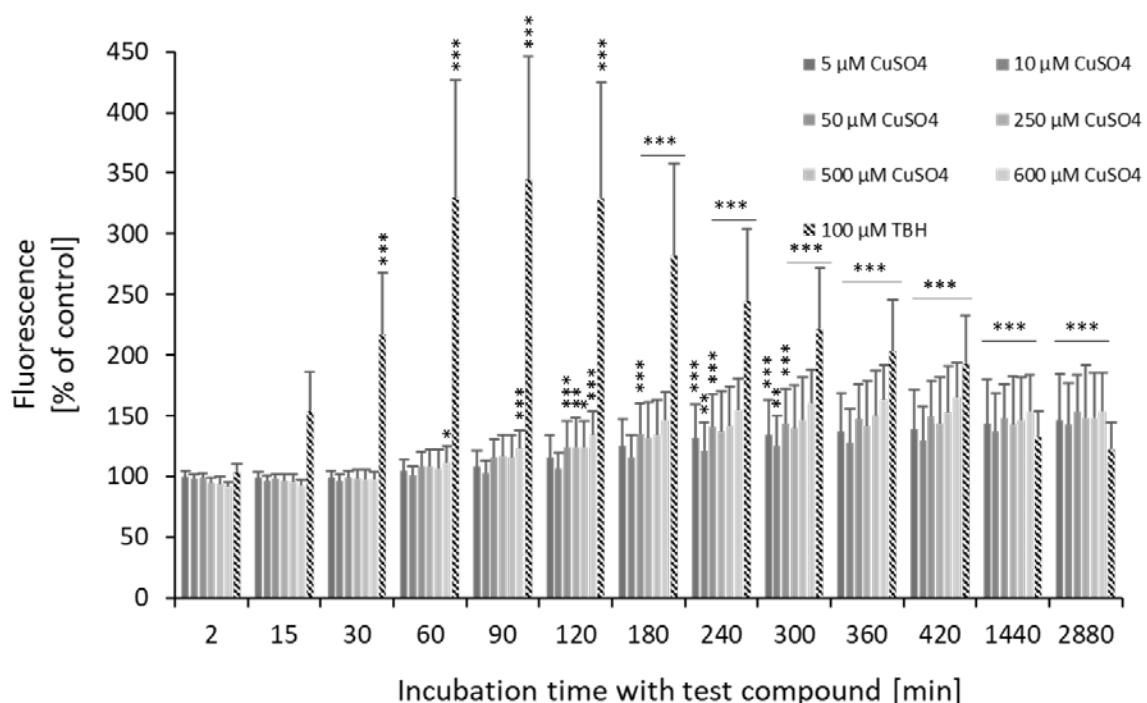
Fig. 4. Reactive oxygen species – Induction of ROS was investigated *via* carboxy-DCFH-DA assay in the human astrocytic cell line (CCF-STTG1) over 48 h following incubation with CuSO$_4$ and the positive control tert-butylhydroperoxide (TBH; 100 μM), respectively. Shown are mean values of at least three independent experiments + SD. * $p < 0.05$, ** $p < 0.01$, *** $p < 0.001$ (compared to untreated control) based on ANOVA-one way test followed by Dunnett's test.

In the next step, focus was set on the detection of superoxides *via* dihydroethidium (DHE). No increase in fluorescence intensity could be observed in the Cu-treated cells compared to controls (see Fig. 5). In contrast, the positive control antimycin A massively induced superoxide-production as observed by increased fluorescence intensity. Antimycin A inhibits the electron transport chain of the mitochondria, thereby disrupting the mitochondrial function and leading to increased ROS release [55]. These results correspond to studies in rat astrocytes, where Cu did not induce ROS as measured by the same endpoint [56]. Since DHE is used to specifically detect superoxides, it seems, that Cu does not generate this type of ROS. However, it cannot be excluded that other reactive species are formed [29]. Studies in human astrocytes showed increased levels of hydroperoxides at excess Cu levels. Moreover, pre-treatment with antioxidants could prevent cellular death of Cu-exposed astrocytes [40,54]. It seems, that oxidative stress caused by ROS plays a critical role in the mode of action of Cu. In the next step, to check for other ROS and to characterize their origin, a mitochondria-targeted DHE conjugate (MitoSOX™ Red) approach was applied to investigate mitochondrial ROS. Another issue, that needs to be considered is, that ROS are highly reactive and non-stable products. It might be, that ROS cannot be detected following 48 h incubation, because they are already reduced within the cells. Therefore, kinetic measurements might be considered to monitor the production and cellular fate of ROS over a certain time periode [29,45].
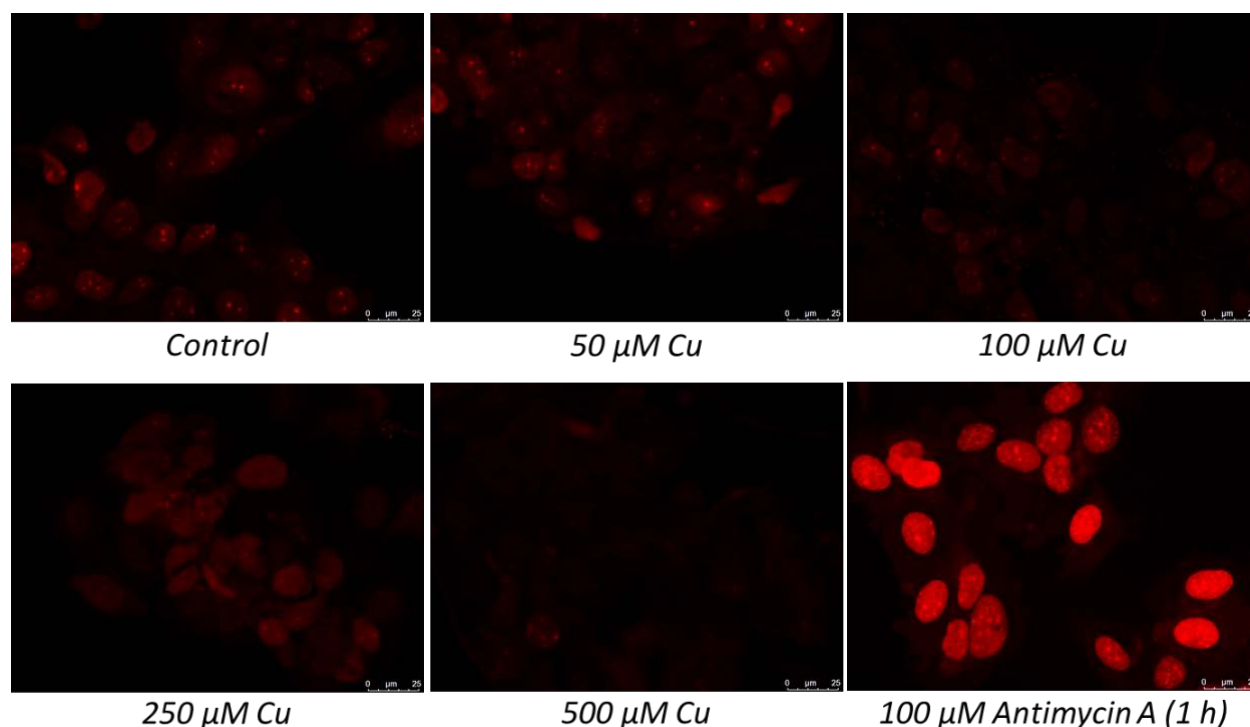
Fig. 5. Reactive oxygen species – Induction of superoxides was assessed via DHE assay in the human astrocytic cell line (CCF-STTG1) following 48 h incubation with CuSO₄ and the positive control antimycin A (100 μM, 1 h), respectively. Shown are exemplary microscopic images (60x magnification).

Application of MitoSOX™ Red enables the selective superoxide detection originating from the mitochondria [57,58]. Performing this approach, a distinct increase in mitochondria-specific superoxides could be detected (see Fig. 6). Following incubation of Cu, a slight increase in fluorescence was already observed at subcytotoxic concentrations of 50 µM. This increase was even more pronounced following incubation of concentrations up to 250 µM. Whereas the fluorescence decreased again at 500 µM Cu, probably since this is already in a cytotoxic concentration range. The positive control antimycin A induced high fluorescence. Antimycin A blocks complex III of respiratory chain. By disrupting electron transport, electrons can be transferred to oxygen and in that way superoxides are formed [56,59]. It has been reported before, that one toxic mode of action of Cu represents the formation of ROS particularly in the target organelles mitochondria [43,49].
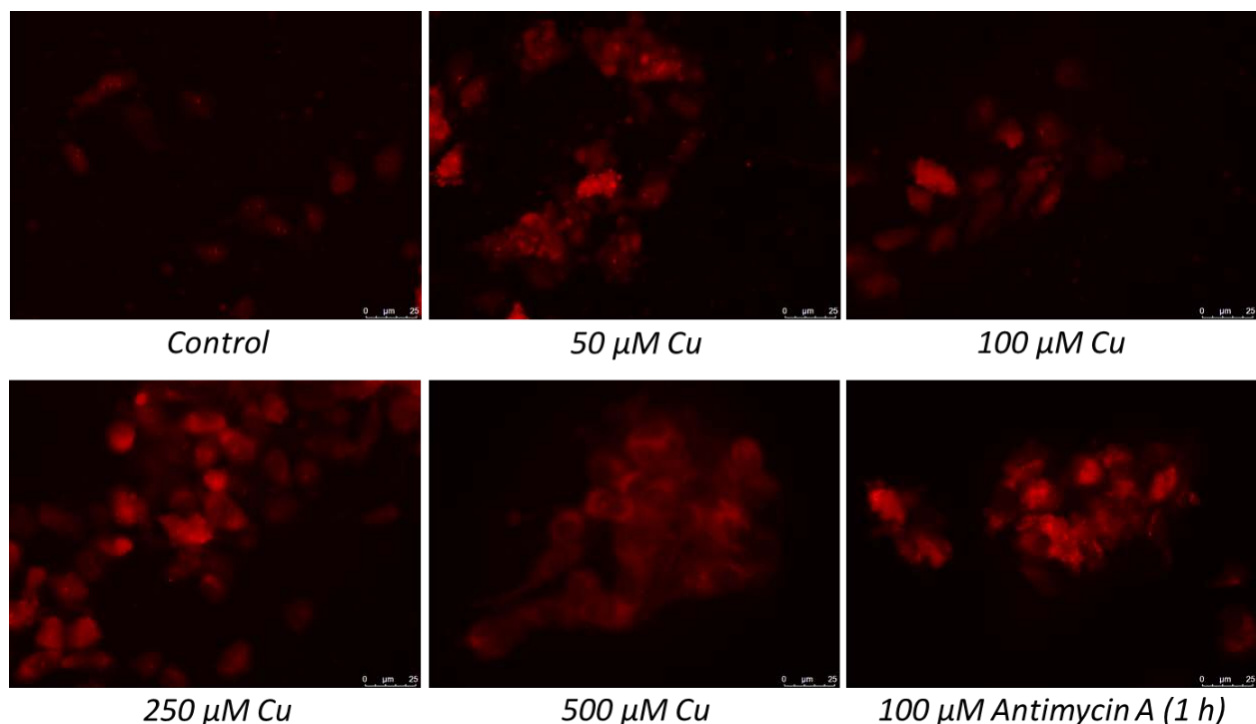
Fig. 6. Reactive oxygen species – Induction of mitochondria-derived superoxides was assessed via MitoSOX™ Red assay in the human astrocytic cell line (CCF-STTG1) following 48 h incubation with CuSO₄ and the positive control antimycin A (100 µM, 1 h), respectively. Shown are exemplary microscopic images (60x magnification). (For interpretation of the references to colour in this figure legend, the reader is referred to the web version of this article).

In vitro studies showed that Cu induced disruption of the mitochondrial membrane potential in connection with induction of mitochondrial ROS leading to mitochondrial dysfunction [49, 54]. Since this approach of MitoSOX™ Red is based on live-cell imaging, it would be interesting to develop a high-throughput assay based on tracking ROS induction in a 96 well approach. In that way, live-cell monitoring *via* kinetic measurements would provide more detailed information on the underlying mechanism and fate of mitochondrial ROS induced by Cu. ROS have been discussed to be induced only

at late stages in the course of Cu toxicity, when mitochondria are already severely damaged [36,60]. ROS seem to be rather a consequence of mitochondrial dysfunction than its cause. However, in this study, mitochondrial ROS could be already detected at low, subcytotoxic Cu levels. If these ROS are responsible and the major cause for Cu toxicity, or if the cells are able to fight against the induced ROS is not clear. Further studies should focus on defense mechanisms particularly with regard to oxidative stress/ROS. The course and fate of mitochondrial ROS caused by Cu needs to be characterized more detailed (*e.g.* kinetic measurement). In addition, potential consequences of oxidative stress, such as oxidation of biomolecules should be investigated [35].

5.5.3   Cellular bioavailability and other trace elements

 To estimate accessibility of Cu in the human astrocytic cell model, cellular bioavailability was investigated. A concentration-dependent Cu accumulation could be observed in the cells (see Fig. 7). Following incubation with 50 µM Cu, cellular Cu concentrations were found to be around 350 µM. The highest incubation concentration of 500 µM lead to cellular Cu concentrations of around 5000 µM Cu. Accumulation factors laid between 7- and 11-fold. Basal levels in human astrocytes were around 0.007 µg Cu/ mg protein. Following incubation with 50 µM Cu, cellular Cu was 0.060 µg Cu/ mg protein. The highest incubation concentration of 500 µM Cu showed the highest cellular Cu levels of 1.061 µg Cu/ mg protein. Cu accumulation factors derived out of this study are comparable to results from cellular bioavailability studies in primary astrocyte-rich cultures from rat brains. There, up to 7-fold accumulation of Cu was observed. Basal Cu levels were 1.1 nmol Cu/mg protein in the untreated astrocyte-rich cultures (corresponds to 0.070 µg Cu/ mg protein) [8]. This slightly elevated Cu level in the untreated controls might be due to species and cell type differences. A threshold level of 10 nmol Cu/ mg protein (corresponds to 0.64 µg/ mg protein) has been discussed as toxicity level for cultured astrocytes [47,61]. This threshold level could be also confirmed by this study, where substantial toxicity was observed starting from 250 µM (EC_{30} concentration, intracellular Cu level: 0.502 µg/ mg protein).

Essential elements, including Mg, Ca, Fe, Mn and Cu play a pivotal role in the brain for fundamental physiological functions and consequently, need to be present at adequate levels [62–64]. Their homeostasis in the brain is tightly regulated *via* distinct barrier systems including the blood-brain barrier and blood-cerebrospinal fluid barrier [65,66]. Altered element homeostasis might contribute to increased oxidative stress associated with neurodegenerative disorders such as Alzheimer's or Wilson disease, supporting the idea, that certain elements, besides Cu, might be involved in the development and progress of such neurological diseases [62,67]. However, studies on homeostasis of elements in the brain and their interaction are scarce. Since the homeostasis of Cu is discussed to be linked to the homeostasis of other essential elements, effects on the levels of Mg, Ca, Fe and Mn, besides Cu, were investigated (see Table 1). While Mg homeostasis was not affected with increasing

Cu concentrations, Ca and Mn levels seem to be slightly elevated. Particularly following incubation with the highest Cu concentration, the homeostasis of Ca and Mn were significantly altered. Contrarily, Fe levels tend to decrease with increasing Cu incubation. Brains of Alzheimer's disease patients have been shown to be lower in Mg [14]. The exact cause and mechanisms are still unknown. This study, however, did not reveal any link between homeostasis of Cu and Mg. An increase in Fe has been reported in brains of Wilson and Parkinson's disease patients, before. While the levels of Fe increased in the brain, being deposited with Cu in the plaques, the remaining brain cells are rather deficient in Cu [3,15,68]. Discussed links between Fe and Cu might be the transporter DMT1 (uptake mechanisms for both elements) and the Cu-binding protein ceruloplasmin (iron metabolism and export) [4,14]. In this study, Fe levels tended to decrease with increasing Cu levels. Probably, both elements are competing for the same uptake mechanisms (DMT1), leading to lower cellular Fe levels, compared to Cu.
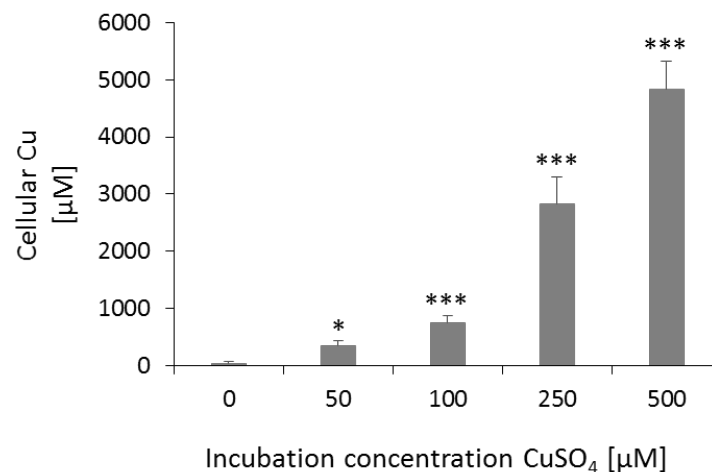
Fig. 7. Cellular bioavailability – cellular Cu levels were assessed in cell lysates *via* ICP-MS/MS in the human astrocytic cell line (CCF-STTG1) following 48 h incubation with CuSO$_4$. Shown are mean values of at least three independent experiments + SD. * $p < 0.05$, *** $p < 0.001$ (compared to untreated control) based on ANOVA-one way test followed by Dunnett's test.

Other elements are supposed to be involved in the formation of plaques in the brain as hallmark of specific brain diseases. Elevated Ca levels are discussed to increase the risk for plaque formation in the brain, associated with Alzheimer's disease [14]. Characterization of the senile plaques indicated, that homeostasis of Fe and Ca are disrupted in these patients, since elevated levels of Fe and Ca are detected [69]. Besides, increased Ca levels can be a sign for induction of apoptosis. Ca acts as a second messenger to trigger cell death *via* intracellular signaling pathways [70]. Interestingly, a slight increase in cellular Ca has been reported in Cu-treated neurons, before. Increase in Ca level could be linked to Cu-induced apoptosis, since the use of a calcium blocker mitigated toxic effects of Cu [34]. Besides, Mn seems to be also connected to the Cu homeostasis. Both elements are discussed to interact with ATP7A, leading to efflux of Cu [16,71]. Consequently, in context of a disrupted Cu homeostasis, other

essential elements need to be taken into account as well, since they might contribute to Cu-mediated toxicity.

5.6 Conclusion

This study aimed to characterize the toxic mode of action of Cu in a human astrocytic cell model, with particular focus on mitochondria and oxidative stress markers. Following 48 h incubation, Cu exerted a substantial cytotoxic potential (EC$_{30}$: 250 µM) and impaired mitochondrial function already at subcytotoxic concentrations as observed *via* effects on mitochondrial membrane potential and formation of ROS, indicating studies should focus on fate and course of ROS in the cells following incubation with Cu. Moreover, Cu showed effects on the GSH metabolism as observed by increased total cellular GSH levels and altered cellular ratios of GSH/GSSG. Besides providing an important antioxidant system, GSH is also involved in the Cu homeostasis. Consequently, it will be of great interest to also consider further copper-related proteins such as metallothioneins. It seems that excess levels of Cu not only affect cellular Cu levels, but also interfere with the homeostasis of other elements such as Ca, Fe and Mn. Altered element homeostasis might contribute to the induction of oxidative stress likely being involved in the course of neurodegenerative diseases. The underlying mechanisms and interplays are poorly understood and need to be elucidated. In this context, it would be interesting to include other relevant elements such as Zn and Se, that might be also involved in the course of Cu-related disorders. These studies provide a basis to get deeper insights in the interrelation of altered homeostasis and development and progression of these diseases. Based on these results, potential biomarkers might be developed and used for early detection of Cu-related disorders before first symptoms appear.

Table 1. Cellular element homeostasis – effects on cellular levels of selected elements (Mg, Ca, Fe, Mn, Cu) were investigated in cell lysates *via* ICP-MS/MS in the human astrocytic cell line (CCF-STTG1) following 48 h incubation with CuSO$_4$. Shown are mean values of at least three independent experiments +/- SD. ** $p < 0.01$, *** $p < 0.001$ (compared to untreated control) based on ANOVA-one way test followed by Dunnett's test.

Element [µg/mg Protein]	0 µM Cu	50 µM Cu	100 µM Cu	250 µM Cu	500 µM Cu
Mg	0.975	0.978	1.082	1.090	0.949
	± 0.190	± 0.155	± 0.199	± 0.139	± 0.105
Ca	2.689	2.757	3.266	3.003	3.500
	± 0.477	± 0.739	± 0.696	± 0.662	± 0.652**
Fe	0.084	0.091	0.102	0.076	0.066
	± 0.030	± 0.039	± 0.046	± 0.033	± 0.029
Mn	0.019	0.020	0.022	0.021	0.025
	± 0.003	± 0.003	± 0.003	± 0.003	± 0.002***
Cu	0.007	0.060	0.143	0.502	1.061
	± 0.003	± 0.013	± 0.037	± 0.094	± 0.159

5.7 Funding

5.8 CRediT authorship contribution statement

Barbara Witt: Conceptualization, Methodology, Formal analysis, Investigation, Writing - original draft, Writing - review & editing, Supervision. **Michael Stiboller:** Methodology, Validation, Formal analysis, Investigation, Writing - review & editing. **Stefanie Raschke:** Investigation, Formal analysis. **Sharleen Friese:** Investigation, Formal analysis. **Franziska Ebert:** Methodology, Supervision. **Tanja Schwerdtle:** Conceptualization, Resources, Supervision, Project administration, Funding acquisition.

5.9 Declaration of Competing Interest

The authors declare no conflict of interest.

5.10 Acknowledgements

5.11 References

[1]   U.B. Barache, A.B. Shaikh, T.N. Lokhande, G.S. Kamble, M.A. Anuse, S.H. Gaikwad, An efficient, cost effective, sensing behaviour liquid-liquid extraction and spectrophotometric determination of copper(II) incorporated with 4-(4'- chlorobenzylideneimino)-3-methyl-5-mercapto-1, 2, 4-triazole: analysis of food samples, leafy vegetables, fertilizers and environmental samples, Spectrochim. Acta A Mol. Biomol. Spectrosc. 189 (2018) 443–453.

[2]   M. Bost, S. Houdart, M. Oberli, E. Kalonji, J.F. Huneau, I. Margaritis, Dietary copper and human health: current evidence and unresolved issues, J. Trace Elem. Med. Biol. 35 (2016) 107–115.

[3]   F. Bulcke, R. Dringen, I.F. Scheiber, Neurotoxicity of copper, Adv. Neurobiol. 18 (2017) 313–343.

[4]   I.F. Scheiber, J.F.B. Mercer, R. Dringen, Metabolism and functions of copper in brain, Prog. Neurobiol. 116 (2014) 33–57.

[5]   M.S. Horning, P.Q. Trombley, Zinc and copper influence excitability of rat olfactory bulb neurons by multiple mechanisms, J. Neurophysiol. 86 (4) (2001) 1652–1660.

[6]   S. Lutsenko, Copper trafficking to the secretory pathway, Metallomics 8 (9) (2016) 840–852.

[7]   I.F. Scheiber, M.M. Schmidt, R. Dringen, Copper export from cultured astrocytes, Neurochem. Int. 60 (3) (2012) 292–300.

[8]   I.F. Scheiber, J.F. Mercer, R. Dringen, Copper accumulation by cultured astrocytes, Neurochem. Int. 56 (3) (2010) 451–460.

[9]   E. Tiffany-Castiglioni, S. Hong, Y. Qian, Copper handling by astrocytes: insights into neurodegenerative diseases, Int. J. Dev. Neurosci. 29 (8) (2011) 811–818.

[10]   D.R. Brown, Role of the prion protein in copper turnover in astrocytes, Neurobiol. Dis. 15 (3) (2004) 534–543.

[11]   B. Sullivan, G. Robison, J. Osborn, M. Kay, P. Thompson, K. Davis, T. Zakharova, O. Antipova, Y. Pushkar, On the nature of the Cu-rich aggregates in brain astrocytes, Redox Biol. 11 (2017) 231–239.

[12]   M. Manto, Abnormal copper homeostasis: mechanisms and roles in neurodegeneration, Toxics 2 (2014) 327–345.

[13]   A.R. White, G. Multhaup, F. Maher, S. Bellingham, J. Camakaris, H. Zheng, A. I. Bush, K. Beyreuther, C.L. Masters, R. Cappai, The Alzheimer's disease amyloid precursor protein modulates copper-induced toxicity and oxidative stress in primary neuronal cultures, J. Neurosci. 19 (21) (1999) 9170–9179.

[14]   P. Wang, Z.Y. Wang, Metal ions influx is a double edged sword for the pathogenesis of Alzheimer's disease, Ageing Res. Rev. 35 (2017) 265–290.

[15]   R.F. Serpa, E.F. de Jesus, M.J. Anjos, L.F. de Oliveira, L.A. Marins, M.G. do Carmo, J.D. Correa Junior, M.S. Rocha, R.T. Lopes, A.M. Martinez, Topographic trace-elemental analysis in the brain of Wistar rats by X-ray microfluorescence with synchrotron radiation, Anal. Sci. 24 (7) (2008) 839–842.

[16]   X. Fu, Y. Zhang, W. Jiang, A.D. Monnot, C.A. Bates, W. Zheng, Regulation of copper transport crossing brain barrier systems by Cu-ATPases: effect of manganese exposure, Toxicol. Sci. 139 (2) (2014) 432–451.

[17]   C. Doguer, J.H. Ha, J.F. Collins, Intersection of Iron and copper metabolism in the mammalian intestine and liver, Compr. Physiol. 8 (4) (2018) 1433–1461.

[18]   H. Kozlowski, A. Janicka-Klos, J. Brasun, E. Gaggelli, D. Valensin, G. Valensin, Copper, iron, and zinc ions homeostasis and their role in neurodegenerative disorders (metal uptake, transport distribution and regulation), Coord. Chem. Rev. 253 (2009) 2665–2685.

[19]   C.F. Brunk, K.C. Jones, T.W. James, Assay for nanogram quantities of DNA in cellular homogenates, Anal. Biochem. 92 (2) (1979) 497–500.

[20]   B. Witt, S. Meyer, F. Ebert, K.A. Francesconi, T. Schwerdtle, Toxicity of two classes of arsenolipids and their water-soluble metabolites in human differentiated neurons, Arch. Toxicol. 91 (9) (2017) 3121–3134.

[21]   J. O'Brien, I. Wilson, T. Orton, F. Pognan, Investigation of the Alamar Blue (resazurin) fluorescent dye for the assessment of mammalian cell cytotoxicity, Eur. J. Biochem. 267 (17) (2000) 5421–5426.

[22]   H. Lohren, L. Blagojevic, R. Fitkau, F. Ebert, S. Schildknecht, M. Leist, T. Schwerdtle, Toxicity of organic and inorganic mercury species in differentiated human neurons and human astrocytes, J. Trace Elem. Med. Biol. 32 (2015) 200–208.

[23]   B. Chazotte, Labeling mitochondria with MitoTracker dyes, Cold Spring Harb. Protoc. 2011 (8) (2011) 990–992.

[24]   S.W. Perry, J.P. Norman, J. Barbieri, E.B. Brown, H.A. Gelbard, Mitochondrial membrane potential probes and the proton gradient: a practical usage guide, Biotechniques 50 (2) (2011) 98–115.

[25]   F. Ebert, M. Thomann, B. Witt, S.M. Muller, S. Meyer, T. Weber, M. Christmann, T. Schwerdtle, Evaluating long-term cellular effects of the arsenic species thio-DMA (V): qPCR-based gene expression as screening tool, J. Trace Elem. Med. Biol. 37 (2016) 78–84.

[26]   I. Rahman, A. Kode, S.K. Biswas, Assay for quantitative determination of glutathione and glutathione disulfide levels using enzymatic recycling method, Nat. Protoc. 1 (6) (2006) 3159–3165.

[27]   L. Leffers, M. Unterberg, M. Bartel, C. Hoppe, I. Pieper, J. Stertmann, F. Ebert, H. U. Humpf, T. Schwerdtle, In vitro toxicological characterisation of the S-containing arsenic metabolites thio-dimethylarsinic acid and dimethylarsinic glutathione, Toxicology 305 (2013) 109–119.

[28]   J. Bornhorst, S. Chakraborty, S. Meyer, H. Lohren, S.G. Brinkhaus, A.L. Knight, K. A. Caldwell, G.A. Caldwell, U. Karst, T. Schwerdtle, A. Bowman, M. Aschner, The effects of pdr1, djr1.1 and pink1 loss in manganese-induced toxicity and the role of alpha-synuclein in C. Elegans, Metallomics 6 (3) (2014) 476–490.

[29]   B. Halliwell, M. Whiteman, Measuring reactive species and oxidative damage in vivo and in cell culture: how should you do it and what do the results mean? Br. J. Pharmacol. 142 (2) (2004) 231–255.

[30]   F. Ebert, V. Ziemann, V.K. Wandt, B. Witt, S.M. Muller, N. Guttenberger, E. E. Bankoglu, H. Stopper, G. Raber, K.A. Francesconi, T. Schwerdtle, Cellular toxicological characterization of a thioxolated arsenic-containing hydrocarbon, J. Trace Elem. Med. Biol. 61 (2020), 126563.

[31]   J. Bornhorst, S. Meyer, T. Weber, C. Boker, T. Marschall, A. Mangerich, S. Beneke, A. Burkle, T. Schwerdtle, Molecular mechanisms of Mn induced neurotoxicity: RONS generation, genotoxicity, and DNA-damage response, Mol. Nutr. Food Res. 57 (7) (2013) 1255–1269.

[32]   L. Zhao, J.L. Wang, Y.R. Wang, X.Z. Fa, Apigenin attenuates copper-mediated beta-amyloid neurotoxicity through antioxidation, mitochondrion protection and MAPK signal inactivation in an AD cell model, Brain Res. 1492 (2013) 33–45.

[33]   E.E. Bankoglu, O. Tschopp, J. Schmitt, P. Burkard, D. Jahn, A. Geier, H. Stopper, Role of PTEN in oxidative stress and DNA damage in the liver of whole-body pten haplodeficient mice, PLoS One 11 (11) (2016), e0166956.

[34]   S.H. Chen, J.K. Lin, S.H. Liu, Y.C. Liang, S.Y. Lin-Shiau, Apoptosis of cultured astrocytes induced by the copper and neocuproine complex through oxidative stress and JNK activation, Toxicol. Sci. 102 (1) (2008) 138–149.

[35]   K. Merker, D. Hapke, K. Reckzeh, H. Schmidt, H. Lochs, T. Grune, Copper related toxic effects on cellular protein metabolism in human astrocytes, Biofactors 24 (1- 4) (2005) 255–261.

[36]   S. Borchard, F. Bork, T. Rieder, C. Eberhagen, B. Popper, J. Lichtmannegger, S. Schmitt, J. Adamski, M. Klingenspor, K.H. Weiss, H. Zischka, The exceptional sensitivity of brain mitochondria to copper, Toxicol. In Vitro 51 (2018) 11–22.

[37]   D. Hu, T.J. Kipps, Reduction in mitochondrial membrane potential is an early event in Fas-independent CTL-mediated apoptosis, Cell. Immunol. 195 (1) (1999) 43–52.

[38]   V.C. Keil, F. Funke, A. Zeug, D. Schild, M. Muller, Ratiometric high-resolution imaging of JC-1 fluorescence reveals the subcellular heterogeneity of astrocytic mitochondria, Pflugers Arch. 462 (5) (2011) 693–708.

[39]   A. Korenic, J. Boltze, A. Deten, M. Peters, P. Andjus, L. Radenovic, Astrocytic mitochondrial membrane hyperpolarization following extended oxygen and glucose deprivation, PLoS One 9 (2) (2014), e90697.

[40]   P.V. Reddy, K.V. Rao, M.D. Norenberg, The mitochondrial permeability transition, and oxidative and nitrosative stress in the mechanism of copper toxicity in cultured neurons and astrocytes, Lab. Invest. 88 (8) (2008) 816–830.

[41]   E. Nam, J. Han, J.M. Suh, Y. Yi, M.H. Lim, Link of impaired metal ion homeostasis to mitochondrial dysfunction in neurons, Curr. Opin. Chem. Biol. 43 (2018) 8–14.

[42]   C.T. Sheline, E.H. Choi, J.S. Kim-Han, L.L. Dugan, D.W. Choi, Cofactors of mitochondrial enzymes attenuate copper-induced death in vitro and in vivo, Ann. Neurol. 52 (2) (2002) 195–204.

[43]   M.J. Hosseini, F. Shaki, M. Ghazi-Khansari, J. Pourahmad, Toxicity of copper on isolated liver mitochondria: impairment at complexes I, II, and IV leads to increased ROS production, Cell Biochem. Biophys. 70 (1) (2014) 367–381.

[44]   F. Bulcke, R. Dringen, Handling of copper and copper oxide nanoparticles by astrocytes, Neurochem. Res. 41 (1-2) (2016) 33–43.

[45]   C. Batandier, E. Fontaine, C. Keriel, X.M. Leverve, Determination of mitochondrial reactive oxygen species: methodological aspects, J. Cell. Mol. Med. 6 (2) (2002) 175–187.

[46]   C.H. Wang, S.B. Wu, Y.T. Wu, Y.H. Wei, Oxidative stress response elicited by mitochondrial dysfunction: implication in the pathophysiology of aging, Exp. Biol. Med. (Maywood) 238 (5) (2013) 450–460.

[47]   I.F. Scheiber, R. Dringen, Copper-treatment increases the cellular GSH content and accelerates GSH export from cultured rat astrocytes, Neurosci. Lett. 498 (1) (2011) 42–46.

[48]   C.M. Saporito-Magrina, R.N. Musacco-Sebio, G. Andrieux, L. Kook, M.T. Orrego, M. V. Tuttolomondo, M.F. Desimone, M. Boerries, C. Borner, M.G. Repetto, Copper-induced cell death and the protective role of glutathione: the implication of impaired protein folding rather than oxidative stress, Metallomics 10 (12) (2018) 1743–1754.

[49]   J. Pourahmad, P.J. O'Brien, A comparison of hepatocyte cytotoxic mechanisms for Cu2+ and Cd2+, Toxicology 143 (3) (2000) 263–273.

[50]   H. Nagasaka, I. Inoue, A. Inui, H. Komatsu, T. Sogo, K. Murayama, T. Murakami, T. Yorifuji, K. Asayama, S. Katayama, S. Uemoto, K. Kobayashi, M. Takayanagi, T. Fujisawa, H. Tsukahara, Relationship between oxidative stress and antioxidant systems in the liver of patients with Wilson disease: hepatic manifestation in Wilson disease as a consequence of augmented oxidative stress, Pediatr. Res. 60 (4) (2006) 472–477.

[51]   R. Dringen, B. Hamprecht, Glutathione restoration as indicator for cellular metabolism of astroglial cells, Dev. Neurosci. 20 (4-5) (1998) 401–407.

[52]   S.A. Pope, R. Milton, S.J. Heales, Astrocytes protect against copper-catalysed loss of extracellular glutathione, Neurochem. Res. 33 (7) (2008) 1410–1418.

[53]   M.A. Martin, S. Ramos, R. Mateos, M. Izquierdo-Pulido, L. Bravo, L. Goya, Protection of human HepG2 cells against oxidative stress by the flavonoid epicatechin, Phytother. Res. 24 (4) (2010) 503–509.

[54]   G. Ferretti, T. Bacchetti, C. Moroni, A. Vignini, G. Curatola, Copper-induced oxidative damage on astrocytes: protective effect exerted by human high density lipoproteins, Biochim. Biophys. Acta 1635 (1) (2003) 48–54.

[55]   W.H. Park, Y.W. Han, S.H. Kim, S.Z. Kim, An ROS generator, antimycin A, inhibits the growth of HeLa cells via apoptosis, J. Cell. Biochem. 102 (1) (2007) 98–109.

[56]   A.V. Gyulkhandanyan, C.J. Feeney, P.S. Pennefather, Modulation of mitochondrial membrane potential and reactive oxygen species production by copper in astrocytes, J. Neurochem. 87 (2) (2003) 448–460.

[57]   R.R. Nazarewicz, A. Bikineyeva, S.I. Dikalov, Rapid and specific measurements of superoxide using fluorescence spectroscopy, J. Biomol. Screen. 18 (4) (2013) 498–503.

[58]   M.E. Kauffman, M.K. Kauffman, K. Traore, H. Zhu, M.A. Trush, Z. Jia, Y.R. Li, MitoSOX-based flow cytometry for detecting mitochondrial ROS, React. Oxyg. Species Apex (Apex) 2 (5) (2016) 361–370.

[59]   D.G. Nicholls, S.L. Budd, Mitochondria and neuronal survival, Physiol. Rev. 80 (1) (2000) 315–360.

[60]   H. Zischka, C. Einer, Mitochondrial copper homeostasis and its derailment in Wilson disease, Int. J. Biochem. Cell Biol. 102 (2018) 71–75.

[61]   F. Bulcke, K. Thiel, R. Dringen, Uptake and toxicity of copper oxide nanoparticles in cultured primary brain astrocytes, Nanotoxicology 8 (7) (2014) 775–785.

[62]   A. Ashraf, C. Michaelides, T.A. Walker, A. Ekonomou, M. Suessmilch, A. Sriskanthanathan, S. Abraha, A. Parkes, H.G. Parkes, K. Geraki, P.W. So, Regional distributions of Iron, copper and zinc and their relationships with glia in a normal aging mouse model, Front. Aging Neurosci. 11 (2019) 351.

[63]   J.S. Cristovao, R. Santos, C.M. Gomes, Metals and neuronal metal binding proteins implicated in alzheimer's disease, Oxid. Med. Cell. Longev. 2016 (2016), 9812178.

[64]   L. Mezzaroba, D.F. Alfieri, A.N. Colado Simao, E.M. Vissoci Reiche, The role of zinc, copper, manganese and iron in neurodegenerative diseases, Neurotoxicology 74 (2019) 230–241.

[65]   W. Zheng, A.D. Monnot, Regulation of brain iron and copper homeostasis by brain barrier systems: implication in neurodegenerative diseases, Pharmacol. Ther. 133 (2) (2012) 177–188.

[66]   N.J. Abbott, A.A. Patabendige, D.E. Dolman, S.R. Yusof, D.J. Begley, Structure and function of the blood-brain barrier, Neurobiol. Dis. 37 (1) (2010) 13–25.

[67]   L. Zhong, A. Dong, Y. Feng, X. Wang, Y. Gao, Y. Xiao, J. Zhang, D. He, J. Cao, W. Zhu, S. Zhang, Alteration of metal elements in radiation injury: radiation-induced copper accumulation aggravates intestinal damage, Dose. 18 (1) (2020), 1559325820904547.

[68]   B.R. Roberts, T.M. Ryan, A.I. Bush, C.L. Masters, J.A. Duce, The role of metallobiology and amyloid-beta peptides in Alzheimer's disease, J. Neurochem. 120 (Suppl 1) (2012) 149–166.

[69]   J. Everett, J.F. Collingwood, V. Tjendana-Tjhin, J. Brooks, F. Lermyte, G. Plascencia-Villa, I. Hands-Portman, J. Dobson, G. Perry, N.D. Telling, Nanoscale synchrotron X-ray speciation of iron and calcium compounds in amyloid plaque cores from Alzheimer's disease subjects, Nanoscale 10 (25) (2018) 11782–11796.

[70]   Y. Yuan, C.Y. Jiang, H. Xu, Y. Sun, F.F. Hu, J.C. Bian, X.Z. Liu, J.H. Gu, Z.P. Liu, Cadmium-induced apoptosis in primary rat cerebral cortical neurons culture is mediated by a calcium signaling pathway, PLoS One 8 (5) (2013), e64330.

[71]   M.L. Schlief, J.D. Gitlin, Copper homeostasis in the CNS: a novel link between the NMDA receptor and copper homeostasis in the hippocampus, Mol. Neurobiol. 33 (2) (2006) 81–90.

6. Selenium homeostasis in human brain cells: Effects of copper (II) and Se species

6.1 Graphical abstract
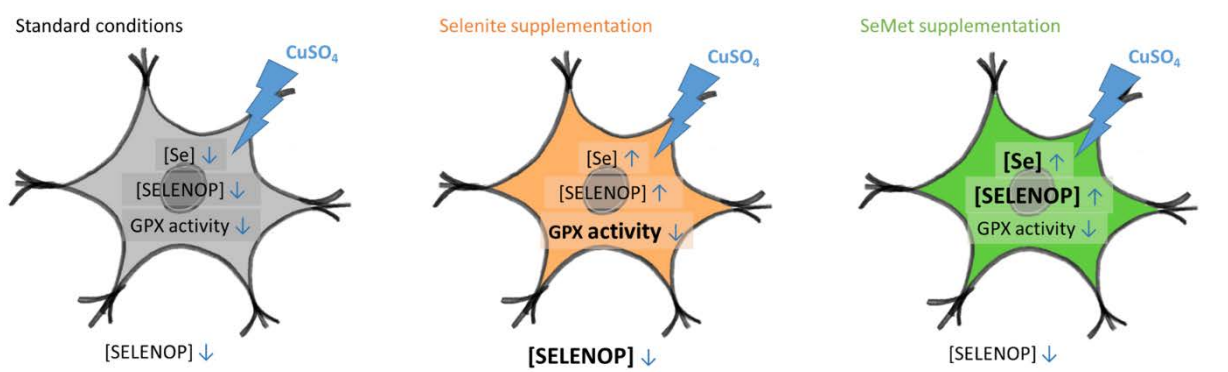
6.2 Abstract

Both essential trace elements selenium (Se) and copper (Cu) play an important role in maintaining brain function. Homeostasis of Cu, which is tightly regulated under physiological conditions, seems to be disturbed in Alzheimer´s (AD) and Parkinson´s disease (PD) patients. Excess Cu promotes the formation oxidative stress, which is thought to be a major cause for development and progression of neurological diseases (NDs). Most selenoproteins exhibit antioxidative properties and may counteract oxidative stress. However, expression of selenoproteins is altered under conditions of Se deficiency. Serum Se levels are decreased in AD and PD patients suggesting Se as an important factor in the development and progression of NDs. The aim of this study was to elucidate the interactions between Cu and Se in human brain cells particularly with respect to Se homeostasis. Firstly, modulation of Se status by selenite or SeMet were assessed in human astrocytes and human differentiated neurons. Therefore, cellular total Se content, intra- and extracellular selenoprotein P (SELENOP) content, and glutathione peroxidase (GPX) activity were quantified. Secondly, to investigate the impact of Cu on these markers, cells were exposed to copper(II)sulphate ($CuSO_4$) for 48 h. In addition, putative protective effects of Se on Cu-induced toxicity, as measured by cell viability, DNA damage, and neurodegeneration were investigated. Modulation of cellular Se status was strongly dependent on Se species. In detail, SeMet increased total cellular Se and SELENOP content, whereas selenite led to increased GPX activity and SELENOP excretion. Cu treatment resulted in 133-fold higher cellular Cu concentration with a concomitant decrease in Se content. Additionally, SELENOP excretion was suppressed in both cell lines, while GPX activity was diminished only in astrocytes. These effects of Cu could be partially prevented by the addition of Se depending on the cell line and Se species used. While Cu-induced oxidative DNA damage could not be prevented by addition of Se regardless of chemical species, SeMet protected against neurite network degeneration triggered by Cu. Cu appears to negatively affect Se status in astrocytes and neurons. Especially with regard to an altered homeostasis of those trace elements during aging, this interaction is of high physiological relevance. Increasing Cu concentrations associated with decreased selenoprotein expression or functionality might be a promoting factor for the development of NDs.

6.3 Introduction

Selenium (Se) is of high relevance in maintaining brain functions. In Se-deficiency, the brain retains Se at the expense of other tissues [1], resulting in particular protection from deficiency. Selenoprotein P (SELENOP) is the main Se-supplier for the brain and responsible for Se distribution in the brain [2]. Deficiency has severe consequences on physiological functions, as demonstrated in different knockout mouse models [3–6]. SELENOP is synthesized not only by liver cells but also by astrocytes, which contributes to Se distribution in the brain. The brain is highly susceptible to oxidative stress [7,8], which is considered as a molecular mechanism for the development of neurodegenerative diseases (NDs). Most selenoproteins possess antioxidant properties, which might counteract development of NDs [9]. In elderly, correlation between decreased plasma Se and cognitive decline could be observed [10]. Additionally, decreased plasma Se and SELENOP levels were found in Alzheimer´s (AD) and Parkinson´s disease (PD) patients [11,12].

Besides Se, copper (Cu) is also essential for brain function, with deficiency leading to neurological dysfunction [13]. Cu deficiency occurs rarely, whereas oversupply develop more frequently. However, it is toxic at high concentration by generating free radicals via Fenton-like reaction and consequently damaging macromolecules [13], emphasizing the need for strict homeostatic regulation. Cu transport into the cell is mainly facilitated by CTR1 as Cu(I), where it is sequestered by GSH and transported to specific chaperones or stored in metallothionein (MT) [14]. Recycling of oxidized GSH occurs via the thioredoxin reductase/thioredoxin (TXNRD/TRX) system, which establishes a connection between Se and Cu [15]. Moreover, NDs are associated with disturbed Cu homeostasis resulting in misdistribution of Cu [16,17]. In brains of PD and AD patients, Cu levels were decreased in brain areas such as the substantia nigra while Cu accumulation occurs in Lewis bodies or senile plaques [18,19]. In mouse neuronal cells, Cu stimulated the aggregation of tau protein and amyloid-β, both associated with AD progression, resulting in higher cytotoxicity which could be ameliorated by addition of SELENOP [20,21]. Recently, it was published that enzymatic activities of glutathione peroxidase (GPX) and thioredoxin reductase (TXNRD) were decreased upon Cu exposure in HepG2 cells, demonstrating interference of Cu with Se metabolism [22].

In view of changes in trace element homeostasis during aging, the investigation of interactions is of relevance [23]. Especially, shifts in the Cu-to-Se ratios are associated with worse outcome of various diseases [24,25]. Therefore, the aim of this study was to characterize the modulation of the Se status of brain-derived cell lines by different Se species and subsequently the influence of Cu on Se homeostasis.

6.4 Material and methods

6.4.1 Materials

RPMI 1640 medium and L-glutamine were obtained from Biochrom (Berlin, Germany), fetal calf serum (FCS, Se low, LOT 118K3395), penicillin/streptomycin and trypsin were purchased from Sigma Aldrich (Steinheim, Germany). Culture dishes were from TPP (Trasadingen, Switzerland). Sodium selenite ($Na_2SeO_3 \cdot 5\ H_2O$, ≥99%), seleno-DL-methionine (≥99%), resazurin dye, ammonium acetate, L-glutathione (reduced, ≥98%), glutathione reductase from baker's yeast (*S. cerevisiae*, LOT SLBX2014), hydrogen peroxide solution (for ultratrace analysis) were obtained from Sigma Aldrich. Standard reference material (SRM) 1950 was obtained from the National Institute of Standards and Technology (NIST, Gaithersburg, MD). Copper(II)sulphate ($CuSO_4$, anhydrous, >99%), ICP-MS elemental standards, NADPH-Tetranatriumsalz (≥95 %) were from Roth (Karlsruhe, Germany). MitoTracker® Orange CMT-MRos were from Life Technologies GmbH (Darmstadt, Germany). Hoechst 33258 and nitric acid (65%, suprapur) were obtained from Merck KGaA (Darmstadt, Germany). Bradford solution were from Bio-Rad (Munich, Germany). Protease inhibitor cocktail set III were obtained from Merck Millipore (Burlington, USA). All other chemicals not stated were purchased from Sigma Aldrich or Roth and were of p.a. grade.

Dilutions were prepared freshly before each experiment. Concentration of stock solutions were regularly checked by ICP-MS/MS measurement (data not shown).

6.4.2 Cell culture and incubation protocol

Human astrocytes (CCF-STTG1)

Human astrocytoma cell line was kindly provided by Prof. Dr. Hans-Joachim Galla (Institute of Biochemistry, University of Münster). Cells were cultured in RPMI 1640 medium supplemented with 10% FCS, 100 U/mL penicillin, 100 mg/mL streptomycin and 1.4 mM L-glutamine at standard conditions (37°C, 5% CO_2 and 100% humidity). Every week, cells were subcultured and medium was exchanged every 2-3 days. Se concentration was below limit of detection (LOD) in RPMI media including all additives. For Cu/Se combination, cells were supplemented with 100 nM of respective Se species directly after seeding. After 48 h, cells were treated with $CuSO_4$ for additional 48 h (Figure S1A).

Human differentiated neurons (LUHMES)

Neuronal cell line was kindly provided by Prof. Dr. Marcel Leist and Dr. Stefan Schildknecht from the University of Konstanz. General cultivation and differentiation processes were performed according to protocols published before [26]. Cell culture flasks and plates were precoated with 50 µg/mL poly-L-ornithine (poly-L-ornithine hydrobromide, Sigma–Aldrich) and 1 µg/mL fibronectin (from bovine plasma, Sigma–Aldrich). For cultivation and differentiation, Advanced Dulbecco's modified Eagle's

medium/F12 (Life Technologies GmbH) supplemented with 1 × N2 supplement (Life Technologies GmbH), 2 mM L-glutamine (Sigma–Aldrich) was used as basic medium. According to the manufacturer, the basic medium contains sodium selenite, which results in a Se content of approximately 50 nM. For proliferation, LUHMES cells were cultivated in proliferation medium (basic medium added with 40 ng/mL recombinant human basic fibroblast growth factor (FGF, R&D Systems, Wiesbaden-Nordenstadt, Germany) at standard conditions (37°C, 5% CO2 and 100% humidity). For differentiation, cells were seeded at a density of 4.5 · 105 cells per cm² and 24 h later the differentiation process was started by replacing the proliferation media by differentiation media (basal medium added with 1 µg/mL tetracycline (Sigma-Aldrich), 1 mM dibutyryl cyclic adenosine monophosphate sodium salt (cAMP, Sigma-Aldrich) and 2 ng/mL recombinant human glial cell-derived neurotrophic factor (GDNF, R&D Systems). After 48 h, cells were trypsinized and seeded on pre-coated dishes (1.5 · 105 cells per cm²) and supplemented with 50 nM selenite or SeMet. Another 48 h later, differentiation media was exchanged and cells were again supplemented with 50 nM selenite or SeMet. Differentiation process was complete on day 6 and cells were exposed to CuSO4 for 48 h (Figure S1B).

6.4.3   Viability studies

To characterize the impact of an adequate Se supply on the cytotoxic effects of $CuSO_4$ in human astrocytes and differentiated neurons, the following cell viability marker were assessed.

Dehydrogenase activity (Cell counting Kit-8): Cytosolic and mitochondrial dehydrogenases are responsible for the reduction of the yellow tetrazolium salt and the amount of the end-product formazan is proportional to the number of cells with sufficient dehydrogenase activity. The assay was performed as described before [27]. Shift in absorbance was measured at 450 nm wavelength using the Tecan infinite 200 Pro plate reader (Tecan Austria GmbH, Grödig, Austria).

Hoechst staining: The bisbenzimidazole dye, Hoechst 33258, intercalate to double stranded DNA resulting in a linear correlation between DNA content and fluorescence [28,29]. Procedure of the assay was done as previously described [30]. The fluorescence was measured using a Tecan infinite 200 Pro plate reader at Ex. 355 nm and Em. 460 nm.

Neutral red uptake: Viable cells are able to take up the neutral red, which has a net charge of zero at physiological pH into lysosomes. Once inside the intact lysosomes the dye gets charged and binds to the lysosomal matrix [31]. The assay was performed as described before [27]. Absorbance at 540 nm was measured using a Tecan infinite 200 Pro plate reader.

Resazurin Assay: The reduction of resazurin to the fluorescent resorufin by cellular dehydrogenases is considered as a marker for cell viability [32]. Detailed procedure has been previously published [26]. Fluorescence of the end-product was measured using a Tecan infinite 200 Pro plate reader at excitation wavelength 540 nM and emission wavelength 590 nM.

6.4.4   Mitochondrial membrane potential

Dependend on the mitochondrial membrane potential (MMP), cells are able to take up the positively charged dye, MitoTracker® Orange CMTMRos [33,34]. The assay was carried out as described elsewhere [35]. For calculation of the mitochondrial activity, the mitochondrial membrane potential was related to the cell number.

6.4.5   Selenium-related markers

To determine the Se status of the cells, GPX activity, SELENOP, and total Se content were measured in cell lysates and medium samples.

GPX activity: Determination of GPX activity based on the consumption of NADPH coupled with glutathione reductase according to Florian et al. adapted to cell lysates [36]. To obtain cell lysates, pellets were lysed in homogenisation buffer (100 mM Tris, 300 mM KCl, 0,1% Triton X-100 added with 1:1000 protease inhibitor cocktail set III) and after sonication, cellular debris were removed by centrifugation (15.000 x g, for 10 min, at 4 °C). Subsequently, assay buffer (100 mM TRIS, 5 mM EDTA, 1 mM NaN3, pH 7.6) containing 10% Triton X-100, 0.2 mM NADPH, 3.4 mM GSH and 2.3 U GR was added to the cell lysates. To start the reaction, hydrogen peroxide at a final concentration of 75 nM was added. Consumption of NADPH was measured using the Synergy 2 (BioTek Instruments, Bad Friedrichshall, Germany) plate reader at 340 nM. After automatic pathlength correction GPX activity was calculated according to Lambert-Beer´s law and was expressed as mU/mg protein (one unit corresponds to the consumption of 1 µmol NADPH per minute). Total protein content was determined according to Bradford [37].

Total Cu and Se content: For determination of total concentrations of Cu and Se, cell lysates or medium were prepared by acidic microwave-assisted digestion. To obtain lysates, cell pellets were lysed in RIPA buffer (100 mM TRIS, 10 mM EDTA, 1 M NaCl, 10% Triton-X100, 10% DOC, 10% SDS). After sonication, cellular debris was removed by centrifugation (15.000 x g, for 10 min, at 4 °C). As internal standard Ge (10 µg/L), Rh (1 µg/L) and Se77 (3 µg/L) were added to the samples. Determination of element contents were carried out by ICP-MS/MS (Agilent 8800 ICP-QQQ-MS, Agilent Technologies, Waldbronn, Germany). The ICP-MS/MS was operated in MS/MS mode using helium (Cu) or oxygen (Se) as collision cell gas at a flow rate of 4.3 mL/min and 3.0 mL/min, respectively. Following mass transitions were measured: Se m/z 78 → 94, Se m/z 80 → 96, Cu m/z 65 → 65. External calibration was performed for Cu quantification by using mixed calibration standards in 20% nitric acid (v/v). For quantification of Se, isotope dilution method was applied as described before [38]. Limits of detection were calculated by mean value of at least three chemical blanks plus three times standard deviation divided by calibration slope. All measured samples were above LOD. For quality control, certified reference material NIST Trace Elements in Natural Water 1640A (LGC Standards GmbH, Wesel, Germany) was used and treated

in the same way like samples. This material has certified values of 85.75 ± 0.51 µg/L for Cu and 20.13 ± 0.17 µg/L for Se with recovery rates of 94.4 ± 1.7% and 90.9 ± 2.1%, respectively. Cellular element concentrations were related to total protein content determined according to Bradford [37].

Selenoprotein P content: Determination of SELENOP content based on affinity chromatography coupled to ICP-MS according to Heitland & Köster [39] adapted to cell lysates and cell culture medium. For preparation of cell lysates, pellets were lysed in homogenisation buffer (100 mM Tris, 300 mM KCl, 0.1% Triton X-100 added with 1:1000 protease inhibitor cocktail set III) and after sonication, cellular debris was removed by centrifugation (15.000 x g, for 10 min, at 4 °C). For SELENOP separation, an Agilent 1200 Infinity (Agilent Technologies, Waldbronn, Germany) HPLC and a HiTrap® Heparin HP column prepacked with Heparin Sepharose® (GE Healthcare, Freiburg, Germany) was employed. Mobile phase A contained 0.17 M and mobile phase B 1.3 M ammonium acetate in 2% ethanol (v/v) at pH 7.0. The gradient program was 0¬1:00 min 100% A, 1:01 to 4:50 min 100% B and 4:51¬ to 5:50 100% A at a constant flow rate of 1 mL/min. The injection volume was 75 µL of 1:4 (v/v) diluted cell lysates and 100 µL of undiluted media. The ICP-MS was operated in MS/MS mode using oxygen as collision cell gas at a flow rate of 3.0 mL/min and 12% CO_2 as option gas. The monitored mass transitions (integration time of 0.1 sec/point) were m/z 78 → 94 and m/z 80 → 96 for Se. External calibration was performed for Se quantification by using Se calibration standards in distilled water (v/v). For quality control, certified reference material NIST® SRM® 1950 (Sigma Aldrich) was used and treated in the same way like samples. This material has certified value of 50.2 ± 4.3 µg/kg and obtained recovery rate was 101.4 ± 3.6%. Limit of detection (LOD) were calculated by mean value of four chemical blanks plus three times standard deviation divided by calibration slope. All measured samples were above LOD. Cellular Se content was related to total protein content determined according to Bradford [37].

6.4.6   Detection of DNA damage via alkaline and Fpg-modified Comet Assay

To assess the effects of an adequate Se supply on the Cu-induced induction of oxidative DNA damage, we performed the alkaline and Fpg-modified comet assay (CA). Briefly, cells were seeded on 12-well plates and treated as described before. After the end of incubation, cells were trypsinized and cell number was measured using an automatic cell counter (Casy TTCs, Omni Life Science). An aliquot of 20 µL of the cell suspension (density of 4 x 106 cells per mL) was added to 180 µL of 0.5% LMP-agarose. 45 µL of the mixture were subjected to slides coated with 1.5% NMP-agarose. Cell suspension was covered with a cover glass and was kept at 4°C to solidify. After removal of the cover glass, slides were placed in cold lysis buffer (10 mM Tris, 2.5 M NaCl, 100 mM EDTA, pH 10, 10% DMSO and 1% Triton-X100) for 1 h at 4°C. Then, slides were washed 3 times in cold Fpg buffer (40 mM Hepes, 100 mM KCl, 0.5 mM EDTA, 0.2 mg/mL BSA, pH 8) and were incubated with the Fpg enzyme (LOT 110240L, New England Biolabs) diluted 1:10,000 for 30 min at 37°C. For DNA unwinding, slides were placed in

electrophoresis buffer (300 mM NaOH, 1 mM EDTA) for 20 min at 4°C, followed by electrophoresis for 20 min at 25 V and 300 mA. Afterwards, slides were neutralized in 400 mM Tris (pH 7.5) for 5 min at 4°C and fixed in methanol for 5 min at 4°C. Finally, slides were stained using GelRed Nucleidacid (Biotum) and blinded prior to analysis. To evaluate inter-assay variation and electrophoretic performance, untreated and MMS-treated HepG2 cells were used as negative and positive controls for the alkaline CA. RO198022 and visible light-irradiated astrocytes were used as positive controls for the Fpg-modified alkaline CA. Fluorescence microscopic evaluation (Leica DM 2000 LED, Leica Microsystems GmbH, Wetzlar, Germany) was done semi-automatically with image analysis software (Comet IV, Perceptive Instruments, Stone, UK). The median percentage of DNA in tail of 100 randomly selected comets was taken as the value for DNA damage for each condition. Net Fpg-sensitive sites were calculated by subtracting the % of DNA in tail obtained after reaction buffer incubation from that obtained after the Fpg incubation with the respective concentrations.

6.4.7   Neuronal network via βIII-tubulin staining

To test whether an adequate Se supply might protect the neuronal network against Cu-induced damage, the cytoskeletal protein βIII-tubulin was assessed via immunostaining. The method was performed as described before [30]. At least 20 images of each sample were taken using a fluorescence microscope (Leica DMB 6, Wetzlar, Germany) and analysed with an image analysis software (LAS X Core 2D, Leica, Wetzlar, Germany).

6.4.8   Statistical analysis

All experiments were performed independently at least three times. Data are shown as mean ± SD. Statistical analysis was done by GraphPad Prism version 8 (San Diego, USA) as indicated in the figure legends. Significance levels are $*/^#p < 0.05$, $**/^{##}p < 0.01$, $***/^{###}p < 0.001$.

6.5 Results

6.5.1   Modulating the Se status of human astrocytes and differentiated neurons by Se species

In initial studies, the cultivation conditions were optimized with regard to the supply of Se to the cells. In astrocytes, selenite supplementation was able to elevate GPX activity in a concentration-dependent manner reaching a plateau with a 63% increase at 100 nM, whereas SeMet did not show this effect (Fig. S2A). Astrocytes are capable of excreting SELENOP into the medium, and incubation with selenite resulted in a dose-dependent increase in these levels by up to 5.3-fold (Fig. S2D). In contrast, cellular Se content (up to 30.6-fold) and cellular SELENOP levels (up to 17.8-fold) were increased in a dose-dependent manner only after SeMet was added (Fig. S2B and C). On this basis, the cell culture medium

was supplemented with the respective Se species for further studies to achieve a Se concentration of 100 nM. The Se concentrations used are in a physiologically relevant range and do not induce cytotoxic effects in astrocytes [47] and differentiated neurons (Fig. S3).

When the two cell lines were cultured under standard conditions, there were no differences in total Se content and cellular and extracellular SELENOP concentrations (Fig. 1A-C, plain bars). However, basal GPX activity in astrocytes was already 2.3-fold higher than in neurons (Fig. 1D, plain bars). Supply with selenite did not affected cellular Se and SELENOP concentration (Fig. 1A and B, vertical striped bars), but significantly increased SELENOP excretion and GPX activity in astrocytes by a factor of 2.6 and 1.6, respectively (Fig. 1C and D, vertical striped bars). Incubation with SeMet resulted mainly in higher cellular Se and SELENOP concentrations in both cell lines (Fig. 1A and B, oblique striped bars), while SELENOP excretion and GPX activity remained unchanged (Fig. 1C and D, oblique striped bars). The effects of Se supplementation on total Se content, cellular and extracellular SELENOP content appear to be similar in both cell lines. However, both cell lines differ with respect to GPX activity, which could only be modulated in astrocytes by selenite supply.
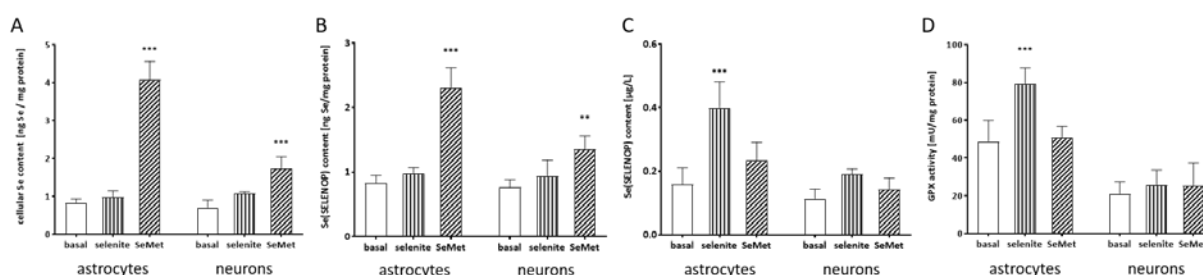
Figure 1. Effect of Se supply on Se-related endpoints in human astrocytes and neurons. Cells were supplemented with either selenite, SeMet (total Se content: 100 nM) or without addition of Se directly after seeding and incubated with CuSO$_4$ for additional 48 h. (A) Cellular Se concentrations were measured utilizing ICP-MS/MS and normalized to protein content of cells. (B) Cellular and (C) extracellular SELENOP concentrations were determined using HPLC-ICP-MS/MS, and cellular concentrations were related to protein content of cells. (D) GPX activities were measured photometrically and normalized to protein content. Data are shown as mean + SD (n ≥ 3). Statistical analysis based on two-way ANOVA with Dunnett´s post-test. *p < 0.05; **p < 0.01; ***p < 0.001 *vs.* non-supplemented cells.

6.5.2   Se supply had no impact on cell viability, mitochondrial integrity and Cu accumulation after Cu exposure

In the following, Cu response of Se-supplied cells was compared with that of cells cultivated under standard conditions. Cu incubation significantly reduced cell viability measured by dehydrogenase activity in both cell lines, while addition of Se did not affect the cytotoxic effects of Cu (Fig. 2A). For astrocytes, dehydrogenase activity measured by CCK8 was the most sensitive endpoint followed by lysosomal integrity with EC30 values of 40 µM and 140 µM CuSO4, respectively (Table S1). In

differentiated neurons, lysosomal integrity was slightly more sensitive (EC30: 50 µM CuSO4) than CCK8 (EC30: 60 µM CuSO4) (Table S1). A number of studies have identified mitochondria as particularly Cu-sensitive organelles [40]. Therefore, the MMP was examined as a more specific endpoint for Cu toxicity. In the cell lines investigated, the Cu-induced effect on MMP was minor and additional Se exerted no impact on Cu-induced decrease in MMP in astrocytes and differentiated neurons (Fig. 2B). Both cell lines were able to accumulate Cu in a dose-dependent manner, which was independent of the Se status of the cells (Fig. 2C). Incubating the cells with 100 µM Cu, cellular concentrations of this element were comparable between the two cell lines. However, exposure to 250 µM CuSO4 resulted in cellular Cu concentrations in astrocytes that were almost twice as high as in neurons. This was accompanied by an about 50-fold increase in MT2a gene expression (Fig. S4E).

6.5.3   Cu negatively affects Se homeostasis in human brain-derived cell lines

To evaluate the impact of Cu on the Se homeostasis of human astrocytes and neurons, Se-related endpoints were measured after 48-hours Cu exposure. Under standard cultivation conditions, cellular Se concentrations were decreased by up to 43% upon Cu treatment in both cell lines (Fig. 3A, plain bars). Similar effect could be observed for cellular SELENOP levels in astrocytes and tendentially also in neurons (Fig. 3B, plain bars). Additionally, excretion of SELENOP into the cell culture medium was strongly inhibited by up to 63% upon Cu incubation in both cell lines (Fig. 3C, plain bars). In astrocytes, Cu resulted in a 36% decline in the enzymatic activity of GPX (Fig. 3D, plain bars, left graph).

To test whether additional supply with Se might counteract the impact of Cu on Se-related markers, cells were supplemented with either selenite or SeMet and then treated with Cu. After 48 hours of Cu incubation, cellular Se concentrations were increased by up to 40% in astrocytes after selenite supplementation, showing an opposite effect compared with non-supplemented cells (Fig. 3A, vertical striped bars, left graph). In contrast, Cu treatment exhibited no effect on cellular Se levels in astrocytes supplemented with SeMet (Fig. 3A, oblique striped bars, left graph). However, these effects could only be observed in astrocytes, as in neurons there was a decline in total Se content of up to 44% despite Se administration (Fig. 3A, right graph). For astrocytes, a similar picture as for the cellular Se concentration could be observed for the cellular SELENOP levels with increasing values after selenite (1.2-fold) and unchanged concentrations after SeMet supply upon 48-hours Cu exposure (Fig. 3B, left graph). In neurons, Cu had no effect on cellular SELENOP concentrations (Fig. 3B, right graph). Supplementation with Se was ineffective in influencing the Cu-induced inhibition of SELENOP excretion in both cell lines (Fig. 3C). In astrocytes, decrease in GPX activity could be prevented by selenite but not by SeMet supply (Fig. 3D, left graph). In contrast, no change in GPX activity could be observed in neurons despite Se supplementation (Fig. 3D, right graph). Taken together, the data suggest that Cu

negatively affects Se homeostasis in both cell lines studied, which could only be partially prevented by an additional supply of Se.
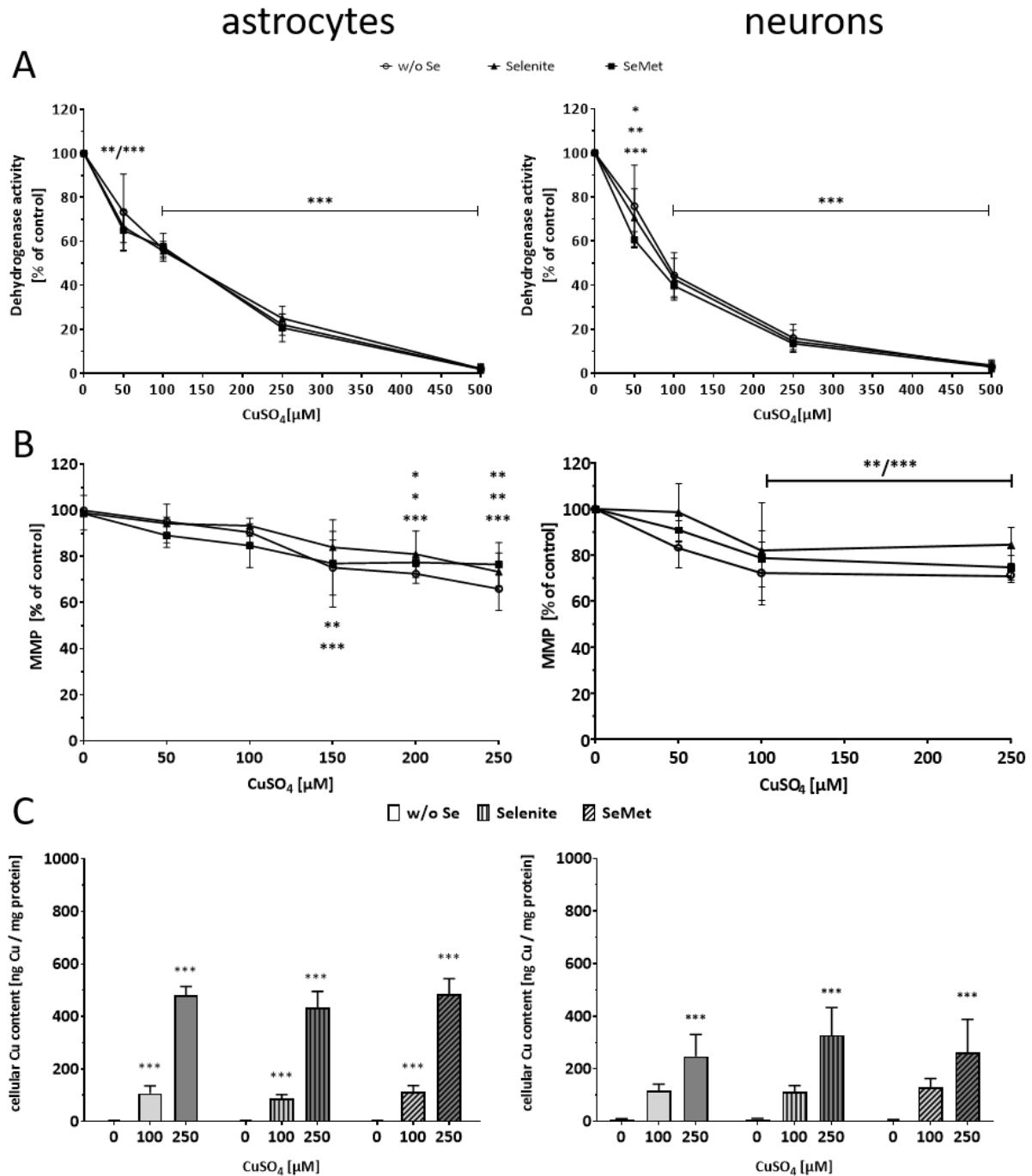
Figure 2. Se supply did not affect Cu cytotoxicity and Cu accumulation in human brain-associated cell lines. Cells were supplemented with either selenite, SeMet (total Se content: 100 nM) or without addition of Se directly after seeding and incubated with $CuSO_4$ for additional 48 h. (A) Dehydrogenase activity measured by using the CCK8 and data were normalized to respective control cells. (B) Mitochondrial membrane potential (MMP) was determined by utilizing MitoTracker Orange and data were normalized to respective control cells. (C) Cellular Cu concentrations were assessed by ICP-MS/MS and related to protein content of cells. Data are shown as mean ± SD (n ≥ 3). *$p < 0.05$; **$p < 0.01$; ***$p < 0.001$ *vs.* 0 µM $CuSO_4$ calculated based on two-way ANOVA with Dunnett´s post-test.
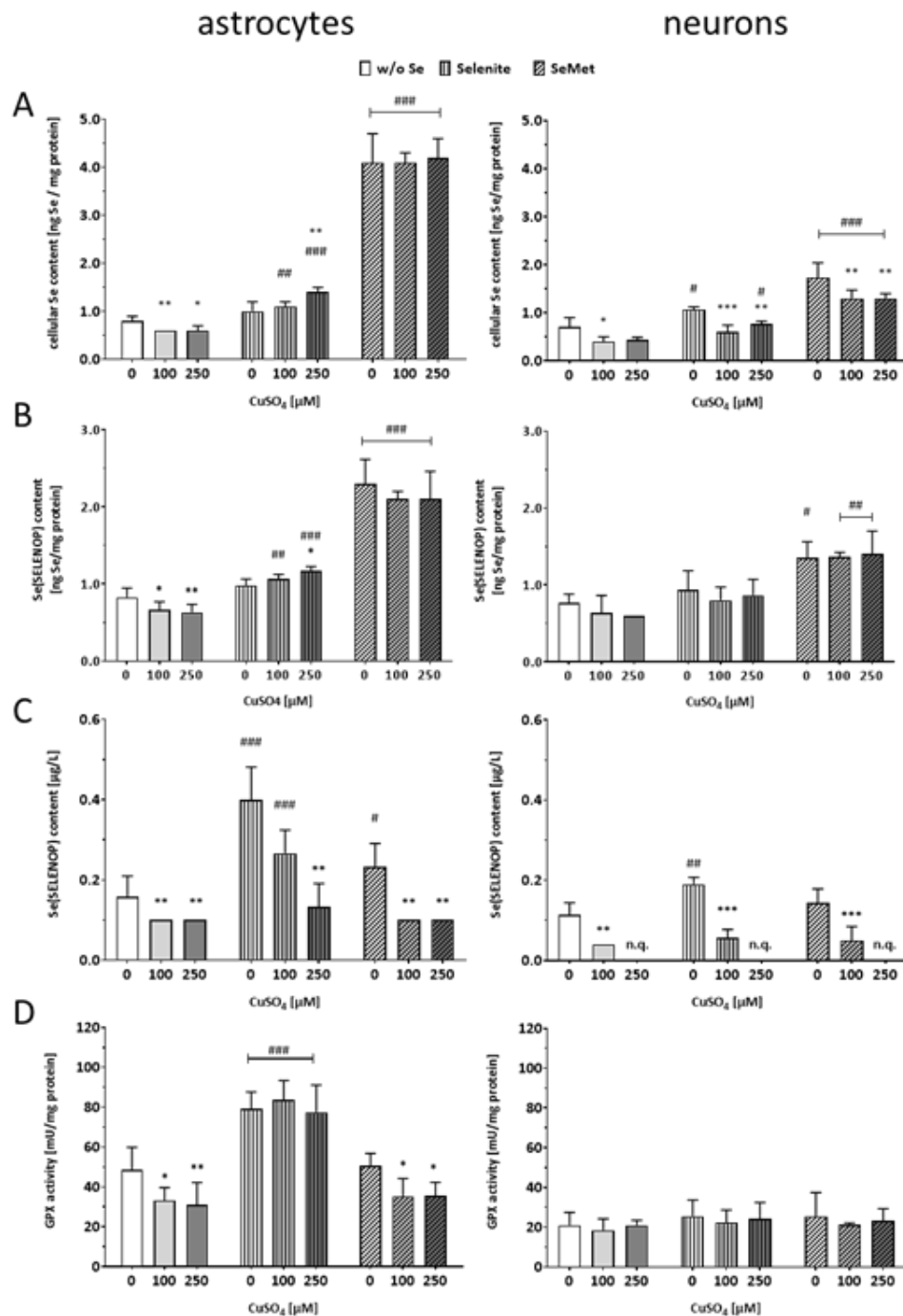
Figure 3. Cu affected Se homeostasis of human astrocytes and neurons. Cells were supplemented with either selenite, SeMet (total Se content: 100 nM) or without addition of Se directly after seeding and incubated with CuSO4 for additional 48 h. (A) Cellular Se concentrations were measured utilizing ICP-MS/MS and normalized to protein content of cells. (B) Cellular and (C) extracellular SELENOP concentrations were determined using HPLC-ICP-MS/MS, and cellular concentrations were related to protein content of cells. (D) GPX activities were measured photometrically and normalized to protein content. Data are shown as mean + SD (n ≥ 3). Statistical analysis based on two-way ANOVA with Dunnett´s post-test: *$p < 0.05$; **$p < 0.01$; ***$p < 0.001$ vs. 0 µM CuSO4. Group analysis based on two-way ANOVA with Tukey´s post-test: #$p < 0.05$; ##$p < 0.01$; ###$p < 0.001$ vs. non-supplemented cells. Abbreviations: n.q. – not quantifiable.

6.5.4 Cu induced oxidative DNA damage in astrocytes and neurite degeneration in differentiated neurons

Cu-induced effects are thought to be mainly due to the induction of oxidative stress, which consequently could damage macromolecules such as the DNA. To elucidate whether Se supply could modulate the induction of DNA damage by Cu, the alkaline and Fpg-modified comet assays were employed. As shown in Fig. 4A, in astrocytes, Cu treatment induced oxidative DNA damage up to 2.2-fold in a concentration-dependent manner, while DNA strand breaks and alkali-labile sites remained unchanged. However, no Se-mediated protection could be observed. Additionally, evaluation of gene expression via qPCR screening revealed no impact of Cu as well as Se on different genes related to base excision repair (BER) such as OGG1, APEX1, NEIL2, PARP1, etc. (Fig. S5). However, damage repair via BER is usually very rapid and it is possible that after 48 h of Cu incubation, this process is already completed and thus no effects are detectable at mRNA as well as DNA damage level. Additionally, a Cu-concentration- and time-dependent increase of ROS formation (Fig. S6A) and a shift of the GSH/GSSG ratio regarding more GSSG (Fig. S6B) could be observed indicating that Cu concentration of 250 µM result in oxidative stress. One defense mechanism against oxidative insults operates via activation of nuclear factor erythroid 2-related factor 2 (NRF2) in order to increase expression of oxidative stress-responsive genes [41]. The NRF2 target genes NQO1, SOD1 and HO-1 were upregulated upon Cu exposure in here used astrocytes (Fig. S4G-I). Additionally, some selenoproteins are also responsive to NRF2 activation like TXNRD1 (Fig. S4D) which was increased in our experiment. These data indicate that Cu is able to modulate the cellular redox homeostasis in astrocytes. In differentiated neurons, basal DNA damage level were already high and no additional damage triggered by Cu administration could be detected. Yet, supplementation with SeMet resulted in a significant reduction in basal oxidative DNA damage in this cell line (Fig. S7).

In addition to the impact on DNA damage, we investigated the impact on the neurite network of differentiated neurons. Although neurite degeneration does not appear to be particularly sensitive to Cu exposure, we detected a decrease in neurite mass (Figure 4B). Cu-induced decrease in neurite mass was observed already at 100 µM Cu in non-supplemented cells. Pre-treatment with SeMet protected the neuronal network against loss of up to 250 µM CuSO$_4$. At this concentration, microscopic images (Figure S8) show accumulation of tubulin signal, suggesting initial neurite degeneration. A loss of neurite network is visible after incubation with 500 µM Cu and could not be prevented by Se.
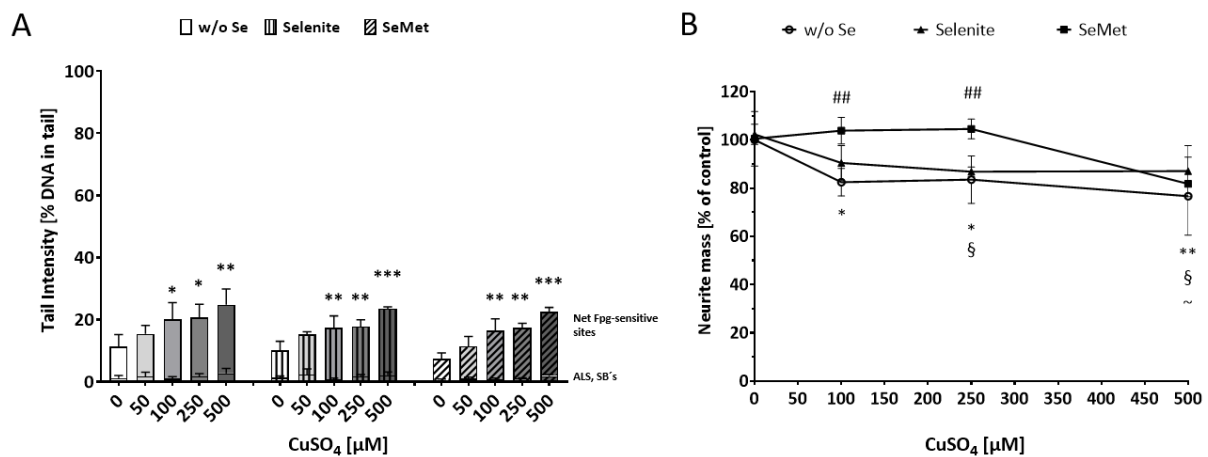
Figure 4. Cu exposure induced oxidative DNA damage and neurodegeneration. (A) DNA damage was quantified by alkaline and Fpg-modified comet assay in human astrocytes. (B) Neurodegeneration was assessed *via* fluorescence microscopy in human differentiated neurons. Data are shown as mean + SD (n = 3). w/o Se (*), selenite (§), SeMet (~). *p < 0.05; **p < 0.01; ***p < 0.001 *vs*. 0 µM CuSO$_4$ based on two-way ANOVA with Dunnett´s post-test. #p < 0.05; ##p < 0.01; ###p < 0.01 *vs*. w/o Se calculated based on two-way ANOVA with Tukey´s post-test. Abbreviations: ALS - alkali-labile sites; SB´s - DNA strand breaks.

6.6 Discussion

Aiming to better characterize the rarely studied interaction between trace elements, this study revealed an interaction between Cu and Se metabolism of human astrocytes and neurons. First, the modulation of Se homeostasis by different Se species was investigated using different Se-related markers. The addition of Se successfully modulated the Se status of both cell lines, although the effects were highly dependent on the Se species used. While inorganic selenite resulted in higher SELENOP excretion into the medium and increased GPX activity, the addition of organic SeMet resulted in higher cellular Se and SELENOP concentrations (Fig. 1). Se in the form of selenite did not increased total cellular Se concentration in astrocytes and neurons compared to SeMet (Fig. 1A), as demonstrated in several cell lines [42]. However, cells were able to utilize selenite for selenoprotein synthesis as demonstrated in higher extracellular SELENOP and increased GPX activity (Fig. 1C and D). Moreover, the organic Se compound SeMet is known to be non-specifically incorporated into proteins instead of methionine [43], which could explain the higher cellular Se concentrations (Fig 1A). Furthermore, cellular SELENOP levels were increased by SeMet supplementation (Fig 1B) without affecting mRNA levels (Fig. S4A). However, regulation of selenoprotein expression is primarily at the translational level [44]. This may hint at a non-specific incorporation of SeMet instead of methionine into the amino acid sequence of SELENOP and may explain why it is not excreted, as in the case of selenite supplementation (Fig. 1C). Additionally, unlike selenite, SeMet did not affect the GPX activity of the cells (Fig. 1D), suggesting that this Se source may not be used for selenoprotein synthesis in these cells. These results are consistent with the observations of Zeng et al. in Caco-2 cells, where the increase in GPX activities was strongly dependent on the added Se form [45]. After supplementation with 31 nM

of different Se species for 72 h GPX activities were measured in medium samples with selenite being more efficient in increasing enzymatic activity compared to SeMet [45].

To investigate the Se status of the cells, Se-related endpoints (cellular Se content, cellular SELENOP, SELENOP excretion and GPX activity) were measured. In cells without additional Se supply, the measured markers of Se status were decreased after Cu loading (Fig. 3), demonstrating disruption of Se homeostasis by Cu. Addition of Se resulted in heterogeneous effects depending on cell line and Se species used. In astrocytes, the addition of selenite as a source of Se led to an increase in total Se and cellular SELENOP levels after Cu exposure. A similar effect was observed in selenite-supplied HepG2 cells, where cellular Se levels were also increased after Cu incubation [22]. However, in the neuronal cell line, selenite had no effect on the Cu-induced decrease in cellular Se concentrations. The organic Se compound SeMet is known to be non-specifically incorporated into proteins instead of methionine, which may explain the higher Se concentration in cells (Fig 3A). The excretion of SELENOP into the cell culture medium was strongly inhibited upon Cu exposure regardless of Se supply in both cell lines tested (Fig. 3C). Together with the decreased mRNA expression in astrocytes (Fig. S4A), SELENOP production appears to be diminished, consistent with the decreased excretion and cellular SELENOP content. Since astrocytes are mainly responsible for Se distribution in the brain [46], Cu-induced inhibition of SELENOP excretion could negatively affect other brain cells such as neurons. These cells are dependent on Se supply, and Se deficiency has serious consequences on the function of these cells. Cu has been shown to have a high binding affinity to SELENOP, which may also play a role in the inhibition mechanism of SELENOP excretion [20]. However, further studies are needed to characterize the mechanism of Cu-induced inhibition of SELENOP excretion. In post-mortem brains of AD patients, the co-localization of SELENOP with Aβ-plaques and neurofibrillary tangles suggests its involvement in the development of AD [47]. Moreover, these areas are enriched in Cu in these patients [19]. In mouse neuroblastoma cells (N2A), the histidine-rich domain of SELENOP protected the cells from the toxicity of Cu-tau and Cu-Aβ complexes [20,21], presumably by forming a ternary complex that could be less toxic [48]. However, complexed SELENOP might not be available for the synthesis of other selenoproteins such as GPX or TXNRD, which are important for the antioxidant defense mechanism. Enzymatic activity of GPX was measured as another functional marker of Se status. In astrocytes, GPX activity was decreased after Cu exposure, whereas it was unchanged in neurons (Fig. 3D). In addition, mRNA of GPX1 was decreased at the level of gene expression, whereas mRNA of GPX4 remained stable in astrocytes (Fig. S4B and C), suggesting that the decrease in activity may be due to decreased GPX synthesis. Similar to our results, GPX activity was decreased after Cu treatment in chicken [49] and rat [50,51] brain tissues. In HepG2 cells, Schwarz et al. also showed a Cu-induced decrease in the enzymatic activities of GPX and TXNRD [22].

In a next step, the cytotoxicity of Cu was examined depending on the Se status of the cells. Our data demonstrated that Cu induced substantial cytotoxic effects in astrocytes and neurons (Fig. 2A and Table S1), which was shown in several studies using cell lines or primary cells [52–56]. Shown data in astrocytes could confirm results of a previous study in the same cell line [55]. In primary rat astrocytes, CuCl2 concentration above 60 µM for 24 h significantly reduced lysosomal integrity measured via neutral red uptake [53]. Chen et al. observed comparable cytotoxic effects by using the MTT assay and received IC50 values for CuCl2 of 180 µM [54]. In the human astrocytoma U87 cell line only CuCl2 concentrations of 250 µM resulted in a significant decrease in MTT reduction capacity [52]. In a study with rat DRG neurons, Cu incubation for 24 h cells resulted in IC50 values of 793 µM CuCl2 measured via MTT assay [56], which is quite comparable with our data from the dehydrogenase activity measured via resazurin assay. In addition, the protective potential of Se against Cu-induced toxicity has been investigated. In a recent study, Nakano et al. demonstrated a protective effect of Se on neuronal cell death after incubation of cells with Cu and Zn. Mouse hypothalamic neurons (GT1-7 cells) were incubated with SeMet (5 - 80 µM) and then treated with a combination of ZnCl2 (30 µM) and CuCl2 (10 µM) for 24 hours [57]. However, it should be noted that supraphysiological concentrations of Se were used. Our data show no Se-dependent effect on Cu-induced cytotoxicity in the cell lines studied. Comparable results were obtained in HepG2 cells supplied with 50 nM selenite and treated with CuSO4 for 72 hours [22].

Mitochondria are discussed as the main target for Cu toxicity, so mitochondrial integrity was assessed after Cu exposure as a function of Se supply. Reddy et al. examined the effects of CuSO4 (20 µM for 24 h) on mitochondria in primary rat astrocytes and neurons [58]. While MMP decreased significantly in astrocytes, Cu did not cause any change in neuronal mitochondrial function but resulted in early cell death due to energy depletion [58]. The authors hypothesized that mitochondrial heterogeneity between cells might account for the differences in Cu-induced mitochondrial dysfunction. However, our data showed no differences between human astrocytes and differentiated neurons (Fig. 2B). Whether this might be an effect of the origin of the cells (human vs. rat) or the use of cell lines, remains unclear. Simultaneous treatment of primary rat cortical neurons with sodium selenite (1 µM for up to 3 h) protected the cells from valporic acid-induced loss of MMP [59]. In another study, mouse hippocampal cells (HT22) were pretreated with sodium selenite (25 - 200 nM, 3 h) followed by 24 h treatment with 2 ppm Ag nanoparticles, which had protective effects on cell viability and mitochondrial function [60]. We could not confirm these protective properties of Se on mitochondrial function (Fig. 2B) and cell viability (Fig. 2A and Table S1). However, it must be emphasized that the incubation period of Se was short in the aforementioned studies, suggesting a direct effect of Se species rather than an effect through selenoprotein metabolism. In our study, the cultivation protocol allowed the cells to

metabolize the Se species for selenoprotein synthesis, and this may be a reason for the differences in the results.

As shown in Fig. 2C, both cell lines accumulated Cu independently of Se supply, consistent with data in HepG2 cells [22]. The results in astrocytes are in line with previously published data in the same astrocyte cell line [55]. The ability of cells to efficiently accumulate Cu has been demonstrated in primary rat astrocytes [53,54] and rat DRG neurons [56]. Consequently, the induction of RONS (Fig. S6A) and the shift in GSH/GSSG ratio (Fig. S6B) indicate oxidative stress after Cu accumulation in cells. One defense mechanism against oxidative stress functions by activating nuclear factor erythroid 2-related factor 2 (NRF2) to increase the expression of oxidative stress-responsive genes [41]. The NRF2 target genes NQO1, SOD1, and HO-1 were upregulated after Cu exposure in the astrocytes used here (Fig. S4G-I). In addition, some selenoproteins also respond to NRF2 activation, such as TXNRD1 (Fig. S4D) which was increased in our experiment. These data indicate that Cu is able to modulate cellular redox homeostasis in astrocytes.

With a more mechanistic focus, the induction of DNA damage after Cu treatment and the impact of Se supply were investigated. Our results demonstrated that oxidative DNA damage increased after Cu treatment (Fig. 4A), consistent with data from other studies [61,62]. However, in astrocytes, Se supply did not appear to affect the prevention of oxidative DNA damage by Cu (Fig. 4A). In neurons, SeMet supply caused some protection against oxidative DNA damage (Fig. S7), but because DNA damage was already high in control cells, this end point is not applicable in this cell line and experimental setting. Therefore, the effects of Cu on the neuronal network were examined. Treatment with Cu resulted in a loss of neurite mass that could be prevented by the addition of SeMet (Fig. 4B). Observations in primary cortical neurons from mice treated with a Cu-tau complex for 12 hours also demonstrated the protective effect of Se administered as the His-rich domain of SELENOP [21]. Consistent with these results, the cellular SELENOP content was significantly higher in neurons supplemented with SeMet (Fig. 3B), which may account for the protective effect. The association between lower serum Se levels and cognitive loss has already been demonstrated in several studies in elderly and AD patients suggesting a protective role of Se and selenoproteins [12,63–65].

In conclusion, elevated Cu levels associated with an increase in oxidative stress and a concomitant decrease in selenoprotein functionality could promote the development of neurodegenerative diseases. As observed in this study, the functionality of selenoproteins was diminished, due to decreased synthesis of selenoproteins after Cu exposure. At the same time, decline in total cellular Se levels indicate involvement of the GSH system, as it plays a role in the complexation of Cu as well as in the metabolization of Se. Therefore, it is of great importance to gain a more comprehensive understanding of the interplay between trace elements and their transporters in order to identify and

achieve health-promoting concentrations of essential trace elements, especially in an aging population.

6.7   Declaration of interest

The authors declare no conflicts of interest.

6.8   Acknowledgments

6.9 References

[1]   R.F. Burk, K.E. Hill, Regulation of Selenium Metabolism and Transport, Annu. Rev. Nutr. 35 (2015) 109–134. https://doi.org/10.1146/annurev-nutr-071714-034250.

[2]   Y. Saito, Selenium Transport Mechanism via Selenoprotein P—Its Physiological Role and Related Diseases, Front. Nutr. 8 (2021). https://doi.org/10.3389/fnut.2021.685517.

[3]   S.W. Caito, D. Milatovic, K.E. Hill, M. Aschner, R.F. Burk, W.M. Valentine, Progression of neurodegeneration and morphologic changes in the brains of juvenile mice with selenoprotein P deleted, Brain Res. 1398 (2011) 1–12. https://doi.org/10.1016/j.brainres.2011.04.046.

[4]   P.R. Hoffmann, S.C. Hoge, P.-A. Li, F.W. Hoffmann, A.C. Hashimoto, M.J. Berry, The selenoproteome exhibits widely varying, tissue-specific dependence on selenoprotein P for selenium supply, Nucleic Acids Res. 35 (2007) 3963–3973. https://doi.org/10.1093/nar/gkm355.

[5]   L. Schomburg, U. Schweizer, B. Holtmann, L. Flohé, M. Sendtner, J. Köhrle, Gene disruption discloses role of selenoprotein P in selenium delivery to target tissues, Biochem. J. 370 (2003) 397–402. https://doi.org/10.1042/bj20021853.

[6]   W.M. Valentine, T.W. Abel, K.E. Hill, L.M. Austin, R.F. Burk, Neurodegeneration in Mice Resulting From Loss of Functional Selenoprotein P or Its Receptor Apolipoprotein E Receptor 2, J. Neuropathol. Exp. Neurol. 67 (2008) 68–77. https://doi.org/10.1097/NEN.0b013e318160f347.

[7]   B. Halliwell, Reactive Oxygen Species and the Central Nervous System, J. Neurochem. 59 (1992) 1609–1623. https://doi.org/10.1111/j.1471-4159.1992.tb10990.x.

[8]   S. Salim, Oxidative Stress and the Central Nervous System, J. Pharmacol. Exp. Ther. 360 (2017) 201–205. https://doi.org/10.1124/jpet.116.237503.

[9]   B.R. Cardoso, B.R. Roberts, A.I. Bush, D.J. Hare, Selenium, selenoproteins and neurodegenerative diseases, Metallomics. 7 (2015) 1213–1228. https://doi.org/10.1039/c5mt00075k.

[10] N.T. Akbaraly, I. Hininger-Favier, I. Carrière, J. Arnaud, V. Gourlet, A.-M. Roussel, C. Berr, Plasma Selenium Over Time and Cognitive Decline in the Elderly, Epidemiology. 18 (2007) 52–58. https://doi.org/10.1097/01.ede.0000248202.83695.4e.

[11] B.R. Cardoso, T.P. Ong, W. Jacob-Filho, O. Jaluul, M.I. d'Ávila Freitas, S.M.F. Cozzolino, Nutritional status of selenium in Alzheimer's disease patients, Br. J. Nutr. 103 (2010) 803–806. https://doi.org/10.1017/S0007114509992832.

[12] A. Shahar, K. V. Patel, R.D. Semba, S. Bandinelli, D.R. Shahar, L. Ferrucci, J.M. Guralnik, Plasma selenium is positively related to performance in neurological tasks assessing coordination and motor speed, Mov. Disord. 25 (2010) 1909–1915. https://doi.org/10.1002/mds.23218.

[13] J. Chen, Y. Jiang, H. Shi, Y. Peng, X. Fan, C. Li, The molecular mechanisms of copper metabolism and its roles in human diseases, Pflügers Arch. - Eur. J. Physiol. 472 (2020) 1415–1429. https://doi.org/10.1007/s00424-020-02412-2.

[14] H. Öhrvik, J. Aaseth, N. Horn, Orchestration of dynamic copper navigation – new and missing pieces, Metallomics. 9 (2017) 1204–1229. https://doi.org/10.1039/C7MT00010C.

[15] A. Holmgren, J. Lu, Thioredoxin and thioredoxin reductase: Current research with special reference to human disease, Biochem. Biophys. Res. Commun. 396 (2010) 120–124. https://doi.org/10.1016/j.bbrc.2010.03.083.

[16] R. Squitti, R. Ghidoni, I. Simonelli, I.D. Ivanova, N.A. Colabufo, M. Zuin, L. Benussi, G. Binetti, E. Cassetta, M. Rongioletti, M. Siotto, Copper dyshomeostasis in Wilson disease and Alzheimer's disease as shown by serum and urine copper indicators., J. Trace Elem. Med. Biol. 45 (2018) 181–188. https://doi.org/10.1016/j.jtemb.2017.11.005.

[17] R. Squitti, D. Lupoi, P. Pasqualetti, G. Dal Forno, F. Vernieri, P. Chiovenda, L. Rossi, M. Cortesi, E. Cassetta, P.M. Rossini, Elevation of serum copper levels in Alzheimer's disease, Neurology. 59 (2002) 1153–1161. https://doi.org/10.1212/WNL.59.8.1153.

[18] S. Genoud, B.R. Roberts, A.P. Gunn, G.M. Halliday, S.J.G. Lewis, H.J. Ball, D.J. Hare, K.L. Double, Subcellular compartmentalisation of copper, iron, manganese, and zinc in the Parkinson's disease brain, Metallomics. 9 (2017) 1447–1455. https://doi.org/10.1039/c7mt00244k.

[19] M. Schrag, C. Mueller, U. Oyoyo, M.A. Smith, W.M. Kirsch, Iron, zinc and copper in the Alzheimer's disease brain: A quantitative meta-analysis. Some insight on the influence of citation bias on scientific opinion, Prog. Neurobiol. 94 (2011) 296–306. https://doi.org/10.1016/j.pneurobio.2011.05.001.

[20] X. Du, Y. Zheng, Z. Wang, Y. Chen, R. Zhou, G. Song, J. Ni, Q. Liu, Inhibitory effect of selenoprotein P on Cu(+)/Cu(2+)-induced Aβ42 aggregation and toxicity, Inorg. Chem. 53 (2014) 1672–8. https://doi.org/10.1021/ic4028282.

[21] X. Du, Y. Zheng, Z. Wang, Y. Chen, R. Zhou, G. Song, J. Ni, Q. Liu, Inhibitory Act of Selenoprotein P on Cu + /Cu 2+ -Induced Tau Aggregation and Neurotoxicity, Inorg. Chem. 53 (2014) 11221–11230. https://doi.org/10.1021/ic501788v.

[22] M. Schwarz, K. Lossow, K. Schirl, J. Hackler, K. Renko, J.F. Kopp, T. Schwerdtle, L. Schomburg, A.P. Kipp, Copper interferes with selenoprotein synthesis and activity, Redox Biol. 37 (2020) 101746. https://doi.org/10.1016/j.redox.2020.101746.

[23] J. Baudry, J.F. Kopp, H. Boeing, A.P. Kipp, T. Schwerdtle, M.B. Schulze, Changes of trace element status during aging: results of the EPIC-Potsdam cohort study, Eur. J. Nutr. 59 (2020) 3045–3058. https://doi.org/10.1007/s00394-019-02143-w.

[24] J. Hackler, M. Wisniewska, L. Greifenstein-Wiehe, W.B. Minich, M. Cremer, C. Bührer, L. Schomburg, Copper and selenium status as biomarkers of neonatal infections, J. Trace Elem. Med. Biol. 58 (2020) 126437. https://doi.org/10.1016/j.jtemb.2019.126437.

[25] Q. Sun, J. Hackler, J. Hilger, H. Gluschke, A. Muric, S. Simmons, L. Schomburg, E. Siegert, Selenium and Copper as Biomarkers for Pulmonary Arterial Hypertension in Systemic Sclerosis, Nutrients. 12 (2020) 1894. https://doi.org/10.3390/nu12061894.

[26] H. Lohren, L. Blagojevic, R. Fitkau, F. Ebert, S. Schildknecht, M. Leist, T. Schwerdtle, Toxicity of organic and inorganic mercury species in differentiated human neurons and human astrocytes, J. Trace Elem. Med. Biol. 32 (2015) 200–208. https://doi.org/10.1016/j.jtemb.2015.06.008.

[27] S.M. Müller, F. Ebert, G. Raber, S. Meyer, J. Bornhorst, S. Hüwel, H.-J. Galla, K.A. Francesconi, T. Schwerdtle, Effects of arsenolipids on in vitro blood-brain barrier model, Arch. Toxicol. 92 (2018) 823–832. https://doi.org/10.1007/s00204-017-2085-8.

[28] C.F. Brunk, K.C. Jones, T.W. James, Assay for nanogram quantities of DNA in cellular homogenates, Anal. Biochem. 92 (1979) 497–500. https://doi.org/10.1016/0003-2697(79)90690-0.

[29] R. Rage, J. Mitchen, G. Wilding, DNA fluorometric assay in 96-well tissue culture plates using Hoechst 33258 after cell lysis by freezing in distilled water, Anal. Biochem. 191 (1990) 31–34. https://doi.org/10.1016/0003-2697(90)90382-J.

[30] B. Witt, S. Meyer, F. Ebert, K.A. Francesconi, T. Schwerdtle, Toxicity of two classes of arsenolipids and their water-soluble metabolites in human differentiated neurons, Arch. Toxicol. 91 (2017) 3121–3134. https://doi.org/10.1007/s00204-017-1933-x.

[31] G. Repetto, A. del Peso, J.L. Zurita, Neutral red uptake assay for the estimation of cell viability/cytotoxicity, Nat. Protoc. 3 (2008) 1125–1131. https://doi.org/10.1038/nprot.2008.75.

[32] J. O'Brien, I. Wilson, T. Orton, F. Pognan, Investigation of the Alamar Blue (resazurin) fluorescent dye for the assessment of mammalian cell cytotoxicity, Eur. J. Biochem. 267 (2000) 5421–5426. https://doi.org/10.1046/j.1432-1327.2000.01606.x.

[33] B. Chazotte, Labeling mitochondria with MitoTracker dyes., Cold Spring Harb. Protoc. 2011 (2011) 990–2. https://doi.org/10.1101/pdb.prot5648.

[34] S.W. Perry, J.P. Norman, J. Barbieri, E.B. Brown, H.A. Gelbard, Mitochondrial membrane potential probes and the proton gradient: a practical usage guide, Biotechniques. 50 (2011) 98–115. https://doi.org/10.2144/000113610.

[35] F. Ebert, M. Thomann, B. Witt, S.M. Müller, S. Meyer, T. Weber, M. Christmann, T. Schwerdtle, Evaluating long-term cellular effects of the arsenic species thio-DMAV: qPCR-based gene expression as screening tool, J. Trace Elem. Med. Biol. 37 (2016) 78–84. https://doi.org/10.1016/j.jtemb.2016.06.004.

[36] S. Florian, S. Krehl, M. Loewinger, A. Kipp, A. Banning, S. Esworthy, F.-F. Chu, R. Brigelius-Flohé, Loss of GPx2 increases apoptosis, mitosis, and GPx1 expression in the intestine of mice, Free Radic. Biol. Med. 49 (2010) 1694–1702. https://doi.org/10.1016/j.freeradbiomed.2010.08.029.

[37] M. Bradford, A Rapid and Sensitive Method for the Quantitation of Microgram Quantities of Protein Utilizing the Principle of Protein-Dye Binding, Anal. Biochem. 72 (1976) 248–254. https://doi.org/10.1006/abio.1976.9999.

[38] T.A. Marschall, N. Kroepfl, K.B. Jensen, J. Bornhorst, B. Meermann, D. Kuehnelt, T. Schwerdtle, Tracing cytotoxic effects of small organic Se species in human liver cells back to total cellular Se and Se metabolites, Metallomics. 9 (2017) 268–277. https://doi.org/10.1039/c6mt00300a.

[39] P. Heitland, H.D. Köster, Biomonitoring of selenoprotein P in human serum by fast affinity chromatography coupled to ICP-MS, Int. J. Hyg. Environ. Health. 221 (2018) 564–568. https://doi.org/10.1016/j.ijheh.2018.02.006.

[40] S. Borchard, F. Bork, T. Rieder, C. Eberhagen, B. Popper, J. Lichtmannegger, S. Schmitt, J. Adamski, M. Klingenspor, K.-H. Weiss, H. Zischka, The exceptional sensitivity of brain mitochondria to copper, Toxicol. Vitr. 51 (2018) 11–22. https://doi.org/10.1016/j.tiv.2018.04.012.

[41] F. He, X. Ru, T. Wen, NRF2, a Transcription Factor for Stress Response and Beyond., Int. J. Mol. Sci. 21 (2020). https://doi.org/10.3390/ijms21134777.

[42] T.A. Marschall, J. Bornhorst, D. Kuehnelt, T. Schwerdtle, Differing cytotoxicity and bioavailability of selenite, methylselenocysteine, selenomethionine, selenosugar 1 and trimethylselenonium ion and their underlying metabolic transformations in human cells, Mol. Nutr. Food Res. 60 (2016) 2622–2632. https://doi.org/10.1002/mnfr.201600422.

[43] M.J. Nasim, M.M. Zuraik, A.Y. Abdin, Y. Ney, C. Jacob, Selenomethionine: A Pink Trojan Redox Horse with Implications in Aging and Various Age-Related Diseases, Antioxidants. 10 (2021) 882. https://doi.org/10.3390/antiox10060882.

[44] C. Vindry, T. Ohlmann, L. Chavatte, Translation regulation of mammalian selenoproteins, Biochim. Biophys. Acta - Gen. Subj. 1862 (2018) 2480–2492. https://doi.org/10.1016/j.bbagen.2018.05.010.

[45] H. Zeng, M.I. Jackson, W.-H. Cheng, G.F. Combs, Chemical Form of Selenium Affects Its Uptake, Transport, and Glutathione Peroxidase Activity in the Human Intestinal Caco-2 Cell Model, Biol. Trace Elem. Res. 143 (2011) 1209–1218. https://doi.org/10.1007/s12011-010-8935-3.

[46] X. Yang, K.E. Hill, M.J. Maguire, R.F. Burk, Synthesis and secretion of selenoprotein P by cultured rat astrocytes, Biochim. Biophys. Acta - Gen. Subj. 1474 (2000) 390–396. https://doi.org/10.1016/S0304-4165(00)00035-0.

[47] F.P. Bellinger, Q.-P. He, M.T. Bellinger, Y. Lin, A. V. Raman, L.R. White, M.J. Berry, Association of Selenoprotein P with Alzheimer's Pathology in Human Cortex, J. Alzheimer's Dis. 15 (2008) 465–472. https://doi.org/10.3233/JAD-2008-15313.

[48] J. Aaseth, J. Alexander, G. Bjørklund, K. Hestad, P. Dusek, P.M. Roos, U. Alehagen, Treatment strategies in Alzheimer's disease: a review with focus on selenium supplementation, BioMetals. 29 (2016) 827–839. https://doi.org/10.1007/s10534-016-9959-8.

[49] X. Sun, J. Li, H. Zhao, Y. Wang, J. Liu, Y. Shao, Y. Xue, M. Xing, Synergistic effect of copper and arsenic upon oxidative stress, inflammation and autophagy alterations in brain tissues of Gallus gallus, J. Inorg. Biochem. 178 (2018) 54–62. https://doi.org/10.1016/j.jinorgbio.2017.10.006.

[50] J. Arowoogun, O.O. Akanni, A.O. Adefisan, S.E. Owumi, A.S. Tijani, O.A. Adaramoye, Rutin ameliorates copper sulfate-induced brain damage via antioxidative and anti-inflammatory activities in rats, J. Biochem. Mol. Toxicol. 35 (2021). https://doi.org/10.1002/jbt.22623.

[51] J. Semprine, N. Ferrarotti, R. Musacco-Sebio, C. Saporito-Magriñá, J. Fuda, H. Torti, M. Castro-Parodi, A. Damiano, A. Boveris, M.G. Repetto, Brain antioxidant responses to acute iron and copper intoxications in rats, Metallomics. 6 (2014) 2083–2089. https://doi.org/10.1039/C4MT00159A.

[52] K. Merker, D. Hapke, K. Reckzeh, H. Schmidt, H. Lochs, T. Grune, Copper related toxic effects on cellular protein metabolism in human astrocytes., Biofactors. 24 (2005) 255–61. https://doi.org/10.1002/biof.5520240130.

[53] I.F. Scheiber, R. Dringen, Copper Accelerates Glycolytic Flux in Cultured Astrocytes, Neurochem. Res. 36 (2011) 894–903. https://doi.org/10.1007/s11064-011-0419-0.

[54] S.H. Chen, J.K. Lin, S.H. Liu, Y.C. Liang, S.Y. Lin-Shiau, Apoptosis of Cultured Astrocytes Induced by the Copper and Neocuproine Complex through Oxidative Stress and JNK Activation, Toxicol. Sci. 102 (2008) 138–149. https://doi.org/10.1093/toxsci/kfm292.

[55] B. Witt, M. Stiboller, S. Raschke, S. Friese, F. Ebert, T. Schwerdtle, Characterizing effects of excess copper levels in a human astrocytic cell line with focus on oxidative stress markers, J. Trace Elem. Med. Biol. 65 (2021) 126711. https://doi.org/10.1016/j.jtemb.2021.126711.

[56] J.J. Liu, Y. Kim, F. Yan, Q. Ding, V. Ip, N.N. Jong, J.F.B. Mercer, M.J. McKeage, Contributions of rat Ctr1 to the uptake and toxicity of copper and platinum anticancer drugs in dorsal root ganglion neurons, Biochem. Pharmacol. 85 (2013) 207–215. https://doi.org/10.1016/j.bcp.2012.10.023.

[57] Y. Nakano, M. Shimoda, S. Okudomi, S. Kawaraya, M. Kawahara, K.I. Tanaka, Seleno-l-methionine suppresses copper-enhanced zinc-induced neuronal cell death: Via induction of glutathione peroxidase, Metallomics. 12 (2020) 1693–1701. https://doi.org/10.1039/d0mt00136h.

[58] P.V.B. Reddy, K. V Rama Rao, M.D. Norenberg, The mitochondrial permeability transition, and oxidative and nitrosative stress in the mechanism of copper toxicity in cultured neurons and astrocytes, Lab. Investig. 88 (2008) 816–830. https://doi.org/10.1038/labinvest.2008.49.

[59] A. Salimi, N. Alyan, N. Akbari, Z. Jamali, J. Pourahmad, Selenium and L-carnitine protects from valproic acid-Induced oxidative stress and mitochondrial damages in rat cortical neurons, Drug Chem. Toxicol. (2020) 1–8. https://doi.org/10.1080/01480545.2020.1810259.

[60] W. Ma, L. Jing, A. Valladares, S.L. Mehta, Z. Wang, P.A. Li, J.J. Bang, Silver Nanoparticle Exposure Induced Mitochondrial Stress, Caspase-3 Activation and Cell Death: Amelioration by Sodium Selenite, Int. J. Biol. Sci. 11 (2015) 860–867. https://doi.org/10.7150/ijbs.12059.

[61] D.R. Lloyd, D.H. Phillips, Oxidative DNA damage mediated by copper(II), iron(II) and nickel(II) Fenton reactions: evidence for site-specific mechanisms in the formation of double-strand breaks, 8-hydroxydeoxyguanosine and putative intrastrand cross-links, Mutat. Res. Mol. Mech. Mutagen. 424 (1999) 23–36. https://doi.org/10.1016/S0027-5107(99)00005-6.

[62] T. Schwerdtle, I. Hamann, G. Jahnke, I. Walter, C. Richter, J.L. Parsons, G.L. Dianov, A. Hartwig, Impact of copper on the induction and repair of oxidative DNA damage, poly(ADP-ribosyl)ation and PARP-1 activity, Mol. Nutr. Food Res. 51 (2007) 201–210. https://doi.org/10.1002/mnfr.200600107.

[63] C. Berr, B. Balansard, J. Arnaud, A.-M. Roussel, A. Alpérovitch, Cognitive Decline Is Associated with Systemic Oxidative Stress: The EVA Study, J. Am. Geriatr. Soc. 48 (2000) 1285–1291. https://doi.org/10.1111/j.1532-5415.2000.tb02603.x.

[64] J. Aaseth, A. V. Skalny, P.M. Roos, J. Alexander, M. Aschner, A.A. Tinkov, Copper, Iron, Selenium and Lipo-Glycemic Dysmetabolism in Alzheimer's Disease, Int. J. Mol. Sci. 22 (2021) 9461. https://doi.org/10.3390/ijms22179461.

[65] R. González-Domínguez, T. García-Barrera, J.L. Gómez-Ariza, Homeostasis of metals in the progression of Alzheimer's disease, BioMetals. 27 (2014) 539–549. https://doi.org/10.1007/s10534-014-9728-5.

6.10 Supplementary material
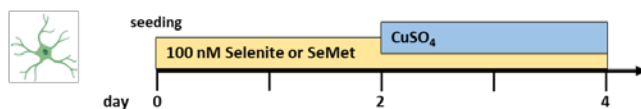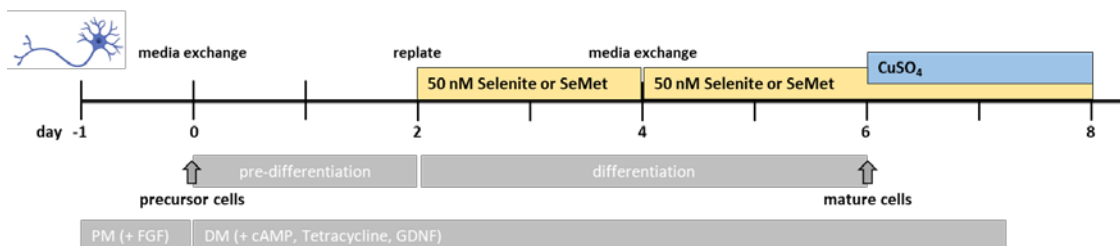
Figure S1. Cultivation and incubation protocol of Cu/Se combination in human astrocytes (CCF-STTG1) (A) and differentiated neurons (LUHMES) (B). Cells were supplemented with either selenite, SeMet (total Se content: 100 nM) or without addition of Se directly after seeding and incubated with $CuSO_4$ for additional 48 h. Abbreviations: cAMP - cyclic adenosine monophosphate, FGF - fibroblast growth factor, GDNF - glial cell-derived neurotrophic factor, PM = proliferation media, DM = differentiation media.

Table S1. Effective concentrations (EC$_{30}$) of CuSO$_4$ in human astrocytes (CCF-STTG1) and differentiated neurons (LUHMES). Cells were supplemented with either selenite, SeMet (total Se content: 100 nM) or without addition of Se directly after seeding and incubated with $CuSO_4$ for additional 48 h.

EC$_{30}$ [µM]	Dehydrogenase activity (CCK8)	Lysosomal integrity (neutral red)	Dehydrogenase activity (resazurin)	Cell number (hoechst)
	CCF-STTG1 / LUHMES	CCF-STTG1 / LUHMES	CCF-STTG1 / LUHMES	CCF-STTG1 / LUHMES
w/o Se	40 / 60	140 / 50	240 / >500	270 / >500
Selenite	40 / 60	130 / 60	240 / >500	290 / >500
SeMet	40 / 60	130 / 50	250 / >500	300 / >500
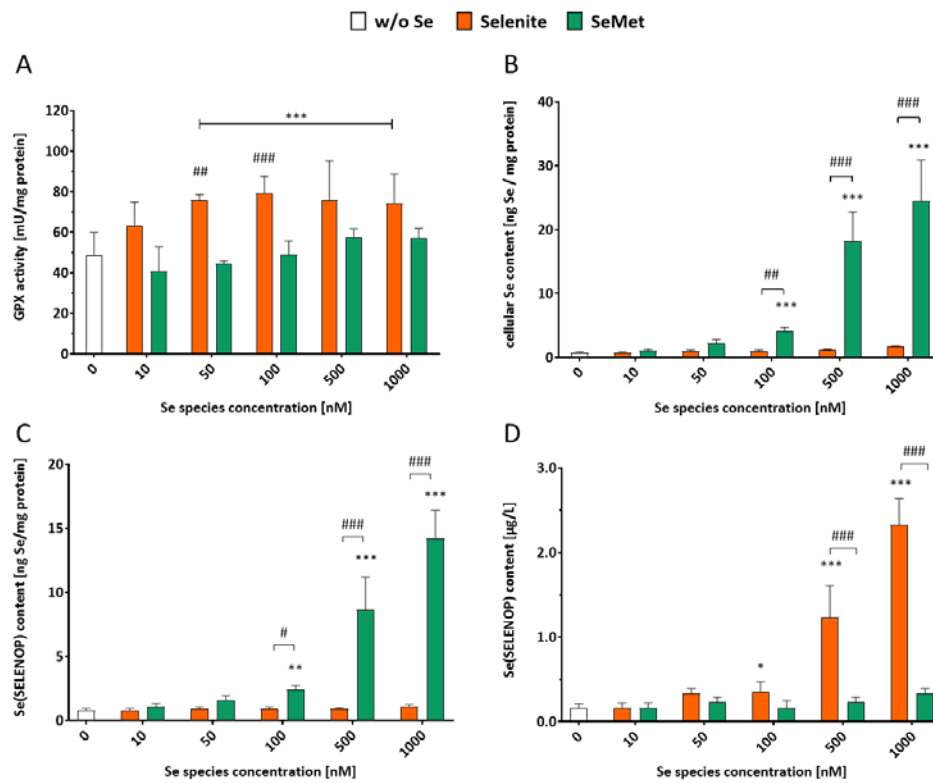
Figure S2. Se species-dependent modulation of Se status in human astrocytes. (A) GPX activity, (B) total Se content, (C) cellular and (D) excreted SELENOP content in human astrocytes supplemented with selenite or SeMet directly after seeding. Data are shown as mean + SD (n ≥ 3). *p < 0.05; **p < 0.01; ***p < 0.001 *vs.* 0 nM Se species based on two-way ANOVA with Dunnett´s post-test. #p < 0.05; ##p < 0.01; ###p < 0.01 *vs.* SeMet calculated based on two-way ANOVA with Dunnett´s post-test.
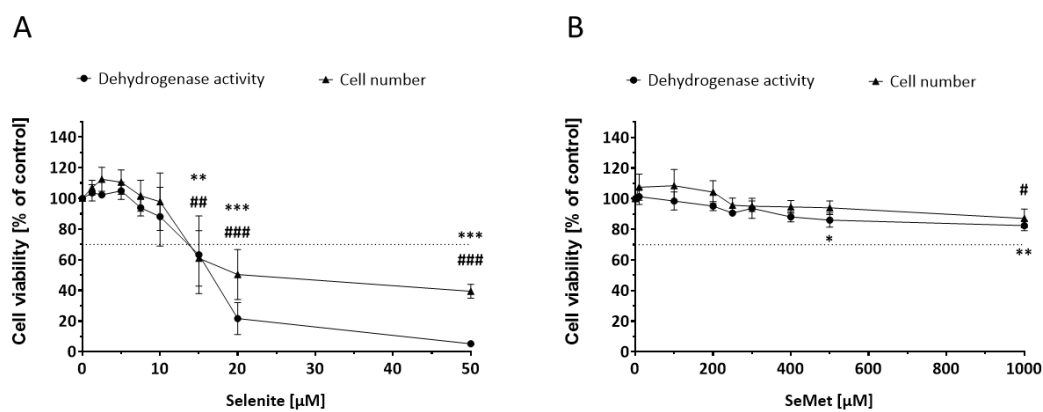
Figure S3. Cytotoxicity of selenite (A) and SeMet (B) in human differentiated neurons. After 48 h incubation with respective Se species dehydrogenase activity (*) *via* Resazurin assay and cell number (#) *via* Hoechst staining were assessed. Data are shown as mean ± SD (n ≥ 3). */# p < 0.05; **/## p < 0.01; ***/### p < 0.001 *vs.* 0 nM Se species based on two-way ANOVA with Dunnett´s post-test.
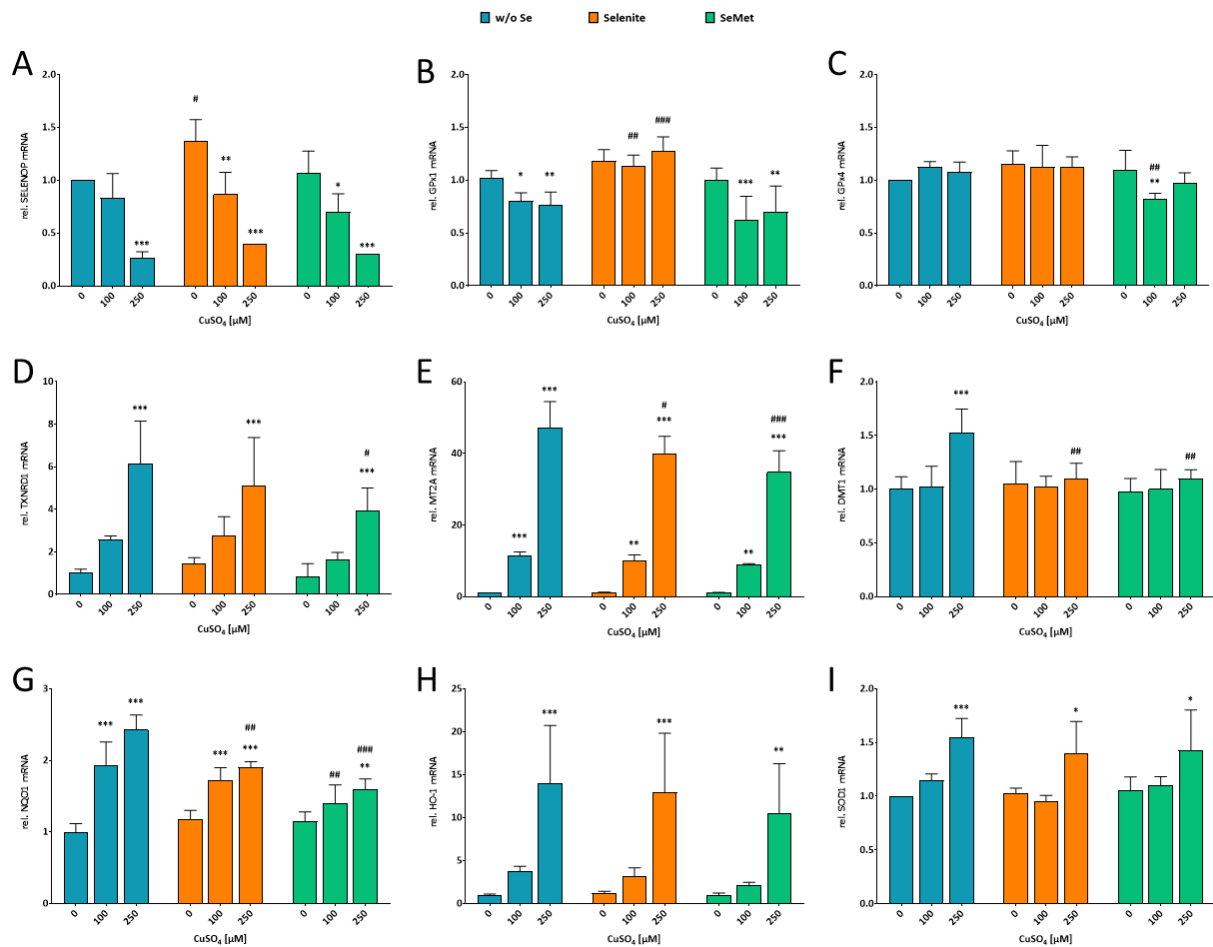
Figure S4. Gene expression of selenoproteins in human astrocytes. Cells were supplemented with either selenite, SeMet (total Se content: 100 nM) or without addition of Se directly after seeding and incubated with CuSO₄ for additional 48 h. Gene expression was determined *via* qPCR and normalized to the reference gene RPL13A. Blue bars represent cells cultivated under standard conditions (w/o Se), while orange and green bars show cells supplemented with selenite or SeMet, respectively. Data are shown as mean + SD (n = 3). *p < 0.05; **p < 0.01; ***p < 0.001 *vs.* 0 µM CuSO₄ based on two-way ANOVA with Dunnett´s post-test. #p < 0.05; ##p < 0.01; ###p < 0.01 *vs.* w/o Se calculated based on two-way ANOVA with Dunnett´s post-test.
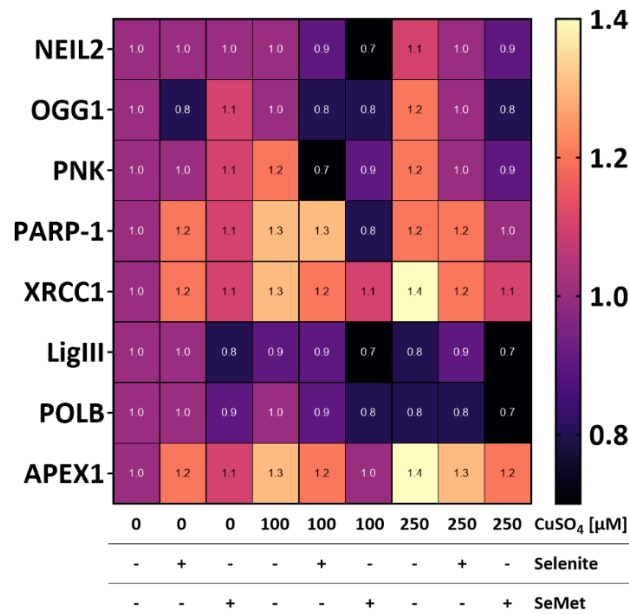
Figure S5. Gene expression of BER-related genes in human astrocytes. Cells were supplemented with either selenite, SeMet (total Se content: 100 nM) or without addition of Se directly after seeding and incubated with $CuSO_4$ for additional 48 h. Gene expression was determined *via* qPCR and normalized to the reference gene RPL13A. Data are shown as mean (n ≥ 2).
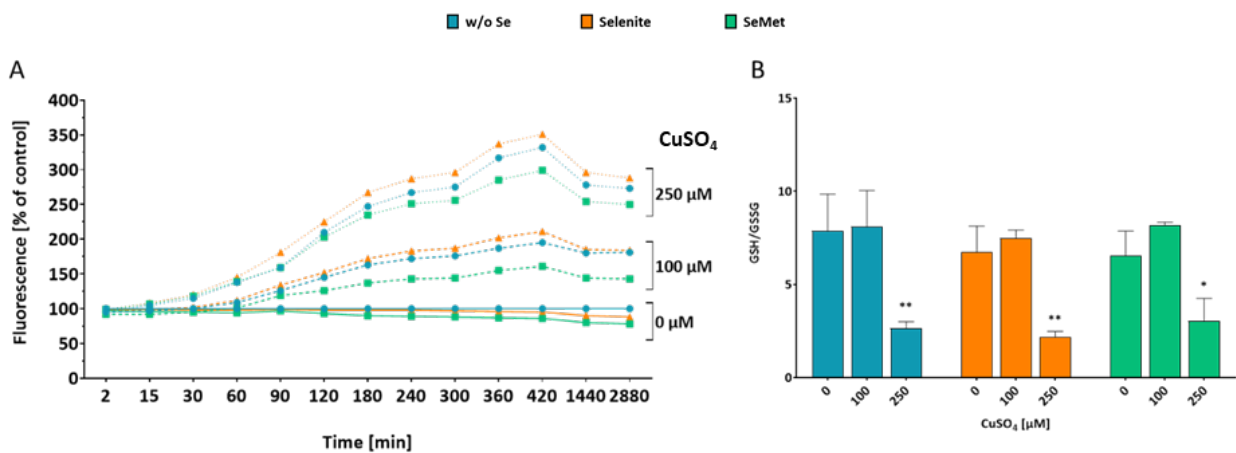
Figure S6. Oxidative stress related marker in human astrocytes. Cells were supplemented with either selenite, SeMet (total Se content: 100 nM) or without addition of Se directly after seeding and incubated with $CuSO_4$ for additional 48 h. (A) Induction of ROS were measured using the carboxy-DCFH-DA assay. Shown are mean (related to control) values of at least three independent experiments. (B) GSH/GSSG ratio was assessed by photometric measurement of DTNB conversion to TNB. Blue bars represent cells cultivated under standard conditions (w/o Se), while orange and green bars show cells supplemented with selenite or SeMet, respectively. Shown are mean values + SD (n ≥ 2). Statistical analysis based on two-way ANOVA with Dunnett´s post-test. *p<0.05; **p<0.01 *vs.* 0 µM $CuSO_4$.
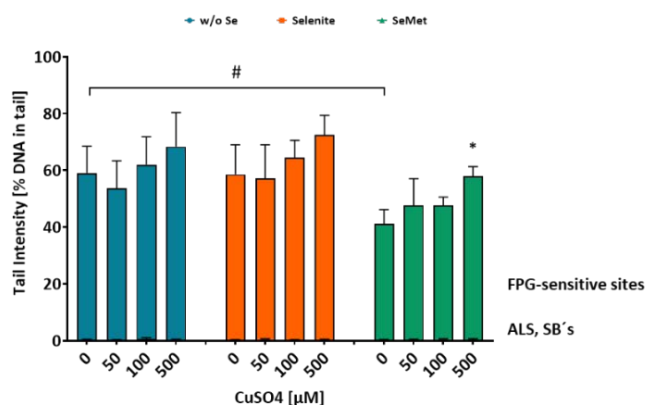
Figure S7. Cu exposure induced oxidative DNA damage in human differentiated neurons (LUHMES). Cells were supplemented with either selenite, SeMet (total Se content: 100 nM) or without addition of Se directly after seeding and incubated with $CuSO_4$ for additional 48 h. DNA damage was quantified by alkaline and FPG-modified comet assay in human astrocytes. ALS - alkali-labile sites; SB´s - DNA strand breaks. Data are shown as mean + SD (n = 3). *p < 0.05 *vs.* 0 µM $CuSO_4$ based on two-way ANOVA with Dunnett´s post-test. #p < 0.05 *vs.* w/o Se calculated based on two-way ANOVA with Tukey´s post-test.
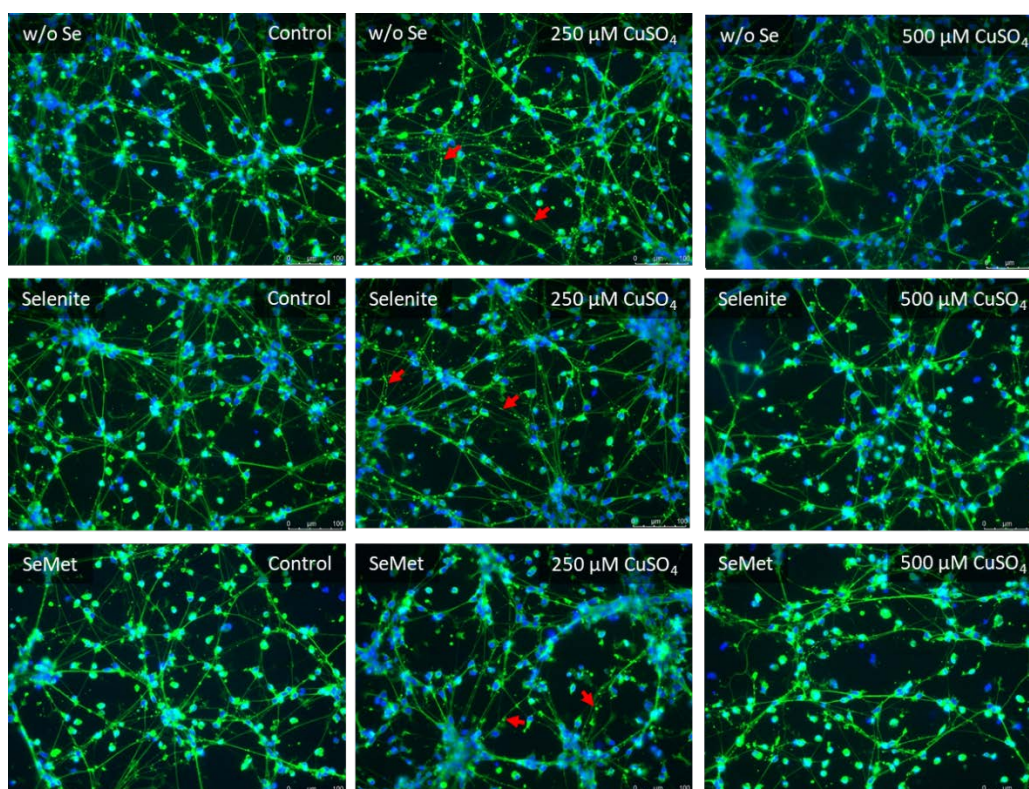
Figure S8. Cu-induced neurodegeneration in human differentiated neurons. Cells were supplemented with selenite or SeMet and then treated with $CuSO_4$ for 48 h. Neurite network was stained by βIII-tubulin antibody and nuclei were stained by DAPI. Arrows show accumulation of tubulin signal indicating loss of neurite network. Shown are exemplary microscopic pictures (20x magnification).

7. GENERAL DISCUSSION

The essentiality of the trace elements Se and Cu has been described for decades and investigation on the individual trace elements is well researched. However, apart from the individual characterization, the consideration of trace element combinations are also crucial. Both, Se and Cu are associated with the development and progression of neurodegenerative diseases (NDs). Decreased Se levels in the brain appear to be linked to Alzheimer´s disease (AD), with hippocampus and temporal lobe particular affected areas which play a role in memory function [286]. A RCT study in AD patients has shown positive effects of Se supplementation on various clinical and biochemical markers [287]. The beneficial effects of Se are mainly attributed to the antioxidant properties of selenoproteins. Furthermore, high Cu concentrations cause increased formation of reactive species and thus oxidative stress, one hallmark of the development of NDs [288]. Accumulation of Cu, resulting from a disturbance of homeostasis is associated with AD and PD progression [266,267]. In affected areas such as cortex and hippocampus, high concentrations of Cu are co-localized with senile-plaques [267]. Accordingly, at the level of a Cu-mediated induction of oxidative stress and the antioxidative selenoproteins, both trace elements seem to be connected. In the present work, the effects of Se and Cu, both as a single substance and in combination, on cells of the neurovascular unit (Figure 6) were studied. Using a versatile *in vitro* model of the blood-brain barrier (BBB), transfer of Se and Cu were quantified as single substances and in combination (chapter 2, 3 and 4). Another part focused on mechanistic relationships of Cu toxicity at the cellular level (chapter 5). Subsequently, *in vitro* experiments were designed to mechanistically elucidate the interactions of both elements in astrocytes and neurons. Particular interest was placed on the effects of Cu on cellular Se homeostasis and the protective potential of Se supplementation (chapter 6).

7.1 Transfer studies using the *in vitro* BBB model

The BBB represents both a chemical and physical barrier between the brain and the bloodstream [178]. Thus, in parallel with the blood-liquor barrier (BCB), the barriers ensure protection of the brain from external factors. Moreover, the internal environment of the brain is regulated to maintain physiological functions [289]. Primary porcine brain capillary endothelial cells (PBCECs) were used as a well-established *in vitro* BBB model (chapter 2, 3 and 4). This model has already been applied to study the transfer of arsenic compounds, manganese and mercury [290–292].

7.1.1   Transfer of the novel selenium compound selenoneine

The brain depends on external Se supply to maintain physiological functions. Besides SELENOP, which is considered the most important systemic Se transporter, other Se species may contribute to Se supply by passing through the BBB [45]. For this reason, it is of particular importance to study the transfer of different Se species. Recently, the novel Se compound selenoneine (SeN) was identified in blood and tissue of blue fin tuna (*Thunnus thynnus*) [271]. This species is highly relevant from two points of view. First, SeN is the Se-containing isologue of the antioxidant ergothioneine (ET), which is found mainly in fungi [293]. Accordingly, similar antioxidative properties are attributed to SeN [271]. And second, SeN is present in high concentrations in edible fish [271,294,295]. This raises the question of whether high fish consumption could contribute to improved Se supply and may have a positive effect on the brain. Consequently, studying the SeN transfer into the brain utilizing a well-established *in vitro* BBB model was the critical first step in answering these questions (cf. *chapter 2: Capabilities of selenoneine to cross the in vitro blood–brain barrier model*).

Initially, cytotoxic potential of SeN was investigated in PBCECs. In the cytotoxicity assays performed, SeN was unable to induce cytotoxic effects up to a concentration of 100 µM over a 72 h period. Similarly, no cytotoxic effects were observed in Caco-2 cells [272]. Not many studies have been done on this Se species yet, but no cytotoxic effects were expected [271]. In comparison, selenite and MeSeCys have been studied as reference compounds. Similar to SeN, MeSeCys excerted no significant cytotoxic effects on PBCECs up to a concentration of 100 µM. Substantial cytotoxicity were observed after incubation with selenite with an EC_{30} value of 15 µM for the most sensitive endpoint, lysosomal activity, which was also observed in other cell lines [272,296,297]. Subsequently, non-toxic concentrations were chosen for transfer experiments, and barrier integrity was monitored continuously during the 72-hour incubation period. Incubation of 1 µM of the respective Se compound into the apical compartment showed no impairment of the barrier integrity. Apical and basolateral medium samples were collected at different time points, and Se content was quantified by ICP-MS/MS. This allowed characterizing the time-dependent transfer of the respective Se species. Compared to the reference compounds, SeN showed the lowest transfer rate in this BBB model. Presumably, the transfer is facilitated *via* transport proteins resulting in a small but significant accumulation in the basolateral compartment. A possible candidate for this would be OCTN1, since it has been described as a transporter for the sulfur analog ET [298]. The presence of this transporter could be demonstrated in the Caco-2 model, which could also explain the side-directed transport observed in this model [272]. However, when applying SeN to both compartments, no side-directed accumulation could be measured on one side in the BBB model. Additionally, expression of *Octn1* could not be detected in rat BBB [299] although ET was found to accumulate in the brain [300]. This suggests an alternative route for SeN *via* the BBB. In contrast to data in Caco-2 cells [272], speciation analyses could not show

significant metabolization of SeN in PBCECs. In summary, this study shows that SeN enters the brain *via* the BBB, but only to a small extent. However, the detailed transfer pathways have not yet been elucidated. Moreover, it was shown that the compound is transferred mostly non-metabolized. Compared to its isolog ET antioxidant properties are several times higher [271]. Furthermore, SeN seems to facilitate detoxification of methylmercury, as shown in zebrafish embryos and dolphin liver [298,301]. Additionally, protective effects against the progression of colorectal cancer in mice [302] and iron-mediated autoxidation in erythrocytes under hypoxic conditions [271] were also observed. A summary of the results from chapter 2 is shown in Figure 9. These data show that SeN has promising physiological properties and therefore further investigations are necessary to characterize them.

	Selenoneine	MeSeCys	Selenite
Cytotoxicity	-	-	+++
Transfer efficiency	+	+++	++
Cellular bioavailability	-	-	-
Metabolism	-	+ (four unknown Species detected)	-
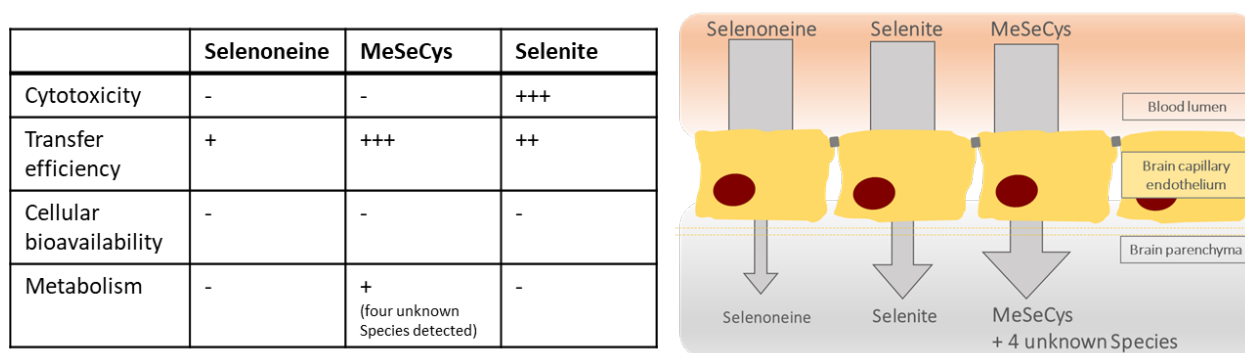
Figure 9. Schematic summary of results obtained from Se transfer study. PBCEC´s incubated with SeN, selenite or MeSeCys for 72 h, regarding their respective transfer behavior, cytotoxicity, metabolism and cellular bioavailability.

7.1.2   Transfer of copper

The homeostatically tightly regulated trace element Cu is essential for the brain. However, a disruption of homeostasis is associated with a number of NDs [265], including genetic heritable WD. These patients have a genetic defect in the Cu transporter *ATP7B* gene [161,170,171], leading to Cu accumulation first in the liver and in later stages also in the brain [273–275]. Excess Cu is deleterious to neuronal tissue and leads to neurological impairment, causing these patients to suffer from symptoms like dysarthria and parkinsonism [276]. One therapeutic approach to prevent Cu accumulation is by treatment with Cu chelators such as DPA. However, 19 to 52% of DPA-treated patients experience a dramatic worsening of symptoms shortly after treatment [277–281]. In contrast, patients treated with a new chelator, tetrathiomolybdate, with a higher Cu affinity, showed no neurological deterioration compared to DPA treatment [282–284]. One of the objectives of chapter 3 (*Bis-choline tetrathiomolybdate prevents copper-induced blood–brain barrier damage*) was to characterize Cu transfer in combination with two chelators, DPA and ALXN1840, *via* the *in vitro* BBB model.

Therefore, loosely bound to albumin Cu was used here to mimic the *in vivo* situation of a Cu pulse during liver cell death, which may occur in WD patients at advanced stages. First, cytotoxicity and effects on barrier integrity of different Cu concentrations were investigated in PBCECs. It was shown that with increasing Cu concentrations, TEER values were decreasing. Whereby only a concentration of 300 µM Cu triggered a cytotoxic effect, measured as an increase in cell capacity, which was also confirmed using the neutral red assay. This indicates that the cells of the BBB are sensitive to Cu exposure and this leads to increased leakiness even without cytotoxic effects. Accordingly, a Cu concentration of 250 µM was chosen for the following transfer experiments in combination with equimolar concentrations of the chelators DPA or ALXN1840. At this concentration without the addition of a chelator, the BBB became leaky over the period of incubation but no cell death occurred. Even the addition of DPA did not prevent the loss of barrier tightness. In contrast, the use of ALXN1840 was able to protect the loss of barrier integrity, resulting in TEER values comparable to untreated controls. To investigate the Cu transfer to the basolateral (brain-facing) compartment, medium samples were collected at different time points, and Cu concentrations were quantified by ICP-MS/MS. The influx of Cu across the BBB into the basolateral compartment was clearly visible in samples treated with Cu alone. Even the combination with DPA did not prevented the Cu transfer. In contrast, co-treatment with ALXN1840 prevented transfer of Cu into the basolateral compartment, resulting in Cu levels similar to untreated controls. In addition, the tight junction proteins claudin-5 and ZO-1 were stained immunhistochemically and examined microscopically. Here, exposure to Cu resulted in the formation of gaps in the distribution of tight junctions that were otherwise uniformly distributed in untreated samples. The formation of gaps could be prevented by addition of ALXN1840, but not by co-treatment with DPA. Similar results were made on electron microscopic images [303]. These results imply a negative effect of Cu on the barrier properties of the BBB, allowing more Cu to enter the brain (Figure 10A). In WD, the export of Cu from the brain is additionally disturbed, since at high Cu concentrations ATP7B is mainly responsible for the export of Cu across the BCB, and mutation of this transporter leads to impaired transport into the blood circulation [262,268]. The development of the high-affinity chelating agent ALXN1840 seems promising in this regard, as the negative effects of Cu on the cells constituting the BBB could be protected.

In addition to WD, AD and PD are also associated with Cu accumulation in some brain areas due to dyshomeostasis of the trace element [266,267]. Studies of trace element concentrations in serum of aging subjects measured increased Cu levels [304], which could be linked to increased levels in the brain. Conversely, the level of Se in the serum of these individuals concurrently declined [304]. The physiological significance of most selenoproteins derives from their ability to participate in redox regulation. Which might imply that a reduced Se supply in the elderly population decreases antioxidant capacity. Especially the brain is vulnerable to oxidative stress [215], whereby decreased expression of

selenoproteins may have adverse effects. Combining this with an increase in redox-active Cu in some brain regions, this suggest a synergistic effect in the development of NDs. The altered homeostasis of trace elements opens the question whether insufficient Se supply to BBB-forming endothelial cells enables higher Cu transfer to the brain. This is addressed in chapter 4 (*Se supplementation to an in vitro blood-brain barrier does not affect Cu transfer into the brain*) by applying the well-established *in vitro* model of the BBB.

Se in the form of selenite (100 or 200 nM) was added during cultivation and differentiation of the PBCECs to both compartments. For transfer studies, 15 or 50 µM CuSO$_4$ was applied apically. The lower Cu concentration was chosen to be in the physiological range of the serum Cu concentration. Additionally, a higher Cu concentration was tested to mimic a Cu pulse presumably occurring during the death of liver cells in the advanced stages of WD. Such an event could be detected in a rat WD model, resulting in elevated serum Cu levels (27 ± 16 µM Cu) [305]. Applied Cu and selenite concentrations were not cytotoxic to the PBCECs, as previously shown [303,306], and did not negatively affect barrier integrity, as confirmed by continuous measurement of TEER values and capacities of the barrier. To quantify total Cu and Se concentrations, medium samples were collected at baseline and after 48 hours of incubation and measured by ICP-MS/MS. As expected, the Se content increased in a concentration-dependent manner after addition of selenite. Moreover, no side-directed Se transfer of the applied Se species was observed, which was described previously [306]. To characterize Se homeostasis more precisely, an attempt was made to quantify SELENOP in the medium by affinity chromatography-coupled ICP-MS/MS. Here, chromatographic separation utilizes the heparin-binding properties of SELENOP to separate it from the other selenoproteins and Se-associated proteins [307]. However, SELENOP levels were too low to allow quantification. Even under Se-supplemented conditions, which increased SELENOP values, but these were still below the limit of quantification. The second fraction, consisting of non-heparin-binding selenoproteins or Se-associated proteins, was significantly elevated after Se supplementation, but this could also be the incubation substance selenite. At this point, further speciation of this fraction would be of interest, since other selenoproteins may be present in this fraction, in order to be able to draw more detailed picture of the Se status. Together with an increased cellular Se content in PBCECs, this may indicate an improved Se status of the cells, which was also not affected by Cu administration. A Se-mediated protection of barrier integrity during oxygen-glucose deprivation under hyperglycemic conditions was previously demonstrated in a co-culture system consisting of murine brain microvascular endothelial (bEnd.3) and astrocytic (MA-h) cell lines [308]. Cu transferred across the BBB in a concentration-dependent manner, while the addition of Se showed no effect on the basolateral Cu concentrations. Interestingly, the permeability coefficients were higher for 15 µM Cu than for the higher incubation concentration. This effect indicates saturation of the Cu transporters, which is mainly mediated by CTR1. In summary,

this study was unable to provide evidence for increased Cu transfer under Se-suboptimal conditions. However, selenite administration was able to improve the Se status of the cells but showed no effect on the permeability coefficients of Cu (Figure 10B).
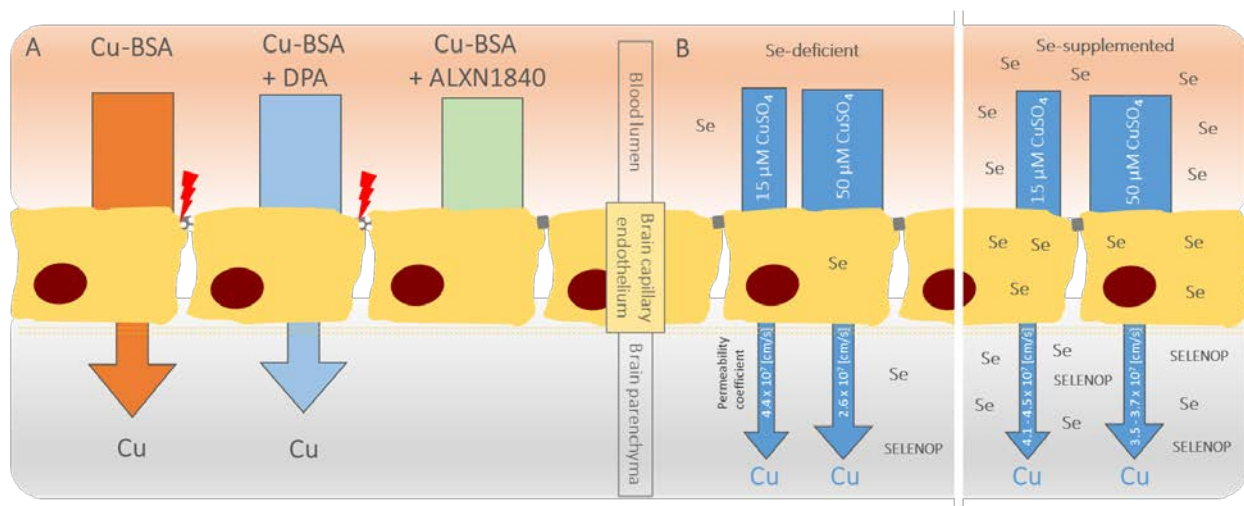
Figure 10. Schematic overview of the results of Cu transfer studies. (A) Investigation of Cu transfer in combination with Cu chelator treatment, regarding the transfer of Cu across the barrier and effects on tight junctions. (B) Study on Cu transfer under Se-suboptimal and Se-supplied conditions, regarding Cu transfer and Cu permeability coefficients as well as Se status.

7.2   Cellular consequences of copper excess and interactions with selenium

Following the discussion of trace element transfer into the brain, this section will now take a closer look on the consequences of Cu overload in the brain. Therefore, chapter 5 (*Characterizing effects of excess copper levels in a human astrocytic cell line with focus on oxidative stress markers*) addresses the impact of Cu overload on a human astrocytic cell line with focusing on oxidative stress. Subsequently, chapter 6 (*Selenium homeostasis in human brain cells: Effects of copper (II) and Se species*) includes Se in the studies to achieve adequate Se supply of the cells. This more closely mimics the *in vivo* situation, where trace elements never act in isolation but in interaction with others. In detail, the protective potential of Se on Cu toxicity will be investigated. Moreover, the impact of Cu on Se homeostasis was addressed to further characterize an interplay of the two trace elements.

7.2.1   Effects of high-dose copper exposure in human astrocytes

Copper(II) sulfate was used as the chemical species for the Cu overload studies. Cupric ions are most abundant in digested food and represent the systemic transport form bound to various proteins in the body (cf. chapter *1.2.4 - Human copper metabolism*) [144]. For cellular uptake, the divalent ions are reduced before being transported into the cells mainly *via* CTR1 [147]. As described in the previous sections, Cu can enter the brain *via* the BBB. Under physiological conditions, Cu homeostasis is under tight control and disturbances in homeostasis are associated with NDs leading to accumulation of Cu

in certain brain regions [265]. Localized between the endothelial cells of the BBB and the neurons, astrocytes occupy a special position in the brain. Substances that enter the brain usually first encounter astrocytes. These cells play a crucial role in Cu homeostasis, as they not only serve to synthesize cuproenzymes, but also store Cu, thus ensuring the protection of other brain cell types from the redox-active properties of Cu. Therefore, the human astrocytic cell line CCF-STTG1 were applied to investigate impact of excess Cu. To observe the cytotoxic potential of Cu, different cytotoxicity assays were used (chapter 5 and 6). All endpoints demonstrated a substantial cytotoxic effect on cells with dehydrogenase activity measured by CCK8 as the most sensitive endpoint. The EC_{30} values ranged from 40 to 270 μM $CuSO_4$ during an incubation period of 48 h. The differences between viability markers are also reflected in the literature [309–311]. In addition, the cell model used also seems to play a role. Data in human glial cells are limited with regard to cytotoxicity of Cu. However, primary cells isolated from rodents seem to be much more sensitive to Cu than cell lines [310,311].

Mitochondria in particular are discussed as a target organelle of Cu toxicity. In a recent publication, high Cu sensitivity of brain mitochondria was shown in comparison to other organs [312]. Therefore, mitochondrial integrity was measured upon Cu exposure in the CCF-STTG1 cells. A concentration-dependent loss of mitochondrial membrane potential was observed, but only at concentrations above 100 μM Cu, which is already in the cytotoxic range. A similar effect has already been observed in primary rat astrocytes [313]. Moreover, structural as well as functional mitochondrial alterations could be shown in another human astrocytic cell line (U87MG) upon Cu exposure [303]. The structural changes provide an explanation for the loss of membrane potential. Consequently, mitochondrial dysfunction lead to elevated formation of reactive species and thus oxidative stress. This was observed in CCF-STTG1 cells after Cu incubation utilizing the MitoSOX™ Red dye, which is used to visualize superoxides from mitochondria [314]. Detection of superoxides *via* DHE assay failed to show increased induction, indicating that this effect appears to be mitochondria-specific. However, the formation of other reactive species could be detected in these cells by the carboxy-DCFH-DA assay, which was also shown in other studies [315,316]. With the help of this dye, reactive species such as peroxyl, alkoxyl, $OH^\bullet$ and $NO_2^\bullet$ can be detected [208]. In addition to the formation of reactive species, cellular GSH levels were quantified as further marker of oxidative stress. A shift of the GSH/GSSG ratio in favor of an increased formation of the oxidized form occurs only at cytotoxic concentrations. However, results from our study are in accordance with published data [317], describing a concentration-dependent increase in total GSH concentrations upon Cu exposure, which suggest an interaction of Cu with the GSH metabolism. This seems plausible, because GSH plays an important role in the intracellular transport of Cu to the specific Cu chaperones. In this context, the increased formation of GSH acts as a compensatory mechanism against the negative effects of redox-active Cu. In this context, increased expression of *MT2a* has been observed in astrocytes upon Cu exposure, which was also seen in HepG2

cells treated with $CuSO_4$ (100 µM for 24 h) [318]. The ability to efficiently take up and store Cu has been demonstrated in primary rat astrocytes [310,311]. Consistent with the results presented in this thesis, Cu accumulation factors of up to 11-fold were observed in CCF-STTG1 cells. These data suggest that the increased binding capacity represents a compensatory mechanism for the massive cellular Cu accumulation upon exposure to this element. Beside the cellular consequences of Cu overload, the interactions with other elements were analysed by quantifying cellular concentrations of Ca, Mg, Mn and Fe. The presented results demonstrated an interaction between investigated elements (except Mg), namely with a Ca and Mn accumulation and a decline in Fe concentration. One possible mechanism of interaction is thought to be *via* shared transporters. DMT1 transports both Cu and Fe and thus a competitive situation of both trace elements arises [262]. The two trace elements are also connected *via* the Cu-containing ceruloplasmin, which functions as a ferroxidase [262]. Similarly, the Cu exporter ATP7A can be affected by Mn, altering Cu homeostasis [260]. Apart from Cu accumulation, levels of Fe and Ca are also elevated in the senile plaques of AD patients and thus associated with disease progression [267,319].

7.2.2   Copper interference with selenium homeostasis

The interactions between Cu and Se, unlike the interactions between Cu and other trace elements, have been poorly studied. Previous *in vivo* studies on the interactions of Se and Cu showed conflicting results ranging from no influence [320,321] to increased hepatic Cu concentrations [322] and elevated circulating Cu [323]. Studies in the brain are rare, showing *in vivo* decreased GPX activity in chickens [324] and rats [325,326] after Cu treatment. These data indicate a possible influence of Cu on Se homeostasis.

To gain a more detailed insight into the interaction between the two trace elements, a combination study was conducted in two human brain cell lines. Of particular interest was how and whether the Se status of the cells was affected by treatment with Cu. Therefore, human astrocytes (CCF-STTG1) and differentiated neurons (LUHMES) were supplemented with Se, either in the form of selenite or SeMet, immediately after seeding. On the one hand, this ensured that the cells had sufficient time to metabolize the Se species. On the other hand, a direct influence of the Se species itself can be excluded. As previously shown from *in vitro* [296] and *in vivo* [327,328] studies, markers used to assess the Se status of the cells were differentially affected by the Se species. Functional markers such as GPX activity and SELENOP excretion were increased only by selenite supplementation but not by SeMet, which elevated only cellular Se and SELENOP levels. This suggests that in the cells applied, SeMet may not be used as a Se source for selenoprotein synthesis. Presumably, SeMet is non-specifically incorporated into proteins instead, resulting in the observed increase in cellular Se levels. Exposure of cells to Cu negatively affected measured Se status markers. Cellular Se uptake was decreased by Cu exposure by

25% in astrocytes and by 43% in neurons. So far, there are no comparable studies in tissue or cells of the brain. However, in HepG2 cells, opposite effects were shown, resulting in a significant increase in cellular Se content after Cu incubation [318]. A similar increase in Se content after Cu exposure was achieved only in astrocytes after supplementation with selenite. However, no hepatic increase in Se content was observed in mice nutritively shifted from Cu-deficient to adequate [318], suggesting that Cu affects Se uptake, but only at supraphysiological Cu concentrations. Decreased Se uptake may also affect the incorporation of SeCys into selenoproteins, leading to more incorporation of Cys instead of SeCys, which has been shown for TXNRD1 [329,330] and SELENOP [331]. Incorporation of amino acids other than SeCys resulted in comparable selenoprotein levels, but these exhibited significantly reduced enzyme activity [332,333]. After Cu exposure decreased GPX activity could also be measured in astrocytes. However, this was accompanied by a decreased *GPX1* mRNA level, suggesting an influence of Cu on GPX synthesis. Studies in brains of rats [325,326] and chicken [324] treated with Cu also showed a decrease in GPX activity as well as decreased protein expression of GPX, supporting the results of this work. In addition to the decline in enzyme activity, cellular SELENOP concentrations were lower in both cell lines upon Cu exposure. This was accompanied with a decrease in *SELENOP* mRNA level, indicating diminished synthesis of SELENOP. Furthermore, Cu strongly inhibited excretion of SELENOP. This strong effect may not be explained by reduced synthesis alone, suggesting that Cu might interfere with the mechanism of SELENOP excretion. Moreover, Cu was shown to have a high binding affinity for SELENOP [237]. In post-mortem brains of AD patients, co-localization of SELENOP and Aβ plaques and neurofibrillary tangles were observed [239]. These areas play a crucial role in the progression of AD and are associated with a higher Cu content [267].

7.2.3   Protective potential of selenium against copper

The protective actions of Se are mainly linked to its antioxidant properties, as it is an essential component of several antioxidant enzymes. The relation between Se and different diseases is summarized in section *1.1.6 – Imbalances of selenium homeostasis*. *In vivo*, Se has been shown to exhibit positive effects on maintenance of locomotor activity and memory function in rat models of PD [334] and AD [335]. Both neurodegenerative diseases are associated with impaired Cu homeostasis, which may lead to Cu accumulation in certain brain areas [266,267]. Apart from that, Se was found to protect from toxicity of different metals and metalloids such as As, Cd, Hg and Pb (reviewed in [336]). However, the protective effect appears to be strongly dose and Se species dependent [337].

Therefore, another focus of the presented Se/Cu combination study was to investigate the protective potential of Se supplementation to counteract Cu-induced toxicity in human astrocytes (CCF-STTG1) and differentiated neurons (LUHMES) (chapter 6: *Selenium homeostasis in human brain cells: Effects of copper (II) and Se species*). Firstly, general cytotoxicity was investigated with dehydrogenase activity

and lysosomal integrity as the most sensitive markers for Cu toxicity. However, Se supplementation did not demonstrate protection in the investigated endpoints. Similar results, in which viability after Cu exposure remained unaffected by Se supplementation (50 nM selenite or 200 nM SeMet), were obtained in HepG2 cells [318]. In contrast, administration of a supraphysiological SeMet concentration (5-80 µM) exhibited a protective effect on neuronal cell viability in murine GT1-7 cells [338]. This illustrates that the used dose of the species has a decisive role in the protective effect. However, it is questionable whether such high concentrations are achievable. As previously discussed (cf. section 7.1.2 - *Transfer of copper*), Cu induces alterations of mitochondrial structure and function. Consequently, the decline in mitochondrial membrane potential (MMP) causes elevated RONS production during oxidative respiration. Therefore, it is reasonable to assume that Se supplementation might have a protective effect on the loss of mitochondrial integrity. However, the data shown did not indicate a preventive effect on Cu-induced loss of MMP. Se-mediated protection of MMP after NaF exposure was observed in a rat renal cell line [339]. In contrast to the study shown in this work, the incubation of selenite and NaF was performed simultaneously in this study, which did not exclude a direct impact of the Se species itself. However, the incubation protocol of the study presented here ensures that the cells have sufficient time to metabolize the Se species, which might explain the discrepancies between the outcomes regarding the protective potential of Se. Exposure to 250 µM Cu resulted in cellular Cu accumulation in astrocytes and neurons by a factor of 133 and 63, respectively. Astrocytes have already been described for their ability to take up and store high amounts of Cu [310,311]. While Se supplementation had no effect on cellular Cu accumulation, the concomitant increase in mRNA levels of *MT2A* was Se-dependent, with lower levels in Se-supplemented cells than in Se-deficient cells. A similar effect on MT expression was observed in liver of Cd-exposed rats supplemented with Se. Both Se and Zn were able to decrease the mRNA levels of *MT1* and *MT2* compared with Cd exposure alone [340]. This was attributed to the antioxidant effect of Se, as MT expression is controlled by cellular redox balance [341]. Another cellular compensatory mechanism to Cu accumulation is an increase in GSH concentration. Only at cytotoxic Cu concentrations the GSSG contents increase at the same time, which reduces the GSH/GSSG ratio. An association between GSH and Se was observed in a study in Se-deficient fed chickens where GSH production was diminished in intestinal tissue [342]. However, no effect of Se supplementation on GSH and GSSG was shown in the study presented in this work. Moreover, the generation of RONS can be attenuated by Se, as demonstrated in patulin-treated mice supplemented with Se [343]. Since Cu is known to produce reactive species mainly through the Fenton-like reaction, the effect of Se supply on RONS formation in our astrocytes was measured. However, the addition of SeMet showed only a slight reduction in RONS level. SeMet supplementation also failed to significantly reduce oxidative DNA damage induced by Cu

exposure, although a protective effect was observed in other cells [344]. A schematic overview of the results from chapter 6 is summarized in Figure 11.

In conclusion, the studies presented provide insight into the mechanism of Cu toxicity in cells forming the neurovascular unit. Moreover, the interactions between Cu and Se homeostasis in these cells were demonstrated. And it is emphasized that the protective effects of Se are not only dependent on the dose and Se species, but also timing of supplementation may be of crucial importance.
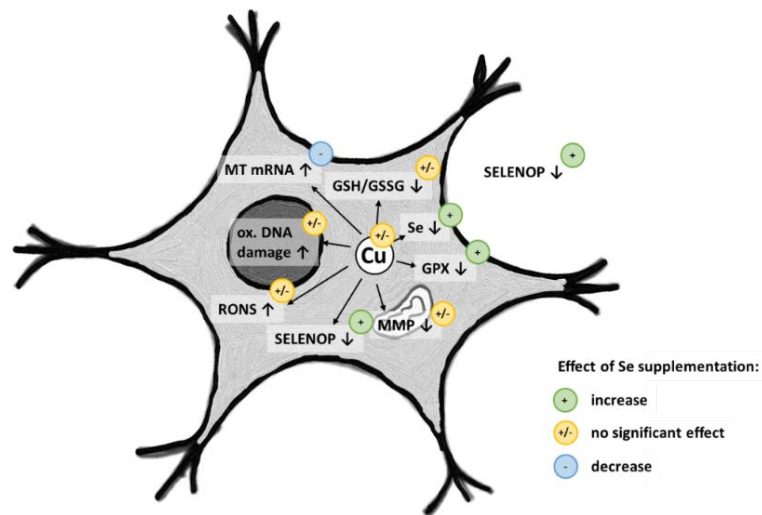
Figure 11. Cellular consequences of Cu exposure and effects of Se supplementation on different general markers as well as endpoints of the Se status in astrocytes.

7.3   Conclusion and outlook

The aim of this work was to investigate the effect of the two trace elements Se and Cu, individually and in combination, on cells of the neurovascular unit. In chapters 2, 3 and 4, using a well-established *in vitro* model of BBB, the transfer of trace elements was studied individually and in combination. Chapter 2 demonstrated that the transfer of the recently discovered species selenoneine *via* the BBB occurs only in small amounts staying in their non-metabolized form. Previous studies on the properties of this substance demonstrated a strong antioxidant effect, but the physiological effects are still largely unexplored. One would be whether this species can be used for the synthesis of selenoproteins. Additionally, selenoneine is found in large amounts in marine fish, which would be nutritionally relevant if consumed in high amounts.

In chapter 3, transfer of Cu across the BBB was examined in the context of genetic WD, in which Cu accumulates in the brain and causes neurological symptoms. It was shown that the barrier function of the endothelial cells forming the BBB is disturbed by Cu, presumably allowing more Cu to transfer. One therapeutic option for WD is the administration of chelating agents. The development of novel chelators, in which side effects are reduced, is of high relevance. The chelator used in this study exhibited promising effects in preventing Cu transfer into the brain, but also in protecting the barrier function. Currently, this chelator is in phase III of development as an alternative therapy for the clinical treatment of WD.

Chapter 4 examines the relationship between adequate Se supplementation and the corresponding consequences for Cu transfer to the brain. The results of this short communication did not show any effect of Se supplementation on Cu transfer in the applied BBB model. However, the administration of Se had a positive effect on the Se status of the endothelial cells. Not only the cellular Se content increased but also the content of SELENOP, although not quantifiable, and presumably other selenoproteins in the basolateral (brain side) compartment. At this point, further investigation of selenoproteins would be interesting, although determination of the low SELENOP concentrations might be methodologically challenging.

The last two chapters the focus has shifted to the assumption that Cu overload is already present in the brain. Accordingly, chapter 5 provided a focused insight into the mechanisms of Cu overload in astrocytes. Mitochondria were shown to be particularly sensitive to Cu, as evidenced by a loss of MMP as well as mitochondria-specific formation of ROS. In addition, Cu affected the GSH balance and homeostasis of other elements such as Fe and Ca.

In chapter 6, the study was extended to investigate the interactions between Se and Cu in astrocytes and neurons. The results demonstrated an interaction of Cu with the Se homeostasis. This negative influence was partially prevented by Se supplementation. The investigation of the protective effects

of Se supplementation on Cu toxicity did not reveal any clear effects. Only in neurons, a protection of the neurite network against Cu exposure was shown by SeMet. In the literature, studies on Se-mediated protection are very heterogeneous. This highlights that, in addition to the dose and the Se substance, the way in which the experiments are performed is also of crucial importance. Simultaneous incubation of Se and stressor cannot exclude an effect of the Se compound itself. In this work, Se was applied prior to incubation with Cu, ensuring sufficient time for Se metabolization, which represented a physiological relevant approach. Concluding, the previous consideration of possible interactions between Se and Cu provided promising approaches for further studies.

Research in recent decades suggest that there are alterations in trace element homeostasis during ND development. However, whether these changes are due to the disease or are a prerequisite for its development remains unclear. Mechanistic studies on the involvement of trace elements in development and progression could provide helpful insights in this regard and identify potential early therapeutic targets.

APPENDIX

A)   THE *IN VITRO* BLOOD-BRAIN BARRIER

The *in vitro* BBB model plays a central role in this thesis and is applied in chapter 2 – 4. The porcine brain capillary endothelial cells (PBCECs) that constitute the BBB were isolated from freshly slaughtered pigs according to published protocols [345,346]. Additionally, already cryopreserved cells kindly provided by the working group of Prof. Dr. H.-J. Galla from the University of Münster were used for transfer experiments. The isolation and cultivation protocol for the PBCECs is shown in Figure 12. For selective cultivation of PBCECs and elimination of unwanted but unintentionally co-isolated cells, cultivation is performed with the addition of puromycin, an effective inhibitor of the protein biosynthesis, at DIV 1 [347]. Here, it is taken advantage of the fact that the capillary endothelial cells, unlike most other cells, express the transporter P-gylcoprotein for the export of puromycin. On DIV 3, cells were cryopreserved until further experiments.

DIV 1
- Isolation from whole brains: mash brains, remove meninx
- Enzymatic digestion I (dispase): 2 h, 37 °C, 5% CO_2, 100% humidity
- Centrifugation (dextran density): 10 min, 4 °C, 6810 x g
- Enzymatic digestion II (collagenase/dispase): 1 h, 37 °C, 5% CO_2, 100% humidity
- Centrifugation: 10 min, room temperature, 150 x g
- Centrifugation (percoll density): 10 min, 4 °C, 1300 x g
- Centrifugation: 10 min, room temperature, 150 x g
- Cultivation with puromycin in collagen G-coated flasks

DIV 2
- Washing with PBS (added with Ca^{2+}/Mg^{2+})

DIV 3
- Trypsin digestion (< 10 s)
- Centrifugation: 10 min, room temperature, 150 x g
- Cryopreservation in FCS with 10% DMSO

DIV 3 – 4
- Thawing
- Centrifugation: 10 min, room temperature, 110 x g
- Cultivation on rat-tail collagen-coated Transwells® or 96 well plates
- Proliferation phase

DIV 4 – 7
- Differentiation phase
- Medium exchange to serum-free medium containing hydrocortisone
- Ready for experiment (DIV 7)

Figure 12. Isolation and cultivation protocol of PBCECs based on [345,346]**.** DIV: days *in vitro*, PBS: phosphate-buffered saline, DMSO: dimethyl sulfoxide.

For transfer experiments, cryopreserved PBCECs were thawed and seeded on rat-tail collagen-coated Transwell® polycarbonate membranes inserts (1.12 cm², 0.4 µm pore size). As depicted in Figure 13,

the resulting two compartments represent the capillary lumen with blood (upper part) and the brain parenchyma with its interstitial fluid (lower part). PBCECs undergo proliferation phase for two days (DIV 3 – 4). On DIV 4, serum-containing medium is exchanged to serum-free medium added with hydrocortisone to start differentiation for further two days. Once the PBCECs are differentiated (DIV 7), the Transwells® inserts are transferred to the CellZscope®. After verification of the barrier properties (TEER of at least 600 $\Omega \cdot cm^2$ and capacitance ranging from $0.45 - 0.6\ \mu F/cm^2$), the test substance can be applied to the apical compartment for investigation of the transfer.
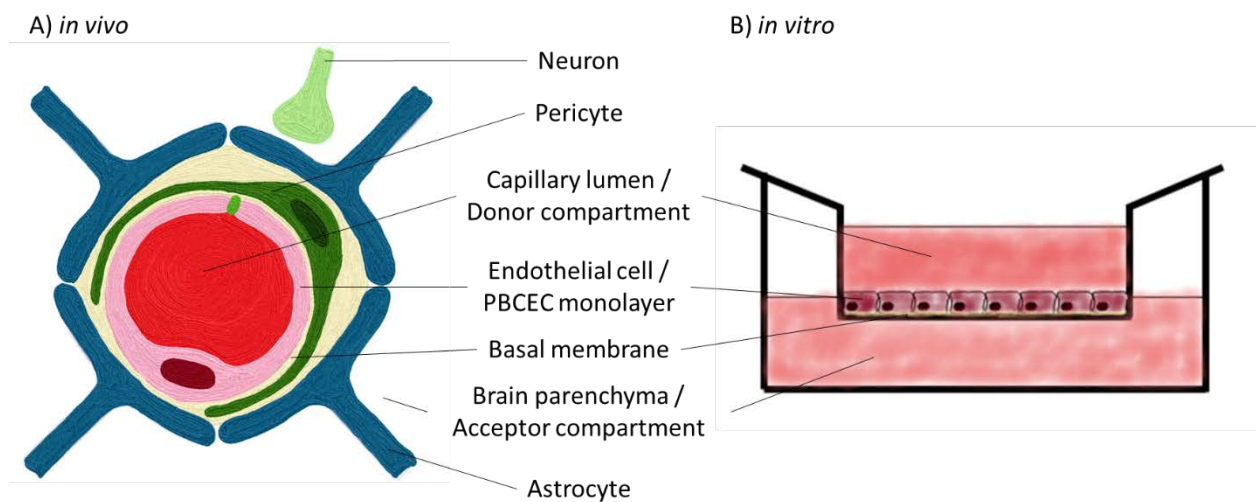
Figure 13. Shematic structure of the blood-brain barrier under (A) *in vivo* conditions and (B) in the applied *in vitro* model.
PBCECs: porcine brain capillary endothelial cells

B)   Impedance spectroscopy for cell monitoring

Impedance spectroscopy with the CellZscope® instrument was applied to monitor barrier- and cell-specific properties during transfer experiments. Particularly relevant are the transendothelial/transepithelial electrical resistance (TEER) and the capacity of the cells. Here, the TEER value is an indicator of barrier integrity, whereas capacitance provides an information about the plasma membrane area of the cell monolayer. The electrical equivalent circuit used to calculate the two values is shown in Figure 14. After applying an alternating current (AC) voltage to the electrodes, both the amplitude and the phase of the AC current are measured. The current can flow either across the gap between the cells (paracellular) or through the cells (transcellular), whereby both paths are accompanied by resistances. Each cell is considered a capacitor due to its lipid bilayer and thus contributes to the resistance of the transcellular pathway. The contribution to the transcellular path or TEER is made by the tight junctions [348].
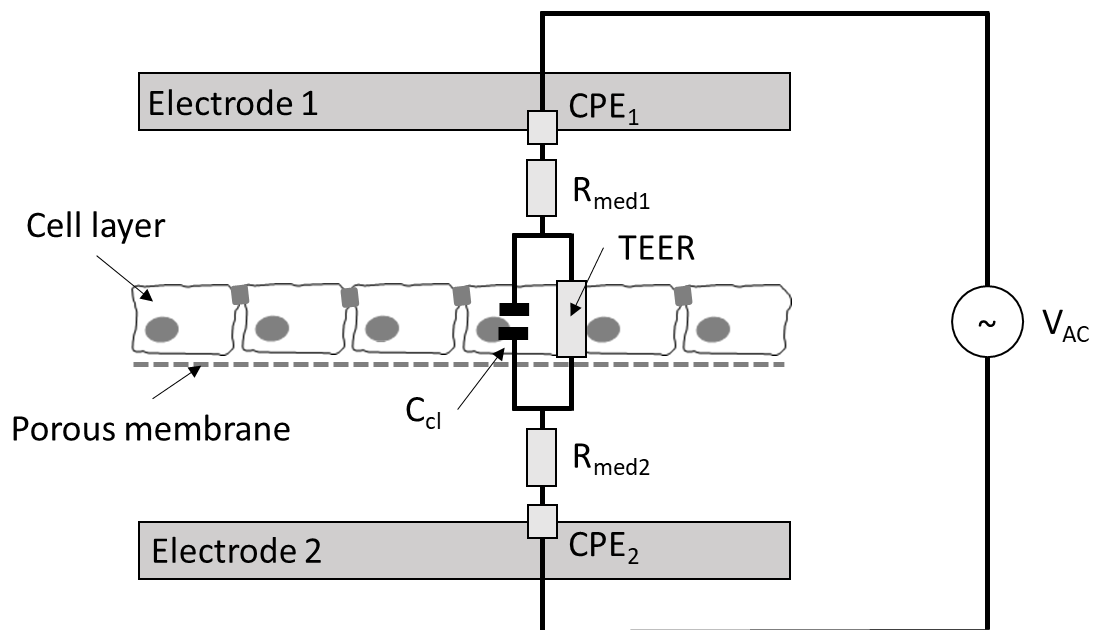
Figure 14. Illustration of an electrical equivalent circuit according to [348]**.** Abbreviations: TEER: transendothelial/transepithelial electrical resistance, C_{cl}: capacitance of the cell layer, CPE: constant phase element, R_{med}: resistance of the culture medium

C)   The *In vitro* neuronal model system

LUHMES (Lund human mesencephalic cells) cells were originally isolated from the ventral mesencephalic tissue of an 8-week-old human embryo. Subsequently, the cells were immortalized using a LINX v-myc retroviral vector whose transcription is regulated by tetracycline [349]. Differentiation is initiated by addition of tetracycline to shut down the myc transgene. After replating of cells into the required cell culture format on day 2, the mature neurons develop with characteristics similar to dopaminergic neurons (e.g. βIII-tubulin immunoreactivity, neuritic processes, dopamine release) [350]. The LUHMES cells provide a useful model to study neurodevelopmental effects as well as neurotoxic effects.
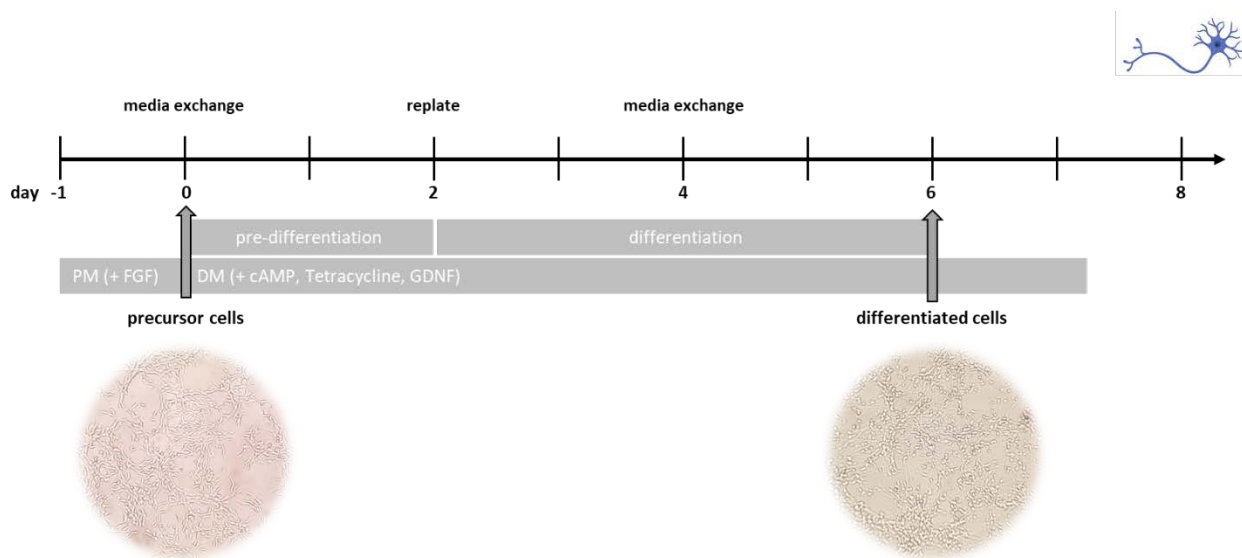
Figure 15. Schematic illustration of the differentiation process of human neurons (LUHMES cells). Abbreviations: cAMP: cyclic adenosine monophosphate, DM: differentiation medium, FGF: fibroblast growth factor, GDNF: glial-derived neurotrophic factor, PM: proliferation medium.

BIBLIOGRAPHY

[1] J. Meija, T.B. Coplen, M. Berglund, W.A. Brand, P. De Bièvre, M. Gröning, N.E. Holden, J. Irrgeher, R.D. Loss, T. Walczyk, T. Prohaska, Atomic weights of the elements 2013 (IUPAC Technical Report), Pure Appl. Chem. 88 (2016) 265–291. https://doi.org/10.1515/pac-2015-0305.

[2] M. Kieliszek, Selenium–Fascinating Microelement, Properties and Sources in Food, Molecules. 24 (2019) 1298. https://doi.org/10.3390/molecules24071298.

[3] J. Meija, T.B. Coplen, M. Berglund, W.A. Brand, P. De Bièvre, M. Gröning, N.E. Holden, J. Irrgeher, R.D. Loss, T. Walczyk, T. Prohaska, Isotopic compositions of the elements 2013 (IUPAC Technical Report), Pure Appl. Chem. 88 (2016) 293–306. https://doi.org/10.1515/pac-2015-0503.

[4] CIAAW, Atomic masses and isotopic abundances. Atomic weights of the elements: Review 2000 by de Laeter et al., Pure Appl. Chem. 2003 (2013) 683–800.

[5] A. Fernández-Martínez, L. Charlet, Selenium environmental cycling and bioavailability: a structural chemist point of view, Rev. Environ. Sci. Bio/Technology. 8 (2009) 81–110. https://doi.org/10.1007/s11157-009-9145-3.

[6] G. Schrauzer, Selenium, in: E. Merian, M. Anke, M. Ihnat, M. Stoeppler (Eds.), Elem. Their Compd. Environ., 2nd ed., WILEY-VCH, 2004: pp. 1365–1406.

[7] L. Schomburg, J. Köhrle, Selen, in: H. Dunkelberg, T. Gebel, A. Hartwig (Eds.), Handb. Der Leb., 5th ed., WILEY-VCH, 2007: pp. 2403–2446.

[8] S. Shini, A. Sultan, W. Bryden, Selenium Biochemistry and Bioavailability: Implications for Animal Agriculture, Agriculture. 5 (2015) 1277–1288. https://doi.org/10.3390/agriculture5041277.

[9] C.M. Weekley, H.H. Harris, Which form is that? the importance of selenium speciation and metabolism in the prevention and treatment of disease, Chem. Soc. Rev. 42 (2013) 8870–8894. https://doi.org/10.1039/c3cs60272a.

[10] J. Alexander, Selenium, in: G. Nordberg, L. Friberg, V. Vouk (Eds.), Handb. Toxicol. Met., 2015.

[11] P.J. White, Selenium in Soils and Crops, in: Selenium, 2018: pp. 29–50. https://doi.org/10.1007/978-3-319-95390-8_2.

[12] Y. Mehdi, J.L. Hornick, L. Istasse, I. Dufrasne, Selenium in the environment, metabolism and involvement in body functions, Molecules. 18 (2013) 3292–3311. https://doi.org/10.3390/molecules18033292.

[13] S.J. Fairweather-Tait, Y. Bao, M.R. Broadley, R. Collings, D. Ford, J.E. Hesketh, R. Hurst, Selenium in Human Health and Disease, Antioxid. Redox Signal. 14 (2011) 1337–1383. https://doi.org/10.1089/ars.2010.3275.

[14] T. Zane Davis, J.O. Hall, Selenium, in: R.C. Gupta (Ed.), Reprod. Dev. Toxicol., 2nd ed., Academic Press: Cambridge, 2017: pp. 595–605.

[15] J.L. Freeman, L.H. Zhang, M.A. Marcus, S. Fakra, S.P. McGrath, E.A.H. Pilon-Smits, Spatial Imaging, Speciation, and Quantification of Selenium in the Hyperaccumulator Plants Astragalus bisulcatus and Stanleya pinnata, Plant Physiol. 142 (2006) 124–134. https://doi.org/10.1104/pp.106.081158.

[16] P.J. White, Selenium metabolism in plants, Biochim. Biophys. Acta - Gen. Subj. 1862 (2018) 2333–2342. https://doi.org/10.1016/j.bbagen.2018.05.006.

[17] L. Winkel, B. Vriens, G. Jones, L. Schneider, E. Pilon-Smits, G. Bañuelos, Selenium Cycling Across Soil-Plant-Atmosphere Interfaces: A Critical Review, Nutrients. 7 (2015) 4199–4239. https://doi.org/10.3390/nu7064199.

[18] R.L.U. Ferreira, K.C.M. Sena-Evangelista, E.P. de Azevedo, F.I. Pinheiro, R.N. Cobucci, L.F.C. Pedrosa, Selenium in Human Health and Gut Microflora: Bioavailability of Selenocompounds and Relationship With Diseases, Front. Nutr. 8 (2021). https://doi.org/10.3389/fnut.2021.685317.

[19] M.P. Rayman, H.G. Infante, M. Sargent, Food-chain selenium and human health: Spotlight on speciation, Br. J. Nutr. 100 (2008) 238–253. https://doi.org/10.1017/S0007114508922522.

[20] Robert-Koch Institut, Selen in der Umweltmedizin, Bundesgesundheitsblatt - Gesundheitsforsch. - Gesundheitsschutz. 49 (2006) 88–101. https://doi.org/10.1007/s00103-005-1185-4.

[21] TrinkwV, Trinkwasserverordnung in der Fassung der Bekanntmachung vom 10. März 2016 (BGBl. I S. 459), die zuletzt durch Artikel 1 der Verordnung vom 22. September 2021 (BGBl. I S. 4343) geändert worden ist, (2021).

[22] A. Frączek, K. Pasternak, Selenium in medicine and treatment, J. Elemntology. (2012). https://doi.org/10.5601/jelem.2013.18.1.13.

[23] M. Kieliszek, S. Błazejak, Current knowledge on the importance of selenium in food for living organisms: A review, Molecules. 21 (2016) 609. https://doi.org/10.3390/molecules21050609.

[24] F. Gorini, L. Sabatino, A. Pingitore, C. Vassalle, Selenium: An Element of Life Essential for Thyroid Function, Molecules. 26 (2021) 7084. https://doi.org/10.3390/molecules26237084.

[25] Richtlinie 2002/46/EG des Europäischen Parlaments und des Rates vom 10. Juni 2002 zur Angleichung der Rechtsvorschriften der Mitgliedstaaten über Nahrungsergänzungsmittel, (2021).

[26] DüMV, Düngemittelverordnung vom 5. Dezember 2012 (BGBl. I S. 2482), die zuletzt durch Artikel 1 der Verordnung vom 2. Oktober 2019 (BGBl. I S. 1414) geändert worden ist, (2019).

[27] Richtlinie der Kommission vom 12. April 1991 zur Änderung der Anhänge der Richtlinie 70/524/EWG des Rates über Zusatzstoffe in der Tierernährung, (n.d.).

[28] Verordnung (EG) Nr. 1831/2003 des Europäischen Parlaments und des Rates vom 22. September 2003 über Zusatzstoffe zur Verwendung in der Tierernährung, (n.d.).

[29] A.P. Kipp, D. Strohm, R. Brigelius-Flohé, L. Schomburg, A. Bechthold, E. Leschik-Bonnet, H. Heseker, Revised reference values for selenium intake, J. Trace Elem. Med. Biol. 32 (2015) 195–199. https://doi.org/10.1016/j.jtemb.2015.07.005.

[30] Y. Xia, K.E. Hill, P. Li, J. Xu, D. Zhou, A.K. Motley, L. Wang, D.W. Byrne, R.F. Burk, Optimization of selenoprotein P and other plasma selenium biomarkers for the assessment of the selenium nutritional requirement: a placebo-controlled, double-blind study of selenomethionine supplementation in selenium-deficient Chinese subjects, Am. J. Clin. Nutr. 92 (2010) 525–531. https://doi.org/10.3945/ajcn.2010.29642.

[31] Institute of Medicine, Dietary Reference Intakes for Vitamin C, Vitamin E, Selenium, and Carotenoids, National Academies Press, Washington, D.C., 2000. https://doi.org/10.17226/9810.

[32] A.J. Duffield, C.D. Thomson, K.E. Hill, S. Williams, An estimation of selenium requirements for New Zealanders, Am. J. Clin. Nutr. 70 (1999) 896–903. https://doi.org/10.1093/ajcn/70.5.896.

[33] G.-Q. Yang, L.-Z. Zhu, S.-J. Liu, L.-Z. Gu, P.-C. Qian, J.-H. Huang, M.-D. Lu, Human Selenium Requirements in China, (1987).

[34] World Health Organization, Vitamin and mineral requirements in human nutrition, 2nd edition, 2004.

[35] K. Renko, Biomarkers of Se Status, in: 2018: pp. 451–465. https://doi.org/10.1007/978-3-319-95390-8_23.

[36] R. Brigelius-Flohé, Selenium in Human Health and Disease: An Overview, in: 2018: pp. 3–26. https://doi.org/10.1007/978-3-319-95390-8_1.

[37] Y. Xia, K.E. Hill, D.W. Byrne, J. Xu, R.F. Burk, Effectiveness of selenium supplements in a low-selenium area of China, Am. J. Clin. Nutr. 81 (2005) 829–834. https://doi.org/10.1093/ajcn/81.4.829.

[38] K. Renko, M. Werner, I. Renner-Müller, T.G. Cooper, C.H. Yeung, B. Hollenbach, M. Scharpf, J. Köhrle, L. Schomburg, U. Schweizer, Hepatic selenoprotein P (SePP) expression restores selenium transport and prevents infertility and motor-incoordination in Sepp -knockout mice, Biochem. J. 409 (2008) 741–749. https://doi.org/10.1042/BJ20071172.

[39] F.P. Phiri, E.L. Ander, R.M. Lark, E.H. Bailey, B. Chilima, J. Gondwe, E.J.M. Joy, A.A. Kalimbira, J.C. Phuka, P.S. Suchdev, D.R.S. Middleton, E.M. Hamilton, M.J. Watts, S.D. Young, M.R. Broadley, Urine selenium concentration is a useful biomarker for assessing population level selenium status, Environ. Int. 134 (2020) 105218. https://doi.org/10.1016/j.envint.2019.105218.

[40] L. Schomburg, Selenoprotein P – Selenium transport protein, enzyme and biomarker of selenium status, Free Radic. Biol. Med. 191 (2022) 150–163. https://doi.org/10.1016/j.freeradbiomed.2022.08.022.

[41] C. Vindry, T. Ohlmann, L. Chavatte, Selenium Metabolism, Regulation, and Sex Differences in Mammals, in: 2018: pp. 89–107. https://doi.org/10.1007/978-3-319-95390-8_5.

[42] L.V. Papp, J. Lu, A. Holmgren, K.K. Khanna, From Selenium to Selenoproteins: Synthesis, Identity, and Their Role in Human Health, Antioxid. Redox Signal. 9 (2007) 775–806. https://doi.org/10.1089/ars.2007.1528.

[43] R.F. Burk, K.E. Hill, Selenoprotein P—Expression, functions, and roles in mammals, Biochim. Biophys. Acta - Gen. Subj. 1790 (2009) 1441–1447. https://doi.org/10.1016/j.bbagen.2009.03.026.

[44] Y. Saito, Selenium Transport Mechanism via Selenoprotein P—Its Physiological Role and Related

Diseases, Front. Nutr. 8 (2021). https://doi.org/10.3389/fnut.2021.685517.

[45] N. Solovyev, E. Drobyshev, B. Blume, B. Michalke, Selenium at the Neural Barriers: A Review, Front. Neurosci. 15 (2021). https://doi.org/10.3389/fnins.2021.630016.

[46] R.F. Burk, K.E. Hill, Regulation of Selenium Metabolism and Transport, Annu. Rev. Nutr. 35 (2015) 109–134. https://doi.org/10.1146/annurev-nutr-071714-034250.

[47] P.A. Tsuji, D. Santesmasses, B.J. Lee, V.N. Gladyshev, D.L. Hatfield, Historical Roles of Selenium and Selenoproteins in Health and Development: The Good, the Bad and the Ugly, Int. J. Mol. Sci. 23 (2021) 5. https://doi.org/10.3390/ijms23010005.

[48] A.-L. Bulteau, L. Chavatte, Update on Selenoprotein Biosynthesis, Antioxid. Redox Signal. 23 (2015) 775–794. https://doi.org/10.1089/ars.2015.6391.

[49] D. Behne, T. Höfer-Bosse, Effects of a Low Selenium Status on the Distribution and Retention of Selenium in the Rat, J. Nutr. 114 (1984) 1289–1296. https://doi.org/10.1093/jn/114.7.1289.

[50] M. Kühbacher, J. Bartel, B. Hoppe, D. Alber, G. Bukalis, A.U. Bräuer, D. Behne, A. Kyriakopoulos, The brain selenoproteome: Priorities in the hierarchy and different levels of selenium homeostasis in the brain of selenium-deficient rats, J. Neurochem. 110 (2009) 133–142. https://doi.org/10.1111/j.1471-4159.2009.06109.x.

[51] K. Schwarz, C. Foltz, Selenium as an integral part of factor 3 against dietary necrotic liver degeneration, J. Am. Chem. Soc. 79 (1957) 3292–3293.

[52] L. Flohe, W.A. Günzler, H.H. Schock, Glutathione peroxidase: A selenoenzyme, FEBS Lett. 32 (1973) 132–134. https://doi.org/10.1016/0014-5793(73)80755-0.

[53] J.T. Rotruck, A.L. Pope, H.E. Ganther, A.B. Swanson, D.G. Hafeman, W.G. Hoekstra, Selenium: Biochemical Role as a Component of Glutathione Peroxidase, Science (80-.). 179 (1973) 588–590. https://doi.org/10.1126/science.179.4073.588.

[54] Y. Zhang, Y.J. Roh, S.-J. Han, I. Park, H.M. Lee, Y.S. Ok, B.C. Lee, S.-R. Lee, Role of Selenoproteins in Redox Regulation of Signaling and the Antioxidant System: A Review, Antioxidants. 9 (2020) 383. https://doi.org/10.3390/antiox9050383.

[55] V.M. Darras, S.L.J. Van Herck, Iodothyronine deiodinase structure and function: from ascidians to humans, J. Endocrinol. 215 (2012) 189–206. https://doi.org/10.1530/JOE-12-0204.

[56] M.A. Reeves, F.P. Bellinger, M.J. Berry, The neuroprotective functions of selenoprotein M and its role in cytosolic calcium regulation., Antioxid. Redox Signal. 12 (2010) 809–18. https://doi.org/10.1089/ars.2009.2883.

[57] A. Chernorudskiy, E. Varone, S.F. Colombo, S. Fumagalli, A. Cagnotto, A. Cattaneo, M. Briens, M. Baltzinger, L. Kuhn, A. Bachi, A. Berardi, M. Salmona, G. Musco, N. Borgese, A. Lescure, E. Zito, Selenoprotein N is an endoplasmic reticulum calcium sensor that links luminal calcium levels to a redox activity, Proc. Natl. Acad. Sci. 117 (2020) 21288–21298. https://doi.org/10.1073/pnas.2003847117.

[58] L. Grumolato, H. Ghzili, M. Montero-Hadjadje, S. Gasman, J. Lesage, Y. Tanguy, L. Galas, D. Ait-Ali, J. Leprince, N.C. Guérineau, A.G. Elkahloun, A. Fournier, D. Vieau, H. Vaudry, Y. Anouar, Selenoprotein T is a PACAP-regulated gene involved in intracellular Ca 2+ mobilization and neuroendocrine secretion, FASEB J. 22 (2008) 1756–1768. https://doi.org/10.1096/fj.06-075820.

[59] B. Ren, M. Liu, J. Ni, J. Tian, Role of Selenoprotein F in Protein Folding and Secretion: Potential Involvement in Human Disease, Nutrients. 10 (2018) 1619. https://doi.org/10.3390/nu10111619.

[60] P.R. Hoffmann, An Emerging Picture of the Biological Roles of Selenoprotein K, in: Selenium, Springer New York, New York, NY, 2011: pp. 335–344. https://doi.org/10.1007/978-1-4614-1025-6_26.

[61] Y. Ye, Y. Shibata, C. Yun, D. Ron, T.A. Rapoport, A membrane protein complex mediates retro-translocation from the ER lumen into the cytosol, Nature. 429 (2004) 841–847. https://doi.org/10.1038/nature02656.

[62] V.M. Labunskyy, D.L. Hatfield, V.N. Gladyshev, Selenoproteins: Molecular Pathways and Physiological Roles, Physiol. Rev. 94 (2014) 739–777. https://doi.org/10.1152/physrev.00039.2013.

[63] A. Nappi, M.A. De Stefano, M. Dentice, D. Salvatore, Deiodinases and Cancer, Endocrinology. 162 (2021). https://doi.org/10.1210/endocr/bqab016.

[64] R. Brigelius-Flohé, L. Flohé, Regulatory Phenomena in the Glutathione Peroxidase Superfamily, Antioxid. Redox Signal. 33 (2020) 498–516. https://doi.org/10.1089/ars.2019.7905.

[65] E.S.J. Arnér, Focus on mammalian thioredoxin reductases — Important selenoproteins with versatile

functions, Biochim. Biophys. Acta - Gen. Subj. 1790 (2009) 495–526. https://doi.org/10.1016/j.bbagen.2009.01.014.

[66] B.C. Lee, A. Dikiy, H.-Y. Kim, V.N. Gladyshev, Functions and evolution of selenoprotein methionine sulfoxide reductases, Biochim. Biophys. Acta - Gen. Subj. 1790 (2009) 1471–1477. https://doi.org/10.1016/j.bbagen.2009.04.014.

[67] X.-M. Xu, B.A. Carlson, R. Irons, H. Mix, N. Zhong, V.N. Gladyshev, D.L. Hatfield, Selenophosphate synthetase 2 is essential for selenoprotein biosynthesis, Biochem. J. 404 (2007) 115–120. https://doi.org/10.1042/BJ20070165.

[68] V. Labunskyy, D. Hatfield, V. Gladyshev, The Sep15 protein family: Roles in disulfide bond formation and quality control in the endoplasmic reticulum, IUBMB Life. 59 (2007) 1–5. https://doi.org/10.1080/15216540601126694.

[69] J. Panee, Z.R. Stoytcheva, W. Liu, M.J. Berry, Selenoprotein H Is a Redox-sensing High Mobility Group Family DNA-binding Protein That Up-regulates Genes Involved in Glutathione Synthesis and Phase II Detoxification, J. Biol. Chem. 282 (2007) 23759–23765. https://doi.org/10.1074/jbc.M702267200.

[70] M. Bertz, K. Kühn, S.C. Koeberle, M.F. Müller, D. Hoelzer, K. Thies, S. Deubel, R. Thierbach, A.P. Kipp, Selenoprotein H controls cell cycle progression and proliferation of human colorectal cancer cells, Free Radic. Biol. Med. 127 (2018) 98–107. https://doi.org/10.1016/j.freeradbiomed.2018.01.010.

[71] C. Ma, V. Martinez-Rodriguez, P.R. Hoffmann, Roles for Selenoprotein I and Ethanolamine Phospholipid Synthesis in T Cell Activation, Int. J. Mol. Sci. 22 (2021) 11174. https://doi.org/10.3390/ijms222011174.

[72] G.J. Fredericks, P.R. Hoffmann, Selenoprotein K and Protein Palmitoylation, Antioxid. Redox Signal. 23 (2015) 854–862. https://doi.org/10.1089/ars.2015.6375.

[73] S. Verma, F.W. Hoffmann, M. Kumar, Z. Huang, K. Roe, E. Nguyen-Wu, A.S. Hashimoto, P.R. Hoffmann, Selenoprotein K Knockout Mice Exhibit Deficient Calcium Flux in Immune Cells and Impaired Immune Responses, J. Immunol. 186 (2011) 2127–2137. https://doi.org/10.4049/jimmunol.1002878.

[74] S. Wang, X. Zhao, Q. Liu, Y. Wang, S. Li, S. Xu, Selenoprotein K protects skeletal muscle from damage and is required for satellite cells-mediated myogenic differentiation, Redox Biol. 50 (2022) 102255. https://doi.org/10.1016/j.redox.2022.102255.

[75] M.A. Reeves, M.J. Berry, Selenoprotein M, in: Selenium, Springer New York, New York, NY, 2011: pp. 197–203. https://doi.org/10.1007/978-1-4614-1025-6_15.

[76] M.J. Jurynec, R. Xia, J.J. Mackrill, D. Gunther, T. Crawford, K.M. Flanigan, J.J. Abramson, M.T. Howard, D.J. Grunwald, Selenoprotein N is required for ryanodine receptor calcium release channel activity in human and zebrafish muscle, Proc. Natl. Acad. Sci. 105 (2008) 12485–12490. https://doi.org/10.1073/pnas.0806015105.

[77] S.-J. Han, B.C. Lee, S.H. Yim, V.N. Gladyshev, S.-R. Lee, Characterization of Mammalian Selenoprotein O: A Redox-Active Mitochondrial Protein, PLoS One. 9 (2014) e95518. https://doi.org/10.1371/journal.pone.0095518.

[78] A. Sreelatha, S.S. Yee, V.A. Lopez, B.C. Park, L.N. Kinch, S. Pilch, K.A. Servage, J. Zhang, J. Jiou, M. Karasiewicz-Urbańska, M. Łobocka, N. V Grishin, K. Orth, R. Kucharczyk, K. Pawłowski, D.R. Tomchick, V.S. Tagliabracci, Protein AMPylation by an Evolutionarily Conserved Pseudokinase., Cell. 175 (2018) 809-821.e19. https://doi.org/10.1016/j.cell.2018.08.046.

[79] N. Solovyev, Selenoprotein P and its potential role in Alzheimer's disease, Hormones. 19 (2020) 73–79. https://doi.org/10.1007/s42000-019-00112-w.

[80] S. Yu, J. Du, Selenoprotein S: a therapeutic target for diabetes and macroangiopathy?, Cardiovasc. Diabetol. 16 (2017) 101. https://doi.org/10.1186/s12933-017-0585-8.

[81] N. Fradejas-Villar, U. Schweizer, Selenium and Neurodevelopment, in: 2018: pp. 177–192. https://doi.org/10.1007/978-3-319-95390-8_9.

[82] A.A. Turanov, M. Malinouski, V.N. Gladyshev, Selenium and Male Reproduction, in: Selenium, Springer New York, New York, NY, 2011: pp. 409–417. https://doi.org/10.1007/978-1-4614-1025-6_32.

[83] L.-L. Chen, J.-Q. Huang, Y. Xiao, Y.-Y. Wu, F.-Z. Ren, X.G. Lei, Knockout of Selenoprotein V Affects Regulation of Selenoprotein Expression by Dietary Selenium and Fat Intakes in Mice, J. Nutr. 150 (2020) 483–491. https://doi.org/10.1093/jn/nxz287.

[84] X. Zhang, W. Xiong, L.-L. Chen, J.-Q. Huang, X.G. Lei, Selenoprotein V protects against endoplasmic reticulum stress and oxidative injury induced by pro-oxidants, Free Radic. Biol. Med. 160 (2020) 670–679.

https://doi.org/10.1016/j.freeradbiomed.2020.08.011.

[85] S.M. Marino, V.N. Gladyshev, A. Dikiy, Structural Characterization of Mammalian Selenoproteins, in: Selenium, Springer New York, New York, NY, 2011: pp. 125–136. https://doi.org/10.1007/978-1-4614-1025-6_10.

[86] H. Kim, K. Lee, J.M. Kim, M.Y. Kim, J.-R. Kim, H.-W. Lee, Y.W. Chung, H.-I. Shin, T. Kim, E.-S. Park, J. Rho, S.H. Lee, N. Kim, S.Y. Lee, Y. Choi, D. Jeong, Selenoprotein W ensures physiological bone remodeling by preventing hyperactivity of osteoclasts, Nat. Commun. 12 (2021) 2258. https://doi.org/10.1038/s41467-021-22565-7.

[87] M.P. Rayman, Selenium intake, status, and health: a complex relationship, Hormones. 19 (2020) 9–14. https://doi.org/10.1007/s42000-019-00125-5.

[88] B.M. Aldosary, M.E. Sutter, M. Schwartz, B.W. Morgan, Case Series Of Selenium Toxicity From A Nutritional Supplement, Clin. Toxicol. 50 (2012) 57–64. https://doi.org/10.3109/15563650.2011.641560.

[89] N. Hadrup, G. Ravn-Haren, Acute human toxicity and mortality after selenium ingestion: A review, J. Trace Elem. Med. Biol. 58 (2020) 126435. https://doi.org/10.1016/j.jtemb.2019.126435.

[90] K.L. Nuttall, Evaluating selenium poisoning., Ann. Clin. Lab. Sci. 36 (2006) 409–20. http://www.ncbi.nlm.nih.gov/pubmed/17127727.

[91] S. Li, T. Xiao, B. Zheng, Medical geology of arsenic, selenium and thallium in China, Sci. Total Environ. 421–422 (2012) 31–40. https://doi.org/10.1016/j.scitotenv.2011.02.040.

[92] EFSA, Tolerable Upper Intake Levels Scientific Committee on Food Scientific Panel on Dietetic Products, Nutrition and Allergies, 2006.

[93] S.C. Koeberle, A.P. Kipp, Selenium and Inflammatory Mediators, in: 2018: pp. 137–156. https://doi.org/10.1007/978-3-319-95390-8_7.

[94] J. Avery, P. Hoffmann, Selenium, Selenoproteins, and Immunity, Nutrients. 10 (2018) 1203. https://doi.org/10.3390/nu10091203.

[95] B. Michalke, Selenium speciation in human serum of cystic fibrosis patients compared to serum from healthy persons, J. Chromatogr. A. 1058 (2004) 203–208. https://doi.org/10.1016/j.chroma.2004.08.063.

[96] P.H. Canter, B. Wider, E. Ernst, The antioxidant vitamins A, C, E and selenium in the treatment of arthritis: a systematic review of randomized clinical trials, Rheumatology. 46 (2007) 1223–1233. https://doi.org/10.1093/rheumatology/kem116.

[97] B. Speckmann, H. Steinbrenner, Selenium and Selenoproteins in Inflammatory Bowel Diseases and Experimental Colitis, Inflamm. Bowel Dis. (2014) 1. https://doi.org/10.1097/MIB.0000000000000020.

[98] W. Alhazzani, J. Jacobi, A. Sindi, C. Hartog, K. Reinhart, S. Kokkoris, H. Gerlach, P. Andrews, T. Drabek, W. Manzanares, D.J. Cook, R.Z. Jaeschke, The Effect of Selenium Therapy on Mortality in Patients With Sepsis Syndrome, Crit. Care Med. 41 (2013) 1555–1564. https://doi.org/10.1097/CCM.0b013e31828a24c6.

[99] S. Hariharan, S. Dharmaraj, Selenium and selenoproteins: it's role in regulation of inflammation, Inflammopharmacology. 28 (2020) 667–695. https://doi.org/10.1007/s10787-020-00690-x.

[100] C.A. Stone, K. Kawai, R. Kupka, W.W. Fawzi, Role of selenium in HIV infection, Nutr. Rev. 68 (2010) 671–681. https://doi.org/10.1111/j.1753-4887.2010.00337.x.

[101] J. Zhang, R. Saad, E.W. Taylor, M.P. Rayman, Selenium and selenoproteins in viral infection with potential relevance to COVID-19, Redox Biol. 37 (2020) 101715. https://doi.org/10.1016/j.redox.2020.101715.

[102] B.C. Lee, Z. Péterfi, F.W. Hoffmann, R.E. Moore, A. Kaya, A. Avanesov, L. Tarrago, Y. Zhou, E. Weerapana, D.E. Fomenko, P.R. Hoffmann, V.N. Gladyshev, MsrB1 and MICALs Regulate Actin Assembly and Macrophage Function via Reversible Stereoselective Methionine Oxidation, Mol. Cell. 51 (2013) 397–404. https://doi.org/10.1016/j.molcel.2013.06.019.

[103] A.J. Goldson, S.J. Fairweather-Tait, C.N. Armah, Y. Bao, M.R. Broadley, J.R. Dainty, C. Furniss, D.J. Hart, B. Teucher, R. Hurst, Effects of Selenium Supplementation on Selenoprotein Gene Expression and Response to Influenza Vaccine Challenge: A Randomised Controlled Trial, PLoS One. 6 (2011) e14771. https://doi.org/10.1371/journal.pone.0014771.

[104] A. Kuria, H. Tian, M. Li, Y. Wang, J.O. Aaseth, J. Zang, Y. Cao, Selenium status in the body and cardiovascular disease: a systematic review and meta-analysis, Crit. Rev. Food Sci. Nutr. 61 (2021) 3616–3625. https://doi.org/10.1080/10408398.2020.1803200.

[105] X. Zhang, C. Liu, J. Guo, Y. Song, Selenium status and cardiovascular diseases: meta-analysis of prospective observational studies and randomized controlled trials, Eur. J. Clin. Nutr. 70 (2016) 162–169.

https://doi.org/10.1038/ejcn.2015.78.

[106] X. Zhang, X. Li, W. Zhang, Y. Song, Selenium and Cardiovascular Disease: Epidemiological Evidence of a Possible U-Shaped Relationship, in: 2018: pp. 303–316. https://doi.org/10.1007/978-3-319-95390-8_16.

[107] A. Shalihat, A.N. Hasanah, Mutakin, R. Lesmana, A. Budiman, D. Gozali, The role of selenium in cell survival and its correlation with protective effects against cardiovascular disease: A literature review, Biomed. Pharmacother. 134 (2021) 111125. https://doi.org/10.1016/j.biopha.2020.111125.

[108] D.J.A. Jenkins, D. Kitts, E.L. Giovannucci, S. Sahye-Pudaruth, M. Paquette, S. Blanco Mejia, D. Patel, M. Kavanagh, T. Tsirakis, C.W.C. Kendall, S.C. Pichika, J.L. Sievenpiper, Selenium, antioxidants, cardiovascular disease, and all-cause mortality: a systematic review and meta-analysis of randomized controlled trials, Am. J. Clin. Nutr. 112 (2020) 1642–1652. https://doi.org/10.1093/ajcn/nqaa245.

[109] M. Vinceti, T. Filippini, K.J. Rothman, Selenium exposure and the risk of type 2 diabetes: a systematic review and meta-analysis, Eur. J. Epidemiol. 33 (2018) 789–810. https://doi.org/10.1007/s10654-018-0422-8.

[110] L. Kohler, J. Foote, C. Kelley, A. Florea, C. Shelly, H.-H. Chow, P. Hsu, K. Batai, N. Ellis, K. Saboda, P. Lance, E. Jacobs, Selenium and Type 2 Diabetes: Systematic Review, Nutrients. 10 (2018) 1924. https://doi.org/10.3390/nu10121924.

[111] S. Stranges, J.R. Marshall, R. Natarajan, R.P. Donahue, M. Trevisan, G.F. Combs, F.P. Cappuccio, A. Ceriello, M.E. Reid, Effects of Long-Term Selenium Supplementation on the Incidence of Type 2 Diabetes, Ann. Intern. Med. 147 (2007) 217. https://doi.org/10.7326/0003-4819-147-4-200708210-00175.

[112] L. Schomburg, The other view: the trace element selenium as a micronutrient in thyroid disease, diabetes, and beyond, Hormones. 19 (2020) 15–24. https://doi.org/10.1007/s42000-019-00150-4.

[113] H. Steinbrenner, L.H. Duntas, M.P. Rayman, The role of selenium in type-2 diabetes mellitus and its metabolic comorbidities, Redox Biol. 50 (2022) 102236. https://doi.org/10.1016/j.redox.2022.102236.

[114] B. Gerardo, M. Cabral Pinto, J. Nogueira, P. Pinto, A. Almeida, E. Pinto, P. Marinho-Reis, L. Diniz, P.I. Moreira, M.R. Simões, S. Freitas, Associations between Trace Elements and Cognitive Decline: An Exploratory 5-Year Follow-Up Study of an Elderly Cohort, Int. J. Environ. Res. Public Health. 17 (2020) 6051. https://doi.org/10.3390/ijerph17176051.

[115] N.T. Akbaraly, I. Hininger-Favier, I. Carrière, J. Arnaud, V. Gourlet, A.-M. Roussel, C. Berr, Plasma Selenium Over Time and Cognitive Decline in the Elderly, Epidemiology. 18 (2007) 52–58. https://doi.org/10.1097/01.ede.0000248202.83695.4e.

[116] X. Yan, K. Liu, X. Sun, S. Qin, M. Wu, L. Qin, Y. Wang, Z. Li, X. Zhong, X. Wei, A cross-sectional study of blood selenium concentration and cognitive function in elderly Americans: National Health and Nutrition Examination Survey 2011–2014, Ann. Hum. Biol. 47 (2020) 610–619. https://doi.org/10.1080/03014460.2020.1836253.

[117] B. Rita Cardoso, V. Silva Bandeira, W. Jacob-Filho, S.M. Franciscato Cozzolino, Selenium status in elderly: Relation to cognitive decline, J. Trace Elem. Med. Biol. 28 (2014) 422–426. https://doi.org/10.1016/j.jtemb.2014.08.009.

[118] V.S. Reddy, S. Bukke, N. Dutt, P. Rana, A.K. Pandey, A systematic review and meta-analysis of the circulatory, erythrocellular and CSF selenium levels in Alzheimer's disease: A metal meta-analysis (AMMA study-I), J. Trace Elem. Med. Biol. 42 (2017) 68–75. https://doi.org/10.1016/j.jtemb.2017.04.005.

[119] M.P. Rayman, Selenium and human health, Lancet. 379 (2012) 1256–1268. https://doi.org/10.1016/S0140-6736(11)61452-9.

[120] A. Mojadadi, A. Au, W. Salah, P. Witting, G. Ahmad, Role for Selenium in Metabolic Homeostasis and Human Reproduction, Nutrients. 13 (2021) 3256. https://doi.org/10.3390/nu13093256.

[121] K.E. Hill, J. Zhou, W.J. McMahan, A.K. Motley, J.F. Atkins, R.F. Gesteland, R.F. Burk, Deletion of Selenoprotein P Alters Distribution of Selenium in the Mouse, J. Biol. Chem. 278 (2003) 13640–13646. https://doi.org/10.1074/jbc.M300755200.

[122] M.J. Ceko, K. Hummitzsch, N. Hatzirodos, W.M. Bonner, J.B. Aitken, D.L. Russell, M. Lane, R.J. Rodgers, H.H. Harris, Correction: X-Ray fluorescence imaging and other analyses identify selenium and GPX1 as important in female reproductive function, Metallomics. 7 (2015) 188–188. https://doi.org/10.1039/C4MT90049A.

[123] L.C. Clark, G.F. Combs, B.W. Turnbull, E.H. Slate, D.K. Chalker, J. Chow, L.S. Davis, R.A. Glover, G.F. Graham, E.G. Gross, A. Krongrad, J.L. Lesher, H.K. Park, B.B. Sanders, C.L. Smith, J.R. Taylor, Effects of selenium supplementation for cancer prevention in patients with carcinoma of the skin: A randomized

controlled trial, J. Am. Med. Assoc. 276 (1996) 1957–1963. https://doi.org/10.1001/jama.276.24.1957.

[124] A.J. Duffield-Lillico, M.E. Reid, B.W. Turnbull, G.F. Combs, E.H. Slate, L.A. Fischbach, J.R. Marshall, L.C. Clark, Baseline characteristics and the effect of selenium supplementation on cancer incidence in a randomized clinical trial: a summary report of the Nutritional Prevention of Cancer Trial., Cancer Epidemiol. Biomarkers Prev. 11 (2002) 630–9. http://www.ncbi.nlm.nih.gov/pubmed/12101110.

[125] A.J. Duffield-Lillico, Selenium Supplementation and Secondary Prevention of Nonmelanoma Skin Cancer in a Randomized Trial, CancerSpectrum Knowl. Environ. 95 (2003) 1477–1481. https://doi.org/10.1093/jnci/djg061.

[126] S.M. Lippman, E.A. Klein, P.J. Goodman, M.S. Lucia, I.M. Thompson, L.G. Ford, H.L. Parnes, L.M. Minasian, J.M. Gaziano, J.A. Hartline, J.K. Parsons, J.D. Bearden, E.D. Crawford, G.E. Goodman, J. Claudio, E. Winquist, E.D. Cook, D.D. Karp, P. Walther, M.M. Lieber, A.R. Kristal, A.K. Darke, K.B. Arnold, P.A. Ganz, R.M. Santella, D. Albanes, P.R. Taylor, J.L. Probstfield, T.J. Jagpal, J.J. Crowley, F.L. Meyskens, L.H. Baker, C.A. Coltman, Effect of Selenium and Vitamin E on Risk of Prostate Cancer and Other Cancers, Jama. 301 (2009) 39. https://doi.org/10.1001/jama.2008.864.

[127] H.R. Harris, L. Bergkvist, A. Wolk, Selenium intake and breast cancer mortality in a cohort of Swedish women, Breast Cancer Res. Treat. 134 (2012) 1269–1277. https://doi.org/10.1007/s10549-012-2139-9.

[128] Y. Zhou, J. Li, X. Xu, M. Zhao, B. Zhang, S. Deng, Y. Wu, 64 Cu-based Radiopharmaceuticals in Molecular Imaging, Technol. Cancer Res. Treat. 18 (2019) 153303381983075. https://doi.org/10.1177/1533033819830758.

[129] A. Ahmedova, B. Todorov, N. Burdzhiev, C. Goze, Copper radiopharmaceuticals for theranostic applications, Eur. J. Med. Chem. 157 (2018) 1406–1425. https://doi.org/10.1016/j.ejmech.2018.08.051.

[130] D.G. Ellingsen, L.B. Møller, J. Aaseth, Copper, in: Handb. Toxicol. Met., Elsevier, 2015: pp. 765–786. https://doi.org/10.1016/B978-0-444-59453-2.00035-4.

[131] B. Zietz, Kupfer, in: H. Dunkelberg, T. Gebel, A. Hartwig (Eds.), Handb. Der Leb., 4th ed., 2007: pp. 2163–2202.

[132] A. Kabata-Pendias, B. Szteke, Copper, in: Trace Elem. Abiotic Biot. Environ., CRC Press, 2015: pp. 97–107. https://doi.org/10.1201/b18198.

[133] N. and A. EFSA NDA Panel (EFSA Panel on Dietetic Products, Scientific Opinion on Dietary Reference Values for copper, EFSA J. 13 (2015) 4253. https://doi.org/10.2903/j.efsa.2015.4253.

[134] D.L. de Romaña, M. Olivares, R. Uauy, M. Araya, Risks and benefits of copper in light of new insights of copper homeostasis, J. Trace Elem. Med. Biol. 25 (2011) 3–13. https://doi.org/10.1016/j.jtemb.2010.11.004.

[135] R. Ginocchio, P.H. Rodríguez, R. Badilla-Ohlbaum, H.E. Allen, G.E. Lagos, Effect of soil copper content and pH on copper uptake of selected vegetables grown under controlled conditions, Environ. Toxicol. Chem. 21 (2002) 1736–1744. https://doi.org/10.1002/etc.5620210828.

[136] V. Chaignon, I. Sanchez-Neira, P. Herrmann, B. Jaillard, P. Hinsinger, Copper bioavailability and extractability as related to chemical properties of contaminated soils from a vine-growing area, Environ. Pollut. 123 (2003) 229–238. https://doi.org/10.1016/S0269-7491(02)00374-3.

[137] J.R. Turnlund, W.R. Keyes, H.L. Anderson, L.L. Acord, Copper absorption and retention in young men at three levels of dietary copper by use of the stable isotope 65Cu, Am. J. Clin. Nutr. 49 (1989) 870–878. https://doi.org/10.1093/ajcn/49.5.870.

[138] J.R. Turnlund, W.R. Keyes, G.L. Peiffer, K.C. Scott, Copper absorption, excretion, and retention by young men consuming low dietary copper determined by using the stable isotope 65Cu, Am. J. Clin. Nutr. 67 (1998) 1219–1225. https://doi.org/10.1093/ajcn/67.6.1219.

[139] J.R. Turnlund, J.C. King, B. Gong, W.R. Keyes, M.C. Michel, A stable isotope study of copper absorption in young men: effect of phytate and alpha-cellulose, Am. J. Clin. Nutr. 42 (1985) 18–23. https://doi.org/10.1093/ajcn/42.1.18.

[140] I. of Medicine, Dietary Reference Intakes for Vitamin A, Vitamin K, Arsenic, Boron, Chromium, Copper, Iodine, Iron, Manganese, Molybdenum, Nickel, Silicon, Vanadium, and Zinc, National Academies Press, Washington, D.C., 2001. https://doi.org/10.17226/10026.

[141] D-A-CH, Referenzwerte für die Nährstoffzufuhr, 2021.

[142] J.F. Collins, Copper nutrition and biochemistry and human (patho)physiology, in: 2021: pp. 311–364. https://doi.org/10.1016/bs.afnr.2021.01.005.

[143] F. Woimant, N. Djebrani-Oussedik, A. Poujois, New tools for Wilson's disease diagnosis: exchangeable copper fraction, Ann. Transl. Med. 7 (2019) S70–S70. https://doi.org/10.21037/atm.2019.03.02.

[144] P.V. van den Berghe, L.W. Klomp, New developments in the regulation of intestinal copper absorption, Nutr. Rev. 67 (2009) 658–672. https://doi.org/10.1111/j.1753-4887.2009.00250.x.

[145] Y. Nishito, T. Kambe, Absorption Mechanisms of Iron, Copper, and Zinc: An Overview, J. Nutr. Sci. Vitaminol. (Tokyo). 64 (2018) 1–7. https://doi.org/10.3177/jnsv.64.1.

[146] J. Chen, Y. Jiang, H. Shi, Y. Peng, X. Fan, C. Li, The molecular mechanisms of copper metabolism and its roles in human diseases, Pflügers Arch. - Eur. J. Physiol. 472 (2020) 1415–1429. https://doi.org/10.1007/s00424-020-02412-2.

[147] J. Lee, M.M.O. Peña, Y. Nose, D.J. Thiele, Biochemical Characterization of the Human Copper Transporter Ctr1, J. Biol. Chem. 277 (2002) 4380–4387. https://doi.org/10.1074/jbc.M104728200.

[148] C. Doguer, J. Ha, J.F. Collins, Intersection of Iron and Copper Metabolism in the Mammalian Intestine and Liver, in: Compr. Physiol., Wiley, 2018: pp. 1433–1461. https://doi.org/10.1002/cphy.c170045.

[149] E.B. Maryon, S.A. Molloy, J.H. Kaplan, Cellular glutathione plays a key role in copper uptake mediated by human copper transporter 1, Am. J. Physiol. Physiol. 304 (2013) C768–C779. https://doi.org/10.1152/ajpcell.00417.2012.

[150] A.M.D.C. Ferreira, M.R. Ciriolo, L. Marcocci, G. Rotilio, Copper(I) transfer into metallothionein mediated by glutathione, Biochem. J. 292 (1993) 673–676. https://doi.org/10.1042/bj2920673.

[151] O.M. Steinebach, H.T. Wolterbeek, Role of cytosolic copper, metallothionein and glutathione in copper toxicity in rat hepatoma tissue culture cells, Toxicology. 92 (1994) 75–90. https://doi.org/10.1016/0300-483X(94)90168-6.

[152] L.S. Field, E. Luk, V.C. Culotta, Copper chaperones: personal escorts for metal ions., J. Bioenerg. Biomembr. 34 (2002) 373–9. https://doi.org/10.1023/a:1021202119942.

[153] V.C. Culotta, L.W.J. Klomp, J. Strain, R.L.B. Casareno, B. Krems, J.D. Gitlin, The Copper Chaperone for Superoxide Dismutase, J. Biol. Chem. 272 (1997) 23469–23472. https://doi.org/10.1074/jbc.272.38.23469.

[154] Y. Takahashi, K. Kako, S. Kashiwabara, A. Takehara, Y. Inada, H. Arai, K. Nakada, H. Kodama, J. Hayashi, T. Baba, E. Munekata, Mammalian Copper Chaperone Cox17p Has an Essential Role in Activation of Cytochrome c Oxidase and Embryonic Development, Mol. Cell. Biol. 22 (2002) 7614–7621. https://doi.org/10.1128/MCB.22.21.7614-7621.2002.

[155] L.W.J. Klomp, S.-J. Lin, D. S.Yuan, R.D. Klausner, V.C. Culotta, J.D. Gitlin, Identification and Functional Expression of HAH1, a Novel Human Gene Involved in Copper Homeostasis, J. Biol. Chem. 272 (1997) 9221–9226. https://doi.org/10.1074/jbc.272.14.9221.

[156] D.W. Cox, S.D.P. Moore, Copper transporting P-type ATPases and human disease., J. Bioenerg. Biomembr. 34 (2002) 333–8. https://doi.org/10.1023/a:1021293818125.

[157] C. Vulpe, B. Levinson, S. Whitney, S. Packman, J. Gitschier, Isolation of a candidate gene for Menkes disease and evidence that it encodes a copper–transporting ATPase, Nat. Genet. 3 (1993) 7–13. https://doi.org/10.1038/ng0193-7.

[158] E.D. Harris, Cellular Copper Transport and Metabolism, Annu. Rev. Nutr. 20 (2000) 291–310. https://doi.org/10.1146/annurev.nutr.20.1.291.

[159] H. Tapiero, D.M. Townsend, K.D. Tew, Trace elements in human physiology and pathology. Copper, Biomed. Pharmacother. 57 (2003) 386–398. https://doi.org/10.1016/S0753-3322(03)00012-X.

[160] J.R. Turnlund, Human whole-body copper metabolism, Am. J. Clin. Nutr. 67 (1998) 960S-964S. https://doi.org/10.1093/ajcn/67.5.960S.

[161] P.C. Bull, G.R. Thomas, J.M. Rommens, J.R. Forbes, D.W. Cox, The Wilson disease gene is a putative copper transporting P–type ATPase similar to the Menkes gene, Nat. Genet. 5 (1993) 327–337. https://doi.org/10.1038/ng1293-327.

[162] K. Nagano, K. Nakamura, K.-I. Urakami, K. Umeyama, H. Uchiyama, K. Koiwai, S. Hattori, T. Yamamoto, I. Matsuda, F. Endo, Intracellular distribution of the Wilson's disease gene product (atpase7b) afterin vitro andin vivo exogenous expression in hepatocytes from the LEC rat, an animal model of Wilson's disease, Hepatology. 27 (1998) 799–807. https://doi.org/10.1002/hep.510270323.

[163] M.C. Linder, Ceruloplasmin and other copper binding components of blood plasma and their functions: an update, Metallomics. 8 (2016) 887–905. https://doi.org/10.1039/C6MT00103C.

[164] E. V. Polishchuk, M. Concilli, S. Iacobacci, G. Chesi, N. Pastore, P. Piccolo, S. Paladino, D. Baldantoni, S.C.D. van IJzendoorn, J. Chan, C.J. Chang, A. Amoresano, F. Pane, P. Pucci, A. Tarallo, G. Parenti, N. Brunetti-Pierri, C. Settembre, A. Ballabio, R.S. Polishchuk, Wilson Disease Protein ATP7B Utilizes Lysosomal Exocytosis to Maintain Copper Homeostasis, Dev. Cell. 29 (2014) 686–700. https://doi.org/10.1016/j.devcel.2014.04.033.

[165] D.C. Twedt, I. Sternlieb, S.R. Gilbertson, Clinical, morphologic, and chemical studies on copper toxicosis of Bedlington Terriers., J. Am. Vet. Med. Assoc. 175 (1979) 269–75. http://www.ncbi.nlm.nih.gov/pubmed/500453.

[166] E.B. Hart, H. Steenbock, J. Waddell, C.A. Elvehjem, E. Van Donk, B.M. Riising, Iron in nutrition: VII. Copper as a supplement to iron for hemoglobin building in the rat, J. Biol. Chem. 77 (1928) 797–812. https://doi.org/10.1016/S0021-9258(20)74028-7.

[167] J.S. McHargue, D.J. Healy, E.S. Hill, The Relation of Copper to the Hemoglobin Content of Rat Blood: Preliminary Report, J. Biol. Chem. 78 (1928) 637–641. https://doi.org/10.1016/S0021-9258(18)83968-0.

[168] Z. Tümer, L.B. Møller, Menkes disease, Eur. J. Hum. Genet. 18 (2010) 511–518. https://doi.org/10.1038/ejhg.2009.187.

[169] A.N. Prasad, S. Levin, C.A. Rupar, C. Prasad, Menkes disease and infantile epilepsy, Brain Dev. 33 (2011) 866–876. https://doi.org/10.1016/j.braindev.2011.08.002.

[170] K. Petrukhin, S.G. Fischer, M. Pirastu, R.E. Tanzi, I. Chernov, M. Devoto, L.M. Brzustowicz, E. Cayanis, E. Vitale, J.J. Russo, D. Matseoane, B. Boukhgalter, W. Wasco, A.L. Figus, J. Loudianos, A. Cao, I. Sternlieb, O. Evgrafov, E. Parano, L. Pavone, D. Warburton, J. Ott, G.K. Penchaszadeh, I.H. Scheinberg, T.C. Gilliam, Mapping, cloning and genetic characterization of the region containing the Wilson disease gene, Nat. Genet. 5 (1993) 338–343. https://doi.org/10.1038/ng1293-338.

[171] R.E. Tanzi, K. Petrukhin, I. Chernov, J.L. Pellequer, W. Wasco, B. Ross, D.M. Romano, E. Parano, L. Pavone, L.M. Brzustowicz, M. Devoto, J. Peppercorn, A.I. Bush, I. Sternlieb, M. Pirastu, J.F. Gusella, O. Evgrafov, G.K. Penchaszadeh, B. Honig, I.S. Edelman, M.B. Soares, I.H. Scheinberg, T.C. Gilliam, The Wilson disease gene is a copper transporting ATPase with homology to the Menkes disease gene, Nat. Genet. 5 (1993) 344–350. https://doi.org/10.1038/ng1293-344.

[172] A. Ala, A.P. Walker, K. Ashkan, J.S. Dooley, M.L. Schilsky, Wilson's disease, Lancet. 369 (2007) 397–408. https://doi.org/10.1016/S0140-6736(07)60196-2.

[173] O.I. Buiakova, J. Xu, S. Lutsenko, S. Zeitlin, K. Das, S. Das, B.M. Ross, C. Mekios, I.H. Scheinberg, T.C. Gilliam, Null Mutation of the Murine ATP7B (Wilson Disease) Gene Results in Intracellular Copper Accumulation and Late-Onset Hepatic Nodular Transformation, Hum. Mol. Genet. 8 (1999) 1665–1671. https://doi.org/10.1093/hmg/8.9.1665.

[174] J.M. Walshe, Penicillamine, a new oral therapy for Wilson's disease, Am. J. Med. 21 (1956) 487–495. https://doi.org/10.1016/0002-9343(56)90066-3.

[175] J.M. Walshe, Treatment of Wilson's disease with trientine (triethylene tetramine) dihydrochloride, Lancet. 319 (1982) 643–647. https://doi.org/10.1016/S0140-6736(82)92201-2.

[176] G.J. Brewer, Zinc acetate for the treatment of Wilson's disease, Expert Opin. Pharmacother. 2 (2001) 1473–1477. https://doi.org/10.1517/14656566.2.9.1473.

[177] D.F. Emerich, S.J.M. Skinner, C. V. Borlongan, A. V. Vasconcellos, C.G. Thanos, The choroid plexus in the rise, fall and repair of the brain, BioEssays. 27 (2005) 262–274. https://doi.org/10.1002/bies.20193.

[178] N.J. Abbott, A.A.K. Patabendige, D.E.M. Dolman, S.R. Yusof, D.J. Begley, Structure and function of the blood–brain barrier, Neurobiol. Dis. 37 (2010) 13–25. https://doi.org/10.1016/j.nbd.2009.07.030.

[179] R. Daneman, A. Prat, The Blood–Brain Barrier, Cold Spring Harb. Perspect. Biol. 7 (2015) a020412. https://doi.org/10.1101/cshperspect.a020412.

[180] A. Kassner, Z. Merali, Assessment of Blood–Brain Barrier Disruption in Stroke, Stroke. 46 (2015) 3310–3315. https://doi.org/10.1161/STROKEAHA.115.008861.

[181] C.D. Arvanitis, G.B. Ferraro, R.K. Jain, The blood–brain barrier and blood–tumour barrier in brain tumours and metastases, Nat. Rev. Cancer. 20 (2020) 26–41. https://doi.org/10.1038/s41568-019-0205-x.

[182] M.D. Sweeney, A.P. Sagare, B. V. Zlokovic, Blood–brain barrier breakdown in Alzheimer disease and other neurodegenerative disorders, Nat. Rev. Neurol. 14 (2018) 133–150. https://doi.org/10.1038/nrneurol.2017.188.

[183] N.J. Abbott, L. Rönnbäck, E. Hansson, Astrocyte–endothelial interactions at the blood–brain barrier, Nat.

Rev. Neurosci. 7 (2006) 41–53. https://doi.org/10.1038/nrn1824.

[184]   U. Kniesel, H. Wolburg, Tight junctions of the blood-brain barrier., Cell. Mol. Neurobiol. 20 (2000) 57–76. https://doi.org/10.1023/a:1006995910836.

[185]   N.J. Abbott, A. Friedman, Overview and introduction: The blood-brain barrier in health and disease, Epilepsia. 53 (2012) 1–6. https://doi.org/10.1111/j.1528-1167.2012.03696.x.

[186]   B. V Zlokovic, The blood-brain barrier in health and chronic neurodegenerative disorders., Neuron. 57 (2008) 178–201. https://doi.org/10.1016/j.neuron.2008.01.003.

[187]   R. Cecchelli, V. Berezowski, S. Lundquist, M. Culot, M. Renftel, M.-P. Dehouck, L. Fenart, Modelling of the blood–brain barrier in drug discovery and development, Nat. Rev. Drug Discov. 6 (2007) 650–661. https://doi.org/10.1038/nrd2368.

[188]   C. Rinaldi, L. Donato, S. Alibrandi, C. Scimone, R. D'Angelo, A. Sidoti, Oxidative Stress and the Neurovascular Unit, Life. 11 (2021) 767. https://doi.org/10.3390/life11080767.

[189]   A. Verkhratsky, M. Nedergaard, Physiology of Astroglia, Physiol. Rev. 98 (2018) 239–389. https://doi.org/10.1152/physrev.00042.2016.

[190]   T.M. Mathiisen, K.P. Lehre, N.C. Danbolt, O.P. Ottersen, The perivascular astroglial sheath provides a complete covering of the brain microvessels: An electron microscopic 3D reconstruction, Glia. 58 (2010) 1094–1103. https://doi.org/10.1002/glia.20990.

[191]   J.I. Alvarez, T. Katayama, A. Prat, Glial influence on the blood brain barrier, Glia. 61 (2013) 1939–1958. https://doi.org/10.1002/glia.22575.

[192]   H.L. McConnell, Z. Li, R.L. Woltjer, A. Mishra, Astrocyte dysfunction and neurovascular impairment in neurological disorders: Correlation or causation?, Neurochem. Int. 128 (2019) 70–84. https://doi.org/10.1016/j.neuint.2019.04.005.

[193]   A. Armulik, G. Genové, M. Mäe, M.H. Nisancioglu, E. Wallgard, C. Niaudet, L. He, J. Norlin, P. Lindblom, K. Strittmatter, B.R. Johansson, C. Betsholtz, Pericytes regulate the blood–brain barrier, Nature. 468 (2010) 557–561. https://doi.org/10.1038/nature09522.

[194]   P. Giannoni, J. Badaut, C. Dargazanli, A.F. De Maudave, W. Klement, V. Costalat, N. Marchi, The pericyte–glia interface at the blood–brain barrier, Clin. Sci. 132 (2018) 361–374. https://doi.org/10.1042/CS20171634.

[195]   L.S. Brown, C.G. Foster, J.-M. Courtney, N.E. King, D.W. Howells, B.A. Sutherland, Pericytes and Neurovascular Function in the Healthy and Diseased Brain, Front. Cell. Neurosci. 13 (2019). https://doi.org/10.3389/fncel.2019.00282.

[196]   M.D. Sweeney, S. Ayyadurai, B. V Zlokovic, Pericytes of the neurovascular unit: key functions and signaling pathways, Nat. Neurosci. 19 (2016) 771–783. https://doi.org/10.1038/nn.4288.

[197]   G. Webersinke, H. Bauer, A. Amberger, O. Zach, H.C. Bauer, Comparison of gene expression of extracellular matrix molecules in brain microvascular endothelial cells and astrocytes, Biochem. Biophys. Res. Commun. 189 (1992) 877–884. https://doi.org/10.1016/0006-291X(92)92285-6.

[198]   L. Xu, A. Nirwane, Y. Yao, Basement membrane and blood–brain barrier, Stroke Vasc. Neurol. 4 (2019) 78–82. https://doi.org/10.1136/svn-2018-000198.

[199]   B. V. Zlokovic, Neurovascular pathways to neurodegeneration in Alzheimer's disease and other disorders, Nat. Rev. Neurosci. 12 (2011) 723–738. https://doi.org/10.1038/nrn3114.

[200]   A. Mahringer, G. Fricker, ABC transporters at the blood–brain barrier, Expert Opin. Drug Metab. Toxicol. 12 (2016) 499–508. https://doi.org/10.1517/17425255.2016.1168804.

[201]   M.M. Patel, B.M. Patel, Crossing the Blood–Brain Barrier: Recent Advances in Drug Delivery to the Brain, CNS Drugs. 31 (2017) 109–133. https://doi.org/10.1007/s40263-016-0405-9.

[202]   J.N. Cobley, M.L. Fiorello, D.M. Bailey, 13 reasons why the brain is susceptible to oxidative stress, Redox Biol. 15 (2018) 490–503. https://doi.org/10.1016/j.redox.2018.01.008.

[203]   B. Halliwell, Reactive Oxygen Species and the Central Nervous System, J. Neurochem. 59 (1992) 1609–1623. https://doi.org/10.1111/j.1471-4159.1992.tb10990.x.

[204]   L. Narciso, E. Parlanti, M. Racaniello, V. Simonelli, A. Cardinale, D. Merlo, E. Dogliotti, The Response to Oxidative DNA Damage in Neurons: Mechanisms and Disease, Neural Plast. 2016 (2016) 1–14. https://doi.org/10.1155/2016/3619274.

[205]   M. Vos, Synaptic mitochondria in synaptic transmission and organization of vesicle pools in health and disease, Front. Synaptic Neurosci. 2 (2010). https://doi.org/10.3389/fnsyn.2010.00139.

[206] R.P. Bazinet, S. Layé, Polyunsaturated fatty acids and their metabolites in brain function and disease, Nat. Rev. Neurosci. 15 (2014) 771–785. https://doi.org/10.1038/nrn3820.

[207] B.R. Stockwell, J.P. Friedmann Angeli, H. Bayir, A.I. Bush, M. Conrad, S.J. Dixon, S. Fulda, S. Gascón, S.K. Hatzios, V.E. Kagan, K. Noel, X. Jiang, A. Linkermann, M.E. Murphy, M. Overholtzer, A. Oyagi, G.C. Pagnussat, J. Park, Q. Ran, C.S. Rosenfeld, K. Salnikow, D. Tang, F.M. Torti, S. V. Torti, S. Toyokuni, K.A. Woerpel, D.D. Zhang, Ferroptosis: A Regulated Cell Death Nexus Linking Metabolism, Redox Biology, and Disease, Cell. 171 (2017) 273–285. https://doi.org/10.1016/j.cell.2017.09.021.

[208] B. Halliwell, M. Whiteman, Measuring reactive species and oxidative damage in vivo and in cell culture: how should you do it and what do the results mean?, Br. J. Pharmacol. 142 (2004) 231–255. https://doi.org/10.1038/sj.bjp.0705776.

[209] R. Musacco-Sebio, N. Ferrarotti, C. Saporito-Magriñá, J. Semprine, J. Fuda, H. Torti, A. Boveris, M.G. Repetto, Oxidative damage to rat brain in iron and copper overloads, Metallomics. 6 (2014) 1410–1416. https://doi.org/10.1039/C3MT00378G.

[210] Wang, Selective neuronal vulnerability to oxidative stress in the brain, Front. Aging Neurosci. (2010). https://doi.org/10.3389/fnagi.2010.00012.

[211] A. Nakayama, K.E. Hill, L.M. Austin, A.K. Motley, R.F. Burk, All Regions of Mouse Brain Are Dependent on Selenoprotein P for Maintenance of Selenium, J. Nutr. 137 (2007) 690–693. https://doi.org/10.1093/jn/137.3.690.

[212] N. Akahoshi, Y. Anan, Y. Hashimoto, N. Tokoro, R. Mizuno, S. Hayashi, S. Yamamoto, K. Shimada, S. Kamata, I. Ishii, Dietary selenium deficiency or selenomethionine excess drastically alters organ selenium contents without altering the expression of most selenoproteins in mice, J. Nutr. Biochem. 69 (2019) 120–129. https://doi.org/10.1016/j.jnutbio.2019.03.020.

[213] B.A. Zachara, H. Pawluk, E. Bloch-boguslawska, K.M. Śliwka, J. Korenkiewicz, Ź. Skok, K. Ryć, Tissue Level, Distribution and Total Body Selenium Content in Healthy and Diseased Humans in Poland, Arch. Environ. Heal. An Int. J. 56 (2001) 461–466. https://doi.org/10.1080/00039890109604483.

[214] O. Oster, G. Schmiedel, W. Prellwitz, The organ distribution of selenium in German adults, Biol. Trace Elem. Res. 15 (1988) 23–45. https://doi.org/10.1007/BF02990125.

[215] V.K. Wandt, N. Winkelbeiner, J. Bornhorst, B. Witt, S. Raschke, L. Simon, F. Ebert, A.P. Kipp, T. Schwerdtle, A matter of concern – Trace element dyshomeostasis and genomic stability in neurons, Redox Biol. 41 (2021) 101877. https://doi.org/10.1016/j.redox.2021.101877.

[216] U. Schweizer, N. Fradejas-Villar, Why 21? The significance of selenoproteins for human health revealed by inborn errors of metabolism, FASEB J. 30 (2016) 3669–3681. https://doi.org/10.1096/fj.201600424.

[217] S. Zhang, C. Rocourt, W.H. Cheng, Selenoproteins and the aging brain, Mech. Ageing Dev. 131 (2010) 253–260. https://doi.org/10.1016/j.mad.2010.02.006.

[218] W.. Markesbery, M.. Lovell, Four-Hydroxynonenal, a Product of Lipid Peroxidation, is Increased in the Brain in Alzheimer's Disease, Neurobiol. Aging. 19 (1998) 33–36. https://doi.org/10.1016/S0197-4580(98)00009-8.

[219] N. López, C. Tormo, I. De Blas, I. Llinares, J. Alom, Oxidative Stress in Alzheimer's Disease and Mild Cognitive Impairment with High Sensitivity and Specificity, J. Alzheimer's Dis. 33 (2013) 823–829. https://doi.org/10.3233/JAD-2012-121528.

[220] A. Yoritaka, N. Hattori, K. Uchida, M. Tanaka, E.R. Stadtman, Y. Mizuno, Immunohistochemical detection of 4-hydroxynonenal protein adducts in Parkinson disease., Proc. Natl. Acad. Sci. 93 (1996) 2696–2701. https://doi.org/10.1073/pnas.93.7.2696.

[221] S. Tsujii, M. Ishisaka, M. Shimazawa, T. Hashizume, H. Hara, Zonisamide suppresses endoplasmic reticulum stress-induced neuronal cell damage in vitro and in vivo, Eur. J. Pharmacol. 746 (2015) 301–307. https://doi.org/10.1016/j.ejphar.2014.09.023.

[222] H. Mitsumoto, R.M. Santella, X. Liu, M. Bogdanov, J. Zipprich, H.-C. Wu, J. Mahata, M. Kilty, K. Bednarz, D. Bell, P.H. Gordon, M. Hornig, M. Mehrazin, A. Naini, M. Flint Beal, P. Factor-Litvak, Oxidative stress biomarkers in sporadic ALS, Amyotroph. Lateral Scler. 9 (2008) 177–183. https://doi.org/10.1080/17482960801933942.

[223] E.P. Simpson, Y.K. Henry, J.S. Henkel, R.G. Smith, S.H. Appel, Increased lipid peroxidation in sera of ALS patients: A potential biomarker of disease burden, Neurology. 62 (2004) 1758–1765. https://doi.org/10.1212/WNL.62.10.1758.

[224] M. Karlík, P. Valkovič, V. Hančinová, L. Krížová, Ľ. Tóthová, P. Celec, Markers of oxidative stress in plasma

and saliva in patients with multiple sclerosis, Clin. Biochem. 48 (2015) 24–28. https://doi.org/10.1016/j.clinbiochem.2014.09.023.

[225] O. Aydin, H.Y. Ellidag, E. Eren, F. Kurtulus, A. Yaman, N. Yilmaz, Ischemia modified albumin is an indicator of oxidative stress in multiple sclerosis, Biochem. Medica. 24 (2014) 383–389. https://doi.org/10.11613/BM.2014.041.

[226] N.D. Solovyev, A. Berthele, B. Michalke, Selenium speciation in paired serum and cerebrospinal fluid samples, Anal. Bioanal. Chem. 405 (2013) 1875–1884. https://doi.org/10.1007/s00216-012-6294-y.

[227] N.D. Solovyev, E. Drobyshev, G. Bjørklund, Y. Dubrovskii, R. Lysiuk, M.P. Rayman, Selenium, selenoprotein P, and Alzheimer's disease: is there a link?, Free Radic. Biol. Med. 127 (2018) 124–133. https://doi.org/10.1016/j.freeradbiomed.2018.02.030.

[228] W.M. Valentine, T.W. Abel, K.E. Hill, L.M. Austin, R.F. Burk, Neurodegeneration in Mice Resulting From Loss of Functional Selenoprotein P or Its Receptor Apolipoprotein E Receptor 2, J. Neuropathol. Exp. Neurol. 67 (2008) 68–77. https://doi.org/10.1097/NEN.0b013e318160f347.

[229] U. Schweizer, M. Michaelis, J. Köhrle, L. Schomburg, Efficient selenium transfer from mother to offspring in selenoprotein-P-deficient mice enables dose-dependent rescue of phenotypes associated with selenium deficiency, Biochem. J. 378 (2004) 21–26. https://doi.org/10.1042/bj20031795.

[230] M. Scharpf, U. Schweizer, T. Arzberger, W. Roggendorf, L. Schomburg, J. Köhrle, Neuronal and ependymal expression of selenoprotein P in the human brain, J. Neural Transm. 114 (2007) 877–884. https://doi.org/10.1007/s00702-006-0617-0.

[231] X. Yang, K.E. Hill, M.J. Maguire, R.F. Burk, Synthesis and secretion of selenoprotein P by cultured rat astrocytes, Biochim. Biophys. Acta - Gen. Subj. 1474 (2000) 390–396. https://doi.org/10.1016/S0304-4165(00)00035-0.

[232] H. Steinbrenner, L. Alili, E. Bilgic, H. Sies, P. Brenneisen, Involvement of selenoprotein P in protection of human astrocytes from oxidative damage, Free Radic. Biol. Med. 40 (2006) 1513–1523. https://doi.org/10.1016/j.freeradbiomed.2005.12.022.

[233] X. Du, H. Li, Z. Wang, S. Qiu, Q. Liu, J. Ni, Selenoprotein P and selenoprotein M block Zn2+-mediated Aβ42 aggregation and toxicity, Metallomics. 5 (2013) 861. https://doi.org/10.1039/c3mt20282h.

[234] X. Du, Y. Zheng, Z. Wang, Y. Chen, R. Zhou, G. Song, J. Ni, Q. Liu, Inhibitory Act of Selenoprotein P on Cu + /Cu 2+ -Induced Tau Aggregation and Neurotoxicity, Inorg. Chem. 53 (2014) 11221–11230. https://doi.org/10.1021/ic501788v.

[235] C. Garza-Lombó, Y. Posadas, L. Quintanar, M.E. Gonsebatt, R. Franco, Neurotoxicity Linked to Dysfunctional Metal Ion Homeostasis and Xenobiotic Metal Exposure: Redox Signaling and Oxidative Stress, Antioxid. Redox Signal. 28 (2018) 1669–1703. https://doi.org/10.1089/ars.2017.7272.

[236] G.T. Sutherland, B. Chami, P. Youssef, P.K. Witting, Oxidative stress in Alzheimer's disease: Primary villain or physiological by-product?, Redox Rep. 18 (2013) 134–141. https://doi.org/10.1179/1351000213Y.0000000052.

[237] X. Du, Y. Zheng, Z. Wang, Y. Chen, R. Zhou, G. Song, J. Ni, Q. Liu, Inhibitory effect of selenoprotein P on Cu(+)/Cu(2+)-induced Aβ42 aggregation and toxicity, Inorg. Chem. 53 (2014) 1672–8. https://doi.org/10.1021/ic4028282.

[238] J.A. Miller, M.C. Oldham, D.H. Geschwind, A Systems Level Analysis of Transcriptional Changes in Alzheimer's Disease and Normal Aging, J. Neurosci. 28 (2008) 1410–1420. https://doi.org/10.1523/JNEUROSCI.4098-07.2008.

[239] F.P. Bellinger, Q.-P. He, M.T. Bellinger, Y. Lin, A. V. Raman, L.R. White, M.J. Berry, Association of Selenoprotein P with Alzheimer's Pathology in Human Cortex, J. Alzheimer's Dis. 15 (2008) 465–472. https://doi.org/10.3233/JAD-2008-15313.

[240] R.H.L.H. Rueli, A.C. Parubrub, A.S.T. Dewing, A.C. Hashimoto, M.T. Bellinger, E.J. Weeber, J.H. Uyehara-Lock, L.R. White, M.J. Berry, F.P. Bellinger, Increased Selenoprotein P in Choroid Plexus and Cerebrospinal Fluid in Alzheimer's Disease Brain, J. Alzheimer's Dis. 44 (2015) 379–383. https://doi.org/10.3233/JAD-141755.

[241] T. Lu, Y. Pan, S.-Y. Kao, C. Li, I. Kohane, J. Chan, B.A. Yankner, Gene regulation and DNA damage in the ageing human brain, Nature. 429 (2004) 883–891. https://doi.org/10.1038/nature02661.

[242] G. Wang, Y. Wu, T. Zhou, Y. Guo, B. Zheng, J. Wang, Y. Bi, F. Liu, Z. Zhou, X. Guo, J. Sha, Mapping of the N-Linked Glycoproteome of Human Spermatozoa, J. Proteome Res. 12 (2013) 5750–5759. https://doi.org/10.1021/pr400753f.

[243] I. Ingold, M. Aichler, E. Yefremova, A. Roveri, K. Buday, S. Doll, A. Tasdemir, N. Hoffard, W. Wurst, A. Walch, F. Ursini, J.P. Friedmann Angeli, M. Conrad, Expression of a Catalytically Inactive Mutant Form of Glutathione Peroxidase 4 (Gpx4) Confers a Dominant-negative Effect in Male Fertility, J. Biol. Chem. 290 (2015) 14668–14678. https://doi.org/10.1074/jbc.M115.656363.

[244] W.S. Yang, R. SriRamaratnam, M.E. Welsch, K. Shimada, R. Skouta, V.S. Viswanathan, J.H. Cheah, P.A. Clemons, A.F. Shamji, C.B. Clish, L.M. Brown, A.W. Girotti, V.W. Cornish, S.L. Schreiber, B.R. Stockwell, Regulation of Ferroptotic Cancer Cell Death by GPX4, Cell. 156 (2014) 317–331. https://doi.org/10.1016/j.cell.2013.12.010.

[245] W.S. Hambright, R.S. Fonseca, L. Chen, R. Na, Q. Ran, Ablation of ferroptosis regulator glutathione peroxidase 4 in forebrain neurons promotes cognitive impairment and neurodegeneration, Redox Biol. 12 (2017) 8–17. https://doi.org/10.1016/j.redox.2017.01.021.

[246] L. Chen, W.S. Hambright, R. Na, Q. Ran, Ablation of the Ferroptosis Inhibitor Glutathione Peroxidase 4 in Neurons Results in Rapid Motor Neuron Degeneration and Paralysis, J. Biol. Chem. 290 (2015) 28097–28106. https://doi.org/10.1074/jbc.M115.680090.

[247] J. Bai, H. Nakamura, Y.-W. Kwon, M. Tanito, S. Ueda, T. Tanaka, I. Hattori, S. Ban, T. Momoi, Y. Kitao, S. Ogawa, J. Yodoi, Does Thioredoxin-1 Prevent Mitochondria- and Endoplasmic Reticulum-Mediated Neurotoxicity of 1-Methyl-4-Phenyl-1,2,3,6-Tetrahydropyridine?, Antioxid. Redox Signal. 9 (2007) 603–608. https://doi.org/10.1089/ars.2006.1513.

[248] C. Jakupoglu, G.K.H. Przemeck, M. Schneider, S.G. Moreno, N. Mayr, A.K. Hatzopoulos, M.H. de Angelis, W. Wurst, G.W. Bornkamm, M. Brielmeier, M. Conrad, Cytoplasmic Thioredoxin Reductase Is Essential for Embryogenesis but Dispensable for Cardiac Development, Mol. Cell. Biol. 25 (2005) 1980–1988. https://doi.org/10.1128/MCB.25.5.1980-1988.2005.

[249] M. Conrad, C. Jakupoglu, S.G. Moreno, S. Lippl, A. Banjac, M. Schneider, H. Beck, A.K. Hatzopoulos, U. Just, F. Sinowatz, W. Schmahl, K.R. Chien, W. Wurst, G.W. Bornkamm, M. Brielmeier, Essential Role for Mitochondrial Thioredoxin Reductase in Hematopoiesis, Heart Development, and Heart Function, Mol. Cell. Biol. 24 (2004) 9414–9423. https://doi.org/10.1128/MCB.24.21.9414-9423.2004.

[250] J. Soerensen, C. Jakupoglu, H. Beck, H. Förster, J. Schmidt, W. Schmahl, U. Schweizer, M. Conrad, M. Brielmeier, The Role of Thioredoxin Reductases in Brain Development, PLoS One. 3 (2008) e1813. https://doi.org/10.1371/journal.pone.0001813.

[251] Y. Takagi, A. Mitsui, A. Nishiyama, K. Nozaki, H. Sono, Y. Gon, N. Hashimoto, J. Yodoi, Overexpression of thioredoxin in transgenic mice attenuates focal ischemic brain damage, Proc. Natl. Acad. Sci. 96 (1999) 4131–4136. https://doi.org/10.1073/pnas.96.7.4131.

[252] Y. Takagi, I. Hattori, K. Nozaki, A. Mitsui, M. Ishikawa, N. Hashimoto, J. Yodoi, Excitotoxic Hippocampal Injury is Attenuated in Thioredoxin Transgenic Mice, J. Cereb. Blood Flow Metab. 20 (2000) 829–833. https://doi.org/10.1097/00004647-200005000-00009.

[253] L. Boukhzar, A. Hamieh, D. Cartier, Y. Tanguy, I. Alsharif, M. Castex, A. Arabo, S. El Hajji, J.-J. Bonnet, M. Errami, A. Falluel-Morel, A. Chagraoui, I. Lihrmann, Y. Anouar, Selenoprotein T Exerts an Essential Oxidoreductase Activity That Protects Dopaminergic Neurons in Mouse Models of Parkinson's Disease, Antioxid. Redox Signal. 24 (2016) 557–574. https://doi.org/10.1089/ars.2015.6478.

[254] Z.-H. Zhang, G.-L. Song, Roles of Selenoproteins in Brain Function and the Potential Mechanism of Selenium in Alzheimer's Disease, Front. Neurosci. 15 (2021). https://doi.org/10.3389/fnins.2021.646518.

[255] U. Schweizer, M. Fabiano, Selenoproteins in brain development and function, Free Radic. Biol. Med. 190 (2022) 105–115. https://doi.org/10.1016/j.freeradbiomed.2022.07.022.

[256] S. Lutsenko, C. Washington-Hughes, M. Ralle, K. Schmidt, Copper and the brain noradrenergic system, J. Biol. Inorg. Chem. 24 (2019) 1179–1188. https://doi.org/10.1007/s00775-019-01737-3.

[257] V. Nischwitz, A. Berthele, B. Michalke, Speciation analysis of selected metals and determination of their total contents in paired serum and cerebrospinal fluid samples: An approach to investigate the permeability of the human blood-cerebrospinal fluid-barrier, Anal. Chim. Acta. 627 (2008) 258–269. https://doi.org/10.1016/j.aca.2008.08.018.

[258] B.-S. Choi, W. Zheng, Copper transport to the brain by the blood-brain barrier and blood-CSF barrier, Brain Res. 1248 (2009) 14–21. https://doi.org/10.1016/j.brainres.2008.10.056.

[259] S.G. Kaler, ATP7A-related copper transport diseases—emerging concepts and future trends, Nat. Rev. Neurol. 7 (2011) 15–29. https://doi.org/10.1038/nrneurol.2010.180.

[260] X. Fu, Y. Zhang, W. Jiang, A.D. Monnot, C.A. Bates, W. Zheng, Regulation of Copper Transport Crossing

Brain Barrier Systems by Cu-ATPases: Effect of Manganese Exposure, Toxicol. Sci. 139 (2014) 432–451. https://doi.org/10.1093/toxsci/kfu048.

[261]   J. Dobrowolska, M. Dehnhardt, A. Matusch, M. Zoriy, N. Palomero-Gallagher, P. Koscielniak, K. Zilles, J.S. Becker, Quantitative imaging of zinc, copper and lead in three distinct regions of the human brain by laser ablation inductively coupled plasma mass spectrometry, Talanta. 74 (2008) 717–723. https://doi.org/10.1016/j.talanta.2007.06.051.

[262]   I.F. Scheiber, J.F.B. Mercer, R. Dringen, Metabolism and functions of copper in brain, Prog. Neurobiol. 116 (2014) 33–57. https://doi.org/10.1016/j.pneurobio.2014.01.002.

[263]   I.F. Scheiber, R. Dringen, Astrocyte functions in the copper homeostasis of the brain, Neurochem. Int. 62 (2013) 556–565. https://doi.org/10.1016/j.neuint.2012.08.017.

[264]   C. Grochowski, E. Blicharska, P. Krukow, K. Jonak, M. Maciejewski, D. Szczepanek, K. Jonak, J. Flieger, R. Maciejewski, Analysis of Trace Elements in Human Brain: Its Aim, Methods, and Concentration Levels, Front. Chem. 7 (2019). https://doi.org/10.3389/fchem.2019.00115.

[265]   G. Gromadzka, B. Tarnacka, A. Flaga, A. Adamczyk, Copper Dyshomeostasis in Neurodegenerative Diseases—Therapeutic Implications, Int. J. Mol. Sci. 21 (2020) 9259. https://doi.org/10.3390/ijms21239259.

[266]   S. Genoud, B.R. Roberts, A.P. Gunn, G.M. Halliday, S.J.G. Lewis, H.J. Ball, D.J. Hare, K.L. Double, Subcellular compartmentalisation of copper, iron, manganese, and zinc in the Parkinson's disease brain, Metallomics. 9 (2017) 1447–1455. https://doi.org/10.1039/c7mt00244k.

[267]   M. Schrag, C. Mueller, U. Oyoyo, M.A. Smith, W.M. Kirsch, Iron, zinc and copper in the Alzheimer's disease brain: A quantitative meta-analysis. Some insight on the influence of citation bias on scientific opinion, Prog. Neurobiol. 94 (2011) 296–306. https://doi.org/10.1016/j.pneurobio.2011.05.001.

[268]   W. Zheng, A.D. Monnot, Regulation of brain iron and copper homeostasis by brain barrier systems: Implication in neurodegenerative diseases, Pharmacol. Ther. 133 (2012) 177–188. https://doi.org/10.1016/j.pharmthera.2011.10.006.

[269]   Y. Yamashita, M. Yamashita, Identification of a novel selenium-containing compound, selenoneine, as the predominant chemical form of organic selenium in the blood of bluefin tuna, J. Biol. Chem. 285 (2010) 18134–18138. https://doi.org/10.1074/jbc.C110.106377.

[270]   N.G. Turrini, N. Kroepfl, K.B. Jensen, T.C. Reiter, K.A. Francesconi, T. Schwerdtle, W. Kroutil, D. Kuehnelt, Biosynthesis and isolation of selenoneine from genetically modified fission yeast, Metallomics. 10 (2018) 1532–1538. https://doi.org/10.1039/C8MT00200B.

[271]   Y. Yamashita, Discovery of the strong antioxidant selenoneine in tuna and selenium redox metabolism, World J. Biol. Chem. 1 (2010) 144. https://doi.org/10.4331/wjbc.v1.i5.144.

[272]   I. Rohn, N. Kroepfl, J. Bornhorst, D. Kuehnelt, T. Schwerdtle, Side-Directed Transfer and Presystemic Metabolism of Selenoneine in a Human Intestinal Barrier Model, Mol. Nutr. Food Res. 63 (2019) 1–11. https://doi.org/10.1002/mnfr.201900080.

[273]   J.N. Cumings, The copper and iron content of brain and liver in the normal and in hepato-lenticular degeneration, Brain. 71 (1948) 410–415. https://doi.org/10.1093/brain/71.4.410.

[274]   G. Faa, M. Lisci, M.P. Caria, R. Ambu, R. Sciot, V.M. Nurchi, R. Silvagni, A. Diaz, G. Crisponi, Brain copper, iron, magnesium, zinc, calcium, sulfur and phosphorus storage in Wilson's disease, J. Trace Elem. Med. Biol. 15 (2001) 155–160. https://doi.org/10.1016/S0946-672X(01)80060-2.

[275]   T. Litwin, G. Gromadzka, G.M. Szpak, K. Jabłonka-Salach, E. Bulska, A. Członkowska, Brain metal accumulation in Wilson's disease, J. Neurol. Sci. 329 (2013) 55–58. https://doi.org/10.1016/j.jns.2013.03.021.

[276]   M.T. Lorincz, Neurologic Wilson's disease, Ann. N. Y. Acad. Sci. 1184 (2010) 173–187. https://doi.org/10.1111/j.1749-6632.2009.05109.x.

[277]   A. Członkowska, T. Litwin, M. Karliński, K. Dziezyc, G. Chabik, M. Czerska, D-penicillamine versus zinc sulfate as first-line therapy for Wilson's disease, Eur. J. Neurol. 21 (2014) 599–606. https://doi.org/10.1111/ene.12348.

[278]   J. Kalita, V. Kumar, A. Ranjan, U.K. Misra, Role of Oxidative Stress in the Worsening of Neurologic Wilson Disease Following Chelating Therapy, NeuroMolecular Med. 17 (2015) 364–372. https://doi.org/10.1007/s12017-015-8364-8.

[279]   J. Kalita, V. Kumar, S. Chandra, B. Kumar, U.K. Misra, Worsening of Wilson Disease following Penicillamine

Therapy, Eur. Neurol. 71 (2014) 126–131. https://doi.org/10.1159/000355276.

[280] U. Merle, M. Schaefer, P. Ferenci, W. Stremmel, Clinical presentation, diagnosis and long-term outcome of Wilson's disease: a cohort study, Gut. 56 (2007) 115–120. https://doi.org/10.1136/gut.2005.087262.

[281] G.J. Brewer, C.A. Terry, A.M. Aisen, G.M. Hill, Worsening of Neurologic Syndrome in Patients With Wilson's Disease With Initial Penicillamine Therapy, Arch. Neurol. 44 (1987) 490–493. https://doi.org/10.1001/archneur.1987.00520170020016.

[282] K.H. Weiss, F.K. Askari, A. Czlonkowska, P. Ferenci, J.M. Bronstein, D. Bega, A. Ala, D. Nicholl, S. Flint, L. Olsson, T. Plitz, C. Bjartmar, M.L. Schilsky, Bis-choline tetrathiomolybdate in patients with Wilson's disease: an open-label, multicentre, phase 2 study, Lancet Gastroenterol. Hepatol. 2 (2017) 869–876. https://doi.org/10.1016/S2468-1253(17)30293-5.

[283] G.J. Brewer, F. Askari, M.T. Lorincz, M. Carlson, M. Schilsky, K.J. Kluin, P. Hedera, P. Moretti, J.K. Fink, R. Tankanow, R.B. Dick, J. Sitterly, Treatment of Wilson Disease With Ammonium Tetrathiomolybdate, Arch. Neurol. 63 (2006) 521. https://doi.org/10.1001/archneur.63.4.521.

[284] G.J. Brewer, P. Hedera, K.J. Kluin, M. Carlson, F. Askari, R.B. Dick, J. Sitterly, J.K. Fink, Treatment of Wilson Disease With Ammonium Tetrathiomolybdate, Arch. Neurol. 60 (2003) 379. https://doi.org/10.1001/archneur.60.3.379.

[285] J. Aaseth, A. V. Skalny, P.M. Roos, J. Alexander, M. Aschner, A.A. Tinkov, Copper, Iron, Selenium and Lipo-Glycemic Dysmetabolism in Alzheimer's Disease, Int. J. Mol. Sci. 22 (2021) 9461. https://doi.org/10.3390/ijms22179461.

[286] S.R. Varikasuvu, S. Prasad V, J. Kothapalli, M. Manne, Brain Selenium in Alzheimer's Disease (BRAIN SEAD Study): a Systematic Review and Meta-Analysis, Biol. Trace Elem. Res. 189 (2019) 361–369. https://doi.org/10.1007/s12011-018-1492-x.

[287] O.R. Tamtaji, R. Heidari-soureshjani, N. Mirhosseini, E. Kouchaki, F. Bahmani, E. Aghadavod, M. Tajabadi-Ebrahimi, Z. Asemi, Probiotic and selenium co-supplementation, and the effects on clinical, metabolic and genetic status in Alzheimer's disease: A randomized, double-blind, controlled trial, Clin. Nutr. 38 (2019) 2569–2575. https://doi.org/10.1016/j.clnu.2018.11.034.

[288] D.S.A. Simpson, P.L. Oliver, ROS Generation in Microglia: Understanding Oxidative Stress and Inflammation in Neurodegenerative Disease, Antioxidants. 9 (2020) 743. https://doi.org/10.3390/antiox9080743.

[289] N.R. Saunders, C.J. Ek, M.D. Habgood, K.M. Dziegielewska, Barriers in the brain: a renaissance?, Trends Neurosci. 31 (2008) 279–286. https://doi.org/10.1016/j.tins.2008.03.003.

[290] S.M. Müller, F. Ebert, G. Raber, S. Meyer, J. Bornhorst, S. Hüwel, H.-J. Galla, K.A. Francesconi, T. Schwerdtle, Effects of arsenolipids on in vitro blood-brain barrier model, Arch. Toxicol. 92 (2018) 823–832. https://doi.org/10.1007/s00204-017-2085-8.

[291] J. Bornhorst, C.A. Wehe, S. Hüwel, U. Karst, H.-J. Galla, T. Schwerdtle, Impact of Manganese on and Transfer across Blood-Brain and Blood-Cerebrospinal Fluid Barrier in Vitro, J. Biol. Chem. 287 (2012) 17140–17151. https://doi.org/10.1074/jbc.M112.344093.

[292] H. Lohren, J. Bornhorst, R. Fitkau, G. Pohl, H.-J. Galla, T. Schwerdtle, Effects on and transfer across the blood-brain barrier in vitro—Comparison of organic and inorganic mercury species, BMC Pharmacol. Toxicol. 17 (2016) 63. https://doi.org/10.1186/s40360-016-0106-5.

[293] I.K. Cheah, B. Halliwell, Ergothioneine; antioxidant potential, physiological function and role in disease, Biochim. Biophys. Acta - Mol. Basis Dis. 1822 (2012) 784–793. https://doi.org/10.1016/j.bbadis.2011.09.017.

[294] Y. Yamashita, M. Yamashita, H. Iida, Selenium Content in Seafood in Japan, Nutrients. 5 (2013) 388–395. https://doi.org/10.3390/nu5020388.

[295] A. Achouba, P. Dumas, N. Ouellet, M. Little, M. Lemire, P. Ayotte, Selenoneine is a major selenium species in beluga skin and red blood cells of Inuit from Nunavik, Chemosphere. 229 (2019) 549–558. https://doi.org/10.1016/j.chemosphere.2019.04.191.

[296] T.A. Marschall, J. Bornhorst, D. Kuehnelt, T. Schwerdtle, Differing cytotoxicity and bioavailability of selenite, methylselenocysteine, selenomethionine, selenosugar 1 and trimethylselenonium ion and their underlying metabolic transformations in human cells, Mol. Nutr. Food Res. 60 (2016) 2622–2632. https://doi.org/10.1002/mnfr.201600422.

[297] K. Lunøe, C. Gabel-Jensen, S. Stürup, L. Andresen, S. Skov, B. Gammelgaard, Investigation of the selenium metabolism in cancer cell lines, Metallomics. 3 (2011) 162–168. https://doi.org/10.1039/c0mt00091d.

[298]   M. Yamashita, Y. Yamashita, T. Suzuki, Y. Kani, N. Mizusawa, S. Imamura, K. Takemoto, T. Hara, M.A. Hossain, T. Yabu, K. Touhata, Selenoneine, a Novel Selenium-Containing Compound, Mediates Detoxification Mechanisms against Methylmercury Accumulation and Toxicity in Zebrafish Embryo, Mar. Biotechnol. 15 (2013) 559–570. https://doi.org/10.1007/s10126-013-9508-1.

[299]   L. Pochini, M. Galluccio, M. Scalise, L. Console, C. Indiveri, OCTN: A Small Transporter Subfamily with Great Relevance to Human Pathophysiology, Drug Discovery, and Diagnostics, SLAS Discov. 24 (2019) 89–110. https://doi.org/10.1177/2472555218812821.

[300]   T. Mayumi, H. Kawanc, Y. Sakamoto, E. Suehisa, Y. Kawai, T. Hama, Studies on Ergothioneine. V.1) Determination by High Performance Liquid Chromatography and Application to Metabolic Research, Chem. Pharm. Bull. 26 (1978) 3772–3778. https://doi.org/10.1248/cpb.26.3772.

[301]   Z. Pedrero Zayas, L. Ouerdane, S. Mounicou, R. Lobinski, M. Monperrus, D. Amouroux, Hemoglobin as a major binding protein for methylmercury in white-sided dolphin liver, Anal. Bioanal. Chem. 406 (2014) 1121–1129. https://doi.org/10.1007/s00216-013-7274-6.

[302]   J. Masuda, C. Umemura, M. Yokozawa, K. Yamauchi, T. Seko, M. Yamashita, Y. Yamashita, Dietary Supplementation of Selenoneine-Containing Tuna Dark Muscle Extract Effectively Reduces Pathology of Experimental Colorectal Cancers in Mice, Nutrients. 10 (2018) 1380. https://doi.org/10.3390/nu10101380.

[303]   S. Borchard, S. Raschke, K.M. Zak, C. Eberhagen, C. Einer, E. Weber, S.M. Müller, B. Michalke, J. Lichtmannegger, A. Wieser, T. Rieder, G.M. Popowicz, J. Adamski, M. Klingenspor, A.H. Coles, R. Viana, M.H. Vendelbo, T.D. Sandahl, T. Schwerdtle, T. Plitz, H. Zischka, Bis-choline tetrathiomolybdate prevents copper-induced blood–brain barrier damage, Life Sci. Alliance. 5 (2022) e202101164. https://doi.org/10.26508/lsa.202101164.

[304]   J. Baudry, J.F. Kopp, H. Boeing, A.P. Kipp, T. Schwerdtle, M.B. Schulze, Changes of trace element status during aging: results of the EPIC-Potsdam cohort study, Eur. J. Nutr. 59 (2020) 3045–3058. https://doi.org/10.1007/s00394-019-02143-w.

[305]   C.D. Quarles, M. Macke, B. Michalke, H. Zischka, U. Karst, P. Sullivan, M.P. Field, LC-ICP-MS method for the determination of "extractable copper" in serum, Metallomics. 12 (2020) 1348–1355. https://doi.org/10.1039/d0mt00132e.

[306]   E. Drobyshev, S. Raschke, R.A. Glabonjat, J. Bornhorst, F. Ebert, D. Kuehnelt, T. Schwerdtle, Capabilities of selenoneine to cross the in vitro blood–brain barrier model, Metallomics. 13 (2021). https://doi.org/10.1093/mtomcs/mfaa007.

[307]   P. Heitland, H.D. Köster, Biomonitoring of selenoprotein P in human serum by fast affinity chromatography coupled to ICP-MS, Int. J. Hyg. Environ. Health. 221 (2018) 564–568. https://doi.org/10.1016/j.ijheh.2018.02.006.

[308]   B. Yang, Y. Li, Y. Ma, X. Zhang, L. Yang, X. Shen, J. Zhang, L. Jing, Selenium attenuates ischemia/reperfusion injury-induced damage to the blood-brain barrier in hyperglycemia through PI3K/AKT/mTOR pathway-mediated autophagy inhibition, Int. J. Mol. Med. 48 (2021) 178. https://doi.org/10.3892/ijmm.2021.5011.

[309]   J.J. Liu, Y. Kim, F. Yan, Q. Ding, V. Ip, N.N. Jong, J.F.B. Mercer, M.J. McKeage, Contributions of rat Ctr1 to the uptake and toxicity of copper and platinum anticancer drugs in dorsal root ganglion neurons, Biochem. Pharmacol. 85 (2013) 207–215. https://doi.org/10.1016/j.bcp.2012.10.023.

[310]   S.H. Chen, J.K. Lin, S.H. Liu, Y.C. Liang, S.Y. Lin-Shiau, Apoptosis of Cultured Astrocytes Induced by the Copper and Neocuproine Complex through Oxidative Stress and JNK Activation, Toxicol. Sci. 102 (2008) 138–149. https://doi.org/10.1093/toxsci/kfm292.

[311]   I.F. Scheiber, R. Dringen, Copper Accelerates Glycolytic Flux in Cultured Astrocytes, Neurochem. Res. 36 (2011) 894–903. https://doi.org/10.1007/s11064-011-0419-0.

[312]   S. Borchard, F. Bork, T. Rieder, C. Eberhagen, B. Popper, J. Lichtmannegger, S. Schmitt, J. Adamski, M. Klingenspor, K.-H. Weiss, H. Zischka, The exceptional sensitivity of brain mitochondria to copper, Toxicol. Vitr. 51 (2018) 11–22. https://doi.org/10.1016/j.tiv.2018.04.012.

[313]   P.V.B. Reddy, K. V Rama Rao, M.D. Norenberg, The mitochondrial permeability transition, and oxidative and nitrosative stress in the mechanism of copper toxicity in cultured neurons and astrocytes, Lab. Investig. 88 (2008) 816–830. https://doi.org/10.1038/labinvest.2008.49.

[314]   D. Puleston, Detection of Mitochondrial Mass, Damage, and Reactive Oxygen Species by Flow Cytometry, Cold Spring Harb. Protoc. 2015 (2015) pdb.prot086298. https://doi.org/10.1101/pdb.prot086298.

[315] G. Ferretti, T. Bacchetti, C. Moroni, A. Vignini, G. Curatola, Copper-induced oxidative damage on astrocytes: protective effect exerted by human high density lipoproteins, Biochim. Biophys. Acta - Mol. Cell Biol. Lipids. 1635 (2003) 48–54. https://doi.org/10.1016/j.bbalip.2003.10.005.

[316] Y. Qian, Y. Zheng, L. Abraham, K.S. Ramos, E. Tiffany-Castiglioni, Differential profiles of copper-induced ROS generation in human neuroblastoma and astrocytoma cells, Mol. Brain Res. 134 (2005) 323–332. https://doi.org/10.1016/j.molbrainres.2004.11.004.

[317] I.F. Scheiber, R. Dringen, Copper-treatment increases the cellular GSH content and accelerates GSH export from cultured rat astrocytes, Neurosci. Lett. 498 (2011) 42–46. https://doi.org/10.1016/j.neulet.2011.04.058.

[318] M. Schwarz, K. Lossow, K. Schirl, J. Hackler, K. Renko, J.F. Kopp, T. Schwerdtle, L. Schomburg, A.P. Kipp, Copper interferes with selenoprotein synthesis and activity, Redox Biol. 37 (2020) 101746. https://doi.org/10.1016/j.redox.2020.101746.

[319] J. Everett, J.F. Collingwood, V. Tjendana-Tjhin, J. Brooks, F. Lermyte, G. Plascencia-Villa, I. Hands-Portman, J. Dobson, G. Perry, N.D. Telling, Nanoscale synchrotron X-ray speciation of iron and calcium compounds in amyloid plaque cores from Alzheimer's disease subjects, Nanoscale. 10 (2018) 11782–11796. https://doi.org/10.1039/C7NR06794A.

[320] W.T. Buckley, S.N. Huckin, L.J. Fisher, G.K. Eigendorf, Effect of Selenium Supplementation on Copper-Metabolism in Dairy-Cows, Can. J. Anim. Sci. 66 (1986) 1009–1018. https://doi.org/10.4141/cjas86-111.

[321] M.S. Fehrs, W.J. Miller, R.P. Gentry, M.W. Neathery, D.M. Blackmon, S.R. Heinmiller, Effect of High but Nontoxic Dietary Intake of Copper and Selenium on Metabolism in Calves, J. Dairy Sci. 64 (1981) 1700–1706. https://doi.org/10.3168/jds.S0022-0302(81)82749-X.

[322] J.B.J. van Ryssen, P.S.M. van Malsen, F. Hartmann, Contribution of dietary sulphur to the interaction between selenium and copper in sheep, J. Agric. Sci. 130 (1998) 107–114. https://doi.org/10.1017/S0021859697005030.

[323] G.G. Thomson, B.M. Lawson, Copper and selenium interaction in sheep, N. Z. Vet. J. 18 (1970) 79–82. https://doi.org/10.1080/00480169.1970.33866.

[324] X. Sun, J. Li, H. Zhao, Y. Wang, J. Liu, Y. Shao, Y. Xue, M. Xing, Synergistic effect of copper and arsenic upon oxidative stress, inflammation and autophagy alterations in brain tissues of Gallus gallus, J. Inorg. Biochem. 178 (2018) 54–62. https://doi.org/10.1016/j.jinorgbio.2017.10.006.

[325] J. Arowoogun, O.O. Akanni, A.O. Adefisan, S.E. Owumi, A.S. Tijani, O.A. Adaramoye, Rutin ameliorates copper sulfate-induced brain damage via antioxidative and anti-inflammatory activities in rats, J. Biochem. Mol. Toxicol. 35 (2021). https://doi.org/10.1002/jbt.22623.

[326] J. Semprine, N. Ferrarotti, R. Musacco-Sebio, C. Saporito-Magriñá, J. Fuda, H. Torti, M. Castro-Parodi, A. Damiano, A. Boveris, M.G. Repetto, Brain antioxidant responses to acute iron and copper intoxications in rats, Metallomics. 6 (2014) 2083–2089. https://doi.org/10.1039/C4MT00159A.

[327] X. Li, Y. Zhang, Y. Yuan, Y. Sun, Y. Qin, Z. Deng, H. Li, Protective Effects of Selenium, Vitamin E, and Purple Carrot Anthocyanins on d-Galactose-Induced Oxidative Damage in Blood, Liver, Heart and Kidney Rats, Biol. Trace Elem. Res. 173 (2016) 433–442. https://doi.org/10.1007/s12011-016-0681-8.

[328] Z. Yao, Y. Zhang, H. Li, Z. Deng, X. Zhang, Synergistic effect of Se-methylselenocysteine and vitamin E in ameliorating the acute ethanol-induced oxidative damage in rat, J. Trace Elem. Med. Biol. 29 (2015) 182–187. https://doi.org/10.1016/j.jtemb.2014.08.004.

[329] X.-M. Xu, A.A. Turanov, B.A. Carlson, M.-H. Yoo, R.A. Everley, R. Nandakumar, I. Sorokina, S.P. Gygi, V.N. Gladyshev, D.L. Hatfield, Targeted insertion of cysteine by decoding UGA codons with mammalian selenocysteine machinery, Proc. Natl. Acad. Sci. 107 (2010) 21430–21434. https://doi.org/10.1073/pnas.1009947107.

[330] J. Lu, L. Zhong, M.E. Lönn, R.F. Burk, K.E. Hill, A. Holmgren, Penultimate selenocysteine residue replaced by cysteine in thioredoxin reductase from selenium-deficient rat liver, FASEB J. 23 (2009) 2394–2402. https://doi.org/10.1096/fj.08-127662.

[331] A.A. Turanov, R.A. Everley, S. Hybsier, K. Renko, L. Schomburg, S.P. Gygi, D.L. Hatfield, V.N. Gladyshev, Regulation of selenocysteine content of human selenoprotein p by dietary selenium and insertion of cysteine in place of selenocysteine, PLoS One. 10 (2015). https://doi.org/10.1371/journal.pone.0140353.

[332] R. Tobe, S. Naranjo-Suarez, R.A. Everley, B.A. Carlson, A.A. Turanov, P.A. Tsuji, M.-H. Yoo, S.P. Gygi, V.N. Gladyshev, D.L. Hatfield, High Error Rates in Selenocysteine Insertion in Mammalian Cells Treated with the Antibiotic Doxycycline, Chloramphenicol, or Geneticin, J. Biol. Chem. 288 (2013) 14709–14715.

https://doi.org/10.1074/jbc.M112.446666.

[333] D.E. Handy, G. Hang, J. Scolaro, N. Metes, N. Razaq, Y. Yang, J. Loscalzo, Aminoglycosides Decrease Glutathione Peroxidase-1 Activity by Interfering with Selenocysteine Incorporation, J. Biol. Chem. 281 (2006) 3382–3388. https://doi.org/10.1074/jbc.M511295200.

[334] J.H. Ellwanger, P. Molz, D.R. Dallemole, A. Pereira dos Santos, T.E. Müller, L. Cappelletti, M. Gonçalves da Silva, S.I. Rech Franke, D. Prá, J.A. Pêgas Henriques, Selenium reduces bradykinesia and DNA damage in a rat model of Parkinson's disease, Nutrition. 31 (2015) 359–365. https://doi.org/10.1016/j.nut.2014.07.004.

[335] B.V.S. Lakshmi, M. Sudhakar, K.S. Prakash, Protective Effect of Selenium Against Aluminum Chloride-Induced Alzheimer's Disease: Behavioral and Biochemical Alterations in Rats, Biol. Trace Elem. Res. 165 (2015) 67–74. https://doi.org/10.1007/s12011-015-0229-3.

[336] M.M. Rahman, K.F.B. Hossain, S. Banik, M.T. Sikder, M. Akter, S.E.C. Bondad, M.S. Rahaman, T. Hosokawa, T. Saito, M. Kurasaki, Selenium and zinc protections against metal-(loids)-induced toxicity and disease manifestations: A review, Ecotoxicol. Environ. Saf. 168 (2019) 146–163. https://doi.org/10.1016/j.ecoenv.2018.10.054.

[337] M. Kiełczykowska, J. Kocot, M. Paździor, I. Musik, Selenium – a fascinating antioxidant of protective properties, Adv. Clin. Exp. Med. 27 (2018) 245–255. https://doi.org/10.17219/acem/67222.

[338] Y. Nakano, M. Shimoda, S. Okudomi, S. Kawaraya, M. Kawahara, K.I. Tanaka, Seleno-l-methionine suppresses copper-enhanced zinc-induced neuronal cell death: Via induction of glutathione peroxidase, Metallomics. 12 (2020) 1693–1701. https://doi.org/10.1039/d0mt00136h.

[339] J. Gao, X. Tian, X. Yan, Y. Wang, J. Wei, X. Wang, X. Yan, G. Song, Selenium Exerts Protective Effects Against Fluoride-Induced Apoptosis and Oxidative Stress and Altered the Expression of Bcl-2/Caspase Family, Biol. Trace Elem. Res. 199 (2021) 682–692. https://doi.org/10.1007/s12011-020-02185-w.

[340] M. Banni, I. Messaoudi, L. Said, J. El Heni, A. Kerkeni, K. Said, Metallothionein Gene Expression in Liver of Rats Exposed to Cadmium and Supplemented with Zinc and Selenium, Arch. Environ. Contam. Toxicol. 59 (2010) 513–519. https://doi.org/10.1007/s00244-010-9494-5.

[341] F. Dondero, L. Piacentini, M. Banni, M. Rebelo, B. Burlando, A. Viarengo, Quantitative PCR analysis of two molluscan metallothionein genes unveils differential expression and regulation, Gene. 345 (2005) 259–270. https://doi.org/10.1016/j.gene.2004.11.031.

[342] J. Yu, H. Yao, X. Gao, Z. Zhang, J.-F. Wang, S.-W. Xu, The Role of Nitric Oxide and Oxidative Stress in Intestinal Damage Induced by Selenium Deficiency in Chickens, Biol. Trace Elem. Res. 163 (2015) 144–153. https://doi.org/10.1007/s12011-014-0164-8.

[343] E. Song, C. Su, J. Fu, X. Xia, S. Yang, C. Xiao, B. Lu, H. Chen, Z. Sun, S. Wu, Y. Song, Selenium supplementation shows protective effects against patulin-induced brain damage in mice via increases in GSH-related enzyme activity and expression, Life Sci. 109 (2014) 37–43. https://doi.org/10.1016/j.lfs.2014.05.022.

[344] B. Laffon, V. Valdiglesias, E. Pásaro, J. Méndez, The Organic Selenium Compound Selenomethionine Modulates Bleomycin-Induced DNA Damage and Repair in Human Leukocytes, Biol. Trace Elem. Res. 133 (2010) 12–19. https://doi.org/10.1007/s12011-009-8407-9.

[345] H. Franke, H.-J. Galla, C.T. Beuckmann, An improved low-permeability in vitro-model of the blood–brain barrier: transport studies on retinoids, sucrose, haloperidol, caffeine and mannitol, Brain Res. 818 (1999) 65–71. https://doi.org/10.1016/S0006-8993(98)01282-7.

[346] H. Franke, H.-J. Galla, C.T. Beuckmann, Primary cultures of brain microvessel endothelial cells: a valid and flexible model to study drug transport through the blood–brain barrier in vitro, Brain Res. Protoc. 5 (2000) 248–256. https://doi.org/10.1016/S1385-299X(00)00020-9.

[347] M.A. Darken, Puromycin inhibition of protein synthesis, Pharmacol Rev. 16 (1964) 223–243.

[348] K. Benson, S. Cramer, H.-J. Galla, Impedance-based cell monitoring: barrier properties and beyond, Fluids Barriers CNS. 10 (2013) 5. https://doi.org/10.1186/2045-8118-10-5.

[349] J. Lotharius, S. Barg, P. Wiekop, C. Lundberg, H.K. Raymon, P. Brundin, Effect of Mutant α-Synuclein on Dopamine Homeostasis in a New Human Mesencephalic Cell Line, J. Biol. Chem. 277 (2002) 38884–38894. https://doi.org/10.1074/jbc.M205518200.

[350] J. Lotharius, Progressive Degeneration of Human Mesencephalic Neuron-Derived Cells Triggered by Dopamine-Dependent Oxidative Stress Is Dependent on the Mixed-Lineage Kinase Pathway, J. Neurosci. 25 (2005) 6329–6342. https://doi.org/10.1523/JNEUROSCI.1746-05.2005.

LIST OF PUBLICATIONS

JOURNAL ARTICLES

- **S. Raschke**, J. Bornhorst, T. Schwerdtle

  Se supplementation to an in vitro blood-brain barrier does not affect Cu transfer into the brain

  Submitted to Journal of Trace Elements in medicine and biology, 13th January 2023 (under review)

- **S. Raschke**, F. Ebert, A. P. Kipp, J. F. Kopp, T. Schwerdtle

  Selenium homeostasis in human brain cells: Effects of copper (II) and Se species

  Resubmitted to Journal of Trace Elements in medicine and biology, 19th January 2023 (under review)

- E. Drobyshev*, **S. Raschke***, R. A. Glabonjat, J. Bornhorst, F. Ebert, D. Kuehnelt & T. Schwerdtle

  (*shared first authorship)

  Capabilities of selenoneine to cross the *in vitro* blood–brain barrier model

  Metallomics, 2021, DOI: 10.1093/mtomcs/mfaa007 (*geteilte Erstautorenschaft)

- Borchard, **S., Raschke**, S., Zak, K. M., Eberhagen, C., Einer, C., Weber, E., ... & Zischka H.

  Bis-choline tetrathiomolybdate prevents copper-induced blood–brain barrier damage

  Life Science Alliance, 2022, DOI: 10.26508/lsa.202101164

- V. K. Wandt, N. Winkelbeiner, J. Bornhorst, B. Witt, **S. Raschke**, L. Simon, F. Ebert, A. P. Kipp, T. Schwerdtle

  A matter of concern – Trace element dyshomeostasis and genomic stability in neurons

  Redox Biology, 2021, DOI: 10.1016/j.redox.2021.101877

- B. Witt, M. Stiboller, **S. Raschke**, S. Friese, F. Ebert, T. Schwerdtle

  Characterizing effects of excess copper levels in a human astrocytic cell line with focus on oxidative stress markers

  Journal of Trace Elements in Medicine and Biology, 2021, DOI: 10.1016/j.jtemb.2021.126711

- Rohn, **S. Raschke**, M. Aschner, S. Tuck, D. Kuehnelt, A. Kipp, T. Schwerdtle & J. Bornhorst

  Treatment of *Caenorhabditis elegans* with small selenium species enhanced antioxidant defense systems

  Molecular Nutrition & Food Research, 2019, DOI: 10.1002/mnfr.201801304

ORAL CONTRIBUTIONS

Meeting of the Society of Food Chemistry North-East, March 15th, 2021

>   **S. Raschke**, F. Ebert, B. Witt, T. Schwerdtle
>
>   *In vitro* Charakterisierung möglicher Selen-vermittelter Protektion gegenüber Kupfer-bedingten toxischen Effekten in humanen suboptimal Se-versorgten Astrozyten

German society for environmental mutation research (GUM), online workshops, March 18th, 2021

>   **S. Raschke**, F. Ebert, B. Witt, T. Schwerdtle
>
>   Cu/Se combination study in Se-suboptimal supplied astrocytes

International Conference of Trace Elements and Minerals (ICTEM), August 2nd, 2021

>   **S. Raschke**, B. Witt, V. K. Wandt, F. Ebert, A. P. Kipp, T. Schwerdtle
>
>   Characterization of Cu/Se combination in human Se-depleted astrocytes

POSTER

European Environmental Mutagenesis and Genomics Society New Investigator (EEMGS NI), June 24th & 25th, 2021

>   **S. Raschke**, B. Witt, V. K. Wandt, F. Ebert, A. P. Kipp, T. Schwerdtle
>
>   Cu/Se combination study in human astrocytes cultured under Se-deficient conditions

SCHOLARSHIPS

02/19 – 07/19   Scholarship for the funding of young scientists of the Faculty of Mathematics and Natural Sciences of the University of Potsdam

08/19 – 07/22   PhD grant of the University of Potsdam/Potsdam Graduate School (PoGS)

CURRICULUM VITAE

Diese Seite enthält persönliche Daten und wurde aus der Arbeit entfernt.

Diese Seite enthält persönliche Daten und wurde aus der Arbeit entfernt.

DANKSAGUNG

An erster Stelle möchte ich Prof. Dr. Tanja Schwerdtle für die Möglichkeit danken, dass ich meine Doktoarbeit in ihrer Arbeitsgruppe anfertigen durfte. Zudem bin ich dankbar für die Chance nach meiner Elternzeit an die Universität zurück kehren zu können. Vielen Dank für die großartige Betreuung und die zahlreichen, hilfreichen Diskussionen während meiner Arbeit.

Ein weiterer Dank geht an Prof. Dr. Julia Bornhorst und Dr. Isabelle Rohn, die mich während meiner Masterarbeit in die Welt des Fadenwurms eingearbeitet haben und somit meine Begeisterung für die Forschung und das Spurenelement Selen geweckt haben. Zudem möchte ich mich bei Prof. Dr. Julia Bornhorst und Dr. Sandra Marie Müller für die Einarbeitung in die komplexe, aber wirklich faszinierende Welt der Schrankenmodelle bedanken. Die Isolierung der primären Zellen ist kompliziert und anstrengend, aber die haben mir immer besonders viel Spaß gemacht. Daran anschließend möchte ich mich bei Herrn Stefan Zimmermann (Metzgerei in Görzke) für die Überlassung des porzinen Gehirngewebes bedanken, vor allem dafür, dass wir bei dem Schlachtprozess geduldet werden. Für die finanzielle Förderung meiner Arbeit bedanke ich mich bei der Kommission zur Vergabe der Graduiertenförderung der Universität Potsdam und der Potsdam Graduate School (PoGS).

Ein großes Dankeschön geht an Dr. Franziska Ebert, die mir nicht nur das Arbeiten in der Zellkultur beigebracht hat, sondern auch eine große Hilfe bei dem Design der Primer und der Genexpressionsstudie gewesen ist. An dieser Stelle möchte ich mich auch ganz herzlich bei allen anderen (ehemaligen und aktuellen) Mitgliedern der Arbeitsgruppe von Prof. Dr. Tanja Schwerdtle bedanken: Dr. Isabelle Rohn, Dr. Vanessa Ziehmann, Dr. Johannes Kopp, Dr. Michael Stiboller, Max Tuchtenhagen, Tom Heinze, Sharleen Friese, Giovanna Ranzini, Denny Pellowski, Gabriele Pohl, Dr. Viktoria Wandt und Dr. Nicola Winkelbeiner. Ich danke euch für die wunderbare Zusammenarbeit, die stetige Motivation und die lustigen Stunden im Labor sowie im Büro.

Meinen fleißigen Korrekturlesern danke ich für ihre Adleraugen, ihre Zeit, die hilfreichen Tipps und für den Feinschliff der vorliegenden Arbeit. Ein spezieller Dank geht auch an Barbara Hertel, die nicht nur wertvolle Anmerkungen zu dieser Arbeit gegeben hat, sondern mir immer mit Rat und Tat im Labor zur Seite stand. Deine Erfahrung im Laboralltag haben mir wirklich viel beigebracht, was ich in Zukunft mit Sicherheit brauchen werde.

Natürlich möchte ich meiner lieben Familie für ihre Geduld und Unterstützung bedanken. Ohne euch hätte ich das nicht geschafft. Danke!